



REPORT

Norwegian GeoTest Sites (NGTS)

IMPACT OF CONE PENETROMETER TYPE ON
CPTU RESULTS AT 4 NGTS SITES. SILT, SOFT CLAY,
SAND AND QUICK CLAY.

DOC. NO.: 20160154-21-R

REV. NO.: 0 / 2020-01-08

Ved elektronisk overføring kan ikke konfidensialiteten eller autentisiteten av dette dokumentet garanteres. Adressaten bør vurdere denne risikoen og ta fullt ansvar for bruk av dette dokumentet.

Dokumentet skal ikke benyttes i utdrag eller til andre formål enn det dokumentet omhandler. Dokumentet må ikke reproduseres eller leveres til tredjemann uten eiers samtykke. Dokumentet må ikke endres uten samtykke fra NGTS.

Neither the confidentiality nor the integrity of this document can be guaranteed following electronic transmission. The addressee should consider this risk and take full responsibility for use of this document.

This document shall not be used in parts, or for other purposes than the document was prepared for. The document shall not be copied, in parts or in whole, or be given to a third party without the owner's consent. No changes to the document shall be made without consent from NGTS.

Project

Project title: Norwegian GeoTest Sites (NGTS)
Document title: Impact of cone penetrometer type on measured CPTU parameters at 4 NGTS sites. Silt, soft clay, sand and quick clay.
Document no.: 20160154-21-R
Date: 2020-01-08
Revision no./rev. date: 0

Client

Client: Research Council of Norway (RCN)
Client contact person: Herman Farbrod
Contract reference: RCN project number 245650

for NGTS

Project manager: Jean-Sebastien L'Heureux
Prepared by: Aleksander S. Gundersen, Anders Lindgård, Tom Lunne
Reviewed by: Eigil Haugen, Jean-Sebastien L'Heureux, Kristoffer Kåsin

Summary

Using cone penetrometers from different manufacturers may yield different results even if the equipment complies with international standards. This report presents a study on differences in CPTU test results as function of cone type.

The Norwegian GeoTest Sites (NGTS) project established five research sites with different characteristic soil types in 2016. This study includes testing at four of the NGTS sites, i.e. soft clay site, silt site, quick clay site and sand site, using twelve different penetrometers from five manufacturers. In total, eighty-seven cone penetration tests are evaluated.

A major contributor to the scatter in CPTU results appear to be the temperature at which zero readings were taken. It was decided to do a temperature correction of all the results. This significantly decreased the scatter in the data. To eliminate this uncertainty, it is recommended to take zero readings with the cone penetrometer at a temperature as close as possible to ground temperature as recommended by ISO 22476-1:2012. If this is not

the case, it is recommended to use cone specific temperature calibration to correct for temperature effects.

Regarding tests with the same cone type, this study suggests that the penetration pore pressure, u_2 , provides the most repeatable results. The corrected cone resistance, q_t , generally varies somewhat more than u_2 . Some of the cone types give good repeatability for sleeve friction, f_s , while some show relatively large variation. These conclusions are valid for all test sites. Comparing results from different cone types reveal that the penetration pore pressure generally produces less scatter compared to the corrected cone resistance and sleeve friction. The measured sleeve frictions are very small for soft soils and vary significantly from one cone type to another, which is in line with previous experience. Hence one should be careful using sleeve friction, and the friction ratio, when interpreting soil parameters for design in soft soils. Since the measured u_2 appears to be the most reliable parameter, it should be used in addition to q_t for deriving soil parameters.

The results show that filter saturation is poor in the start of some tests and this could be improved as emphasized by ISO 22476-1:2012. Following the ISO code it is recommended to carry out the testing with a minimum distance between a CPT and adjacent boreholes of 2 m. The thrust machine should push the rods so that the axis of the pushing force is as close to vertical as possible. The deviation from the intended axis of the cone should be less than 2° .

For some of the tests at the soft clay sites, measured sleeve friction, not corrected for temperature, can be as low as zero. For subtraction cones, the measured values may be this low due to the way the sleeve friction is calculated. A small offset in the measured cone resistance may lead to erroneous values of sleeve friction. As remedy it is suggested to correct the cone resistance and resistance behind sleeve for temperature effects before doing the subtraction.

Some cone penetrometers are sensitive to temperature changes and it was decided to study the time necessary to get stable readings of the cone resistance, sleeve friction and penetration pore pressure at zero load level. The penetrometers were placed in a bucket of water and in free air. The results show the importance of good procedures for taking zero readings and indicate that cone temperature may seriously affect the readings. The importance of waiting for the readings to stabilize at ground temperature is evident from the results. It was also observed that stabilization is quicker and more uniform when taking readings in water compared to taking readings in air. A procedure for taking stable zero readings close to ground temperature has been suggested.

Content

1	Introduction	8
1.1	Background	8
1.2	Main objective	9
2	Test sites	9
2.1	General	9
2.2	Soft clay site – Onsøy	9
2.3	Silt site – Halden	11
2.4	Sand site – Øysand	13
2.5	Quick clay site – Tiller-Flotten	14
3	Cone penetrometers	16
4	Tests carried out	18
4.1	General	18
4.2	Soft clay site – Onsøy	19
4.3	Silt site – Halden	20
4.4	Sand site – Øysand	21
4.5	Quick clay site – Tiller-Flotten	23
5	Processing and interpretation of results	25
5.1	Correction of measured results	25
5.2	Representative results	28
5.3	Derived CPTU parameters	29
6	Test results for each cone type at each site with evaluation of scatter and anomalies	31
6.1	General	31
6.2	Soft clay site – Onsøy	31
6.3	Silt site – Halden	42
6.4	Sand site – Øysand	50
6.5	Quick clay site – Tiller-Flotten	62
7	Comparison of representative results	74
7.1	Soft clay site – Onsøy	74
7.2	Silt site – Halden	77
7.3	Sand site – Øysand	79
7.4	Quick clay site – Tiller-Flotten	84
7.5	Overall evaluation of differences	87
8	Zero readings as function of time	90
9	Recommendations for future testing	93
10	Summary and conclusions	95
11	Acknowledgements	97
12	References	98

Tables

Table 3-1	Properties of the cone penetrometers.
Table 3-2	Pore pressure measurement systems.
Table 4.1-1	Number of tests carried out at each site.
Table 5.1-1	Change in pressure readings with change in temperature
Table 5.3-1	Unit weights used in interpretation – all sites.
Table 6.2-1	Summary of CPTU tests with remarks – soft clay site.
Table 6.3-1	Summary of CPTU tests with remarks – silt site.
Table 6.4-1	Summary of CPTU tests with remarks – sand site.
Table 6.5-1	Summary of CPTU tests with remarks – quick clay site.
Table 7.5-1	Overview of temperature corrections – Tiller-Flotten and Onsøy
Table 7.5-2	Ranges in measured values for the three sensor types at Tiller-Flotten, Onsøy and Halden
Table 8-1	Temperatures in water and air at calibration before and after tests. "-" indicates that no data was recorded.

Figures

Figure 2.2.1	Overview map of the Onsøy area.
Figure 2.2.2	Borehole log. Soft clay site.
Figure 2.3.1	Borehole log. Silt site.
Figure 2.4.1	Typical stratigraphy at the Øysand research site (middle, not to scale).
Figure 2.4-2	Borehole log. Sand site.
Figure 2.5.1	Borehole log. Quick clay site.
Figure 4.2.1	Overview map of test locations – soft clay site. Grid size: 50x50 cm.
Figure 4.3.1	Overview map of test locations – silt site. Grid size: 50x50 cm.
Figure 4.4.1	Overview map of test locations – sand site. Grid size: 50x50 cm.
Figure 4.5.1	Overview map of test locations – quick clay site. Grid size: 50x50 cm.
Figure 5.1.1	Cone resistance versus change in temperature.
Figure 5.1.2	Sleeve friction versus change in temperature.
Figure 5.1.3	Pore pressure versus change in temperature.
Figure 5.3.1	In-situ pore pressure used in interpretation – all sites.
Figure 6.2.1	Measured and derived CPTU parameters. Cone type 1. Soft clay site.
Figure 6.2.2	Measured and derived CPTU parameters. Cone type 2. Soft clay site.
Figure 6.2.3	Measured and derived CPTU parameters. Cone type 3. Soft clay site.
Figure 6.2.4	Measured and derived CPTU parameters. Cone type 4. Soft clay site.
Figure 6.2.5	Measured and derived CPTU parameters. Cone type 5. Soft clay site.
Figure 6.2.6	Measured and derived CPTU parameters. Cone type 6. Soft clay site.
Figure 6.2.7	Measured and derived CPTU parameters. Cone type 7. Soft clay site.
Figure 6.3.1	Measured and derived CPTU parameters. Cone type 1. Silt site.
Figure 6.3.2	Measured and derived CPTU parameters. Cone type 5. Silt site.
Figure 6.3.3	Measured and derived CPTU parameters. Cone type 6. Silt site.
Figure 6.3.4	Measured and derived CPTU parameters. Cone type 7. Silt site.

Figures – continued

- Figure 6.3.5 Measured and derived CPTU parameters. Cone type 9. Silt site.
- Figure 6.4.1 Measured and derived CPTU parameters. Cone type 1. Sand site.
- Figure 6.4.2 Measured and derived CPTU parameters. Cone type 2. Sand site.
- Figure 6.4.3 Measured and derived CPTU parameters. Cone type 3. Sand site.
- Figure 6.4.4 Measured and derived CPTU parameters. Cone type 4. Sand site.
- Figure 6.4.5 Measured and derived CPTU parameters. Cone type 5. Sand site.
- Figure 6.4.6 Measured and derived CPTU parameters. Cone type 6. Sand site.
- Figure 6.4.7 Measured and derived CPTU parameters. Cone type 7. Sand site.
- Figure 6.4.8 Measured and derived CPTU parameters. Cone type 11. Sand site.
- Figure 6.4.9 Measured and derived CPTU parameters. Cone type 12. Sand site.
- Figure 6.5.1 Measured and derived CPTU parameters. Cone type 1. Quick clay site.
- Figure 6.5.2 Measured and derived CPTU parameters. Cone type 2. Quick clay site.
- Figure 6.5.3 Measured and derived CPTU parameters. Cone type 3. Quick clay site.
- Figure 6.5.4 Measured and derived CPTU parameters. Cone type 5. Quick clay site.
- Figure 6.5.5 Measured and derived CPTU parameters. Cone type 6. Quick clay site.
- Figure 6.5.6 Measured and derived CPTU parameters. Cone type 7. Quick clay site.
- Figure 6.5.7 Measured and derived CPTU parameters. Cone type 8. Quick clay site.
- Figure 6.5.8 Measured and derived CPTU parameters. Cone type 12. Quick clay site.
- Figure 7.1.1 Measured and derived CPTU parameters. All cone types. Soft clay site.
- Figure 7.2.1 Measured and derived CPTU parameters. All cone types. Silt site.
- Figure 7.3.1 Measured and derived CPTU parameters. All cone types. Sand site.
- Figure 7.3.2 Profile through CPTUs OYC21-OYC32 showing the interpreted structure of the sand deposit at Øysand (from Hammer, 2019).
- Figure 7.3.3 Comparison of derived CPTU parameters for all cone types at Øysand after depth adjustment (from Hammer, 2019).
- Figure 7.3.4 Average error for derived CPTU parameters for given cone types.
- Figure 7.3.5 Comparison of representative profiles for cone types 3, 4, 5, 11 and 12 at Øysand (from Hammer, 2019).
- Figure 7.4.1 Measured and derived CPTU parameters. All cone types. Quick clay site.

Appendices

- Appendix A Individual CPTU results
- Appendix B Zero readings as function of time

Review and reference page

1 Introduction

1.1 Background

It is a well-known fact that even if cone penetrometers comply with international standards (e.g. ISO 22476-1:2012), using equipment from different manufacturers can give different results (e.g. Lunne et al., 1986, Gauer et al., 2002, Powell & Lunne, 2005, Tiggemann & Beukema, 2008, Lunne, 2010 and Cabal & Robertson, 2014). This is particularly a problem when soil investigation contractors, using different cones, operate in the same area, and especially on the same project. Lunne et al. (1986) carried out a comprehensive laboratory and field study comparing test results from cone penetrometers from 8 different manufacturers. That study included tests at Onsøy soft clay site and Holmen/Drammen sand sites and it was shown that all three parameters q_c , f_s and u_2 could vary significantly, depending on the equipment used.

A later study by NGI (Gauer et al., 2002), based on several different cone penetrometers tested in Onsøy clay, showed that the situation had to some extent improved. The cone resistance showed relatively small scatter, and the penetration pore pressure was even more repeatable from one cone type to another. However, the scatter in the measured sleeve friction, and hence the friction ratio, was very significant.

Powell & Lunne (2005) showed that if calibration of all cone penetrometers used was done in a consistent manner by one organization which also carried out all tests, then the variation in results would be reduced.

Over the last few years further improvements in cone design and electronics have occurred by some cone manufactures. The establishment of 5 new national test sites in Norway (L'Heureux and Lunne 2019) has given the opportunity to revisit the problem of uncertainties in CPTU test results by inviting several companies to do testing at 4 of the sites.

This report includes results from 4 sites; the soft clay site at Onsøy, the silt site at Halden, the sand site at Øysand and the quick clay site at Tiller-Flotten.

For the tests reported herein the calibrations were carried out by each cone manufacturer. It is thought that the test results will then be more representative for general practice in the soil investigation industry. Each cone manufacturer has tried to follow requirements and recommendations in international standards and guidelines. Some of the tests were carried out by the cone manufacturers themselves and some were carried out by NGI and NRPA. This report does not include calibration sheets because the cone manufacturers are treated anonymously. However, the calibration sheets will be forwarded upon request from the reader.

1.2 Main objective

The main objective of the testing program is to investigate if recent advancements in cone design and electronics have led to improved repeatability and less scatter in CPTU measurements for tests conducted in different types of soil.

2 Test sites

2.1 General

The Research Council of Norway's (RCN) infrastructure project "Norwegian GeoTest Sites (NGTS)" ("*Nasjonale forsøksfelt*") has established five test sites across mainland Norway and Svalbard. Each test site has a characteristic soil type. The test sites are full scale field laboratories for testing in situ equipment and foundation solutions, and they will also contribute to improved knowledge of each soil type. More details about the four main land test sites included in this study is presented in the following subchapters.

2.2 Soft clay site – Onsøy

Due to the thickness of the clay deposit and its highly uniform nature, the Onsøy area has been used for research purposes by NGI for many years. The area is in south-eastern Norway, about 100 km from Oslo just north of the town of Fredrikstad and to the west of the Seut River, see Figure 2.2.1.

Early investigations at previous Onsøy sites (blue rectangles in Figure 2.2.1) included a series of vane tests, which were aimed at examining anisotropy and rate effects (Kjærnsli and Aas, 1969). Work at Onsøy continues to the present time with tests on a variety of different penetration devices and studies of sample disturbance effects using high quality Sherbrooke block samples, several piston tube samplers and the GeoDelft continuous sampler. A summary of the major phases of the work is given by Lunne et al. (2003) and in a recent paper by Gundersen et al. (2019).

Prior to 2000, all the test areas were grouped closely together within an area of about 140 m x 120 m (largest blue rectangle in Figure 2.2.1). However due to development of this area a new test site was established some 200 m to 300 m to the northwest. NGI used this site for 10 years.

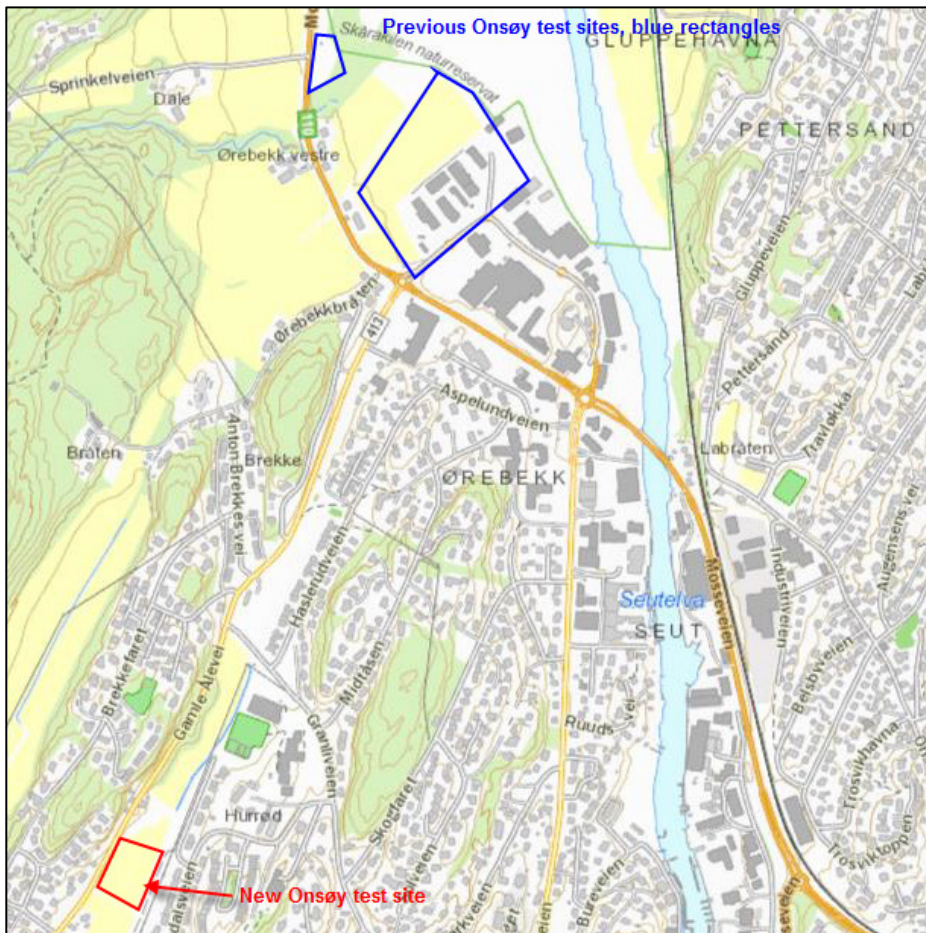


Figure 2.2.1 Overview map of the Onsøy area

In connection with the NGTS project a new test site was established located along the road Gamle Ålevei, 1.3 km southwest of the previous test site along Pancoveien, see Figure 2.2.1.

Figure 2.2.2 shows a borehole log for the NGTS soft clay site. This area is valley shaped and depth to bedrock varies across the site. Soil conditions are not as uniform as the old Onsøy sites. An intermediate clay layer with medium to high plasticity index is encountered between approximately 8.5 m to 13.5 m depending on the location within the site. The main soil volume is the plastic Onsøy clay which is also encountered at the old Onsøy sites.

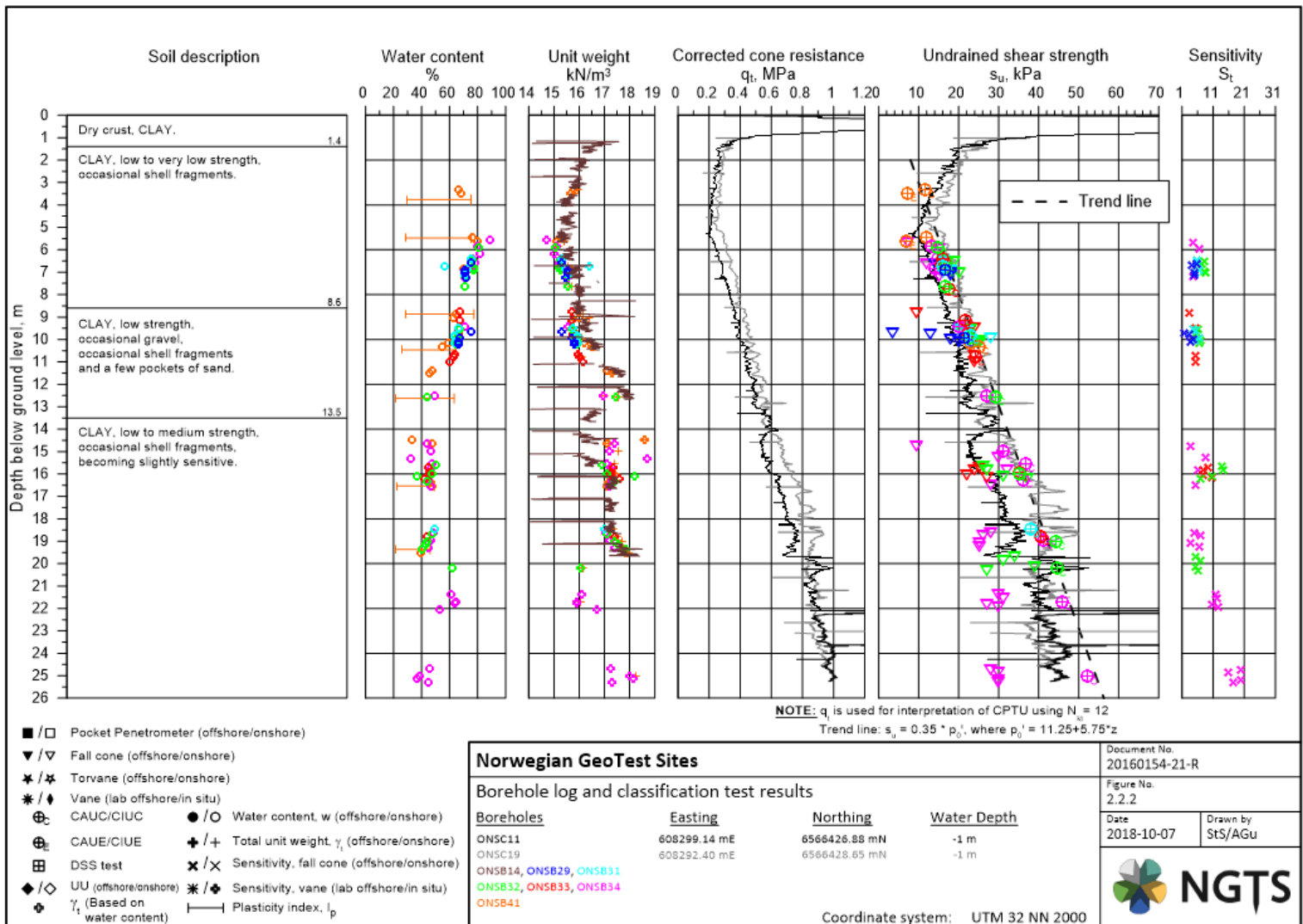


Figure 2.2.2 Borehole log. Soft clay site.

2.3 Silt site – Halden

The silt deposit at Halden was first investigated by NGI in 2011 after a landslide in the area (Blaker et al., 2016). More recently, the deposit has been studied with the aim of developing a National GeoTest Site for silty soils as part of NGI's internal strategic project 8 (SP8) and NGTS. A full overview of the geotechnical data available at Halden thorough site characterization is given in Blaker et al. (2019).

The Halden Research Site is located in south-eastern Norway, approximately 120 km south of Oslo in the municipality of Halden. Here the marine silt deposit is up to 10 m thick and uniform in nature. Over the last two years a series of geophysical, geological and geotechnical investigations have been carried out in the field and in the laboratory to characterize the natural silt deposit. This information will provide a basis for

understanding the main factors controlling the engineering properties and behavior for this silt. Figure 2.3.1 presents the borehole log for location HALB01. Further details of the test site is presented in NGTS reports 20160154-04-R and 20160154-05-R.

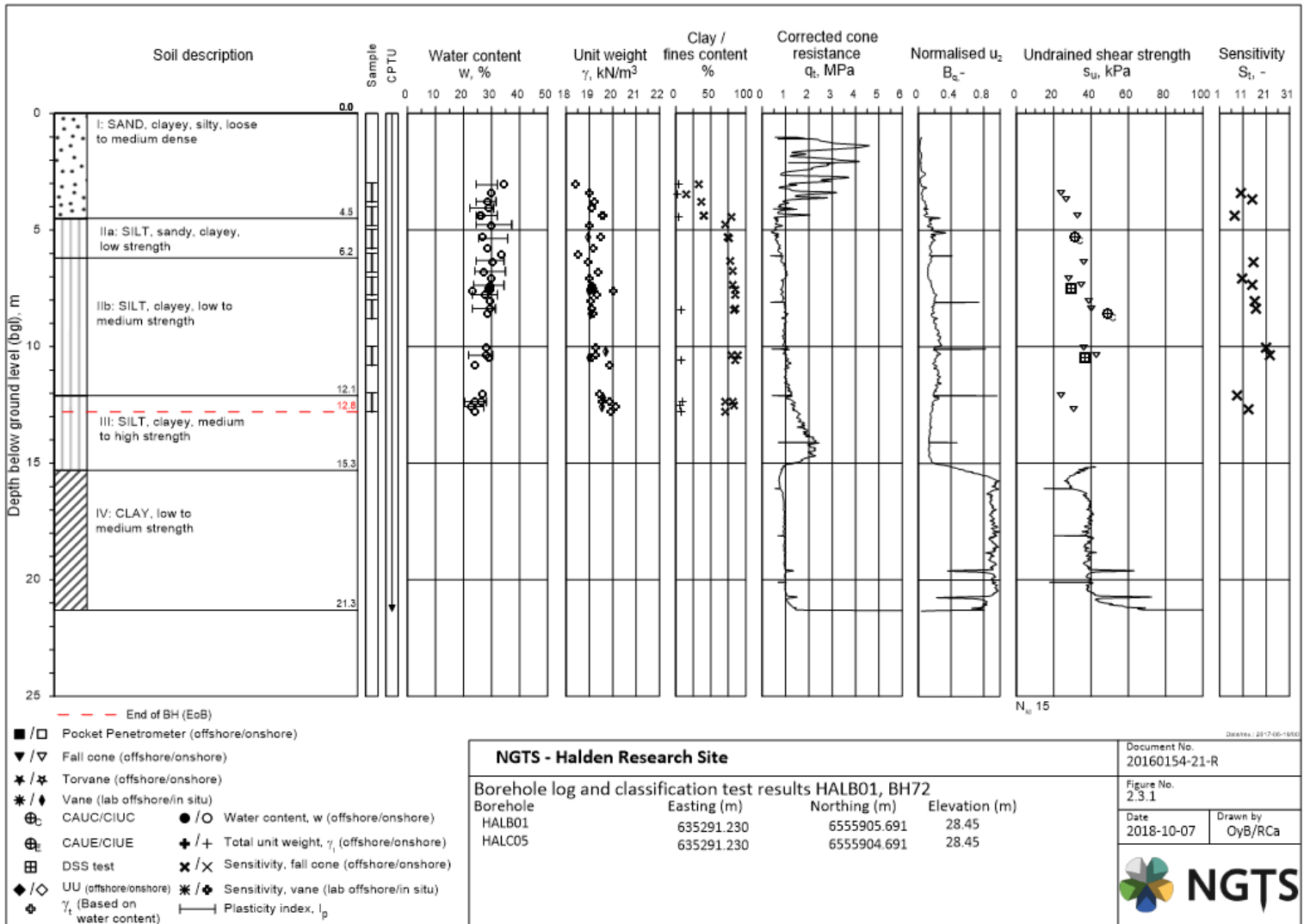


Figure 2.3.1 Borehole log. Silt site.

2.4 Sand site – Øysand

The Øysand research site is in central Norway, approximately 15 km south of Trondheim. The locality sits on the south side of the Gaula River, at the head of the Gaulosen, an arm off the main Trondheim Fjord. Over the past thousand years, the river has mostly prograded westwards in the fjord. The ground surface at the site is at an elevation of 2.7 m above mean sea level.

The fluvial and deltaic deposit at Øysand consists of a 20–25 m fine silty sand with occasional high gravel content. Figure 2.4.1 presents a schematic longitudinal cross-section of a deltaic deposit, depicting its characteristic tripartite architecture (topset, foreset and bottomset). At Øysand, the stratigraphy features a general coarsening upward sequence as typically observed in deltaic deposits with topset, foreset and bottomset units). The layers in these units can have different properties, geometry, fall and dip that can be linked to the depositional history at the mount of the river delta.

Figure 2.4.1 presents a snapshot of the stratigraphy and index properties of the soils at the site, as obtained from in situ and laboratory tests¹. The borehole log is for Borehole OYSB09, which is located very close to CPTU OYSC09. The deposits at the site are somewhat layered, as one may expect from a fluvial deposit. The terrain at the site is flat, located at 2-3 m above sea level. Multi-sensor core logging (MSCL) technique was utilized to estimate unit weight and water content as illustrated in the figure. For details see Gerland & Villinger (1995). Relative density, D_r , is computed according to Jamiolkowski et al. (2003).

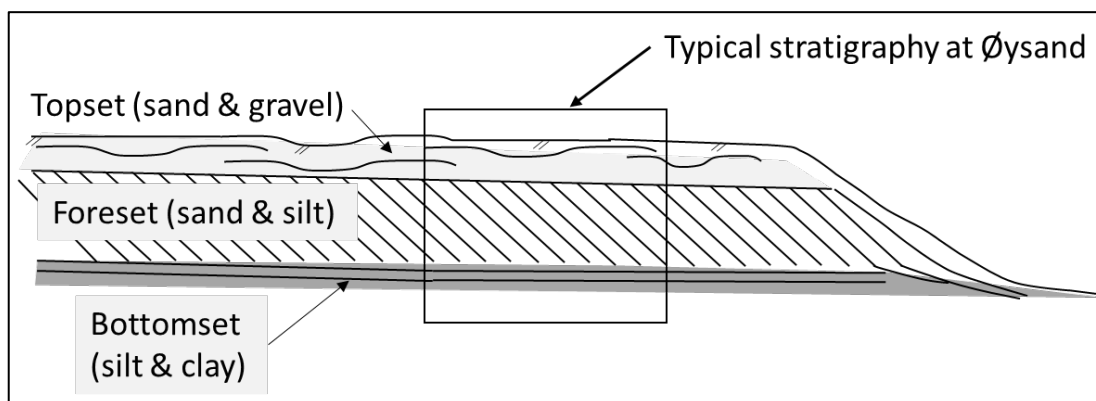


Figure 2.4.1. Typical stratigraphy at the Øysand research site (middle, not to scale).

¹ The symbols used in Figure 2.4.1 are defined either in the figure text above each profile or at the bottom of the table. Other symbols not directly defined are γ_s , the density of solids and D_{10} and D_{60} , the particle diameter (in mm) on the grain size distribution curve with 10 and 60% of the particles by weight passing.

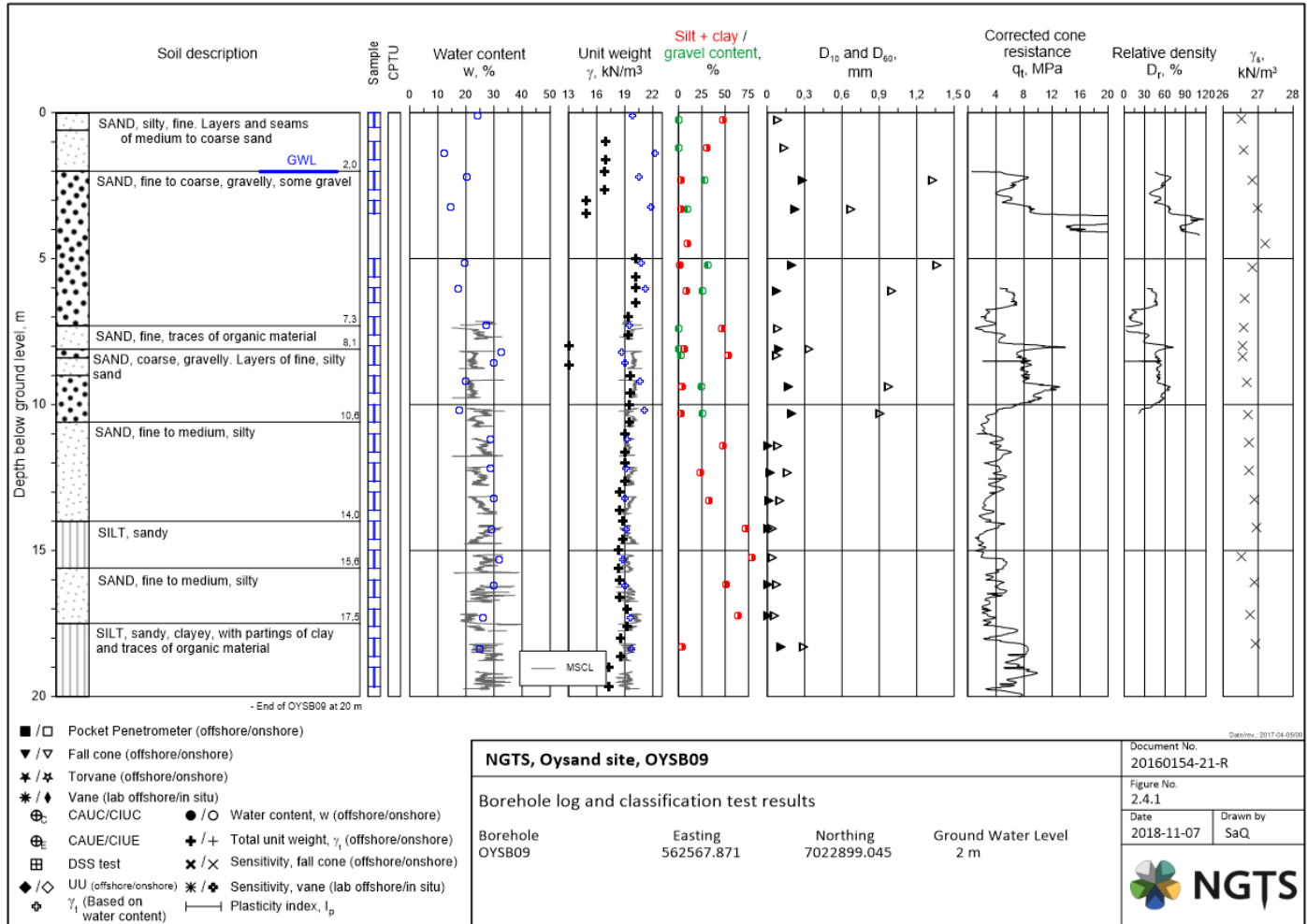


Figure 2.4.2 Borehole log. Sand site.

2.5 Quick clay site – Tiller-Flotten

The Tiller-Flotten research site was developed through the Norwegian GeoTest site (NGTS) project and it is situated approximately 10 km south of Trondheim (L'Heureux et al. 2019). The site consists of a more than 50 m thick marine clay deposit. The top 7.5 m of the deposit shows a low to medium sensitivity, while sensitivity increases up to approximately 200 from 7.5 to 20 m below the ground surface. A wide variety of in situ and laboratory data have been acquired to investigate the geotechnical, geological and geophysical properties of the material. The sensitive clay shows low to medium plasticity and a liquidity index (I_L) above 1.6. It shows some overconsolidation ($OCR \approx 1.5-3.0$) linked to the glacial history of the area. Its strength and stiffness properties show good agreement with some well-known correlations for sensitive clays. Anisotropy in undrained shear strength is also similar to other sensitive clays of Norway.

The water level is located approximately 1.5m below ground level. There is a coarser draining layer located about 20m bgl. where the in-situ pore pressure is significantly lower than a potential hydrostatic profile. Figure 2.5.2 presents a typical borehole log with results from laboratory and in situ geotechnical soundings at Tiller-Flotten.

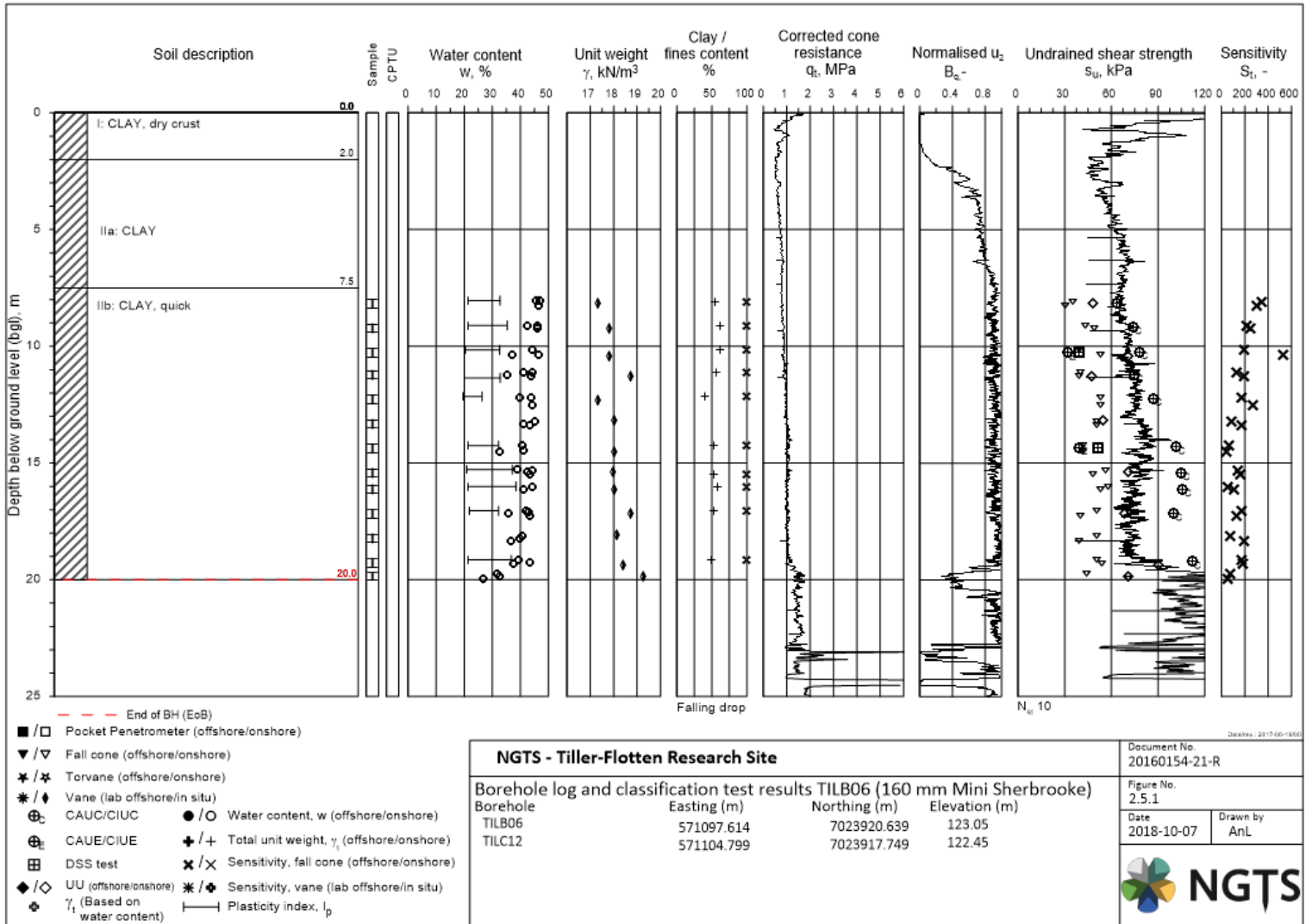


Figure 2.5.1 Borehole log. Quick clay site.

3 Cone penetrometers

Twelve cone penetrometers from five manufacturers were used in the present study. Some key dimensions and other information are given in Table 3-1. Ten of the penetrometers have a cross section area of 10 cm^2 while two have 15 cm^2 . Ten are of the compression type with separate load cells for q_c and f_s , while two are of the subtraction type where one compression load cell measures q_c , and another load cell measures $q_c + f_s$. Then f_s can be calculated by subtraction.

Units and notes to Table 3-1 are as follows:

- ↗ All dimensions are in millimeter and all areas are in mm^2
- ↗ The capacities of the cones are given in MPa
- ↗ Nominal means average values given by the manufacturers
- ↗ D_1 is the diameter of the cylindrical cone tip part and D_2 is the sleeve diameter
- ↗ h is the height of the cylindrical cone tip part
- ↗ L_1 is the length of the friction sleeve
- ↗ A_c is the cone tip area
- ↗ A_{sb} is the area where pore water pressure can act at bottom of the friction sleeve
- ↗ A_{st} is the area where pore water pressure can act at top of friction sleeve
- ↗ A_s is the sleeve area
- ↗ a is the area ratio of the cone and b is the area ratio of the sleeve

The penetration pore pressure, u_2 , is measured at the location just above the conical part of the penetrometer. The pore pressure measurement systems vary as shown in Table 3-2 where the filter type and saturation fluid are summarized.

Eleven of the cones use filter made of bronze, brass or stainless steel. Eight of these use silicon oil as saturation fluid and three uses glycerin. One of the cone penetrometers use a so-called slot filter. As described in ISO 22476-1:2012, in this system the pore pressure is measured by an open system with a 0.3 mm slot immediately behind the conical part. The slot communicates with the pressure chamber through several channels. De-aired water, antifreeze (glycol) or other liquids can be used to saturate the pressure chamber, whereas the channels are saturated with gelatin or a similar liquid. All cone penetrometers used also measure inclination during penetration as required in ISO 22476-1:2012. Tables 3-1 and 3-2 summarize information about all cones used.

Table 3-1 Properties of the cone penetrometers used.

Cone type	D ₁	D ₂	h	L ₁	A _c	A _{sb}	A _{st}	A _s	a-nom	b-nom	Cone type	Cone capacity		
												q _c	f _s	u ₂
1	35.8	35.8	10.0	134	1004	200	200	15015	0.8	0	Comp	50	1.6	2.5
2	35.9	36.0	10.0	134	1012	163	163	15155	0.85	0	Comp	25	0.5	2
3	36.0	36.1	10.0	135	1000	219	219	15000	0.8	0	Subtr	100	1	2
4	36.0	36.1	10.0	135	1000	219	219	15000	0.8	0	Comp	100	1	2
5	36.0	36.1	10.0	135	1000	219	219	15000	0.8	0	Comp	50	0.5	2
6	36.0	36.0	10.0	135	1017	297	168	15268	0.69	0.008	Comp	50	1	2
7	35.7	35.9	7-10	134	1000	263	263	15000	0.75	0	Comp	75	1	2
8	35.7	35.9	7-10	134	1000	263	263	15000	0.75	0	Comp	7.5	0.15	2
9	35.9	36.0	10	134	1012	163	163	15155	0.85	0	Comp	100	0.5	2.5
10	35.9	36.0	10.0	134	1012	163	163	15155	0.85	0	Comp	50	0.5	2
11	44.1	44.2	12.2	165	1500	309	309	22500	0.8	0	Subtr	100	1	2
12	44.1	44.2	12.2	165	1500	309	309	22500	0.8	0	Comp	100	1	2

Table 3-2 Pore pressure measurement systems.

Cone type	Filter type	Saturation fluid
1	Bronze	Silicone ISOVG 100
2	Bronze	Glycerine
3	Brass 38 micron (SIKA B-20)	Silicone oil 200 fluid 50 cSt
4	Brass 38 micron (SIKA B-20)	Silicone oil 200 fluid 50 cSt
5	Brass 38 micron (SIKA B-20)	Silicone oil 200 fluid 50 cSt
6	Slot	Grease/Oil
7	Stainless steel, S/S 10 μ	Silicone oil, DC200, 50 cSt
8	Stainless steel, S/S 10 μ	Silicone oil, DC200, 50 cSt
9	Bronze	Glycerine
10	Bronze	Glycerine
11	Brass 38 micron (SIKA B-20)	Silicone oil 200 fluid 50 cSt
12	Brass 38 micron (SIKA B-20)	Silicone oil 200 fluid 50 cSt

4 Tests carried out

4.1 General

The initial plan was that at least 3 tests should be carried out with each penetrometer type at each of the test sites. The tests should be done at least 2 m apart. Due to various circumstances, not all the tests were carried out in accordance with the initial plan. Therefore, in the following the testing is described as it was performed at each site.

For the first tests, no scheme had been planned for recording the temperature at which the zero readings were taken. For these tests, meteorological records have been used to find the representative air temperature at the time of testing. For most of the tests, the party carrying out the tests performed the zero measurements the way they were used to.

Tests with cone penetrometer type 6 were carried out by NGI, and tests with types 7 and 8 were carried out by NPRA. Tests with the other cone penetrometer types were carried out by the manufacturers. Appendix A gives results of all CPTUs in terms of measured parameters q_c , f_s and u_2 .

During the NGTS project several cone penetration tests have been carried out with different motivations. The test results drawn upon in this study were in general carried out for this study. Table 4.1-1 summarizes the number of included tests with each cone type at each test site. Some of the tests were carried out with an add-on shear wave velocity measurement device (seismic module, s-cone), but the results of these seismic tests are not included in this report. Resistivity measurements and dissipation measurements are also not included in this report.

Table 4.1-1 Number of tests carried out at each site.

Cone type	Sand	Quick clay	Silt	Soft clay
1	4	4	3	4
2	3	3	-	3
3	2	2	-	2
4	2	-	-	4
5	4	4	3	4
6	4	4	2	3
7	3	3	3	3
8	-	3	-	-
9	-	-	2	-
10	-	-	-	-
11	2	-	-	-
12	2	2	-	-
SUM	26	25	13	23

4.2 Soft clay site – Onsøy

The tests included in this report were carried out between 4th September and 17th November 2017 within an area of 5 m by 12 m. All tests were carried out to a depth of 25 m below ground level except for cone 1 which was stopped at 21 m. In situ pore pressure measurements show that the water table has been at about 1.0 m below ground surface throughout the testing period. Due to various circumstances the number of tests carried out with each cone varied from 2 to 4. Predrilling to 1 or 2 m was used for the tests with cones 2, 6 and 7. Figure 4.2.1 shows the tests that are included in the comparative testing in this report except for tests ONSC15-17 which have been superseded by tests ONSC26-28. It should be noted that tests identified as ONSC11, 12 and 13 (A and B as well) were carried out with approximately 0.5m to neighboring tests. The remaining tests were carried out with a distance no less than 1.5m.

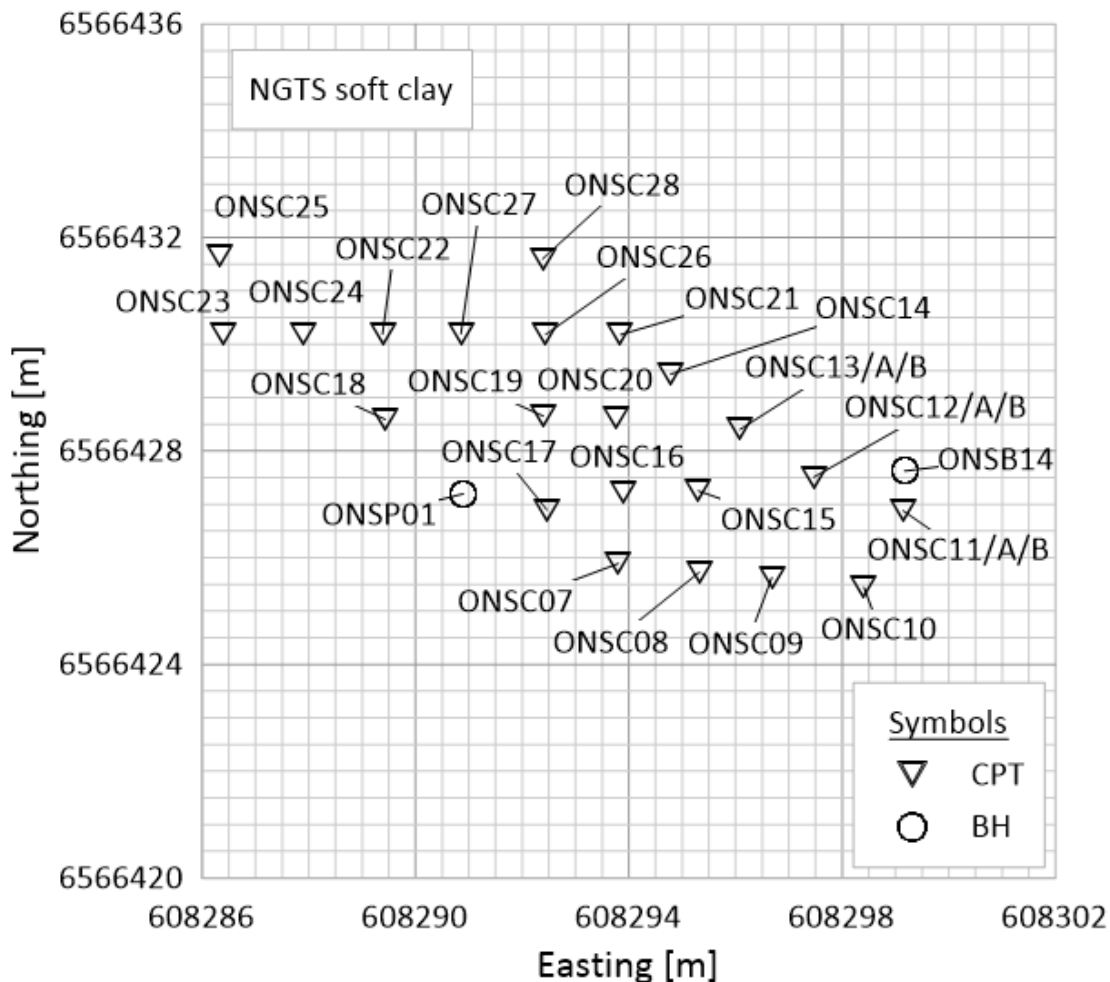


Figure 4.2.1 Overview map of test locations – soft clay site. Grid size: 50x50 cm.

4.3 Silt site – Halden

Figure 4.3.1 illustrates the tests at Halden included in this study. The tests were carried out within an area of 20m by 15m. Test HALC10 was carried out as part of the initial screening of the site in October 2015. HALC11 was done in June 2016 while the remaining tests were carried out from September to December 2017. The air temperature at the time of testing has been taken from meteorological records.

All tests were carried out with a minimum distance of 1.5m to neighboring tests. Due to various circumstances the number of tests carried out with each cone varied from 2 to 4. Pore pressure measurements show that the water table has been at about 2 m below ground surface throughout the testing period. On that note see also the in-situ pore pressure assumed for interpretation presented in Section 5.3. A target depth of 20m below ground level (bgl.) was specified and reached for all tests included in the study.

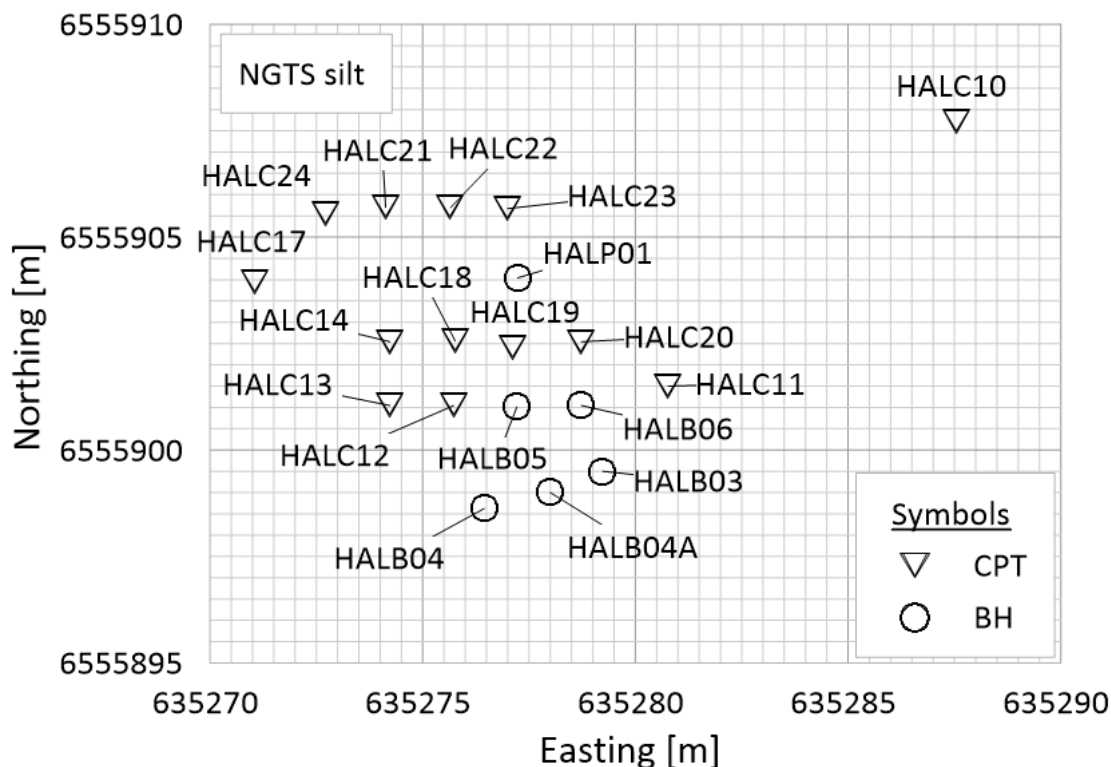


Figure 4.3.1 Overview map of test locations – silt site. Grid size: 50x50 cm.

4.4 Sand site – Øysand

All the tests included in this report except OYSC50, OYSC51 and OYSC52 were carried out within an area of 18 m by 15 m. Figure 4.4.1 illustrates the locations of the tests included in this study. The original plan was to have a minimum distance of 1.5 m to 2 m between two tests. Tests with cone type 1 were performed approximately 1.5 m away from other boreholes while CPTU soundings OYSC21 to OYSC32 were performed approximately 0.5 m apart. The tests with cone types 7 and 8 were performed 2 m away from other boreholes. Some tests were performed with a seismic add-on. These results are not reported herein. On several occasions, predrilling and drilling through gravelly layers was found necessary to prevent damaging of equipment.

The air temperature at the time of testing was taken from meteorological records for all tests except tests with cone types 7 and 8 for which the air temperature was measured on site.

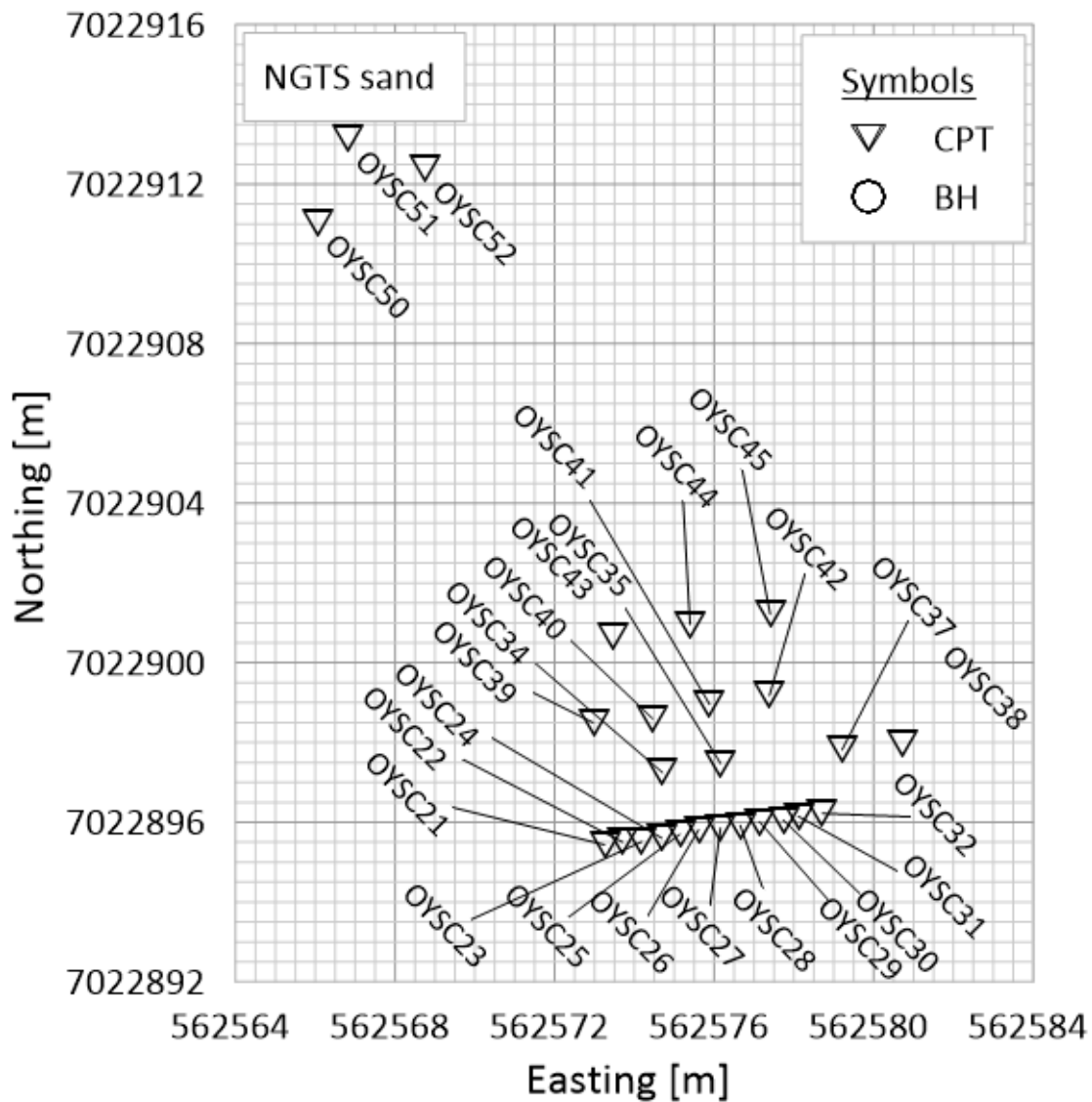


Figure 4.4.1 Overview map of test locations – sand site. Grid size: 50x50 cm.

4.5 Quick clay site – Tiller-Flotten

All the tests included in this report were carried out within an area of 8 m by 17 m. Figure 4.5.1 illustrates the locations of the tests included in this study. The original plan was to have a minimum distance of 2 m between two adjacent tests. The tests with cone type 1 were performed 2 m away from other boreholes, except for TILC16 which was done 0.6 m away from TILC01. TILC01 was the only test with cone type 10 and is therefore only included in the map for reference. TILC15 was performed as a seismic test. Predrilling was not used.

The tests with cone type 2 were performed 2 m away from other boreholes, except TILC30 which was 1.9 m away. Predrilling was performed to 2 m depth. The zero readings were taken in air after stabilizing the temperature in a bucket of water. The water temperature was quite a bit higher than in situ temperature.

The tests with cone type 3, 4, 5, 11 and 12 were performed 1 m apart, except for TILC12. TILC12 was done 0.6 m away from a rotary pressure sounding and less than 2 m away from a 54 mm piston sampling borehole. TILC12 was performed as a seismic test. Predrilling was not used. The zero readings before the tests were taken just above the terrain surface quite immediately before the start of the tests. The zero readings after the tests were taken just above ground surface quite immediately after the cone had left the ground, before the cone had been cleaned.

The tests with cone type 6 were performed 2 m away from other boreholes, except for TILC17 which was performed 1.75 m away. Predrilling was not used.

The tests with cone types 7 and 8 were performed 2 m away from other boreholes. For tests with these cone types, predrilling was done to approximately 2 m depth. TILC25 was executed as a seismic test.

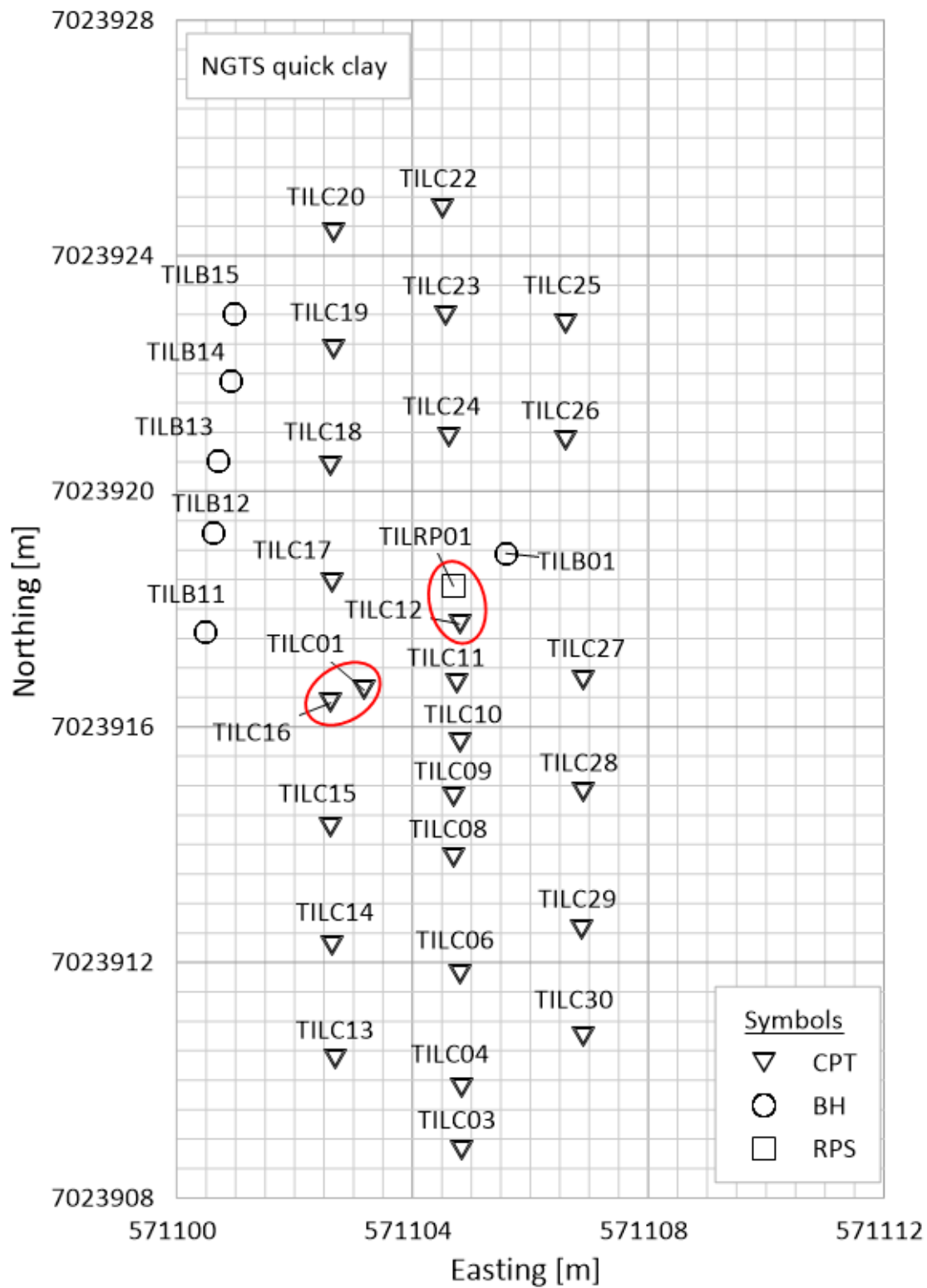


Figure 4.5.1 Overview map of test locations – quick clay site. Grid size: 50x50 cm. Red circles show tests influenced by neighboring boreholes.

5 Processing and interpretation of results

5.1 Correction of measured results

5.1.1 Correction for inclination

All penetrometers used at the NGTS sites measure the inclination of the penetrometer. This inclination was used to correct the measured penetration depth as described in ISO 22467-1:2012 and given in the following:

$$z_i^{corr} = z_{i-1}^{corr} + (z_i^{uncorr} - z_{i-1}^{uncorr}) * \cos(TA_{i-1})$$

Here, i denotes the depth index and TA denotes the tilt angle.

5.1.2 Correction for temperature

For the soft clay site, measurements with cone types 1, 3, 4 and 5 showed significantly lower values compared to other tests. The a -values for these cones were not much lower than the others, so this effect could not explain the differences. Based on previous experience it was suspected that zero shift caused by different temperature at ground level and soil temperature could occur. On that basis, measured results were corrected for temperature assuming a linear relationship between CPTU readings and temperature. The temperature correction was applied to all results from all four sites, except for cone type 6 for which no temperature calibration data are available.

A ground temperature of 8°C was assumed for the soft clay site and the silt site based on CPTU and thermistor string results. Thermistor string and CPTU results indicate a ground temperature of 5°C and 6°C for the quick clay site and the sand site, respectively. Figure 5.1.1 to Figure 5.1.3 illustrate the assumptions made for the different cone types. Change in cone resistance, sleeve friction and pore pressure measurements at zero load are plotted with change in temperature as provided by the manufacturers. The stapled lines present the assumed linear relationships between temperature change and CPTU measurements. These stapled lines were used to correct the CPTU measurements. Table 5.1-1 gives the inclination of the stapled lines in Figures 5.1.1 to 5.1.3. No data were available for cone type 6, hence the measurements with this cone type have not been corrected. Table 6.2-1, Table 6.3-1, Table 6.4-1 and Table 6.5-1 present the air temperatures used to correct the measured results. The air temperatures have been taken from meteorological records or in-situ measurements. Meteorological records from Norwegian Meteorological Institute were utilized. The list of weather stations used is given below:

- Onsøy – Råde (Tomb)
- Halden – Sarpsborg
- Øysand – Skjetlein
- Tiller – Skjetlein

For cone type 1, a cone similar to the ones used was checked for temperature zero drift. The data is illustrated in Figure 5.1.1 to Figure 5.1.3. It is assumed that the zero-drift due to temperature of all the cones of this type are the same. For cone types 2, 9 and 10, only the maximum zero drift for a given temperature interval is given. These two data points form the basis for the linear relationship used for these cones as illustrated in Figure 5.1.1 to Figure 5.1.3. For cone types 3, 4, 5, 11 and 12, it is assumed that the temperature zero drift values of cone 3 (subtraction cone) may be applied to all the cones, since all of them are from the same manufacturer. It is assumed that the zero drift values for cone 8 is the same as for cone 7 since they are both from the same manufacturer.

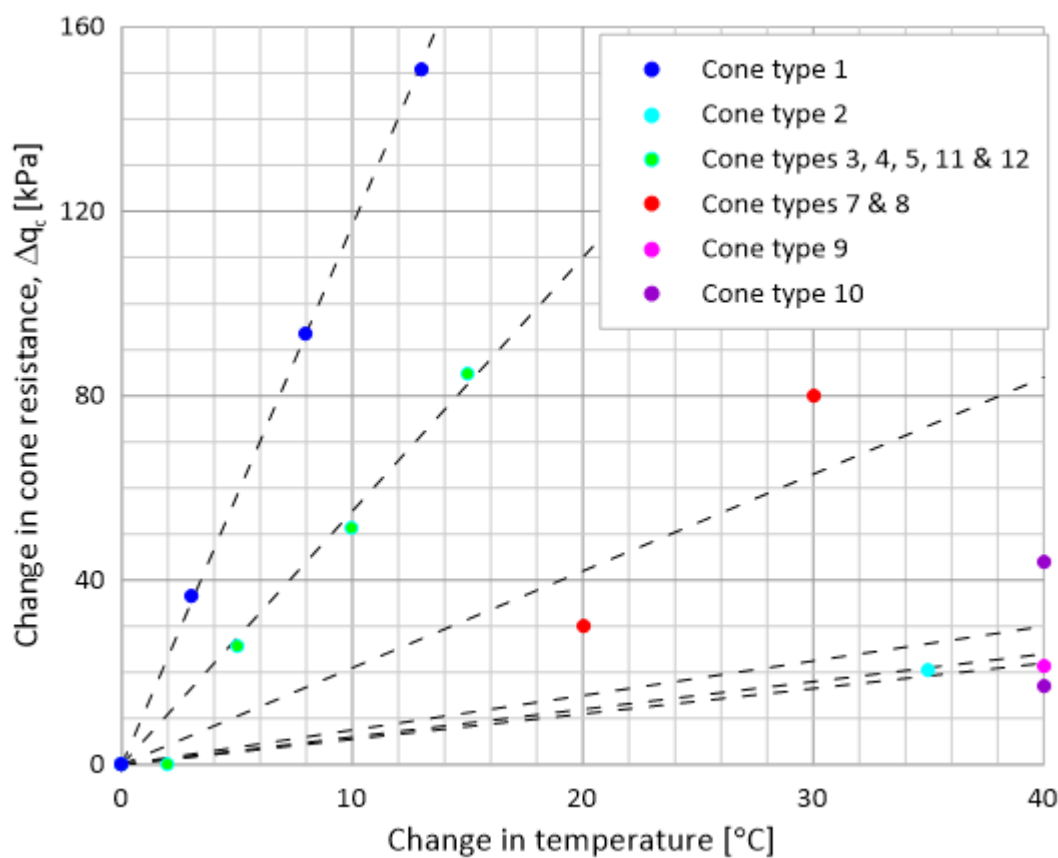


Figure 5.1.1 Cone resistance at zero load versus change in temperature.

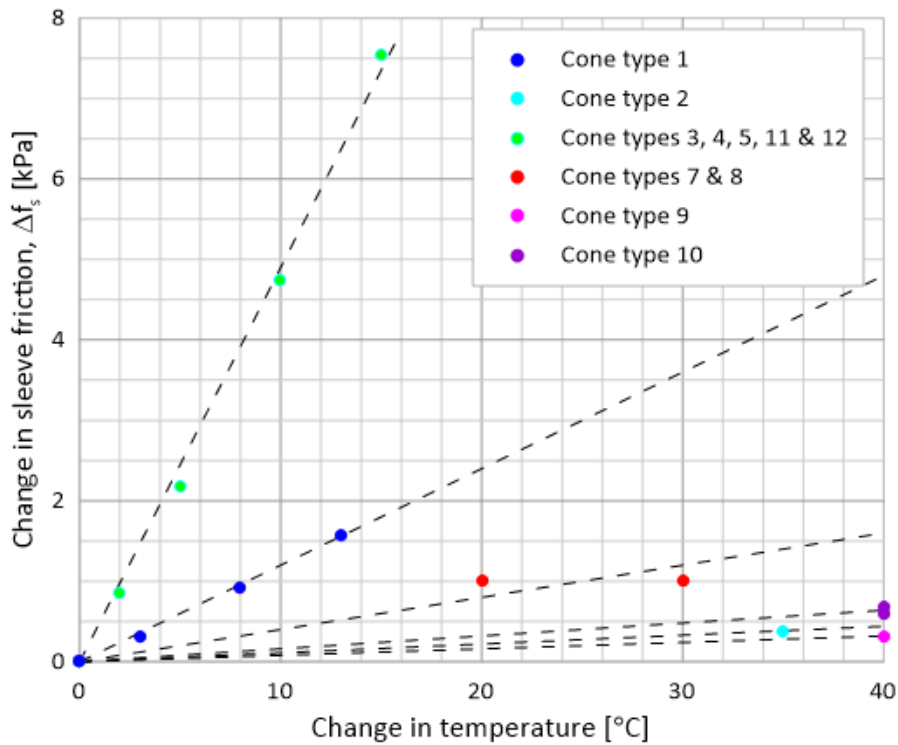


Figure 5.1.2 Sleeve friction at zero load versus change in temperature.

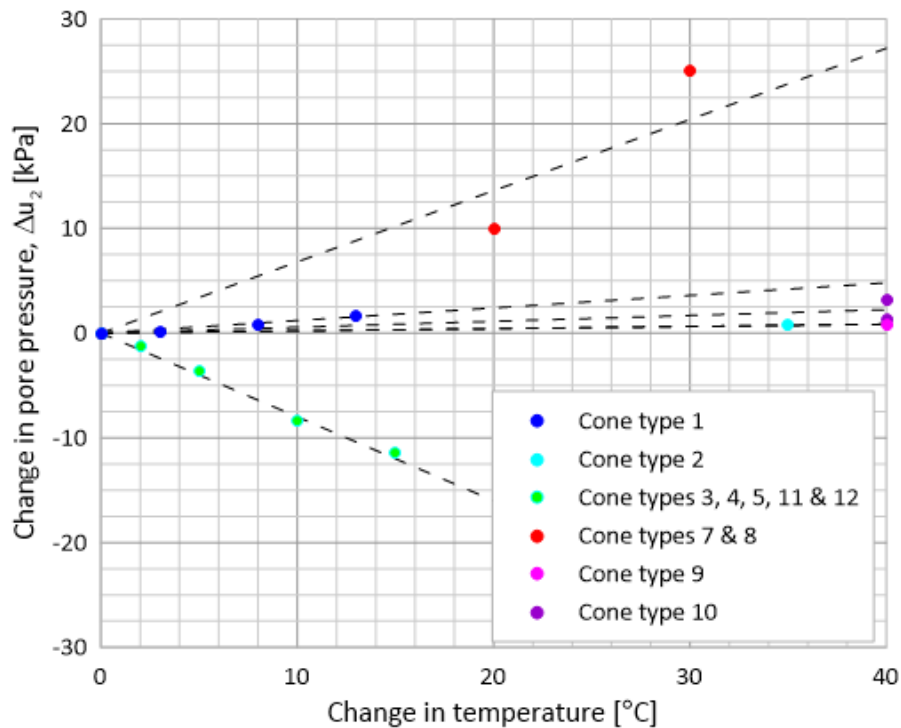


Figure 5.1.3 Pore pressure at zero load versus change in temperature.

Table 5.1-1 Change in pressure readings with change in temperature

Cone type	Pressure rate of change [kPa/Δ°C]		
	q _c	f _s	u ₂
1	11.70	0.120	0.120
2	0.60	0.011	0.021
3	5.50	0.490	-0.800
4	5.50	0.490	-0.800
5	5.50	0.490	-0.800
6	NA	NA	NA
7	2.10	0.040	0.680
8	2.10	0.040	0.680
9	0.55	0.008	0.021
10	0.75	0.016	0.056
11	5.50	0.490	-0.800
12	5.50	0.490	-0.800

5.2 Representative results

Several soundings have been carried out with each cone type at the different NGTS sites. Only cones with more than one sounding have been included in the comparison. Before comparing individual test results, and results from different cone types it is important to define representative results for each test and each cone type excluding anomalies and obviously erroneous measurements. Measurements that are considered not to be reliable have been excluded from further comparison. The list below provides general reasons for partially or completely leaving out some tests from the representative profiles:

1. Pore pressure measurements just below dissipation tests.
2. Measurements where penetration rate was significantly different from 20 mm per second.
3. Measurements with significant zero drifts.
4. Measurements indicating interference with neighboring soil investigations.

There are several potential causes for zero drifts that could occur at any time during testing. Hence, whether the results are representative or not must be decided based on inspection of the results. ISO 22476-1:2012 defines application classes and corresponding allowable minimum accuracy. For application class 1, the minimum allowable accuracy for cone resistance, sleeve friction and penetration pore pressure are 35 kPa, 5 kPa and 10 kPa, respectively (or 5 %, 10 % and 2 % of the measured values, respectively). These limiting stresses have been used to distinguish significant zero drifts for the soft clay site, quick clay site and the silt site. The allowable accuracy for application class 2 (100 kPa, 15 kPa and 25 kPa for q_c, f_s and u₂, respectively) has been used to comment on significant zero drifts for the sand site.

After disregarding results that are considered not to be reliable, a simple procedure defines the representative CPTU results for each cone type as illustrated below (the corrected cone resistance is used in the example).

$$q_{t,repr}^i = \frac{1}{n} \sum_{j=1}^{j=n} q_{t,meas}^j$$

Here n is the number of CPTU tests carried out with a specific penetrometer type, j is the CPTU test index and i is the depth index.

5.3 Derived CPTU parameters

Sleeve friction and pore pressure measurements from different cone penetrometer types can generally be compared directly. A correction for unequal end areas must be applied to the measured cone resistance before comparison between different penetrometer types. The corrected cone resistance, q_t , is given as:

$$q_t = q_c + u_2(1 - a)$$

Here, a, is the area ratio specific to each cone as measured according to ISO 22476-1: 2012. It should be noted that the a-factors used may deviate slightly from the nominal values given in Table 3-1.

The effect of cone type on friction ratio, R_f , normalized friction ratio, F_r , and pore pressure ratio, B_q , is investigated further in Section 7. These parameters have been derived as follows:

$$R_f = \frac{f_s}{q_t}$$

$$F_r = \frac{f_s}{q_n} = \frac{f_s}{q_t - \sigma_{v0}}$$

$$B_q = \frac{\Delta u}{q_n} = \frac{u_2 - u_0}{q_t - \sigma_{v0}}$$

Here, q_n is the net cone resistance, σ_{v0} is the in-situ total overburden stress and u_0 is the in-situ pore pressure. Table 5.3-1 presents the total unit weights used to derive the above parameters. Figure 5.3.1 illustrates the in-situ pore pressure used in the interpretation. Piezometer measurements and pore pressure response from cone penetration tests form

the basis for these profiles. More information on piezometer readings can be found in the factual reports for each test site (NGI 2018a,b,c,d).

Table 5.3-1 Unit weights used in interpretation – all sites

Parameter	Soft clay	Silt	Sand	Quick clay
Total unit weight, γ [kN/m ³]	16.8	19.2	19.0	17.5

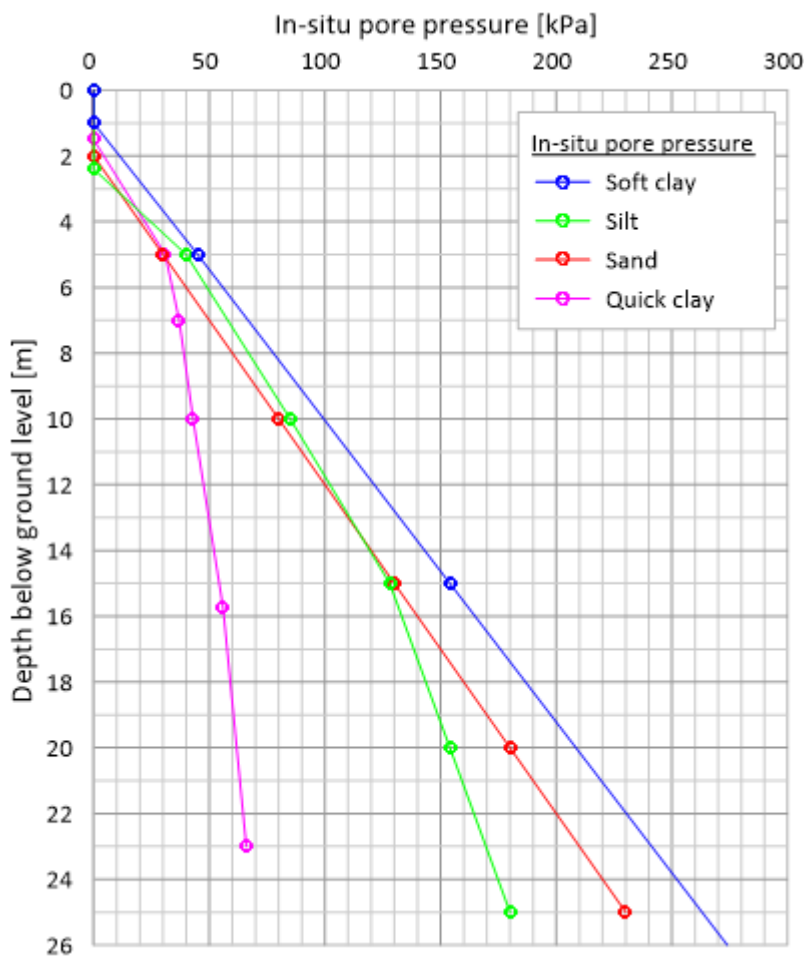


Figure 5.3.1 In-situ pore pressure used for interpretation – all sites.

6 Test results for each cone type at each site with evaluation of scatter and anomalies

6.1 General

The subsequent sections provide summary plots in terms of measured parameters (q_c , f_s and u_2 corrected for temperature effects according to Table 5.1-1.) and derived parameters (q_t , F_r and B_q) for each cone type and site. The measured parameters have been corrected for temperature as described in Section 5.1.2. The results are plotted with depth corrected for inclination as described in Section 5.1.1. These figures also include estimated representative profiles for each cone type as described in Section 5.2.

Details of each individual test including zero shifts are summarized in tables in each subsection. Observed scatter and anomalies are discussed for each site in the following.

6.2 Soft clay site – Onsøy

Figure 6.2.1 to Figure 6.2.7 provide measured and derived CPTU parameters for the 7 cone penetrometer types studied at the Onsøy soft clay site and interpreted representative average profiles. Table 6.2-1 provides zero drifts, air temperature used in correction of measured results and remarks for each test.

Cone type 1

Tests ONSC07 and 08 were carried out on the 4th of September 2017 and ONSC09 and 10 on the 3rd. ONSC07 and 08 were carried out as seismic cone penetration test with seismic measurements every 1.5 m. Figure 6.2.1 illustrates how cone resistance, sleeve friction and pore pressure decreases at the depths where seismic tests were carried out. The different tests compare remarkably well for the cone resistance and pore pressure. ONSC09 shows less resemblance to the other tests judging from cone resistance and sleeve friction response. The sleeve friction capacity of cone type 1 is 1600 kPa and a typical response value for the soft clay site is 7 kPa (0.44% of the capacity). A small nonlinearity may cause the results for ONSC09. Low filter saturation in the top of the soundings seems to cause less responsive pore pressure measurements.

Cone type 2

Figure 6.2.2 illustrates the test results from ONSC26, 27 and 28 which were carried out on the 17th of November 2017. Pre-drilling was done to 2 m below ground level. The top 1-2 meters is dry crust at Onsøy. Pore pressure behind cone show highest repeatability and sleeve friction show lowest repeatability. The decrease in cone resistance and sleeve friction at certain depths is believed to be due to the process of adding new rods. If the rig does not maintain the pressure on the cone this is typical response. This is not so evident for the pore pressure because this parameter is more dependent on time than the pressure from the rig in soft clays.

Cone type 3

ONSC11B and ONS12B were carried out on the 18th of September 2017. Figure 6.2.3 shows that all parameters vary with test, especially sleeve friction which produces zero values at 3 m for test ONSC11B. This cone type is a subtraction cone which means that the sleeve friction is determined by subtraction of the cone resistance from a total resistance measured above sleeve. ONSC11B demonstrates large zero drift for the cone resistance and it is believed that this zero shift have caused the large scatter in the sleeve friction. The repeatability of the pore pressure is about the same as the cone resistance. Poor filter saturation in the top of the profile seems to be the cause of less responsive pore pressure readings as noted for numerous other soundings at the cohesive soil sites presented herein.

Cone type 4

ONSC11A, ONC12A, ONSC13A and ONSC13B were carried out the 18th of September 2017 and Figure 6.2.4 plots the representative results. ONSC12A probably hit a neighboring borehole at approximately 19.5 m depth below grade as these tests were carried out with a center-to-center distance of approximately 0.5 m. All parameters show generally good repeatability. ONSC13B differs from the remaining tests with respect to cone resistance and pore pressure deeper than approximately 14 m depth bgl. Figure 6.2.5 illustrate similar response for ONSC14 which is the neighboring sounding. On that note, this difference is believed to be due to small variations in soil behavior.

Cone type 5

ONSC11, ONC12, ONSC13 and ONSC14 were carried out the 18th of September 2017. Figure 6.2.5 shows that ONSC14 differs from the remaining tests on cone resistance and pore pressure from about 14 m depth bgl. This is believed to be due to some small change in soil property also seen for ONSC13B (neighboring sounding). From 4 m to about 14 m depth bgl the cone resistance and pore pressure show remarkable repeatability. The sleeve friction is also interpreted as fairly repeatable.

Cone type 6

Figure 6.2.6 verifies that predrilling was carried out to 1 m bgl before testing with cone type 6. The measurements show generally good repeatability. It is believed that ONSC20 hit a neighboring borehole at around 18 m depth bgl measurements deeper than this have been excluded from representative results. The sleeve friction for ONSC20 deviates from the other tests below 12.8 m depth bgl. This may be due to hitting a small rock and changing the zero value, but the zero drift for the sleeve friction is 0. If the operators waited for some time before doing the zero reading it may have stabilized. The pore pressure is less responsive and lower for ONSC21 than the other test in depth range 4.5 m to 10.5 m. The excess pore pressure at 1 m depth bgl is consistently around 100 kPa for this cone. This value is highly unlikely considering the fact that the ground water table is located approximately 1 m bgl. It should be noted that this is the only cone in this study using a slot filter.

Cone type 7

Figure 6.2.7 presents the results of soundings with cone type 7 at Onsøy. Table 6.2-1 reveal large zero shifts for ONSC22 in both cone resistance and pore pressure and have been excluded from the representative results. It is believed that this is due to insufficient tightening of the cone before test. It seems that an offset of +86 kPa and -60 kPa makes the measurements very similar to results from ONSC23 and ONSC25. ONSC22 was carried out on the 14th of November 2017 and the air temperature was around and below 0 °C. The temperature calibration range illustrated in Figure 5.1.1 to Figure 5.1.3 was 10 to 40 °C for this cone and the cold weather may provide an explanation to the shift seen for ONSC22.

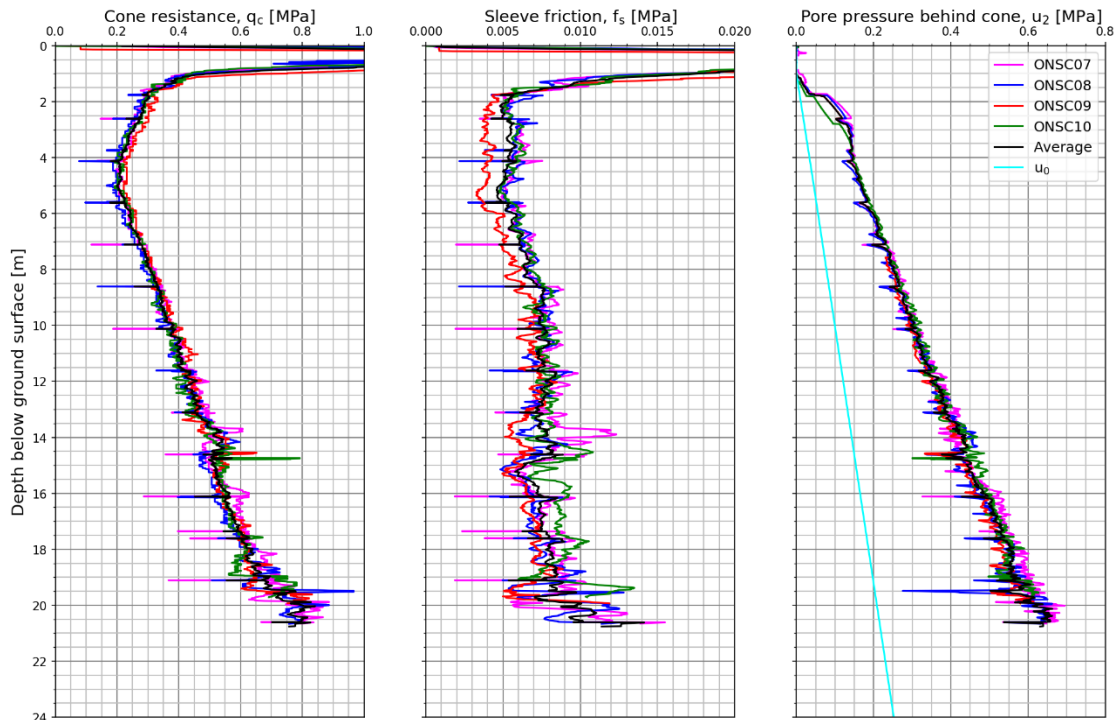
Overall note

It should be noted that soil behavior variations seem to be relatively small and contribute little to the observed scatter. Numerous tests demonstrate low filter saturation in the top of the tests. The presence of a 1 to 2 m thick dry crust seems to be the main cause of that and predrilling has a clear positive effect. Filter saturation is improved for the tests with predrilling. Cone 6 produce unlikely results close to location of ground water table. Pore pressure and cone resistance show significantly less scatter compared to the sleeve friction. The pore pressure is the most repeatable parameter at the soft clay site.

Table 6.2-1 Summary of CPTU tests with remarks – soft clay site.

Test ID	Cone Type	Zero drifts			Test date	Temp. ¹⁾	Remark
		q _c , kPa	f _s , kPa	u ₂ , kPa		°C	
ONSC07	1	16.0	0.4	2.0	2017-09-04	12	Seismic test.
ONSC08	1	21.0	0.2	3.0	2017-09-04	12	Seismic test.
ONSC09	1	27.0	0.1	5.0	2017-09-03	15	
ONSC10	1	22.0	0.2	0.4	2017-09-03	15	
ONSC11	5	-46.5	0.0	6.7	2017-09-18	15	Large zero drift q _c – included in representative profile.
ONSC11A	4	-14.2	-0.7	7.0	2017-09-18	13	
ONSC11B	3	96.4	1.5	8.7	2017-09-18	14	Large zero drift q _c – excluded from representative profile.
ONSC12	5	-27.9	0.0	4.5	2017-09-18	15	
ONSC12A	4	-19.0	-0.9	4.8	2017-09-18	15	
ONSC12B	3	14.3	0.1	13.0	2017-09-18	15	Large zero drift u ₂ – included in representative profile.
ONSC13	5	-22.4	-0.1	6.1	2017-09-18	15	
ONSC13A	4	-16.3	-0.8	5.5	2017-09-18	15	
ONSC13B	4	-17.7	0.9	5.1	2017-09-18	15	
ONSC14	5	-19.9	-0.1	3.7	2017-09-18	15	
ONSC19	6	2.0	0.5	5.2	2017-11-13	0	
ONSC20	6	-6.0	0.0	7.2	2017-11-13	0	
ONSC21	6	-10.0	0.0	1.3	2017-11-13	0	
ONSC22	7	-64.5	-0.5	55.3	2017-11-14	0	Large zero drifts q _c and u ₂ – excluded from representative profile.
ONSC23	7	9.9	-0.5	-6.4	2017-11-13	0	Seismic test.
ONSC25	7	30.8	-0.9	-5.5	2017-11-14	0	
ONSC26	2	-6.7	0.5	1.3	2017-11-17	6	
ONSC27	2	-19.6	0.3	-2.4	2017-11-17	6	
ONSC28	2	NA	NA	NA	2017-11-17	6	No zero readings.

¹⁾ Representative air temperature used to correct measured results



Cone type 1

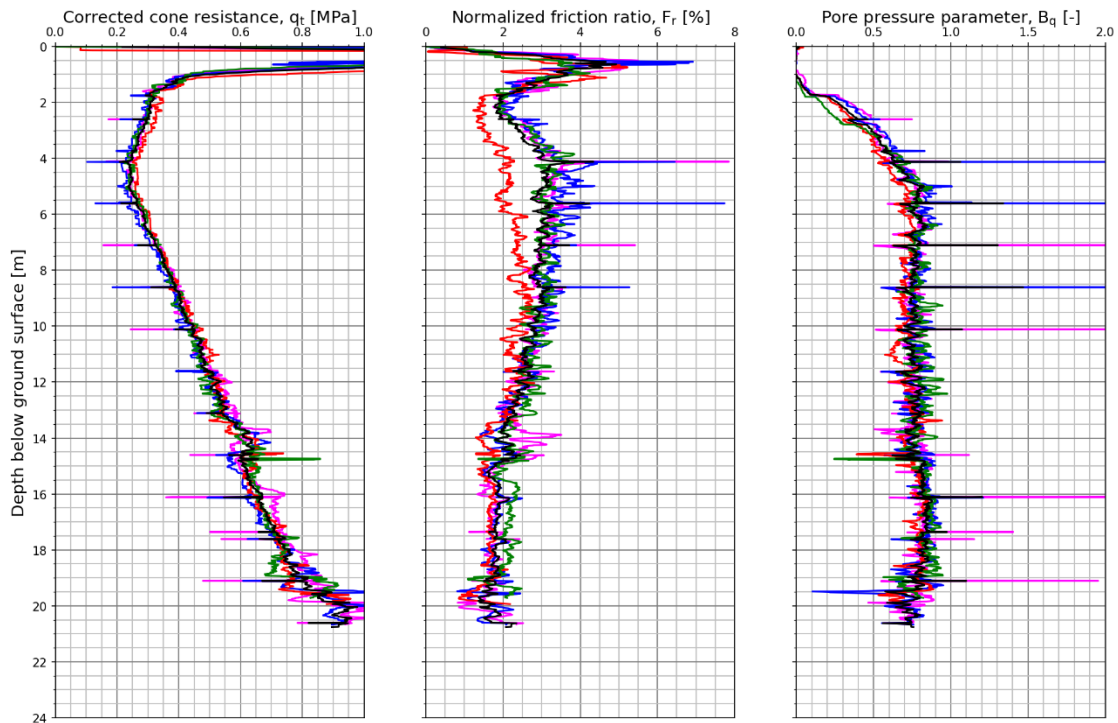


Figure 6.2.1 Measured and derived CPTU parameters. Cone type 1. NGTS soft clay site.

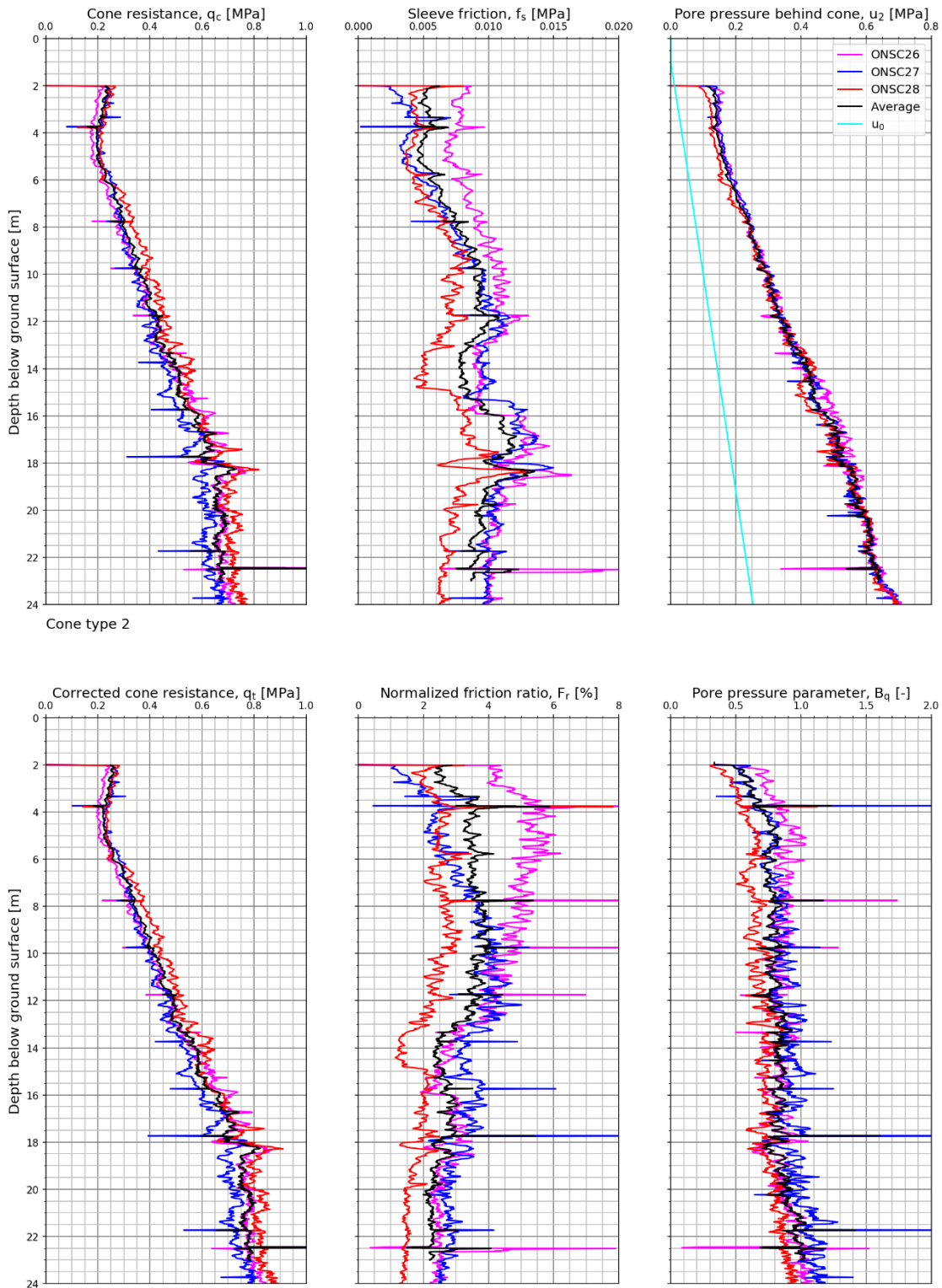


Figure 6.2.2 Measured and derived CPTU parameters. Cone type 2. NGTS soft clay site.

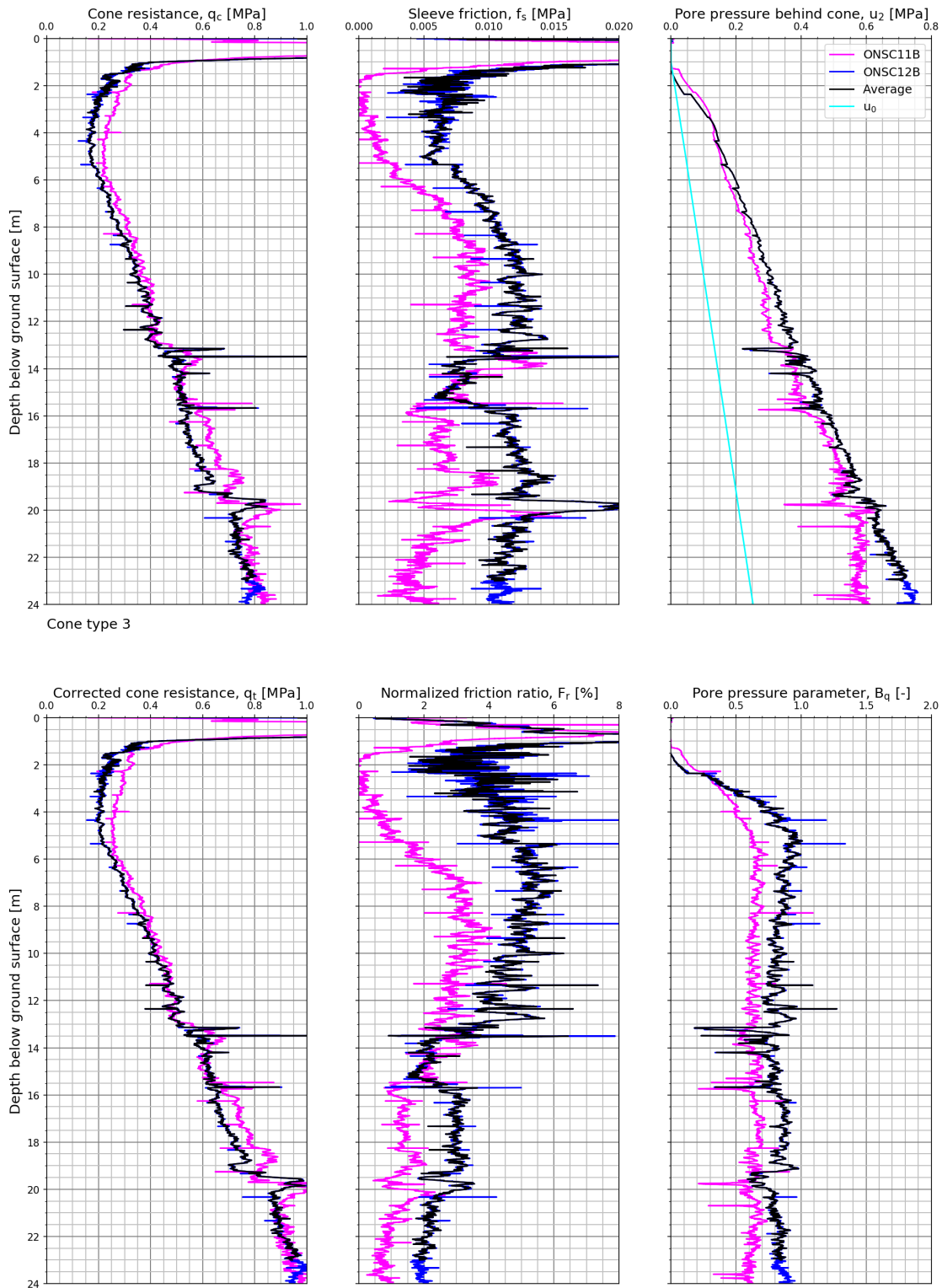
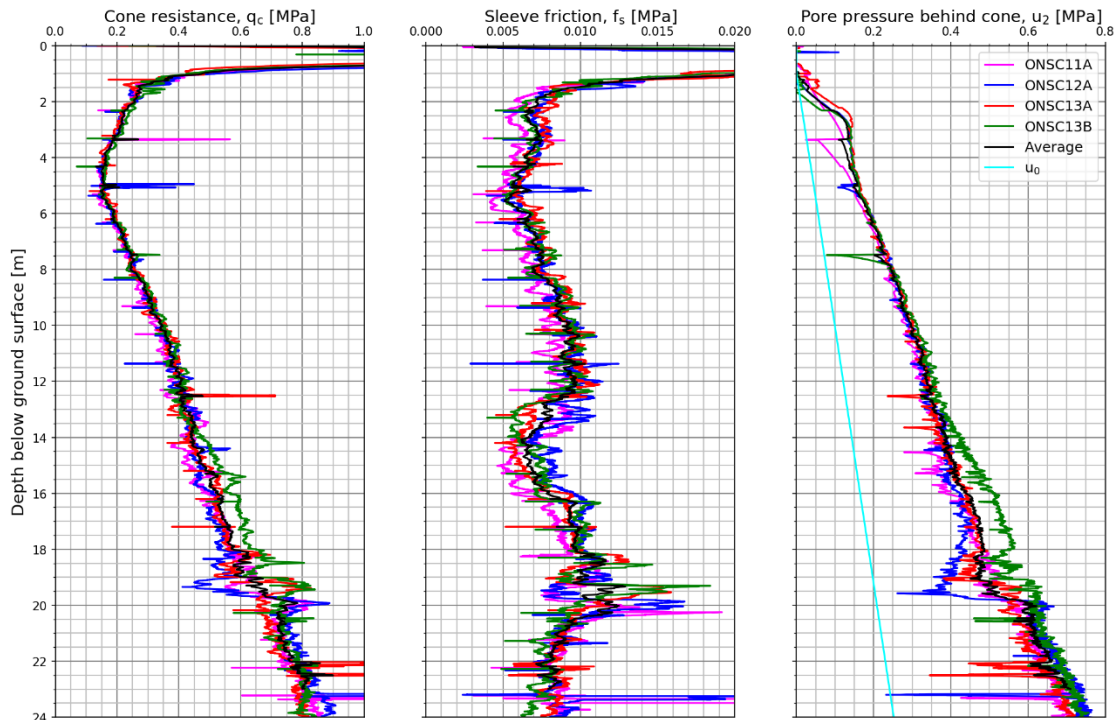


Figure 6.2.3 Measured and derived CPTU parameters. Cone type 3. NGTS soft clay site.



Cone type 4

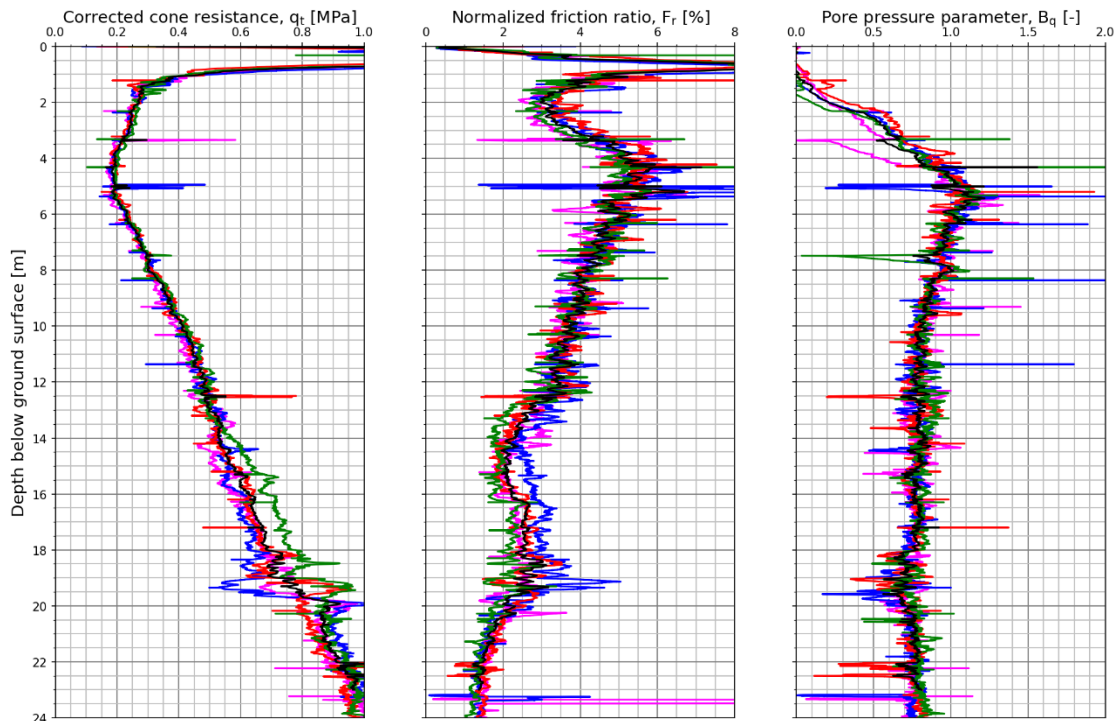
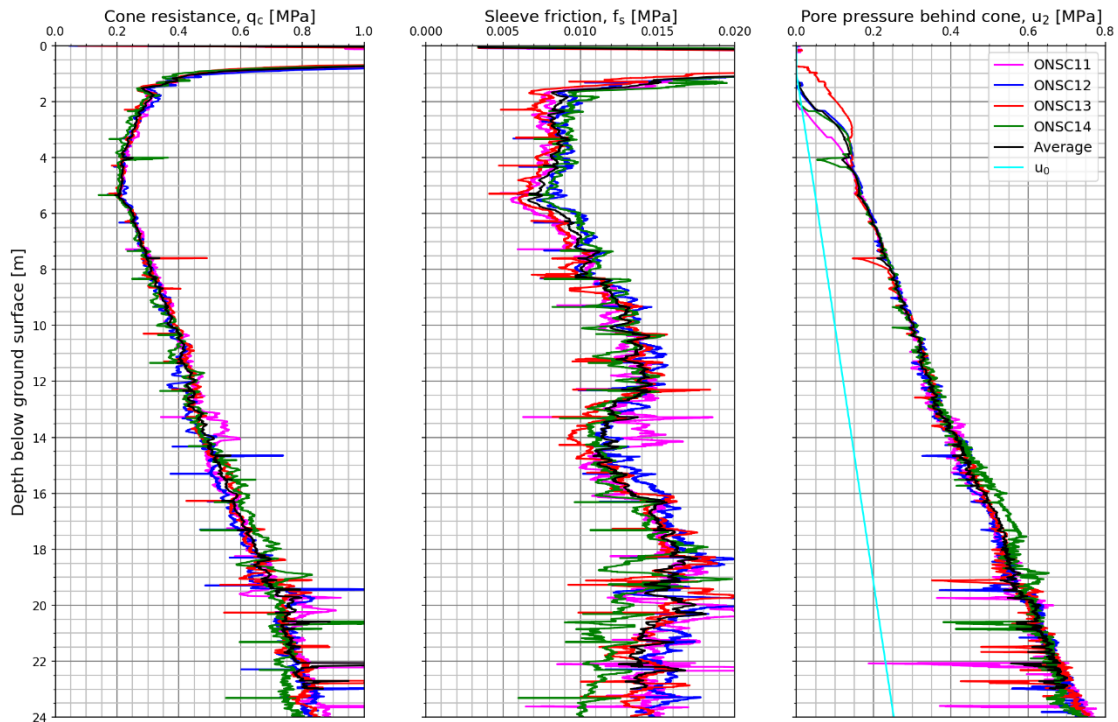


Figure 6.2.4 Measured and derived CPTU parameters. Cone type 4. NGTS soft clay site.



Cone type 5

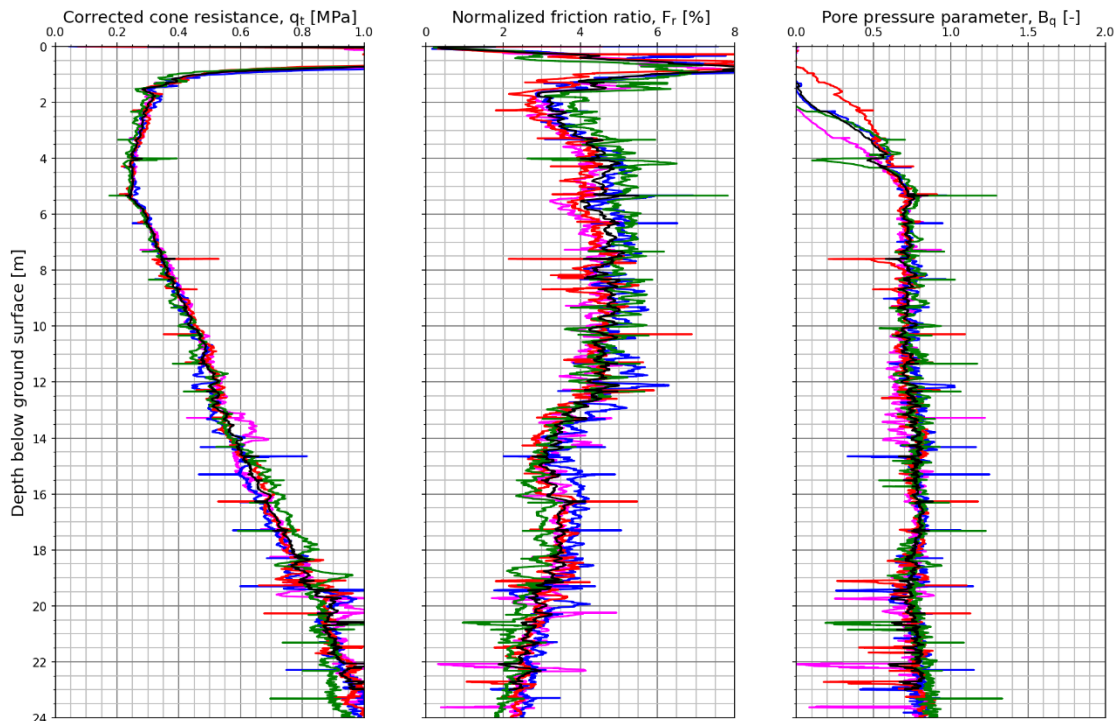
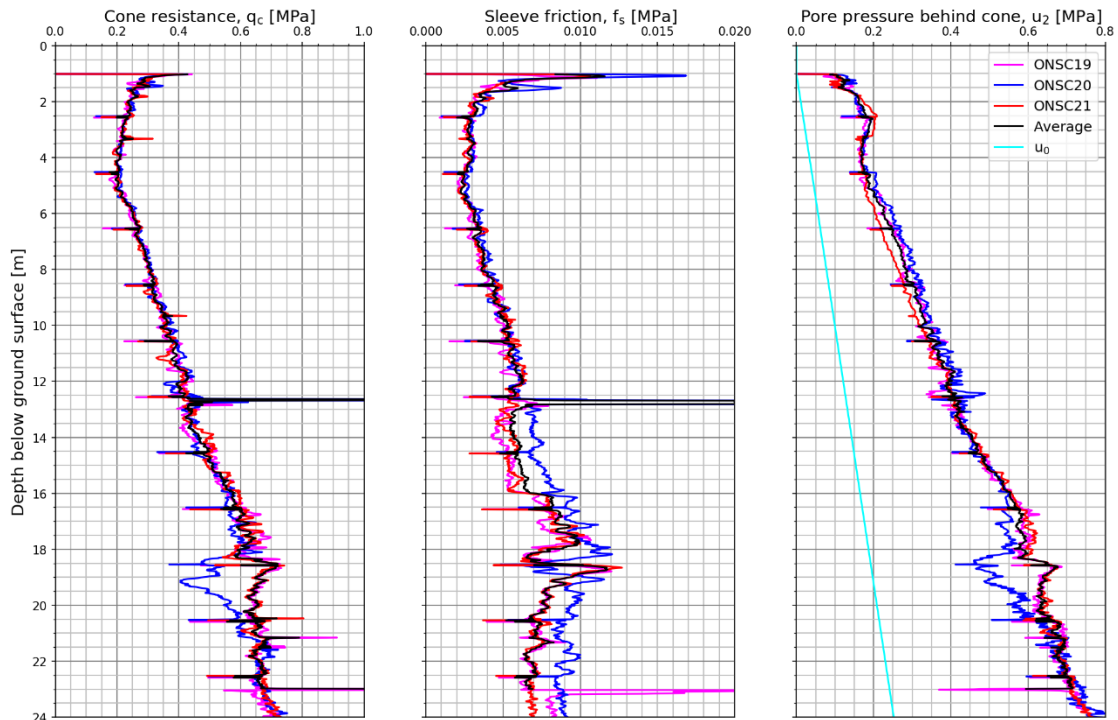


Figure 6.2.5 Measured and derived CPTU parameters. Cone type 5. NGTS soft clay site.



Cone type 6

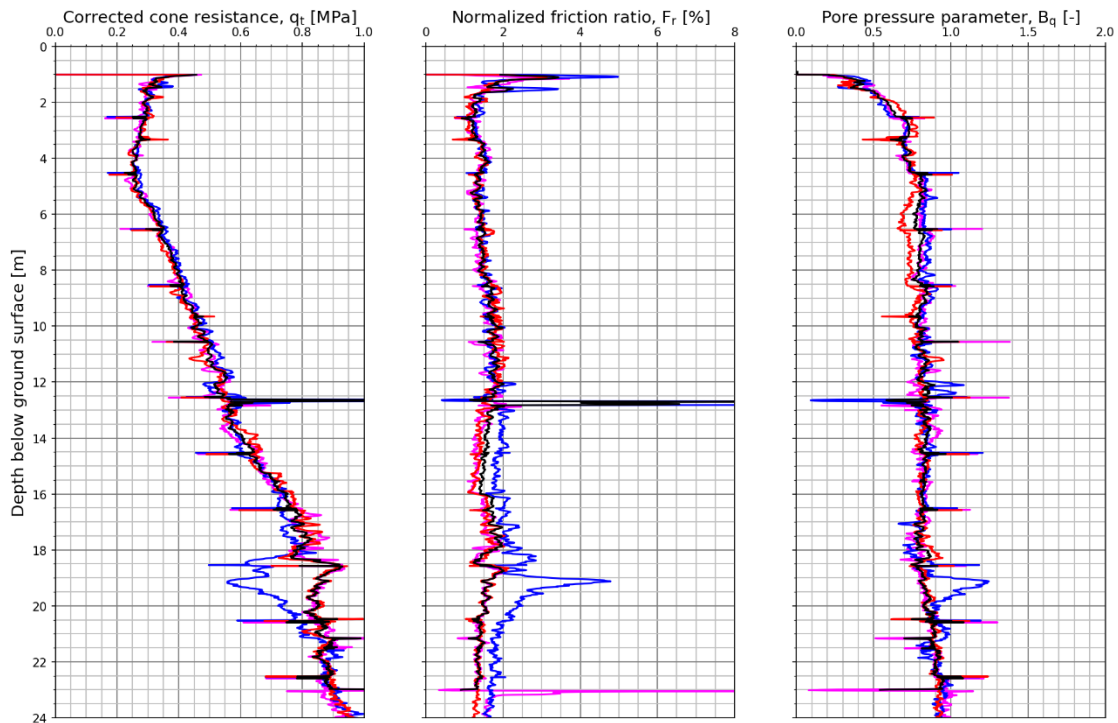
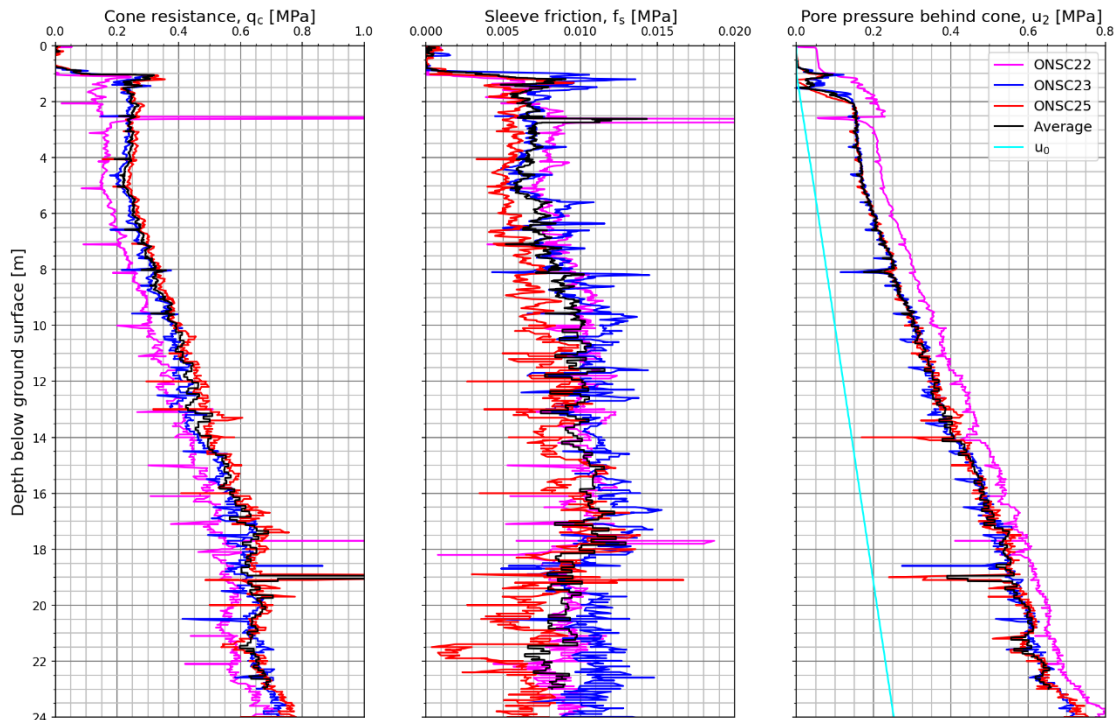


Figure 6.2.6 Measured and derived CPTU parameters. Cone type 6. NGTS soft clay site.



Cone type 7

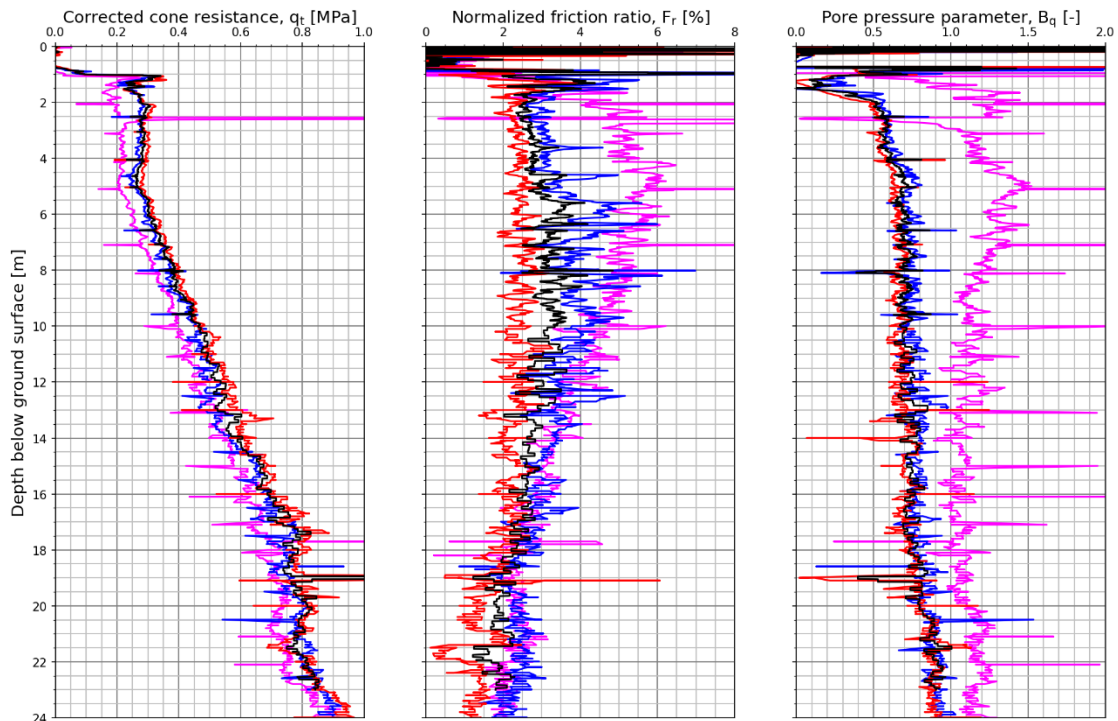


Figure 6.2.7 Measured and derived CPTU parameters. Cone type 7. NGTS soft clay site.

6.3 Silt site – Halden

Figure 6.3.1 to Figure 6.3.5 provide measured and derived CPTU parameters for the 5 cone penetrometer types studied at the Halden silt site and interpreted representative average profiles. The representative average profiles for all cones studied at this site are illustrated in Figure 7.2.1.

At the silt site, a range of different tests have been combined with the standard cone penetration test. The portfolio of tests includes seismic tests, resistivity tests, pore pressure dissipation tests and tests with variable rate. The aim of this study is to quantify the influence of cone type on the standard CPTU parameters and hence, the effect of dissipation tests and variable rate has been excluded from representative profiles herein. Table 6.3-1 summarises the cone penetration testing at the silt site including remarks on corrections etc. The characteristic soil depth range is from 6 m to 15.5 m depth bgl. The evaluations presented herein are based on results in this depth range.

Cone type 1

HALC12 to HALC14 were carried out the 5th and 6th of September 2017. The measurements show good repeatability. Pore pressure dissipation tests and seismic tests were carried out at specific depths for HALC13 and HALC14. The depths at which the dissipation tests were carried out is evident from the pore pressure response in Figure 6.3.1. HALC14 was carried out with variable penetration rate which can be observed in the sleeve friction plot. As discussed in Section 5.2, measurements that are influenced by the additional tests (seismic, dissipation, variable rate) have been excluded from the representative profiles.

Cone type 5

Figure 6.3.2 illustrates the results with cone type 5. HALC18 to HALC20 were carried out the 19th of September 2017. The measurements show good repeatability in the depth range of interest. The pore pressure and cone resistance have less scatter than the sleeve friction. HALC18 show large zero shift for cone resistance, but that is not evident from the plotted results.

Cone type 6

Figure 6.3.3 demonstrates results for HALC10 and HALC11 which were carried out approximately 2 and 1 year before most other tests in this study respectively (see Table 6.3-1). Two different cones of same type were used. Both these tests show large q_c zero shifts. The dataset for cone type 6 is small because HALC10 has an information gap from about 13 m to 17 m depth bgl. Comparable measurements can be seen for the two tests which were carried out approximately 9.2 m apart. As planned, it was predrilled down to 2 m below ground level before starting the test. At the depth of ground water table, the pore pressure reads approximately 50 kPa. There are some variations in in-situ pore pressure, but significantly less than this value. It should be noted that pore pressure measurements with cone type 6 is significantly higher than for the other cone types.

Cone type 7

Tests with cone 7 show good repeatability for all parameters as illustrated in Figure 6.3.4. The effect of different penetration rates and dissipation testing were evident from the sleeve friction and pore pressure response and have been disregarded in representative results. Predrilling was carried out down to 1 m depth while the penetrometer started logging at ground level. The measurements above 1 m depth bgl is not representative of the material in the top 1 m strata and have been excluded from the representative results.

Cone type 9

HALC17 and HALC24 were carried out on the 22nd and 23rd of November 2017 respectively. There was a shift in temperature over night between these two days. Figure 6.3.5 illustrates the results with cone type 9. One meter predrilling was carried out. The results show little scatter, but the effect of variable rate (HALC17) and dissipation testing (both tests) is evident from the sleeve friction and pore pressure response, see for instance depth 7.5 and 10.5 m bgl. The pore pressure response shows excess pore pressure at around 1 m bgl. The ground water table was located approximately 2 m bgl, so the pore pressure response in the start of the sounding is questionable. Similar type of pore pressure response was also observed for cone type 6.

Overall note

A significant number of tests with add-on sensors to the standard cone penetrometer have been carried out at the Halden silt site. These influence the results of the standard CPTU parameters investigated herein. Most of the tests show good repeatability. The pore pressure is the parameter which produces less scatter compared to sleeve friction and cone resistance. Sleeve friction displays the most test dependent results. Cone types 6 and 9 produces some odd results for the pore pressure close to the location of the ground water table as seen also for cone type 6 at the soft clay site. The two tests with this cone type were carried out with different cones.

Table 6.3-1 Summary of CPTU tests with remarks – silt site.

Test ID	Cone Type	Zero drifts			Test date	Temp. ¹⁾	Remark
		q _c , kPa	f _s , kPa	u ₂ , kPa		°C	
HALC10	6	-120.0	-0.7	9.8	2015-10-21	7	Dissipation. Resistivity. Large zero shift, but results are considered representative.
HALC11	6	164.0	-0.8	8.2	2016-06-08	15	Large zero shift, but results are considered representative.
HALC12	1	20.8	0.2	0.5	2017-09-05	13	
HALC13	1	46.8	0.5	0.9	2017-09-05	13	Dissipation. Seismic. Large zero shifts, but results are considered representative.
HALC14	1	104.0	0.8	2.3	2017-09-06	13	Dissipation. Seismic. Variable rate. Large zero shift, but results are considered representative.
HALC17	9	-33.2	0.3	-8.3	2017-11-22	-3	Dissipation. Seismic. Variable rate.
HALC18	5	-18.1	0.0	8.7	2017-09-19	13	Dissipation. Seismic.
HALC19	5	-27.1	-0.1	-24.2	2017-09-19	13	Large zero drift u ₂ – included in representative profile.
HALC20	5	-15.0	0.1	-0.5	2017-09-19	13	Dissipation. Variable rate.
HALC21	7	20.8	-1.9	7.7	2017-12-13	-1	Seismic.
HALC22	7	-12.1	-0.4	-0.1	2017-12-12	-4	Dissipation. Seismic.
HALC23	7	55.2	0.6	-4.3	2017-12-12	-4	Dissipation. Variable rate. Large zero shifts, but included in representative profile.
HALC24	9	-8.9	0.0	7.4	2017-11-23	9	Dissipation.

¹⁾ Representative air temperature used to correct measured results

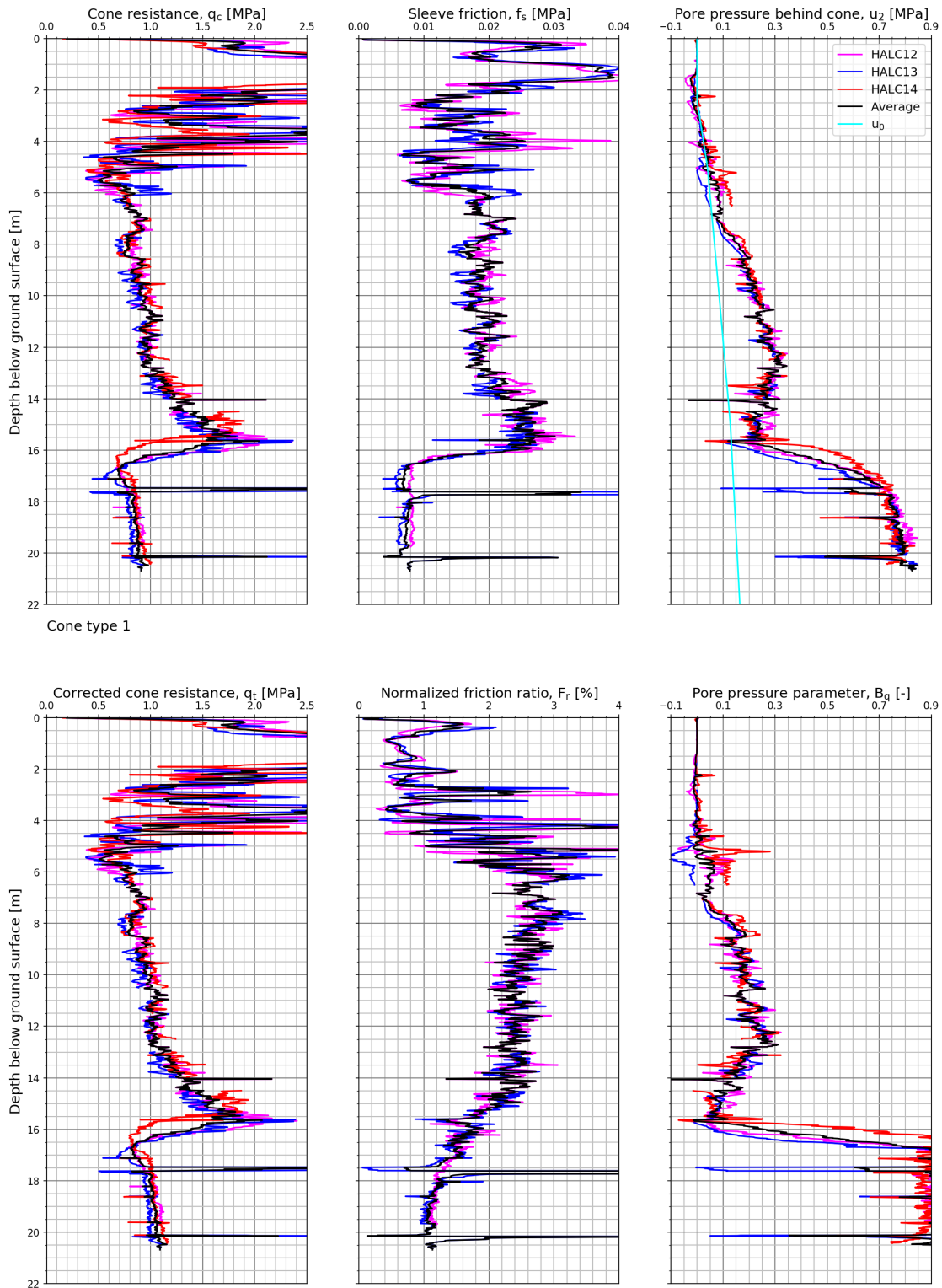
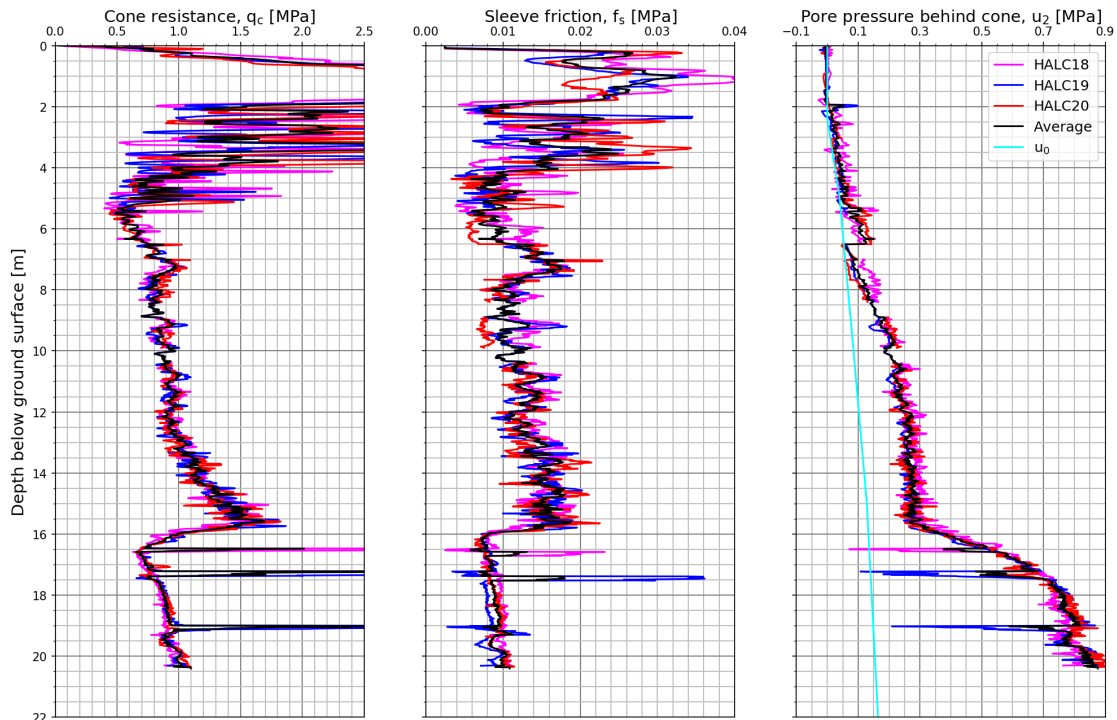


Figure 6.3.1 Measured and derived CPTU parameters. Cone type 1. NGTS silt site.



Cone type 5

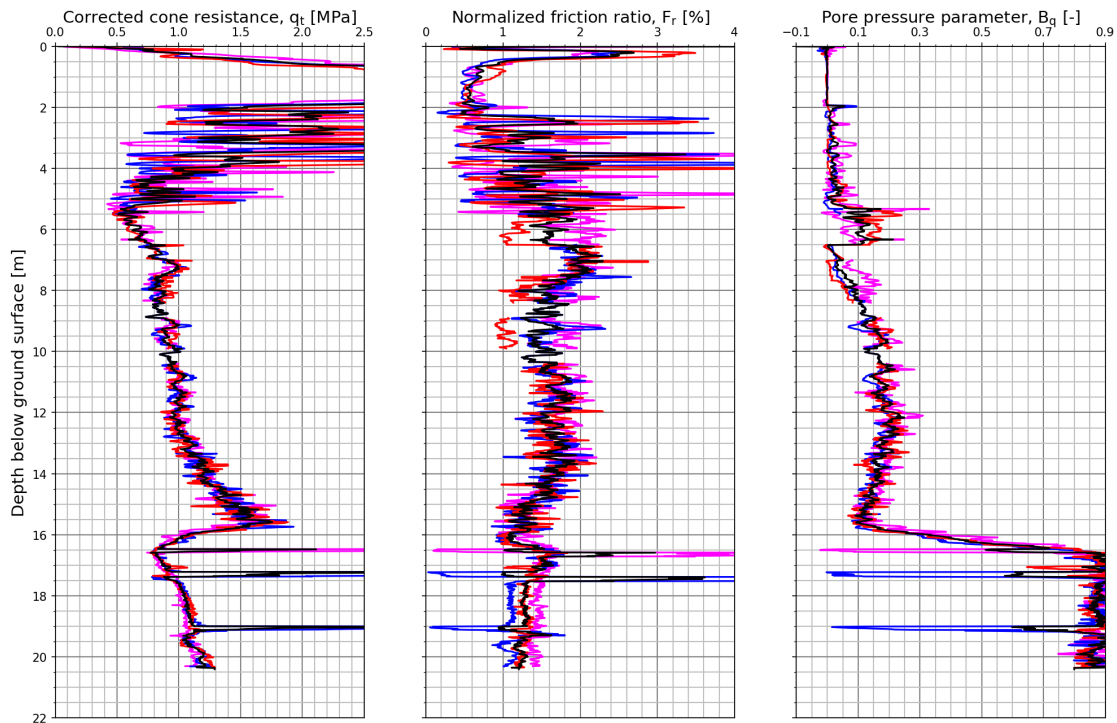


Figure 6.3.2 Measured and derived CPTU parameters. Cone type 5. NGTS silt site.

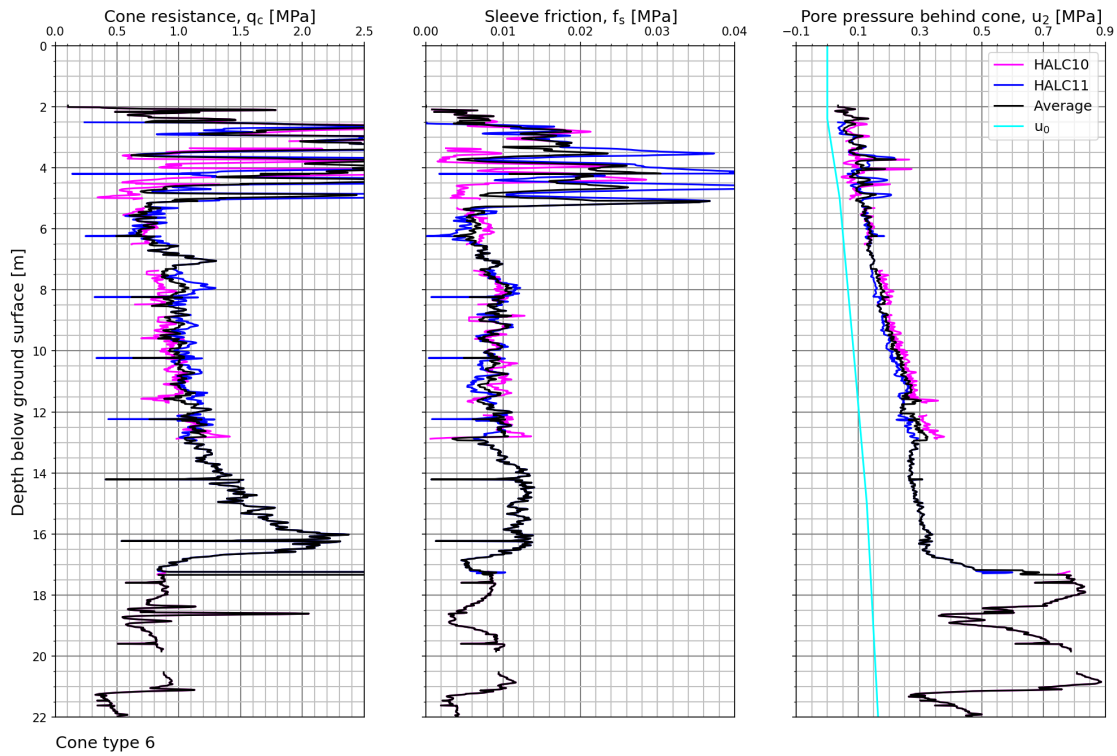
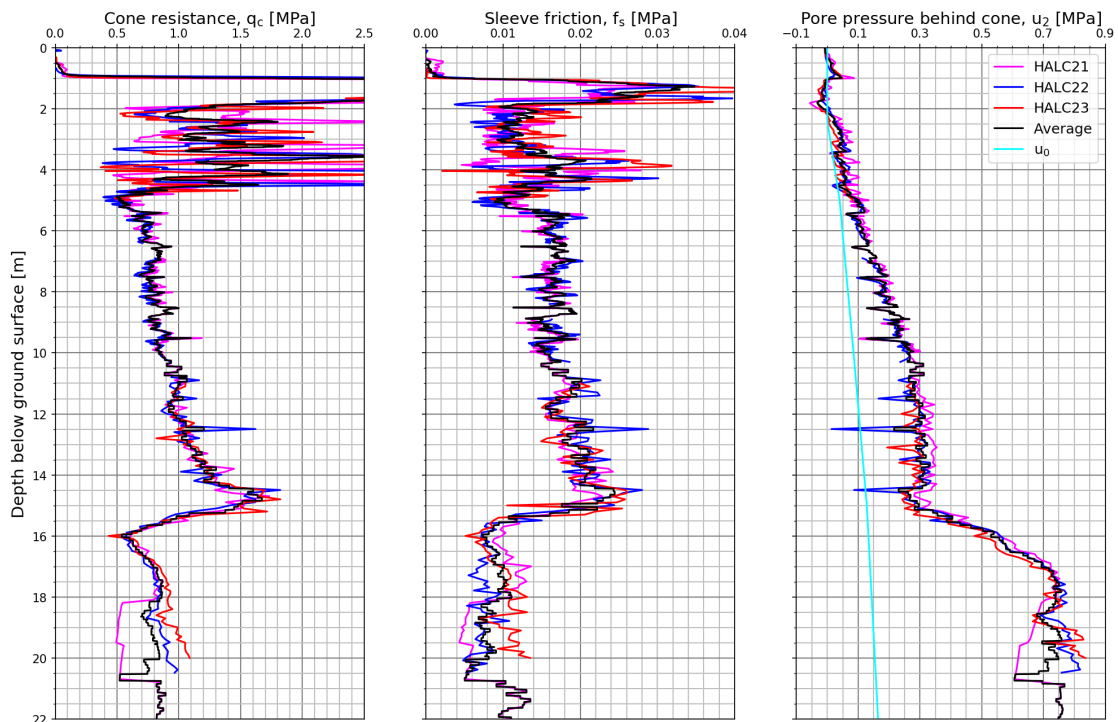


Figure 6.3.3 Measured and derived CPTU parameters. Cone type 6. NGTS silt site.



Cone type 7

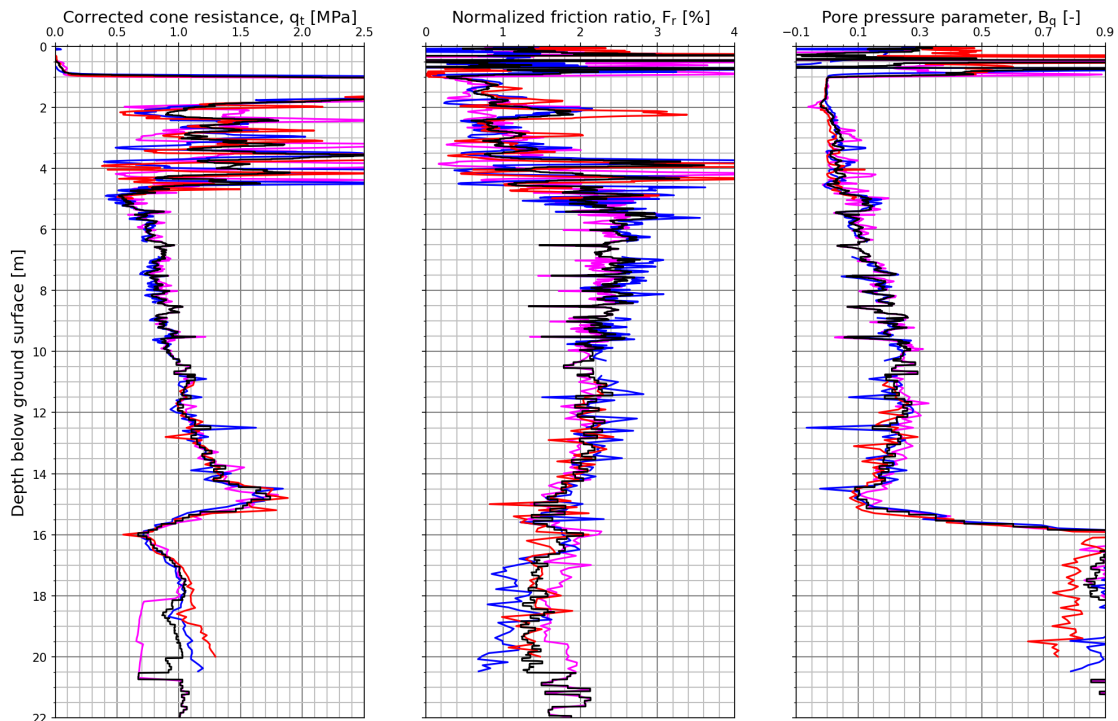
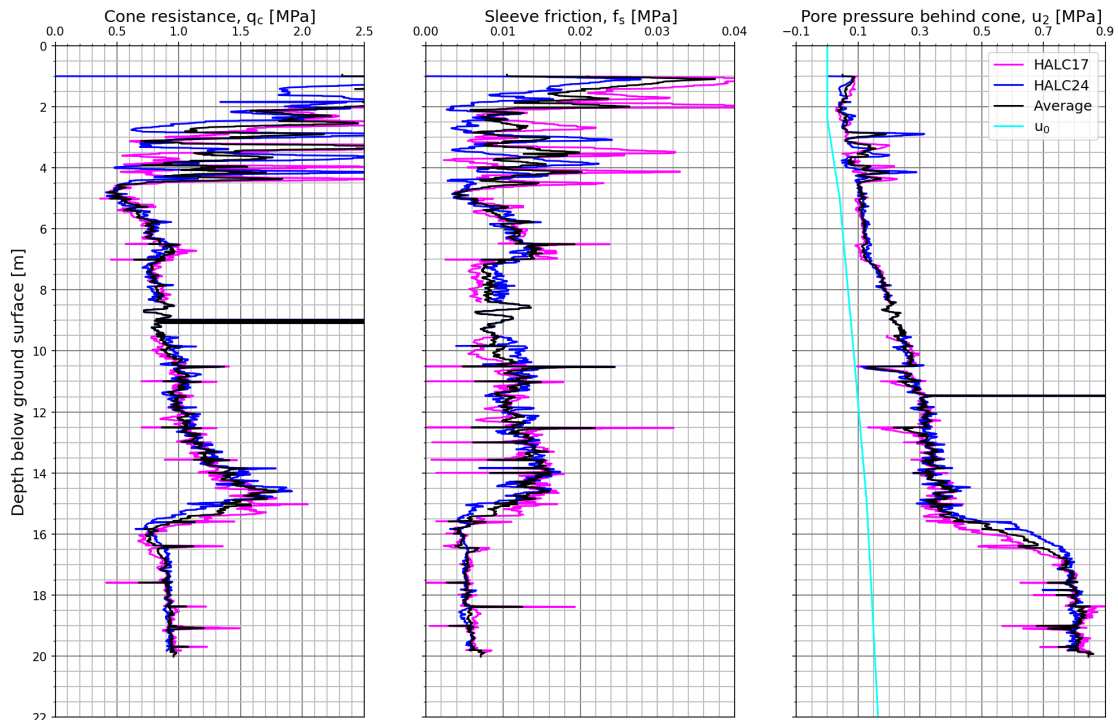


Figure 6.3.4 Measured and derived CPTU parameters. Cone type 7. NGTS silt site.



Cone type 9

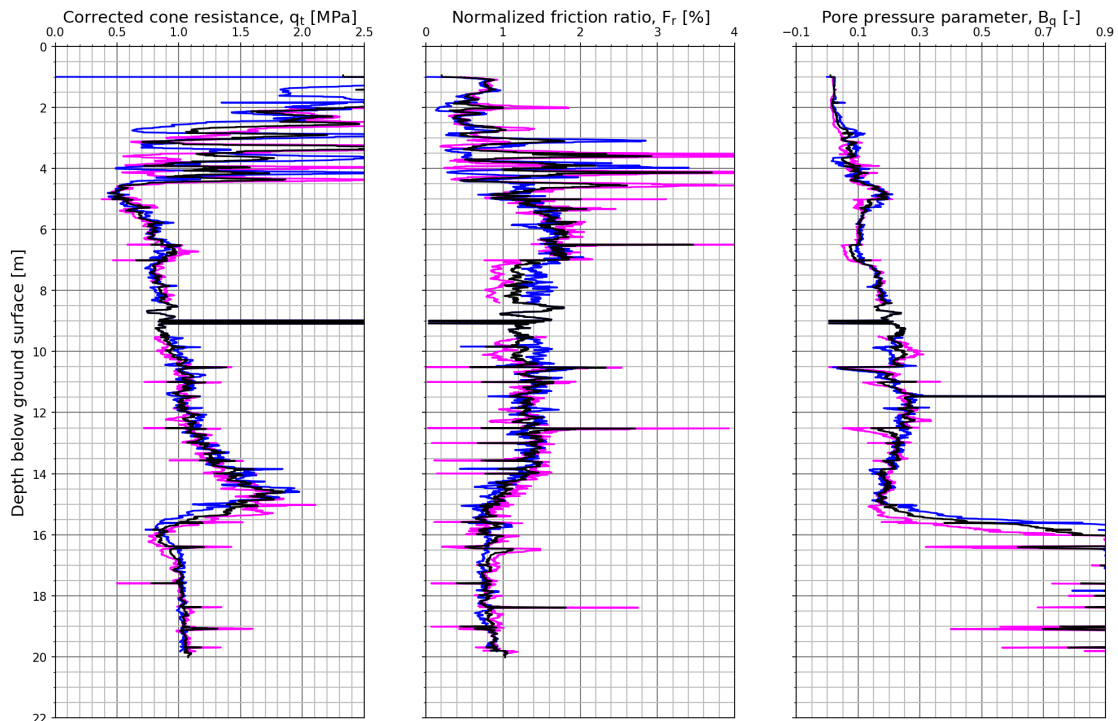


Figure 6.3.5 Measured and derived CPTU parameters. Cone type 9. NGTS silt site.

6.4 Sand site – Øysand

Figure 6.4.1 to Figure 6.4.9 present measured and derived CPTU parameters for the 9 cone penetrometer types studied at the Øysand sand site and interpreted representative average profiles. The representative average profiles for all cones studied at this site are illustrated in Figure 7.3.1.

Cone type 1

Tests with cone type 1 were carried out the 27th and 28th of September 2017 and the results are plotted in Figure 6.4.1. The tests with this cone type show relatively similar results for all measurements except for OYSC38. For this test, q_c and f_s show very different readings compared to the remaining tests in the top 6 m. It seems that predrilling was undertaken down to about 2.5 m and that the cone resistance and sleeve friction reaches the same level as remaining test at about 6 m depth. That is why the data has been taken out from the representative results presented in Figure 6.4.1.

Cone type 2

OYSC50 to OYSC52 were carried out the 31st of May 2018. Figure 6.4.2 illustrates the measured results with cone 2. It was predrilled to 6 m bgl to prevent potential break down of equipment due to the gravelly top layer. The measured parameters generally display good repeatability. The results suggest a shift in material behaviour approximately 11 m bgl. This is consistent for all measured parameters. It can be seen from Figure 4.4.1 that the three soundings with cone 2 were carried out approximately 15 m away from the rest of the tests in this study. The results suggest the presence of a denser sand mixture.

Cone type 3

The cone resistance and pore pressure compare well for cone 3 as illustrate in Figure 6.4.3. The sleeve friction from the two tests differ significantly. It has been demonstrated that sleeve friction from subtraction cones are susceptible to changes in cone resistance. From the figure, there seems to be a constant in difference between the two. Some differences in layering is evident from the figure, see for instance 15.5 m bgl.

Cone type 4

There is generally good repeatability between the two tests with cone type 4 as illustrated in Figure 6.4.4. For instance, at 14 m, a difference can be seen in all the measured parameters. This difference in response is believed to be due to local variations in soil behaviour type. OYSC32 generally represents the upper bound of the two tests with respect to measured cone resistance.

Cone type 5

The results of cone 5 are plotted in Figure 6.4.5. OYSC22, 25, 28 and 31 were carried out the 21st of September 2017. The scatter is generally low for the tests with this cone down to 13 m bgl. Below this depth OYSC31 show different results compared to the other three tests for the cone resistance and sleeve friction. A potential zero drift could

explain these results, but from Table 6.4-1 that is not the case. It seems that the pore pressure behind the cone show less scatter than the other measurements. At 17.5m bgl it can be seen from the figure that all tests suggest close to zero excess pore pressure. At this depth it seems that there is a somewhat different material than at the other depths.

Cone type 6

OYSB41A and OYSB41B have been combined into OYSB41, and OYSB42A and OYSB42B have been combined into OYSB42. The four tests with cone 6 were carried out the 28th of September 2017, and Figure 6.4.6 illustrates the results. Sleeve friction and normalised sleeve friction from test OYSC39 was excluded from representative results due to large zero shift. Results from OYSC41 show that a neighbouring borehole was hit at around 16 m depth bgl and these results have been omitted from further comparison.

Cone type 7

For this cone it was decided to predrill to 6 m bgl to prevent breakdown of equipment. The results of the soundings are illustrated in Figure 6.4.7. Seismic measurements for OYSC44 were carried out at depths every meter from 8 to 18 m bgl. The raw data show obviously erroneous measurements after seismic testing at specific depths such as 9 m bgl, 16 m bgl and 18 m bgl. The erroneous readings have been excluded from the representative profile. The q_c –profile showed variations down to 8 m bgl. It was assumed that this effect was caused by extension of the gravelly sand top layer at locations OYSC44 (to 6.7 m bgl) and 43 (to 8.5 m bgl). These results were removed from the representative results in Figure 6.4.7.

Cone type 11

The two tests with this cone type give generally similar results as illustrated in Figure 6.4.8. It is believed that the variations are mainly due to change in soil behaviour. For example, test OYSC24 at 16.5 m depth bgl both q_c and f_s decrease while the pore pressure increases.

Cone type 12

Figure 6.4.9 shows the representative results for cone type 12. Obviously erroneous measurements around 2 m bgl from test OYSC27 have been removed from representative results. The variations between the tests are believed to be mainly due to variations in the soil stratigraphy. For instance, at 16.7 m similar response is seen for OYSC21 and OYSC24 except a bit deeper. There is generally good agreement between the two tests.

Overall note

Differences in the results seem to be more dependent on the varying soil conditions for the sand site than the remaining sites studied. Thin layers of varying content of clay, silt, sand and gravel dominates the soil profile and hence the measurement results vary significantly over short depth ranges. This is expected because the sand site naturally deposited in the interface between the fiord and river Gaula. On a general note, all

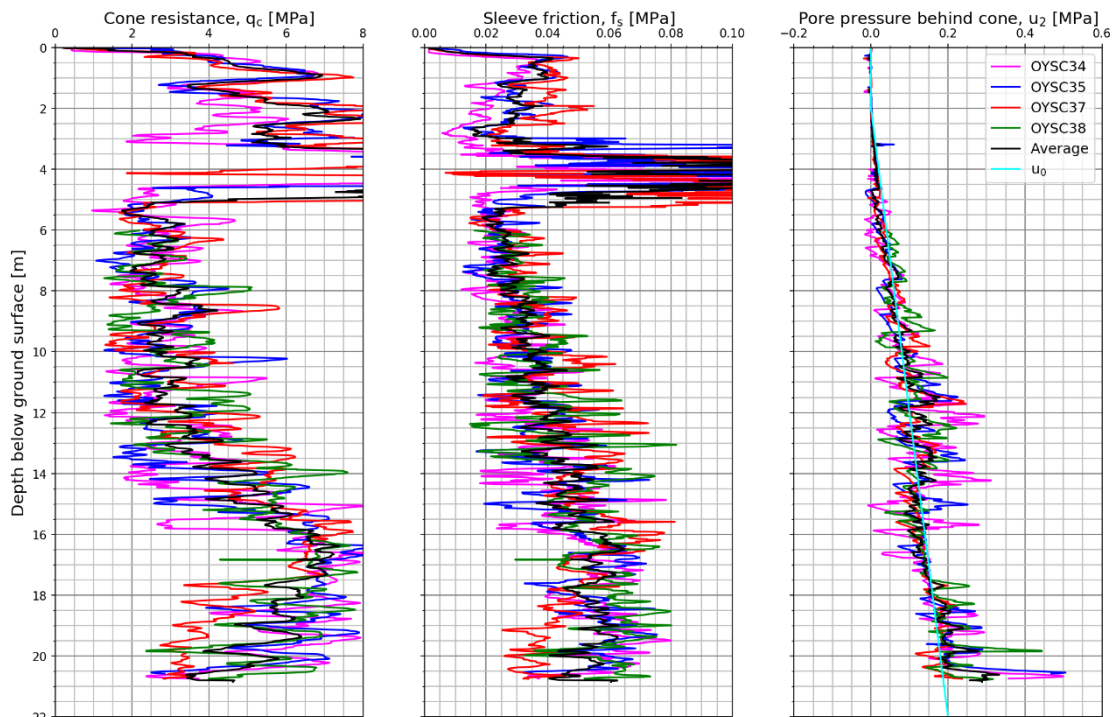
parameters compare reasonably well. The sleeve friction is as repeatable as the other two parameters. All parameters produce more scatter than for the remaining NGTS sites.

Table 6.4-1 Summary of CPTU tests with remarks – sand site.

Test ID	Cone Type	Zero drifts			Test date	Temp. ¹⁾	Remark
		q_c , kPa	f_s , kPa	u_2 , kPa		°C	
OYSC21	12	-71.4	0.2	-5.8	2017-09-21	12	
OYSC22	5	9.8	0.4	-11.1	2017-09-21	12	
OYSC23	3	5.1	-3.9	-20.2	2017-09-21	12	
OYSC24	11	-48.5	0.9	14.9	2017-09-21	12	
OYSC25	5	-44.5	0.0	-0.7	2017-09-21	12	
OYSC26	4	-28.5	-0.5	-33.2	2017-09-21	12	Large zero drift u_2 , but results are considered representative ²⁾ .
OYSC27	12	-41.6	-0.5	2.8	2017-09-21	12	
OYSC28	5	-4.5	0.0	-4.5	2017-09-21	12	
OYSC29	11	-127.3	-6.4	15.6	2017-09-21	12	Large zero drift q_c , but results are considered representative.
OYSC30	3	-19.4	-0.9	-31.1	2017-09-21	12	Large zero drift u_2 , but results are considered representative.
OYSC31	5	-21.7	-0.1	-0.9	2017-09-21	12	
OYSC32	4	-62.2	-1.1	7.5	2017-09-21	12	
OYSC34	1	5.4	0.6	0.0	2017-09-27	18	
OYSC35	1	21.7	0.1	0.2	2017-09-27	17	Seismic.
OYSC37	1	21.7	0.2	0.2	2017-09-28	18	
OYSC38	1	16.3	0.2	0.1	2017-09-28	17	
OYSC39	6	168.0	80.3	2.0	2017-09-28	17	Large zero drifts. Sleeve friction excluded from further comparison.
OYSC40	6	64.0	-1.1	-19.5	2017-09-28	17	
OYSC41	6	56.0	-0.9	-12.8	2017-09-28	17	
OYSC42	6	26.0	62.6	-23.1	2017-09-28	17	Large zero drift f_s – results above 4 m depth not included in representative profile.
OYSC43	7	6.1	0.5	-1.9	2018-05-03	10	Three result files combined.
OYSC44	7	-13.4	-1.5	0.4	2018-05-03	10	Seismic.
OYSC45	7	-20.2	0.0	13.1	2018-05-04	10	
OYSC50	2	4.2	0.3	1.0	2018-05-31	16	
OYSC51	2	-18.9	0.3	-1.0	2018-05-31	16	
OYSC52	2	-26.3	0.5	-1.1	2018-05-31	16	

¹⁾ Representative air temperature used to correct measured results

²⁾ It is assumed that the zero shift has occurred at end of test when hitting harder layer



Cone type 1

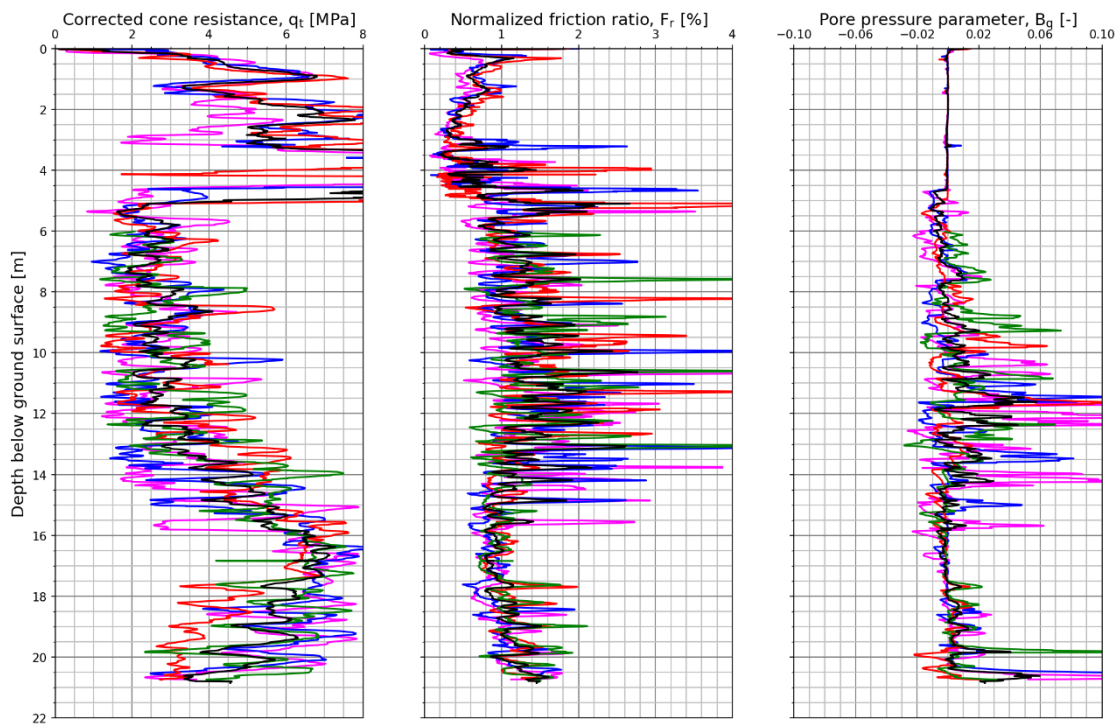
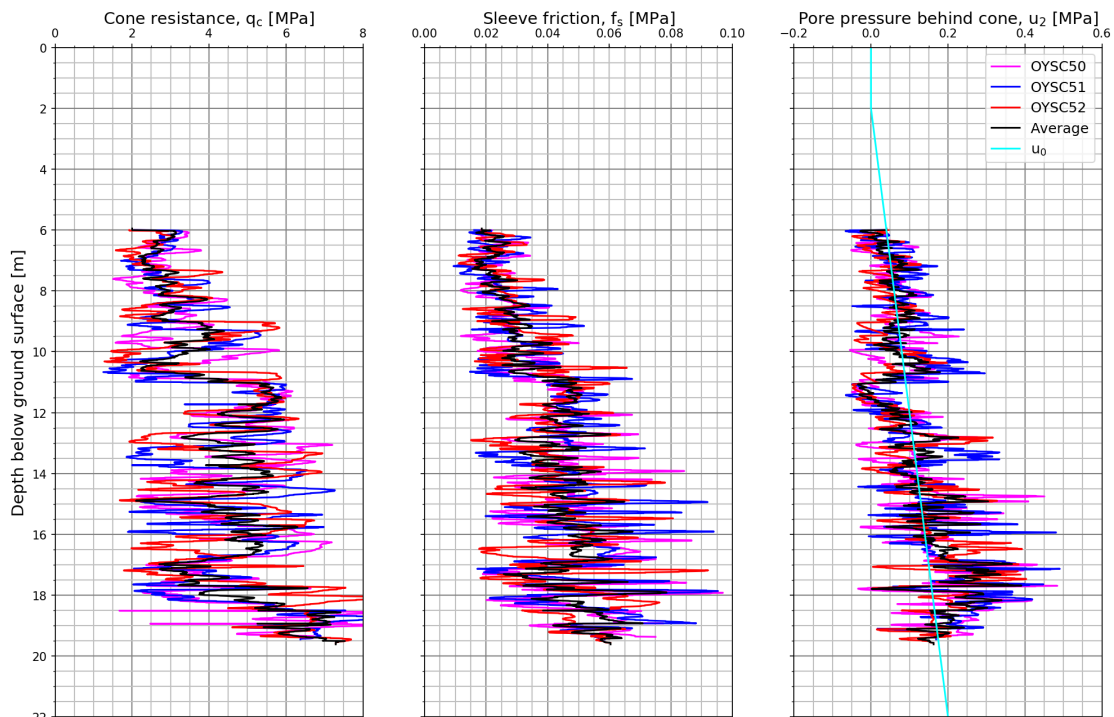


Figure 6.4.1 Measured and derived CPTU parameters. Cone type 1. NGTS sand site.



Cone type 2

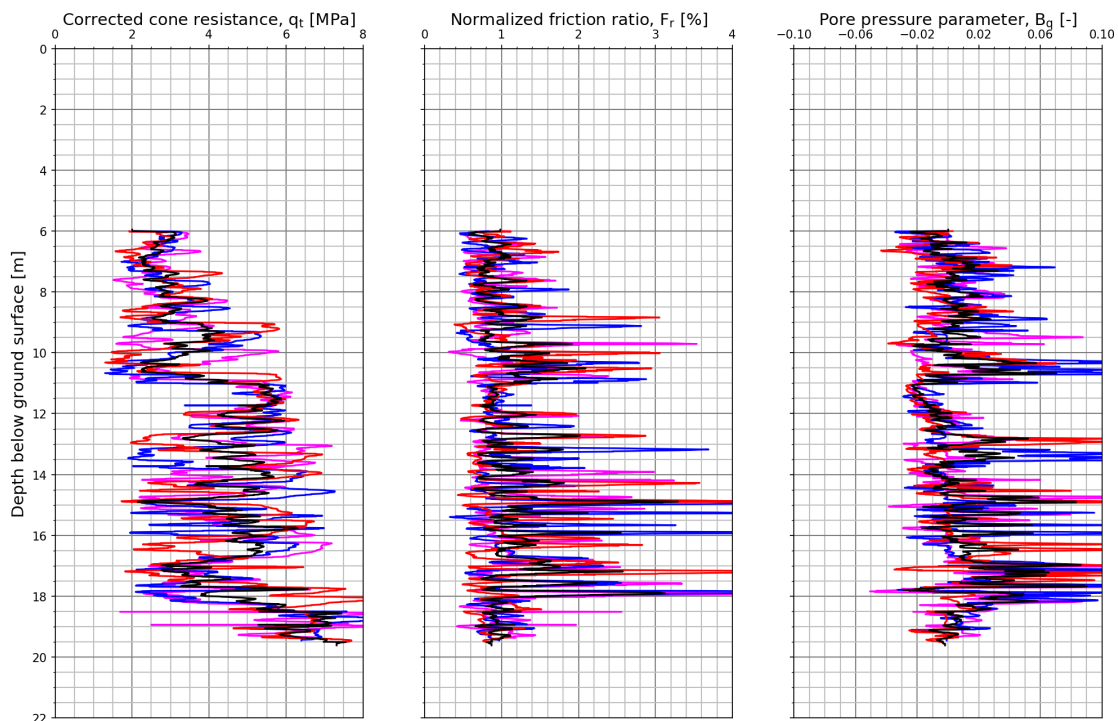
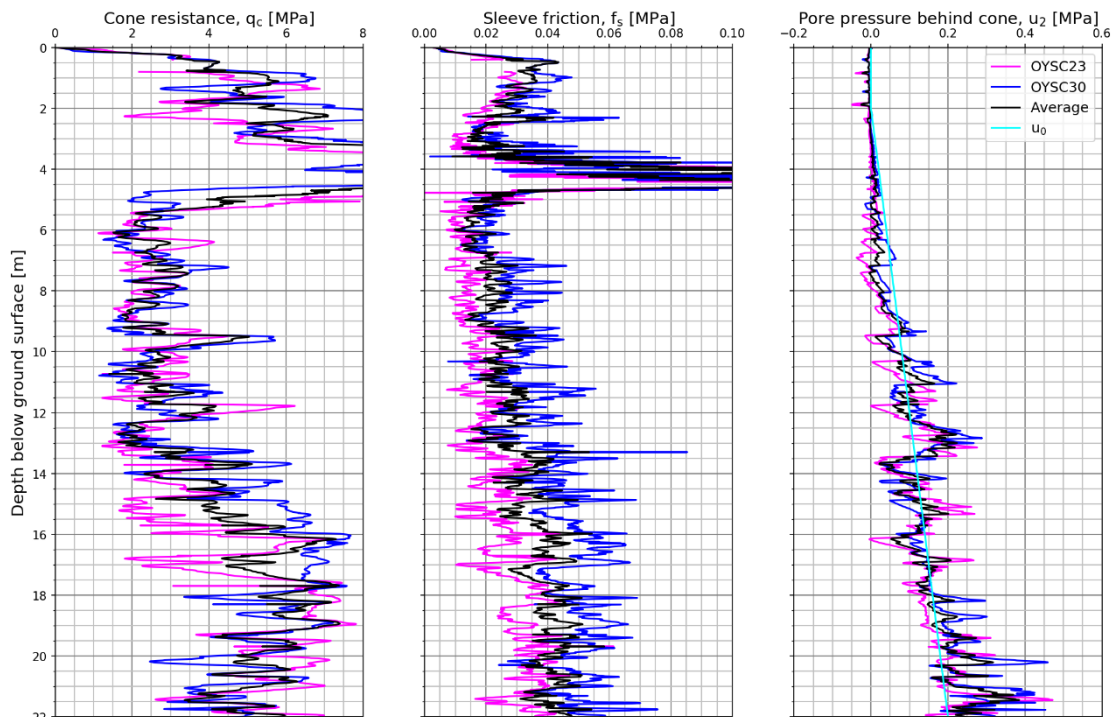


Figure 6.4.2 Measured and derived CPTU parameters. Cone type 2. NGTS sand site.



Cone type 3

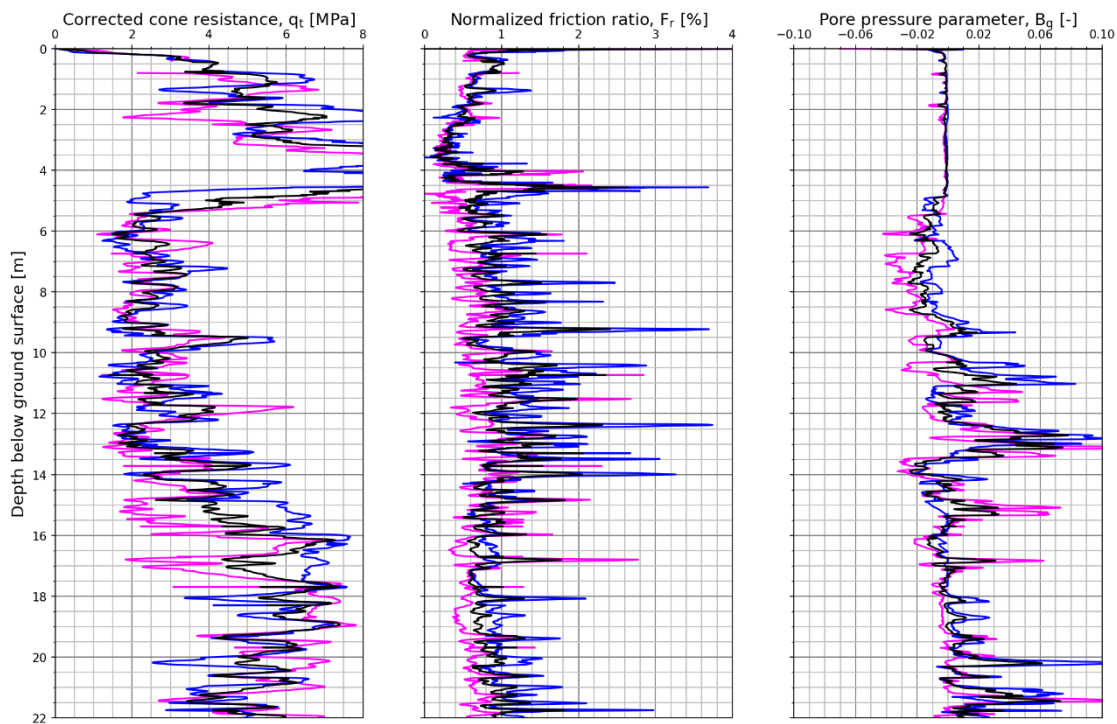


Figure 6.4.3 Measured and derived CPTU parameters. Cone type 3. NGTS sand site.

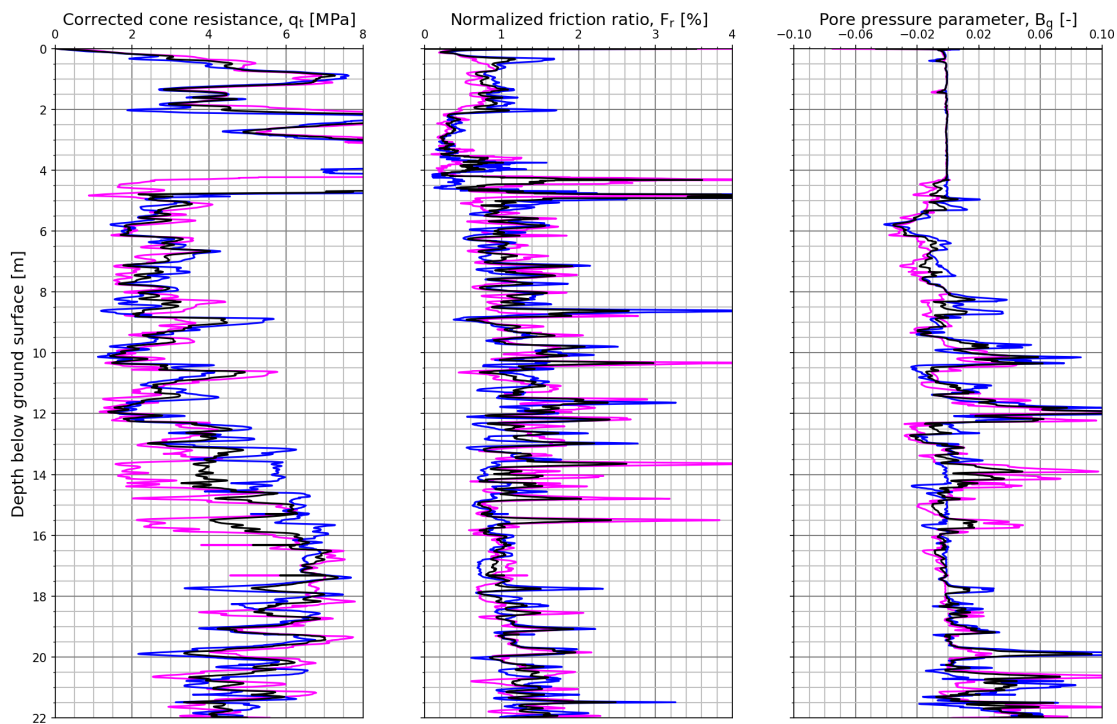
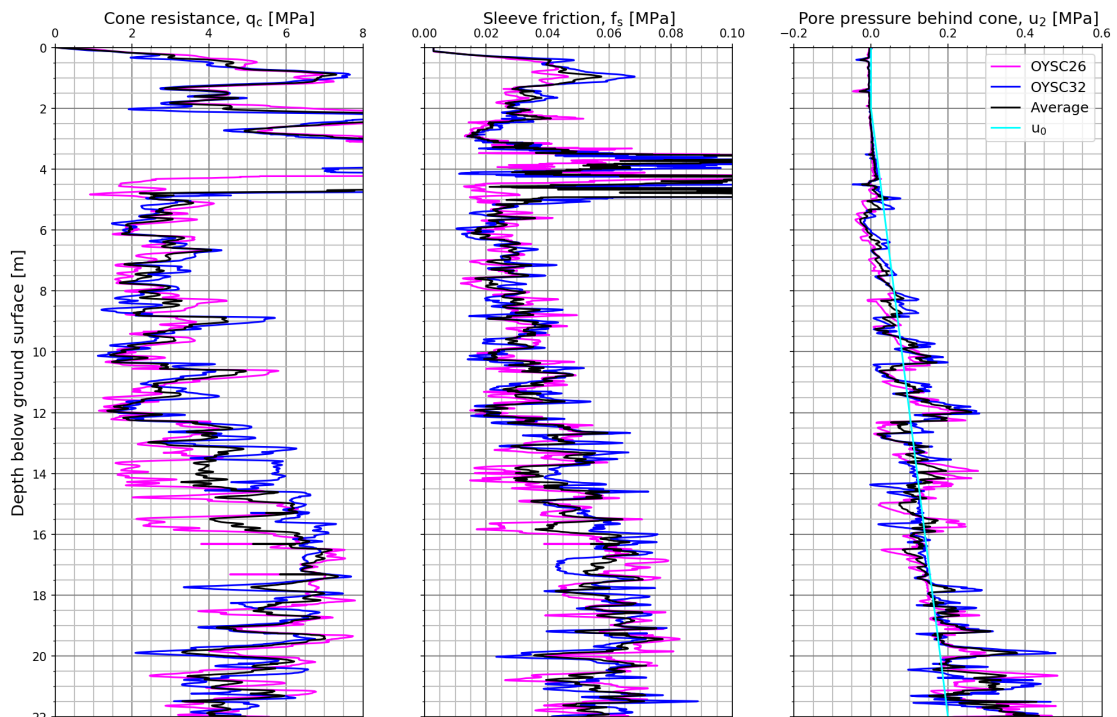


Figure 6.4.4 Measured and derived CPTU parameters. Cone type 4. NGTS sand site.

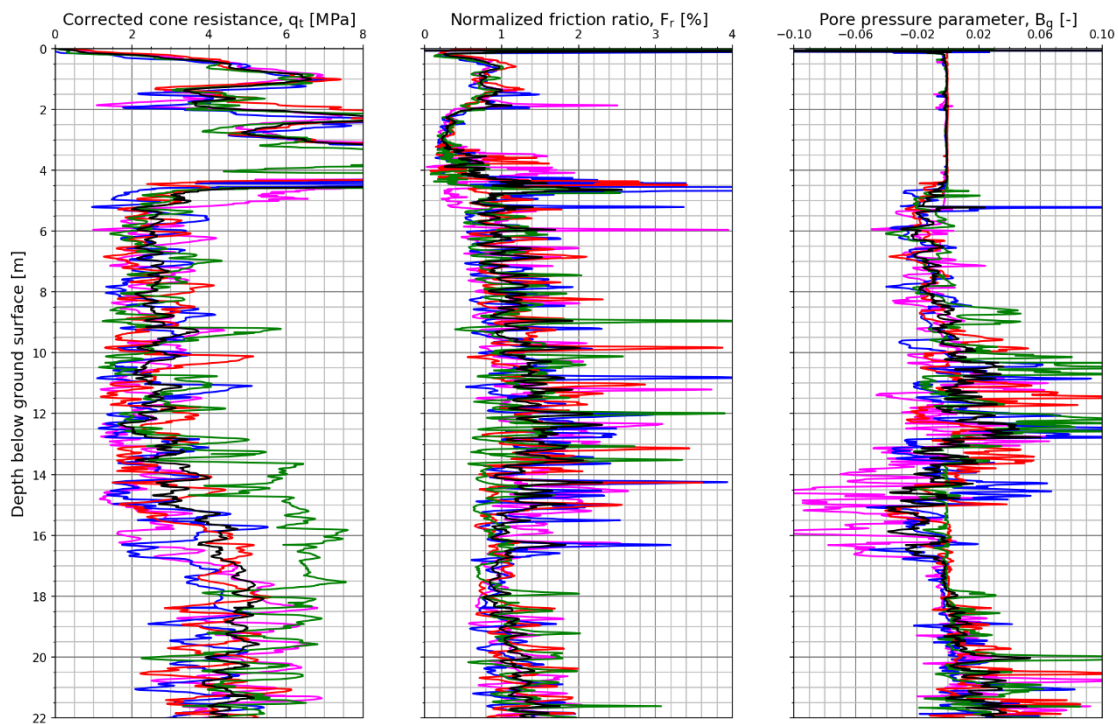
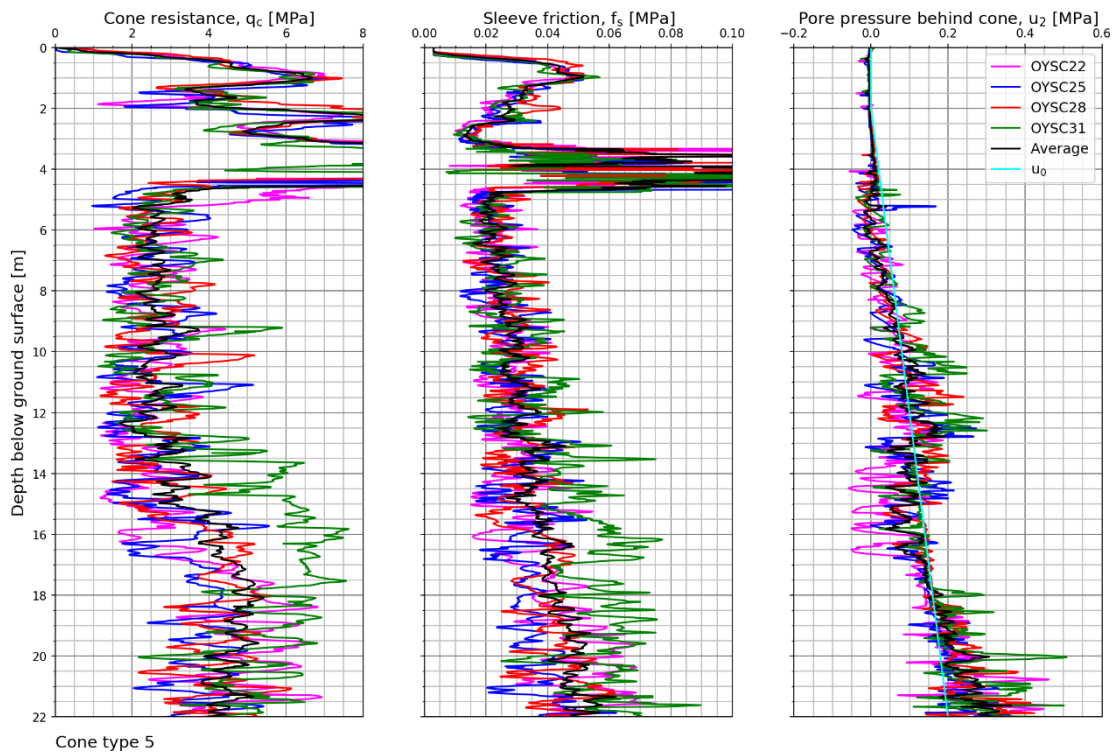


Figure 6.4.5 Measured and derived CPTU parameters. Cone type 5. NGTS sand site.

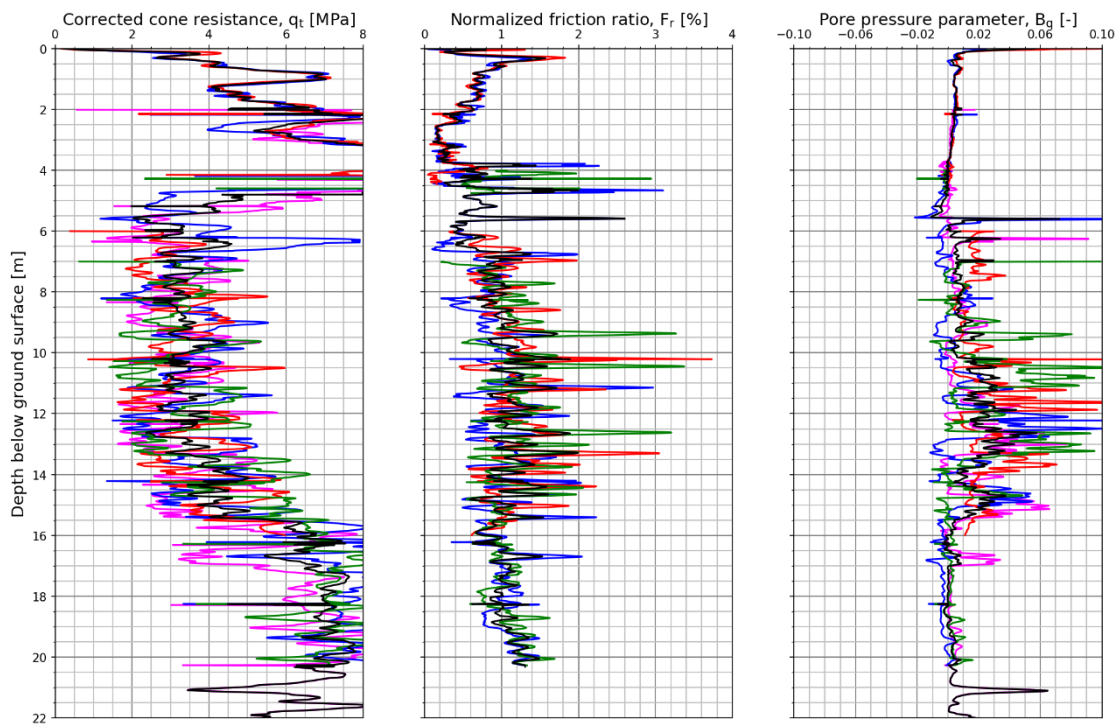
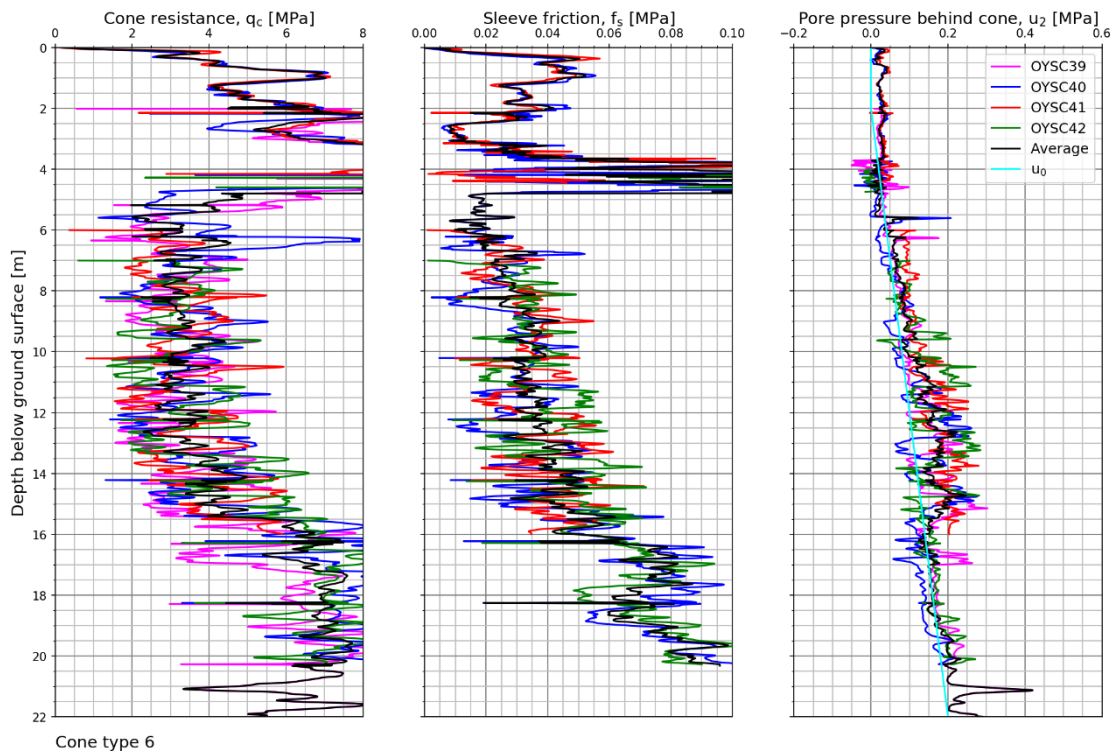


Figure 6.4.6 Measured and derived CPTU parameters. Cone type 6. NGTS sand site.

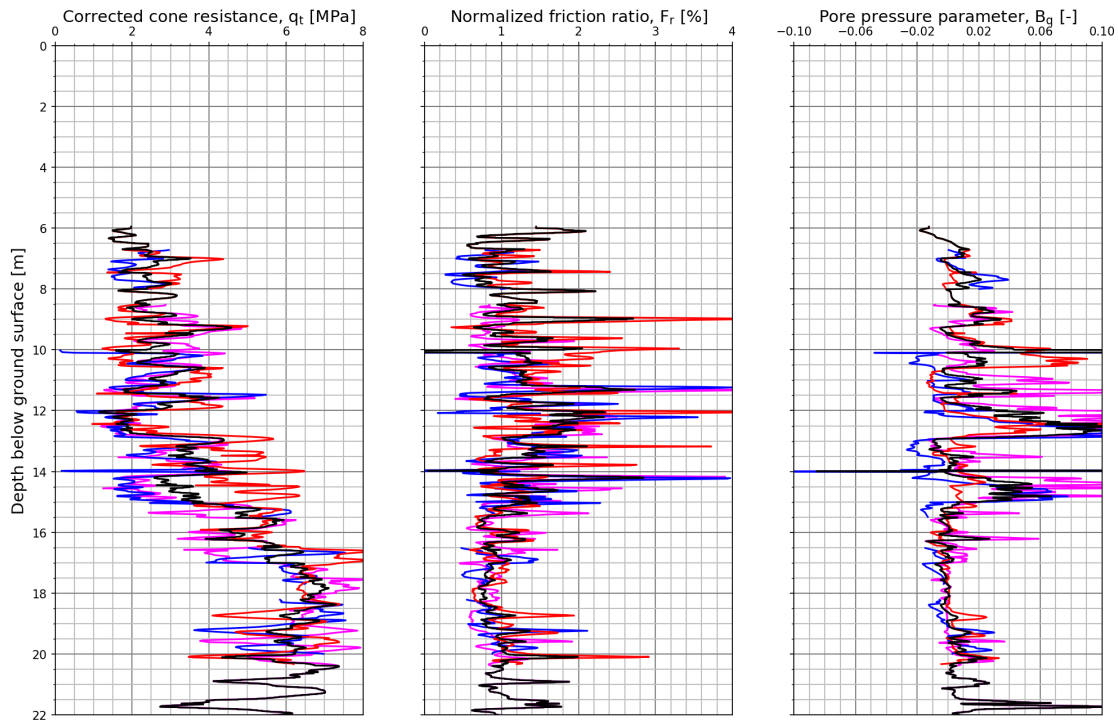
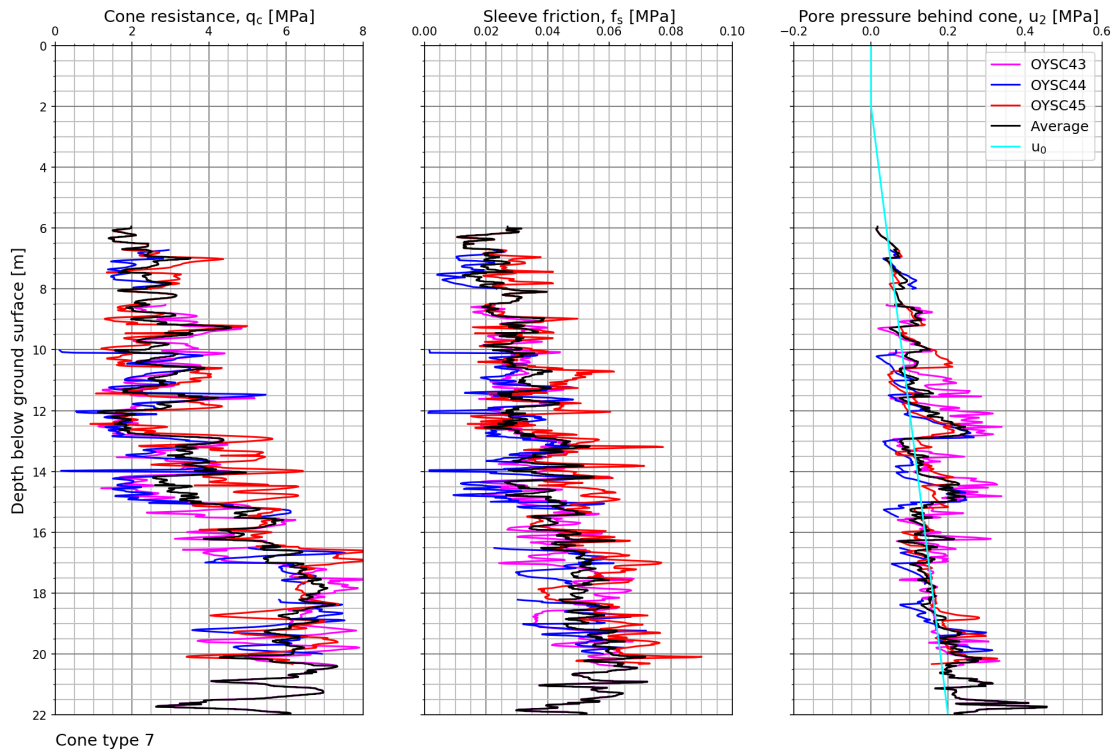
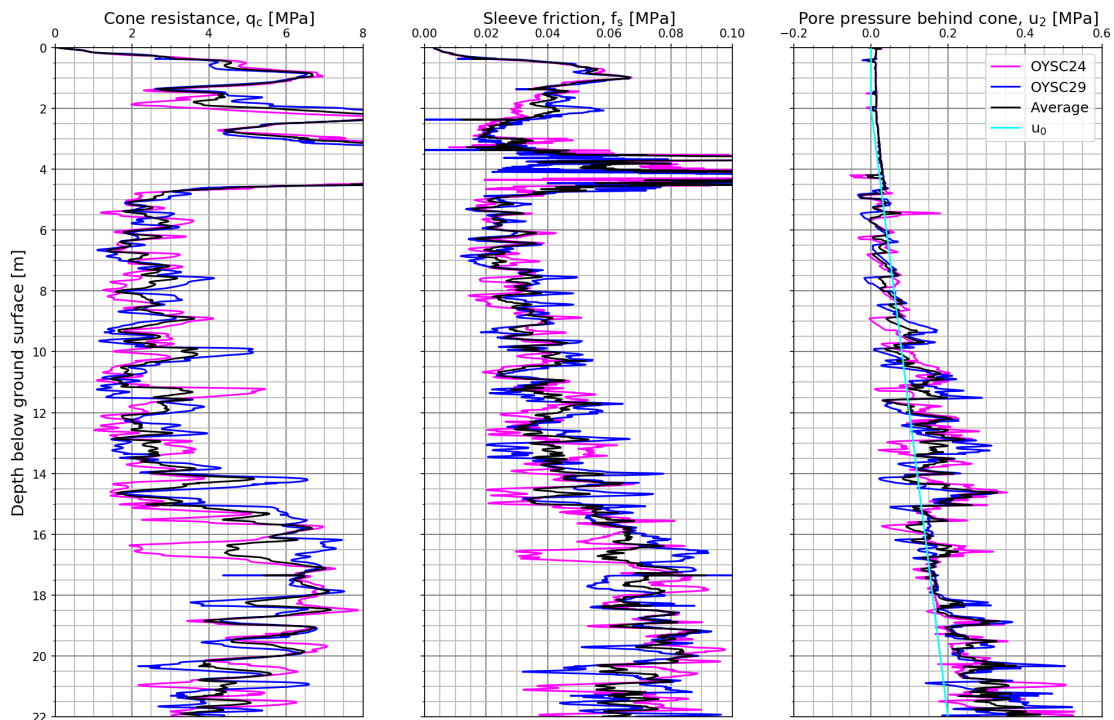


Figure 6.4.7 Measured and derived CPTU parameters. Cone type 7. NGTS sand site.



Cone type 11

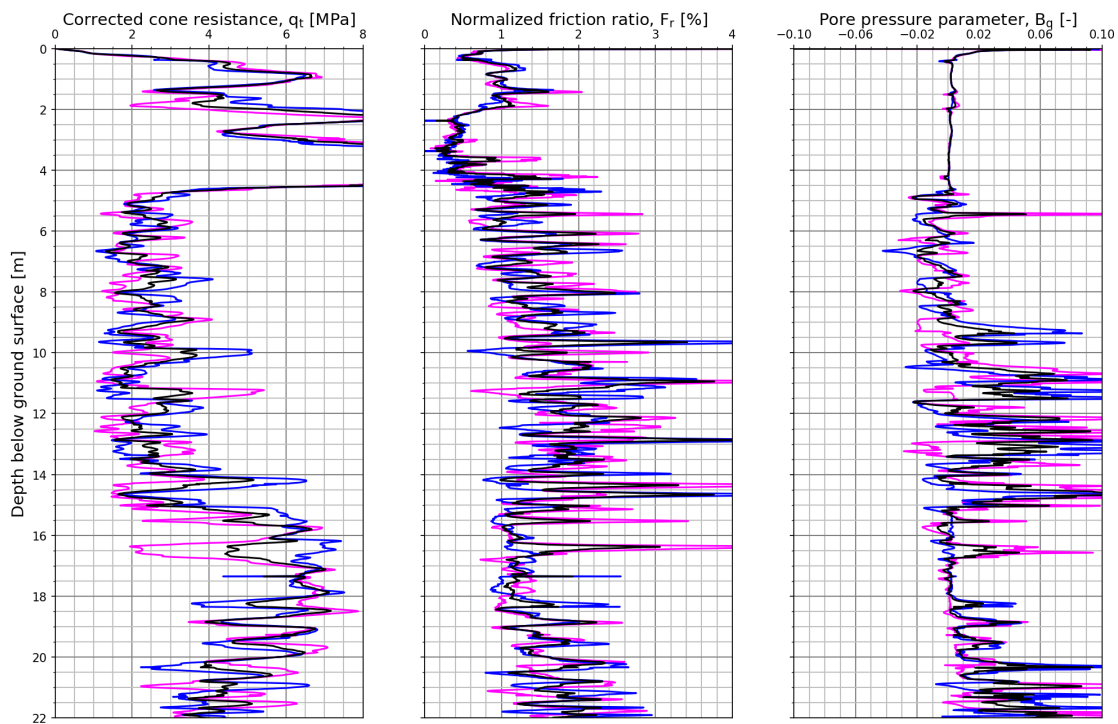


Figure 6.4.8 Measured and derived CPTU parameters. Cone type 11. NGTS sand site.

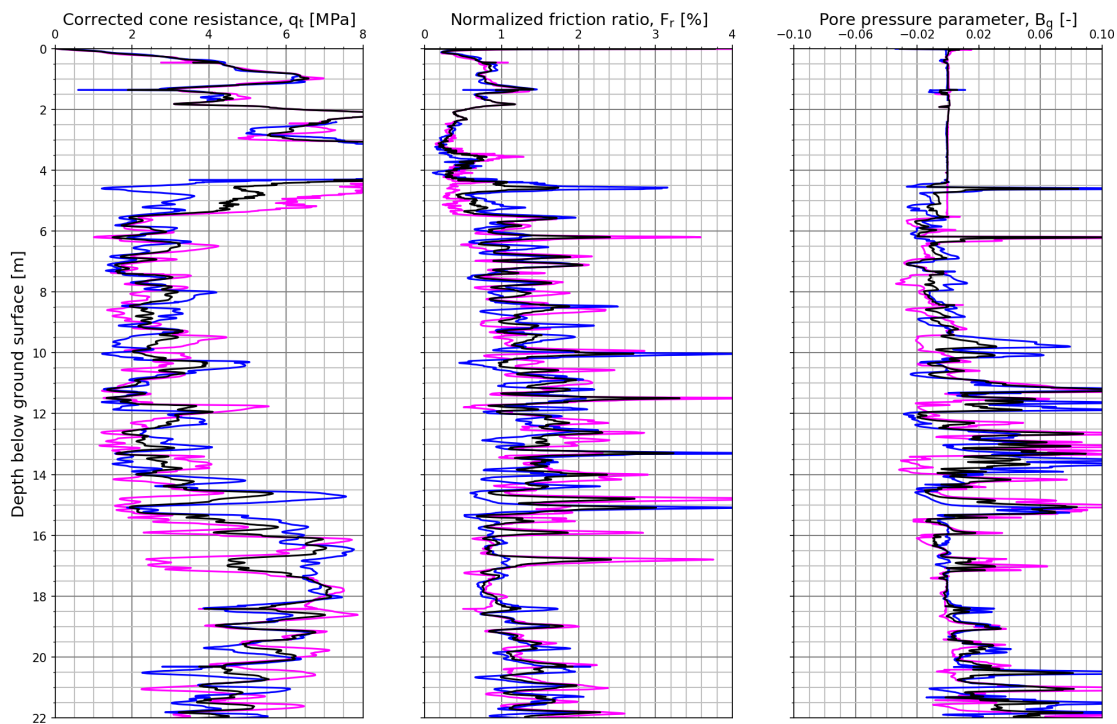
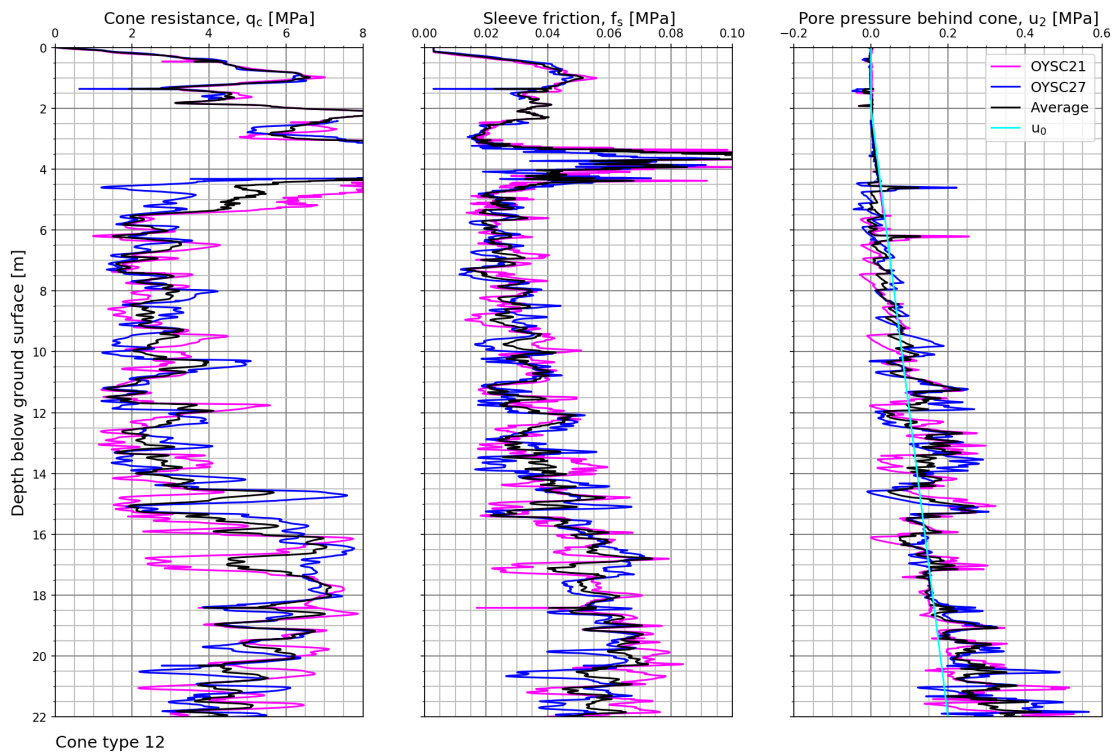


Figure 6.4.9 Measured and derived CPTU parameters. Cone type 12. NGTS sand site.

6.5 Quick clay site – Tiller-Flotten

Figure 6.5.1 to Figure 6.5.8 provide measured and derived CPTU parameters for the 8 cone penetrometer types studied at the Tiller-Flotten quick clay site and interpreted representative average profiles. The representative average profiles for all cones studied at this site are illustrated in Figure 7.4.1.

Cone type 1

The tests with cone type 1 show very good repeatability of the pore pressure measurements below 5 m depth. The cone resistance shows good repeatability except for test TILC13, which represents an upper bound to the measured results. This test illustrates the same trend with depth as the other results except with an offset. The offset seems to be around 100 kPa and the zero drift of 96 kPa can explain this difference in results. For this cone, the sleeve friction again confirms most scatter of the measured parameters. The pore pressure measurements indicate poor saturation for some of the tests down to 4 m depth.

Cone type 2

The tests with this cone show remarkably good comparison for both the cone resistance and the pore pressure, as seen in Figure 6.5.2. The scatter in the sleeve friction is especially evident down to 6 m bgl where the measured value is in the range of approximately 8-13 kPa. The scatter in sleeve friction decreases below 6 m depth.

Cone type 3

Figure 6.5.3 illustrates the measured results with cone type 3 in accordance with Section 5. The cone resistance shows relatively good repeatability down to about 16 m where TILC11 is clearly influenced by another borehole and has been excluded from the representative profiles. The pore pressure measurements show somewhat less repeatability. The sleeve friction plots show more scatter, and this may be because cone type 3 is a subtraction cone. The zero drifts for q_c , f_s and u_2 are very large.

Cone type 5

Figure 6.5.4 displays the representative results with cone type 5. The results show small variations in cone resistance and pore pressure. All measurements for test TILC12 showed increasing deviation from the other tests from approximately 7 m bgl. It is believed that interference with rotary pressure sounding TILRP01 caused this response. This test was performed 0.6 m away. All measurements from TILC12 below 7 m depth have been excluded from the representative results. Neglecting the measurements from TILC12 below 7 m depth, one may observe that the pore pressure measurements from cone type 5 show good repeatability. The cone resistance also shows relatively good repeatability. The sleeve friction of TILC03 and TILC09 are very similar, but TILC06 deviates significantly.

Cone type 6

Figure 6.5.5 illustrates good repeatability for the pore pressure measurements and cone resistance. The pore pressure response from TILC18 suggests poor saturation of the filter in the top 6 m. The results from TILC17 clearly show that the sounding crosses another borehole below 14-15 m depth. Above this depth, the side friction for TILC17 and TILC20 coincide well. Therefore, the results below 14 m are left out of the representative profiles. The measured sleeve friction for sounding TILC18 was in the order of 10 times greater than the remaining CPT sleeve friction measurements. The zero drift of this test was also high, and the results have been excluded from further comparison. The sleeve friction of TILC19 is quite a bit higher. All tests with cone type 6 have an inclination at end above 20°.

Cone type 7

Figure 6.5.6 illustrates the results with cone type 7. The figure shows relatively good repeatability for the pore pressure and cone resistance down to 18 m depth, where TILC25 seems to cross another borehole. Results from TILC25 is left out below 18 m. The sleeve friction shows more scattered results as is seen for the majority of tests at the quick clay site.

Cone type 8

Cone type 8 shows relatively good repeatability for the pore pressure measurements and cone resistance illustrated in Figure 6.5.7. TILC22 shows obvious erroneous measurements above 3 m depth which have been excluded from further comparison. Sleeve friction is quite repeatable below approximately 4 m depth.

Cone type 12

Figure 6.5.8 illustrate the representative results with cone type 12. All parameters show reasonably good repeatability. The repeatability of cone resistance and pore pressure are however relatively low compared to other tests at this site. The sleeve friction is low in the quick clay layer below 7-8 m depth.

Overall note

All tests with each cone show generally good repeatability for measurements on pore pressure and cone resistance while the sleeve friction varies more with each sounding. It should be noted that the measured values for sleeve friction are relatively low and in the absolute lower end of what the cones are designed for.

After testing at Tiller-Flotten, calibration was controlled by the producer for the cone of type 7 (standard cone) used for TILC23 and TILC25, as well as the cone of type 8 (sensitive cone) used for tests TILC22, TILC26 and TILC27. The results indicate that there were problems with the cone resistance and sleeve friction calibration of the cone of type 8. An attempt to correct the cone resistance measurements of the tests with cone type 8 by 8 % made the results more equal to those from cone type 7 (tests TILC23, TILC24 and TILC25). However, the calibration error of the sleeve friction was

inconsistent, and attempts to correct the sleeve friction measurements only resulted in more scatter.

Table 6.5-1 Summary of CPTU tests with remarks – quick clay site.

Test ID	Cone Type	Zero drifts			Test date	Temp. ¹⁾	Remark
		q _c , kPa	f _s , kPa	u ₂ , kPa		°C	
TILC03	5	-48.0	0.0	-1.6	2017-09-22	14	Large zero drift q _c , but results are considered representative. ²⁾
TILC04	12	-69.5	-1.1	-30.4	2017-09-22	14	Large zero drifts, but results are considered representative.
TILC06	5	-35.1	0.0	-71.6	2017-09-22	14	Large zero drifts, but results are considered representative.
TILC08	3	0.6	0.7	2.6	2017-09-22	14	
TILC09	5	-31.7	-0.1	-59.4	2017-09-22	14	Large zero drift u ₂ , but results are considered representative.
TILC10	12	-40.9	-0.6	-20.5	2017-09-22	14	Large zero drifts, but results are considered representative.
TILC11	3	973.0	71.9	588.2	2017-09-22	14	Large zero drifts, but results are considered representative.
TILC12	5	-37.1	0.0	2.4	2017-09-22	14	Dissipation. Large zero drift q _c , results are considered representative.
TILC13	1	93.6	1.7	1.4	2017-09-25	17	Large zero drift q _c , but results are considered representative.
TILC14	1	83.2	1.6	0.9	2017-09-25	17	Large zero drift q _c , but results are considered representative.
TILC15	1	46.8	0.7	1.3	2017-09-26	17	Seismic. Large zero drift q _c , but results are considered representative.
TILC16	1	31.2	0.3	0.7	2017-09-25	17	
TILC17	6	22.0	-0.5	-15.7	2017-09-27	10	Large zero drift u ₂ , but results are considered representative.
TILC18	6	50.0	71.7	-16.4	2017-09-27	16	Large zero drifts, but results are considered representative.
TILC19	6	14.0	0.1	-11.2	2017-09-27	17	Large zero drift u ₂ , but results are considered representative.
TILC20	6	32.0	-0.9	-22.3	2017-09-27	18	Large zero drift u ₂ , but results are considered representative.
TILC22	8	3.5	0.4	1.6	2018-05-08	8	
TILC23	7	8.9	0.5	0.3	2018-05-08	18	
TILC24	7	6.3	2.4	1.3	2018-05-08	19	
TILC25	7	6.6	0.1	0.0	2018-05-08	11	Seismic.
TILC26	8	17.2	2.9	1.3	2018-05-09	16	
TILC27	8	9.2	2.4	1.8	2018-05-09	19	
TILC28	2	-24.2	1.7	2.5	2018-05-30	16	
TILC29	2	-26.2	0.4	2.4	2018-05-30	16	
TILC30	2	-9.7	0.3	-1.8	2018-05-30	16	

¹⁾ Representative air temperature used to correct measured results

²⁾ It is assumed that zero shifts have occurred towards the end of the test

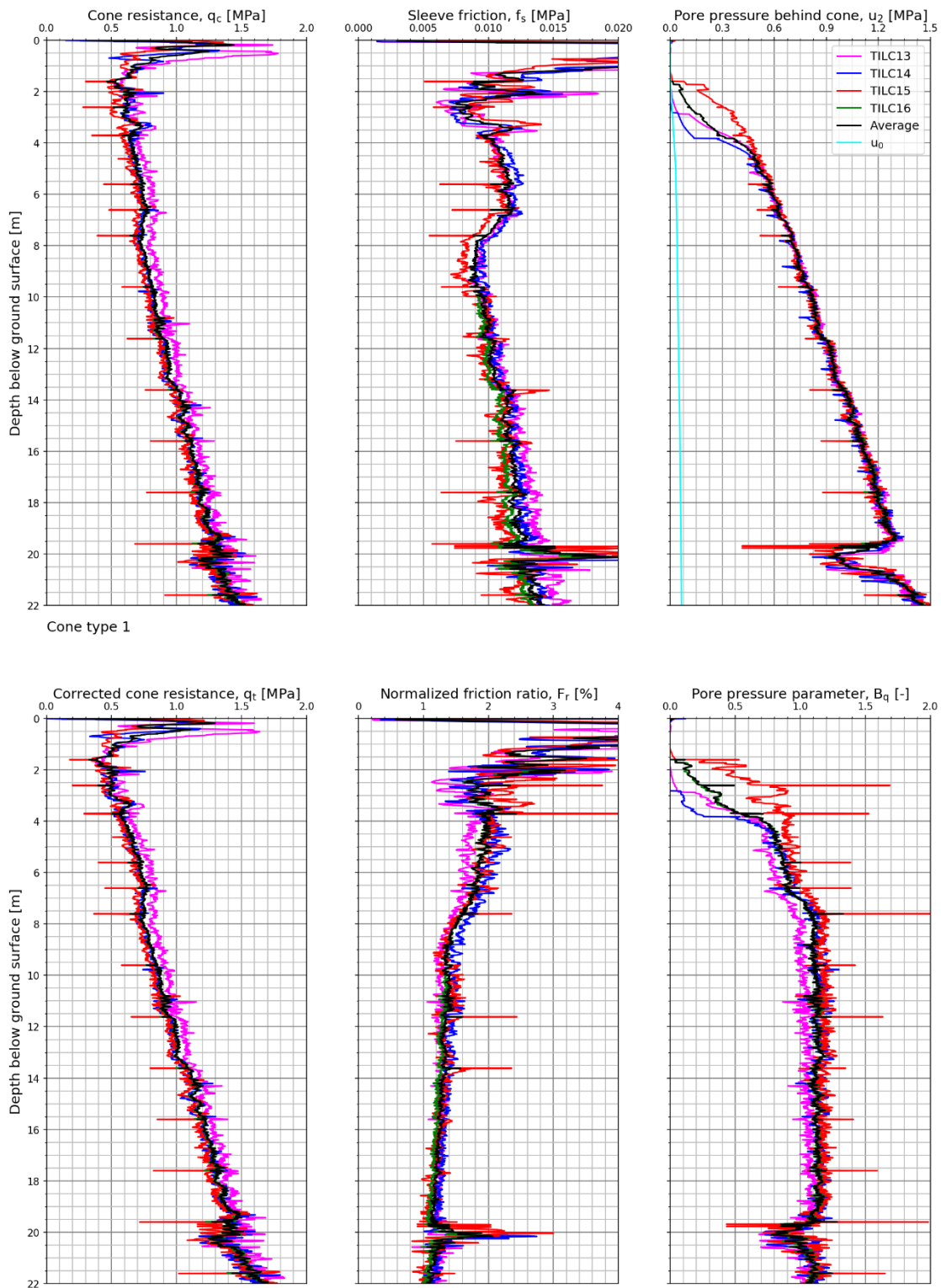


Figure 6.5.1 Measured and derived CPTU parameters. Cone type 1. NGTS quick clay site.

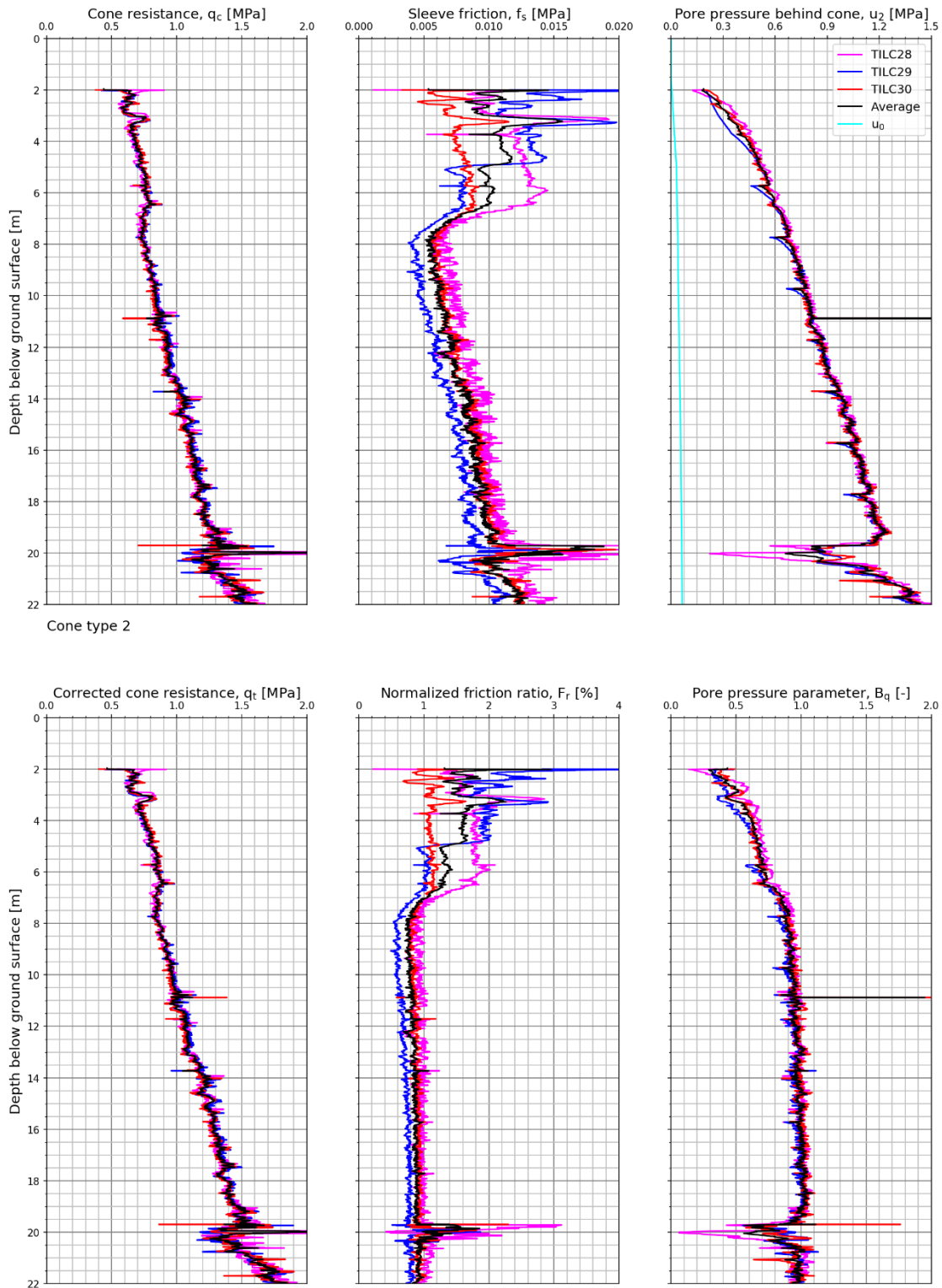


Figure 6.5.2 Measured and derived CPTU parameters. Cone type 2. NGTS quick clay site.

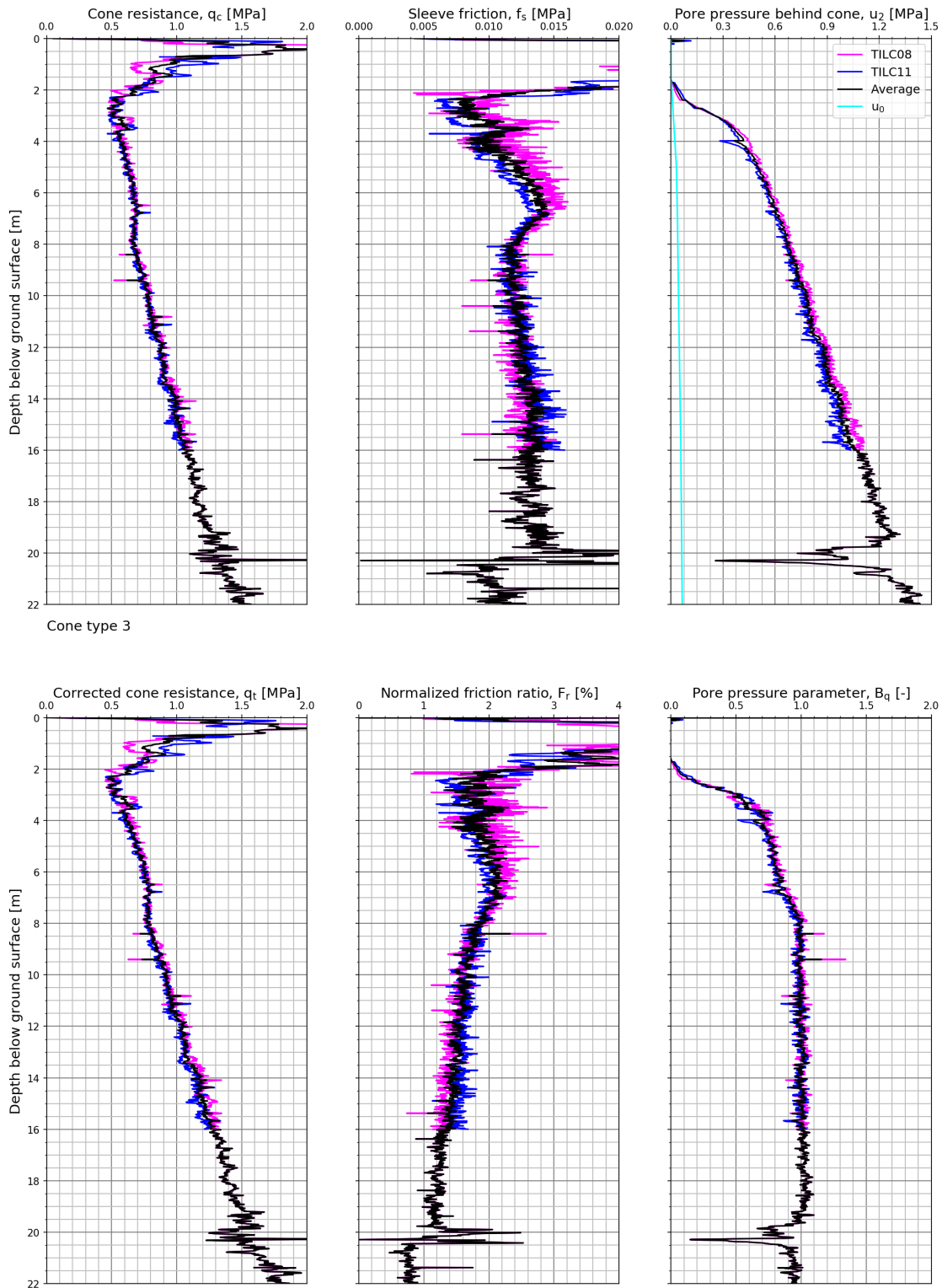


Figure 6.5.3 Measured and derived CPTU parameters. Cone type 3. NGTS quick clay site.

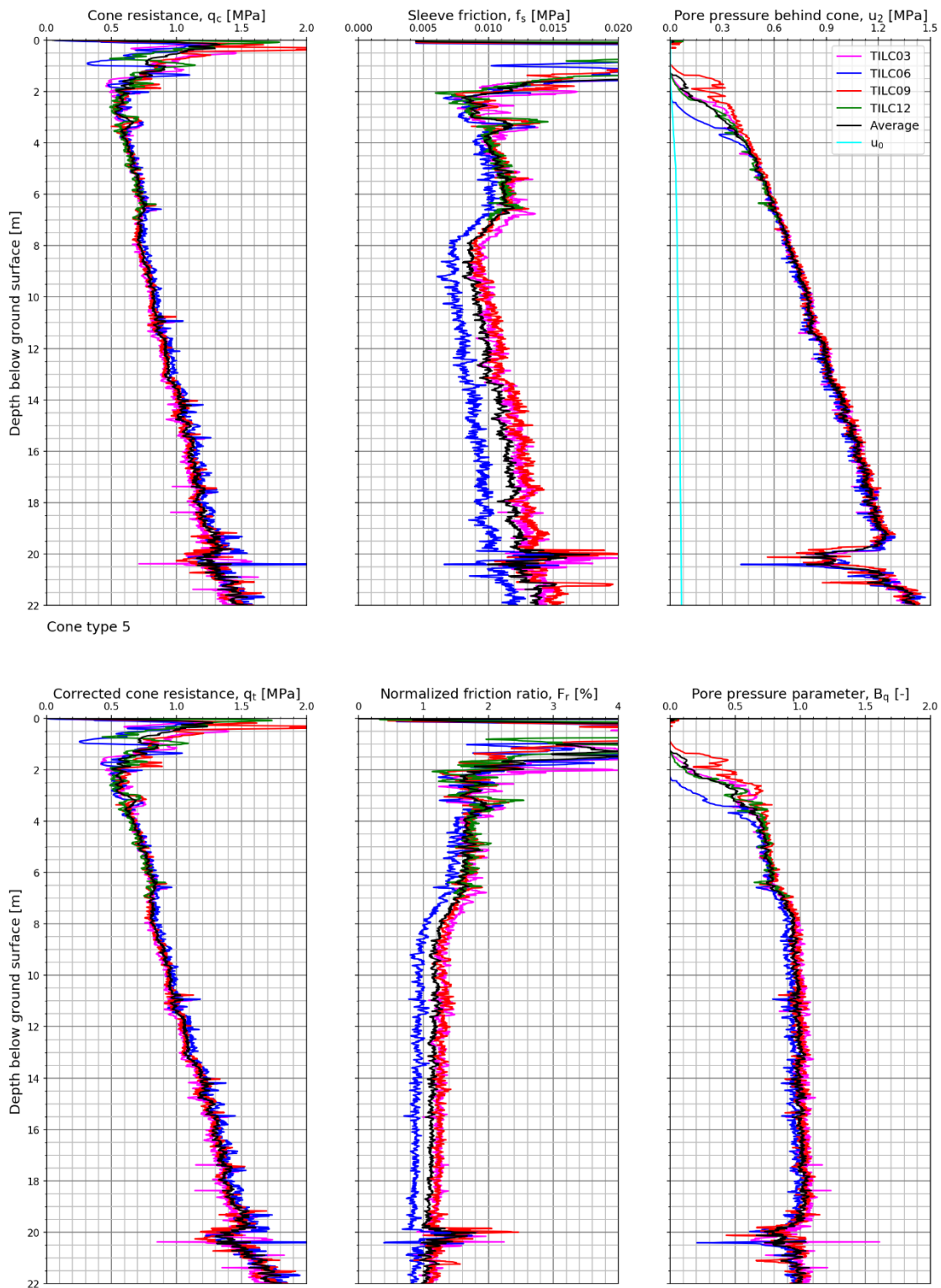


Figure 6.5.4 Measured and derived CPTU parameters. Cone type 5. NGTS quick clay site.

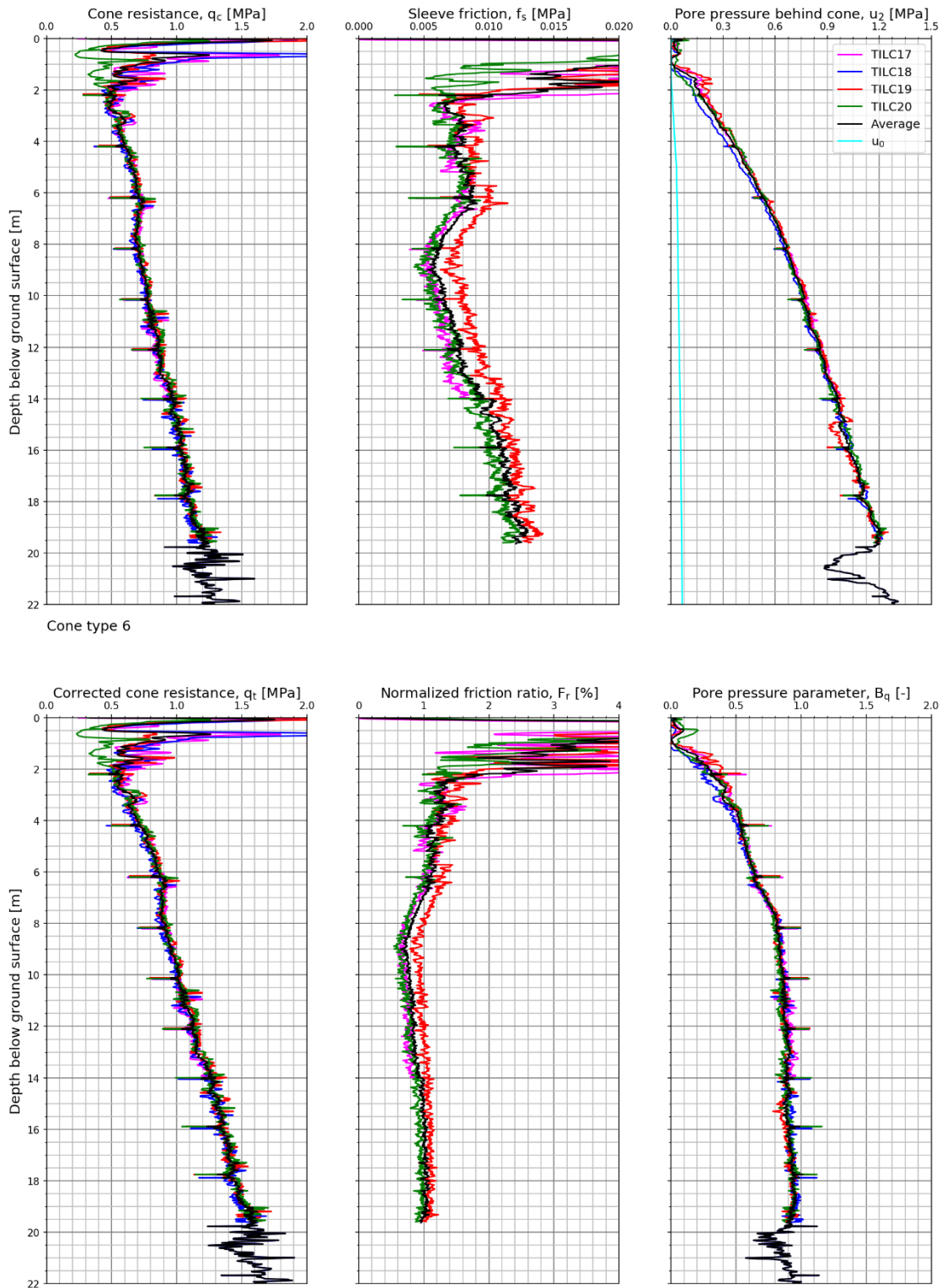


Figure 6.5.5 Measured and derived CPTU parameters. Cone type 6. NGTS quick clay site

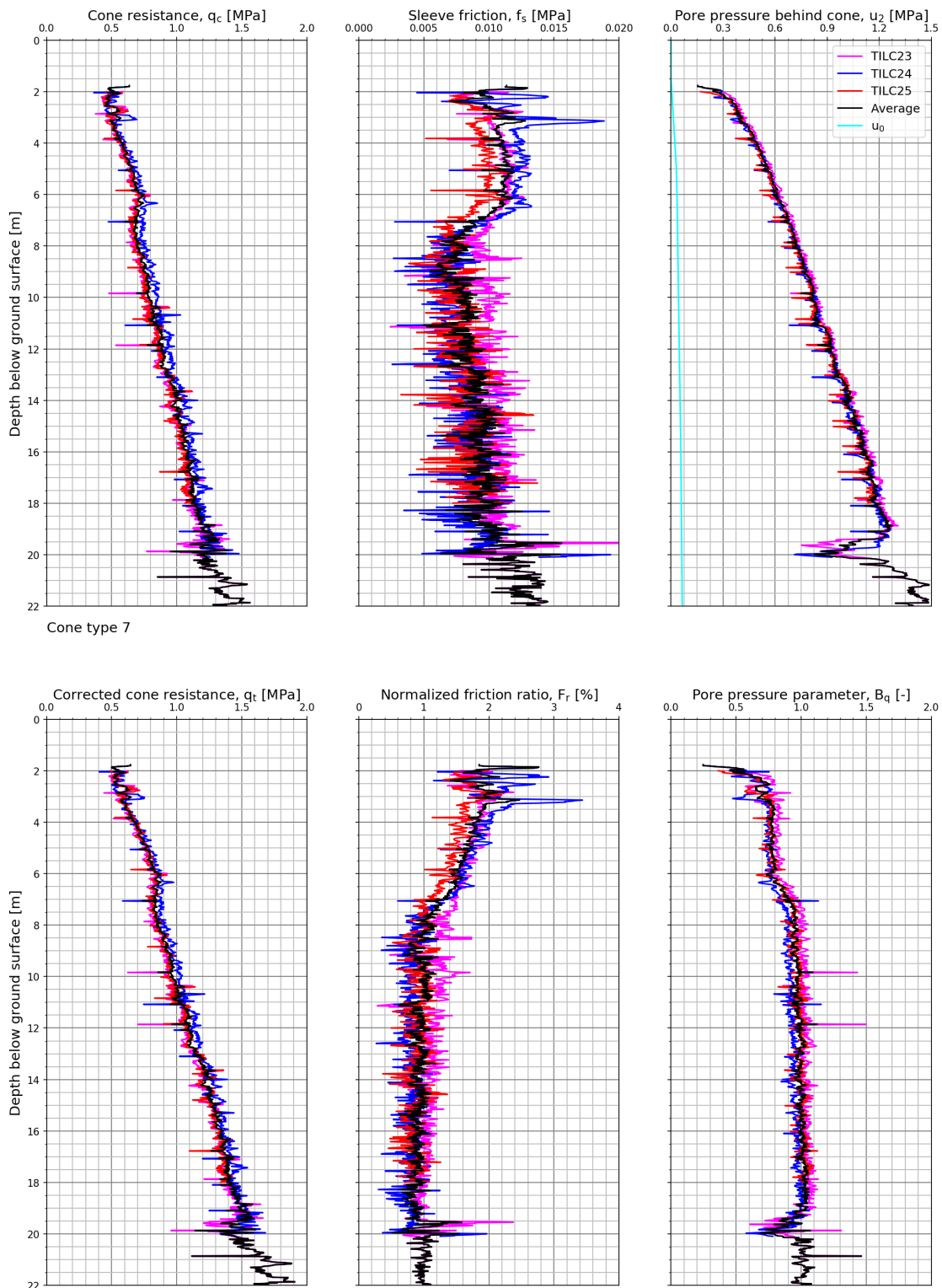


Figure 6.5.6 Measured and derived CPTU parameters. Cone type 7. NGTS quick clay site.

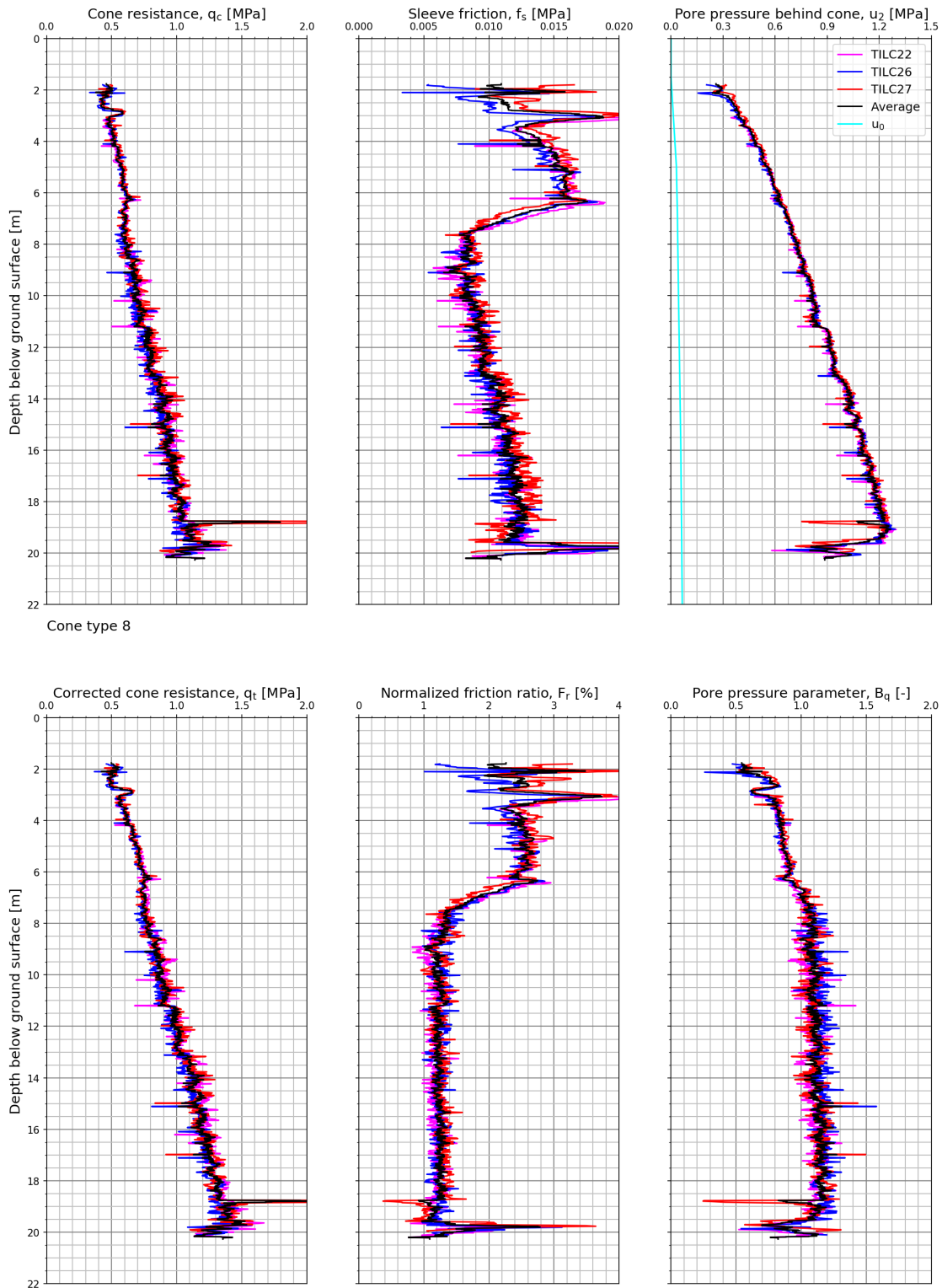


Figure 6.5.7 Measured and derived CPTU parameters. Cone type 8. NGTS quick clay site.

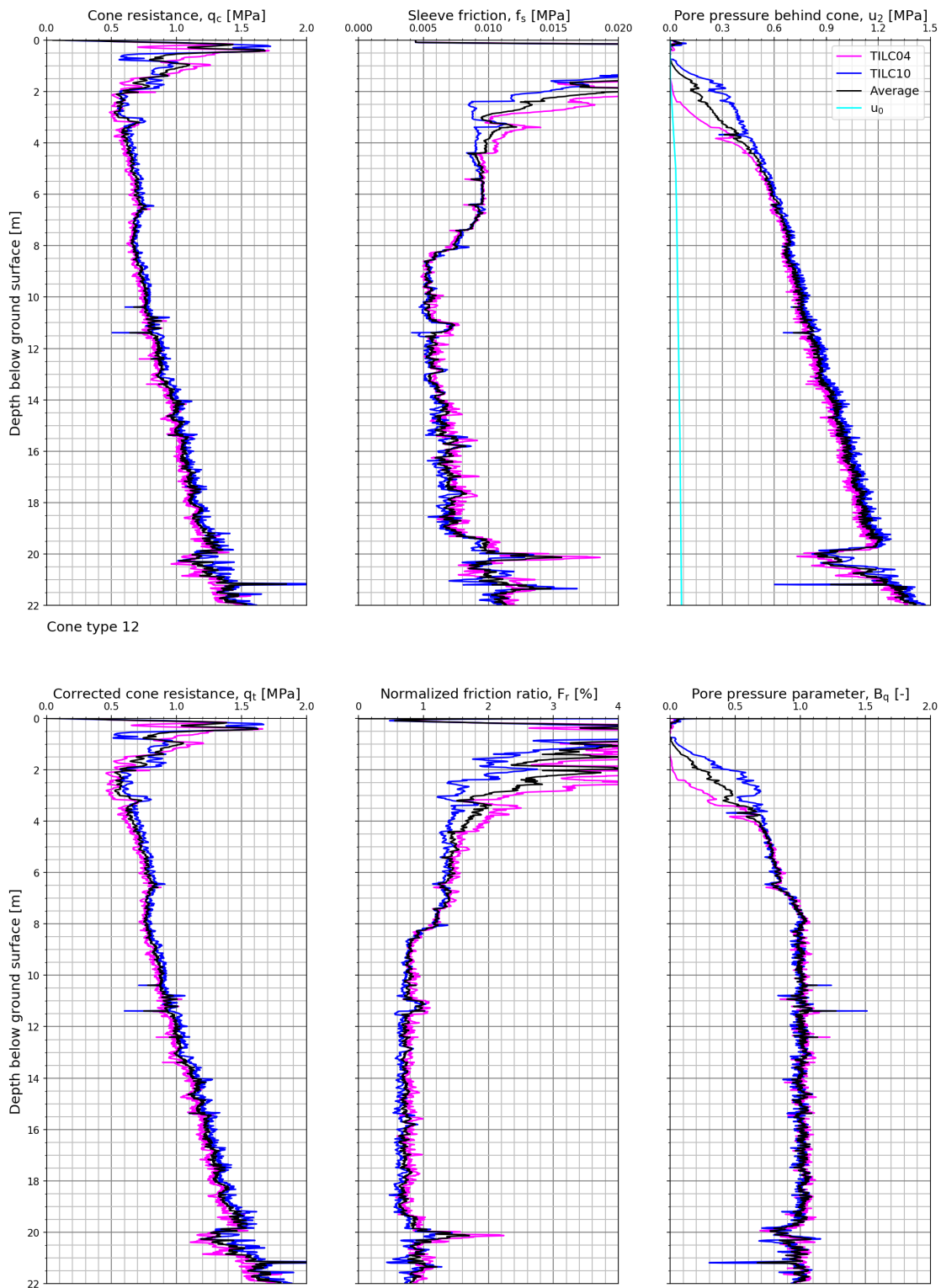


Figure 6.5.8 Measured and derived CPTU parameters. Cone type 12. NGTS quick clay site.

7 Comparison of representative results

7.1 Soft clay site – Onsøy

The representative average profiles for all cones studied at the soft clay site are illustrated in Figure 7.1.1.

A general trend of poor filter saturation in the first 1-2 meters of testing can be observed for multiple tests and these results have not been used as basis for comparison.

Figure 7.1.1 suggests that the repeatability of the corrected cone resistance is higher than the sleeve friction, but lower than the pore pressure behind the cone. For cone resistance, cone types 3 and especially 4 represent low values compared to the other cones although the repeatability of the different tests with this cone was excellent. The low values of corrected cone resistance between 4 m and 8 m bgl is the major contribution to the observed scatter in pore pressure parameter B_q . It is evident from Figure 5.1.1 that temperature effects play an important role for some of the cone penetrometers when the cone resistance is as low as for the soft clay site. Results with cone type 4 have been corrected with the same temperature calibration results as obtained for cone type 3. This may be a potential source of error in the cone resistance data for cone type 4 relative to cone type 3.

Sleeve friction shows less repeatability compared to cone resistance and pore pressure behind the cone. Results with cone type 6 represent a range of low values of the sleeve friction while cone types 3 and 5 represents the upper range of measurements. As described in Section 5.1.2, a temperature correction has been applied to the measured results for all cones except cone type 6 where no temperature calibration was available. This may explain the very low values compared to the other cone types as shown in Figure 7.1.1. Cone type 3 is a subtraction cone which means that the results are dependent on measurements of two load cells. In the case of soft clay sites, the sleeve friction may be very low compared to the cone resistance, therefore the level of sleeve friction accuracy depends on the level of accuracy for the cone resistance. At 10 m depth bgl the sleeve friction ranges from 5 kPa to 12 kPa, which is significant because the values are so low. Measuring 5 kPa when the correct reading is 12 kPa means a difference of 140 %.

Except for cone type 6, u_2 shows remarkably good comparison among the cone types. Cone 6 is the only cone using a slot (filter) instead of a filter. This may be an explanation why u_2 is higher (20 – 80 kPa in depth interval 5m – 15m) compared to the other cones. However, neither NGI nor NPRA, who have many years of experience with using slot filters have observed such deviations earlier. Cone type 6 suggests a pore pressure of approximately 100 kPa at 1m depth bgl, which is the location of the ground water table. For many tests the filter saturation is poor in the top 4 m of strata.

The variations in normalized friction ratio are large. The variations in pore pressure parameter are relatively low compared to normalized friction ratio. The most significant contribution to the scatter in B_q is cone type 4 which may be strongly influenced by temperature effects as discussed above.

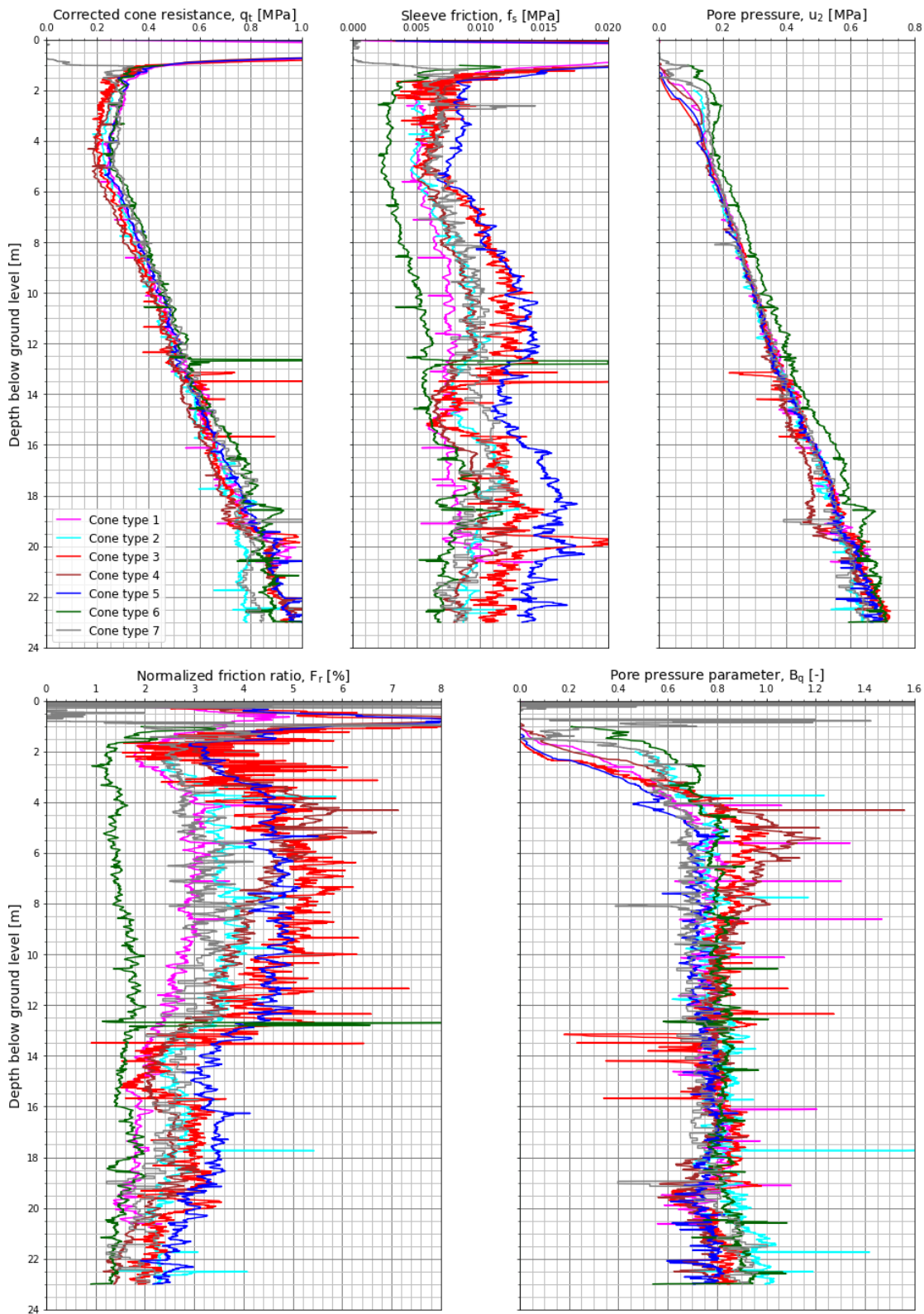


Figure 7.1.1 Measured and derived CPTU parameters. All cone types used at NGTS soft clay site.

7.2 Silt site – Halden

The representative average profiles for all cones studied at the silt site are illustrated in Figure 7.2.1.

It is evident from the measurements that there is a change in material type at some depth between 15 m and 16.5 m. The depth range of interest is from 5 m to 15 m depth bgl approximately and only the results within this depth range are compared herein.

The corrected cone resistance shows approximately the same level of scatter as the pore pressure, but far less scatter compared to the sleeve friction. Cone 6 produces the highest readings especially around 8 m depth bgl. Test HALC11 is the main contributor to the response seen at 7 m depth bgl for cone 6. It is believed that this could be the effect of hitting a cobble.

The sleeve friction demonstrates considerable scatter between the representative average profiles. Similar scatter was observed for the soft clay site. Cone 6 represents, in general, the lower bound measurements and cone type 1 represents the upper bound measurements. It is generally expected that most of the tests show results towards an average value of the upper and lower bound results. This is not the case for the sleeve friction response at Halden. The results can generally be clustered in two, cones 1 and 7 and cones 5, 6 and 9.

The pore pressure response shows reasonable repeatability except for cones 6 and 9. These cones produce excess pore pressure from 2 and 1 m bgl respectively. The ground water table is located around 2 m bgl and a permeable layer is generally encountered down to 5 m bgl. On that basis the pore pressure response from these two cones are somewhat unlikely.

For the derived parameters F_r and B_q the scatter is seen to be larger than the measured parameters which is expected from combining several parameters with scatter. The pore pressure parameter B_q shows less scatter than the normalized friction ratio. The lower and upper bound cones from sleeve friction are also the lower bound and upper bound for the normalized sleeve friction. The pore pressure parameter B_q is influenced by the unlikely results produced by cones 6 and 9.

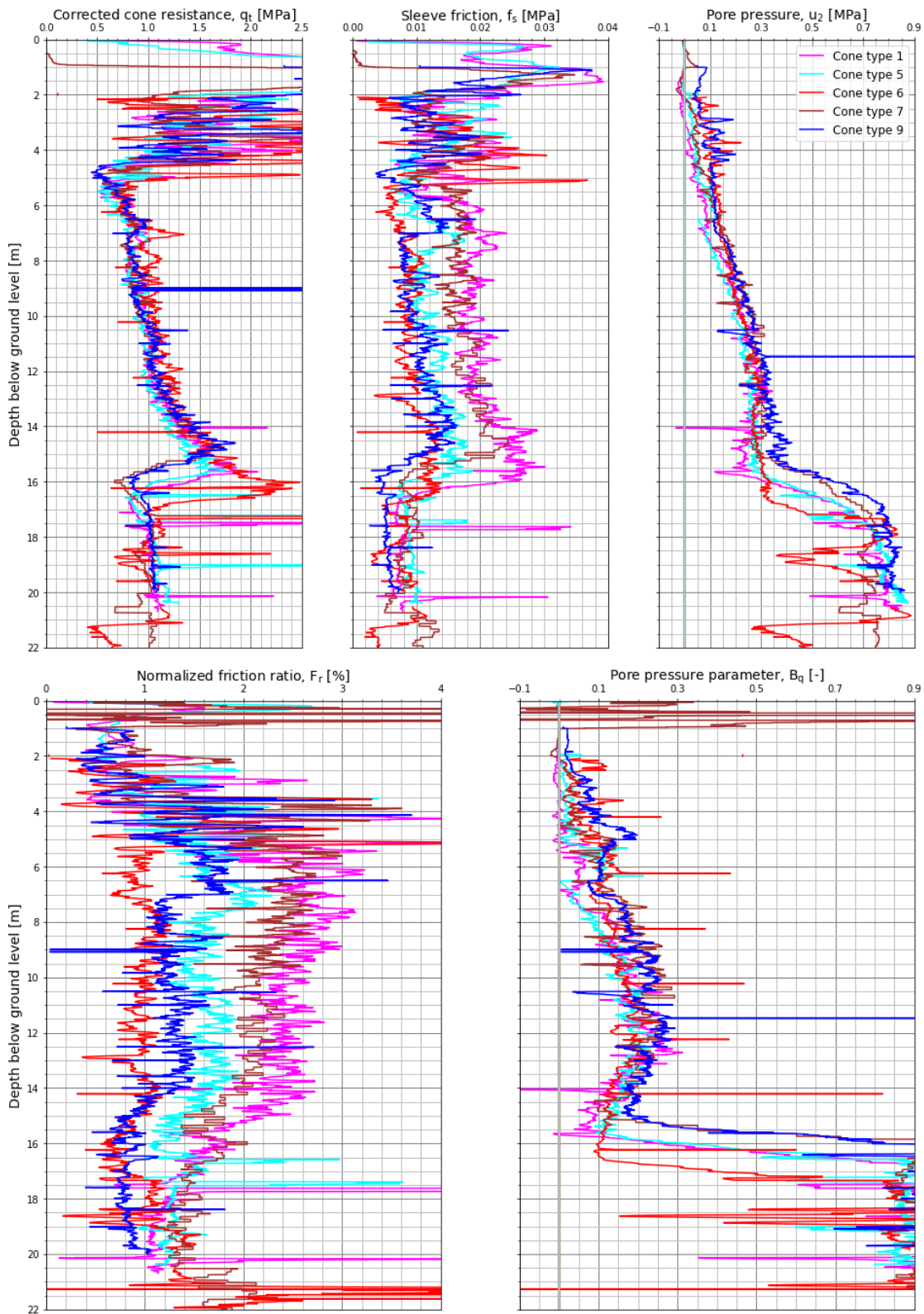


Figure 7.2.1 Measured and derived CPTU parameters. All cone types used at NGTS silt site.

7.3 Sand site – Øysand

The representative average profiles for all cones studied at the sand site are illustrated in Figure 7.3.1. Results show a very wide variability in the corrected cone resistance derived from the cone penetration measurements and the measured pore pressure u_2 , as q_t varies between 1.5 and 4.5 MPa or more in the depth interval 7 to 12 m. This is not unexpected and links to the depositional history at the site. The layers found in the delta foreset (Figure 2.4.1) can have varying geometry.

While examining the data, it was observed that the CPTUs are slightly out of phase depth-wise because of the structure (strike and dip) in the foreset of the deltaic deposits. A simple depth adjustment was made by shifting the corrected cone resistance q_t data in each CPTU sounding up or down to match the peaks and troughs in the corrected cone resistances. The depth adjustment was made after an interpretation of the structure/layering at the site as shown in Figure 7.3.2. Figure 7.3.3 presents a depth adjusted comparison of the CPTU data at Øysand. The relative variation in net tip resistance and measured pore pressure is small and for all practical purposes negligible. However, sleeve friction results show a large scatter between the different cone types with up to 75 kPa in variation at 20 m depth. The variation in sleeve friction also seems to increase with depth.

In his study, Hammer (2019) defined the average error in CPTU parameter for a given cone type as the difference between a given measurement and the average representative value (i.e. average measurement at a given depth for a given cone type). Results presented in Figure 7.3.4 and Figure 7.3.5 show differences in accuracy for 5 cone types (i.e. 3, 4, 5, 11 and 12). All in all, the accuracy in the q_{net} is better than for u_2 and f_s . Accuracy in f_s measurements for cone types 3 and 11 is rather poor compared to the others.

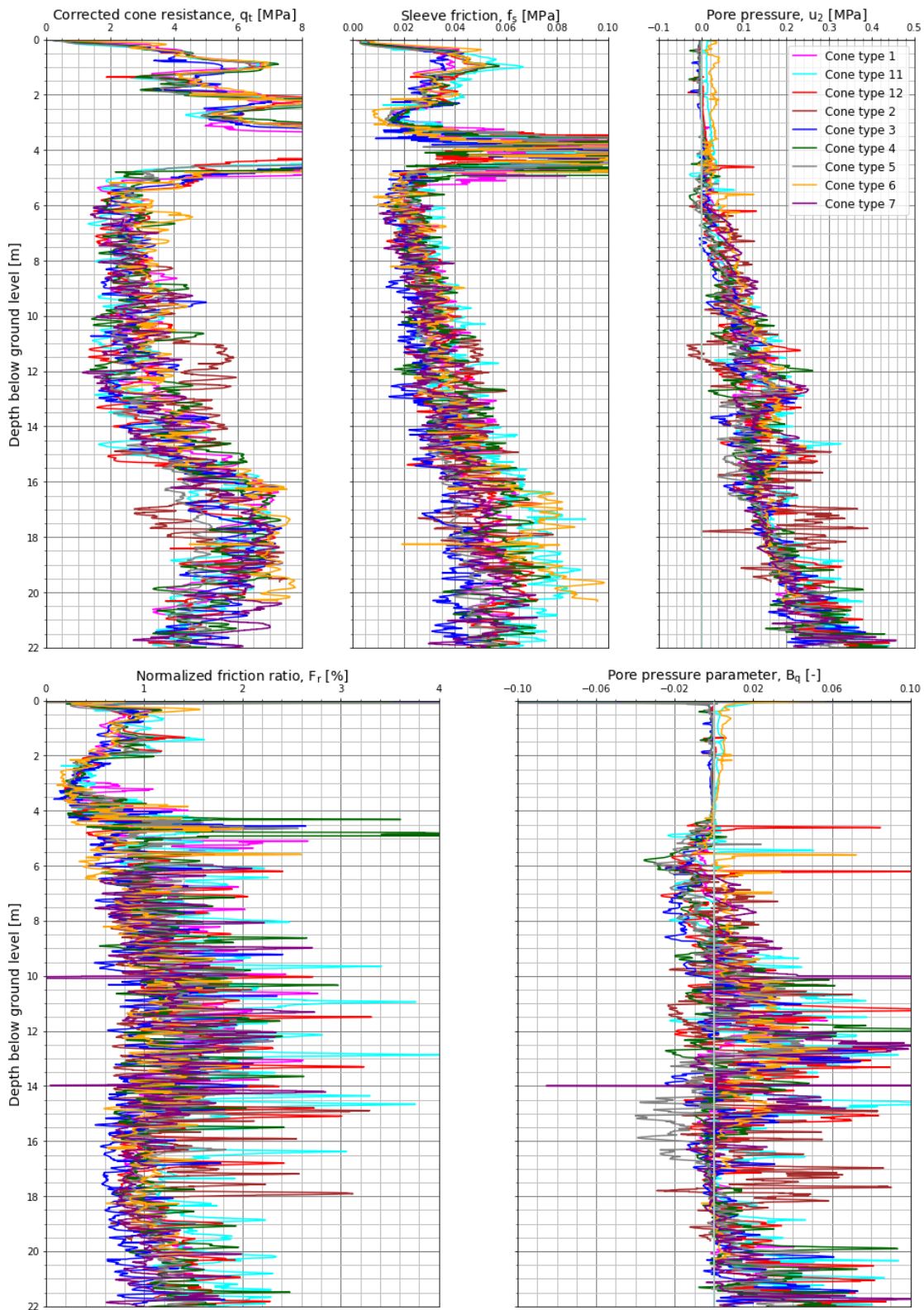


Figure 7.3.1 Measured and derived CPTU parameters. All cone types used at NGTS sand site.

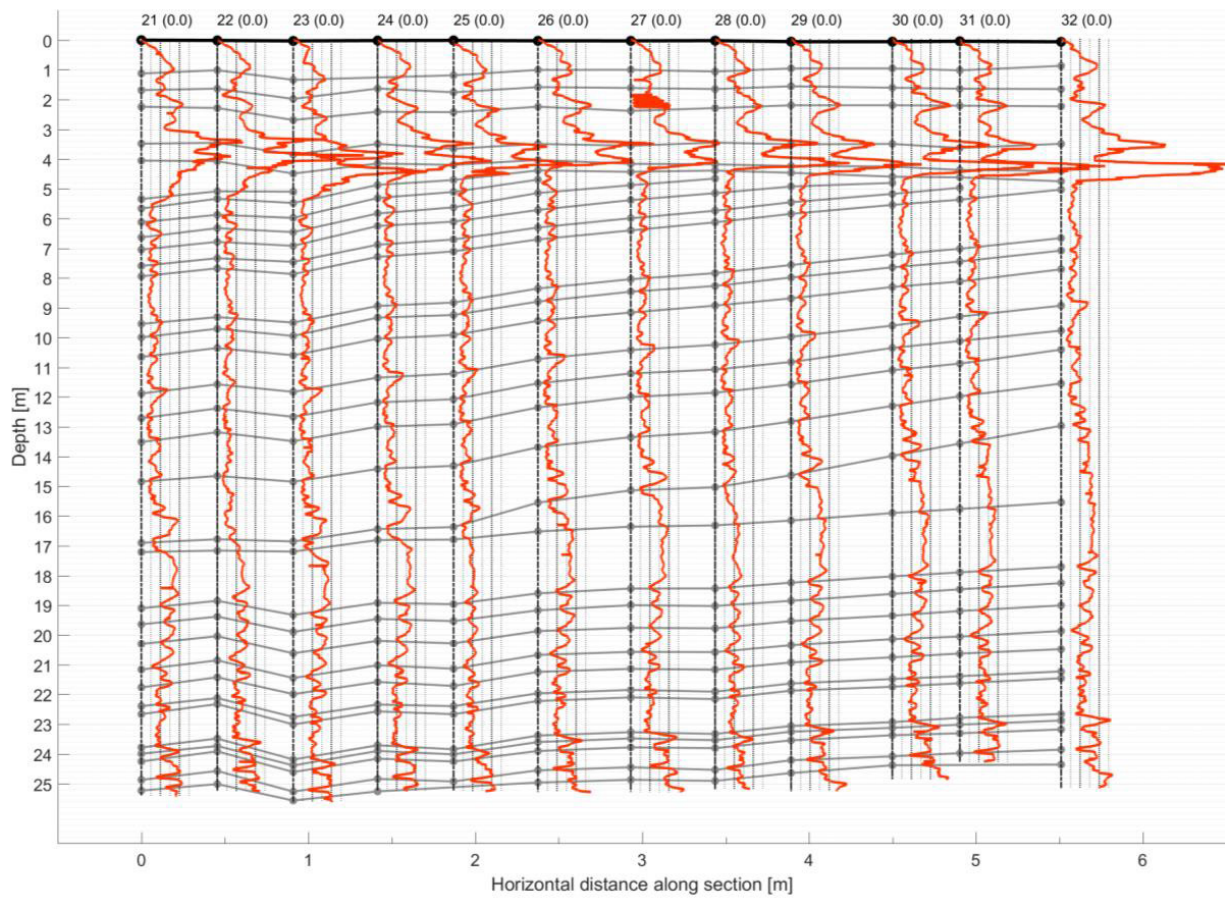


Figure 7.3.2. Profile through CPTUs OYC21-OYC32 showing the interpreted structure of the sand deposit at Øysand (from Hammer, 2019).

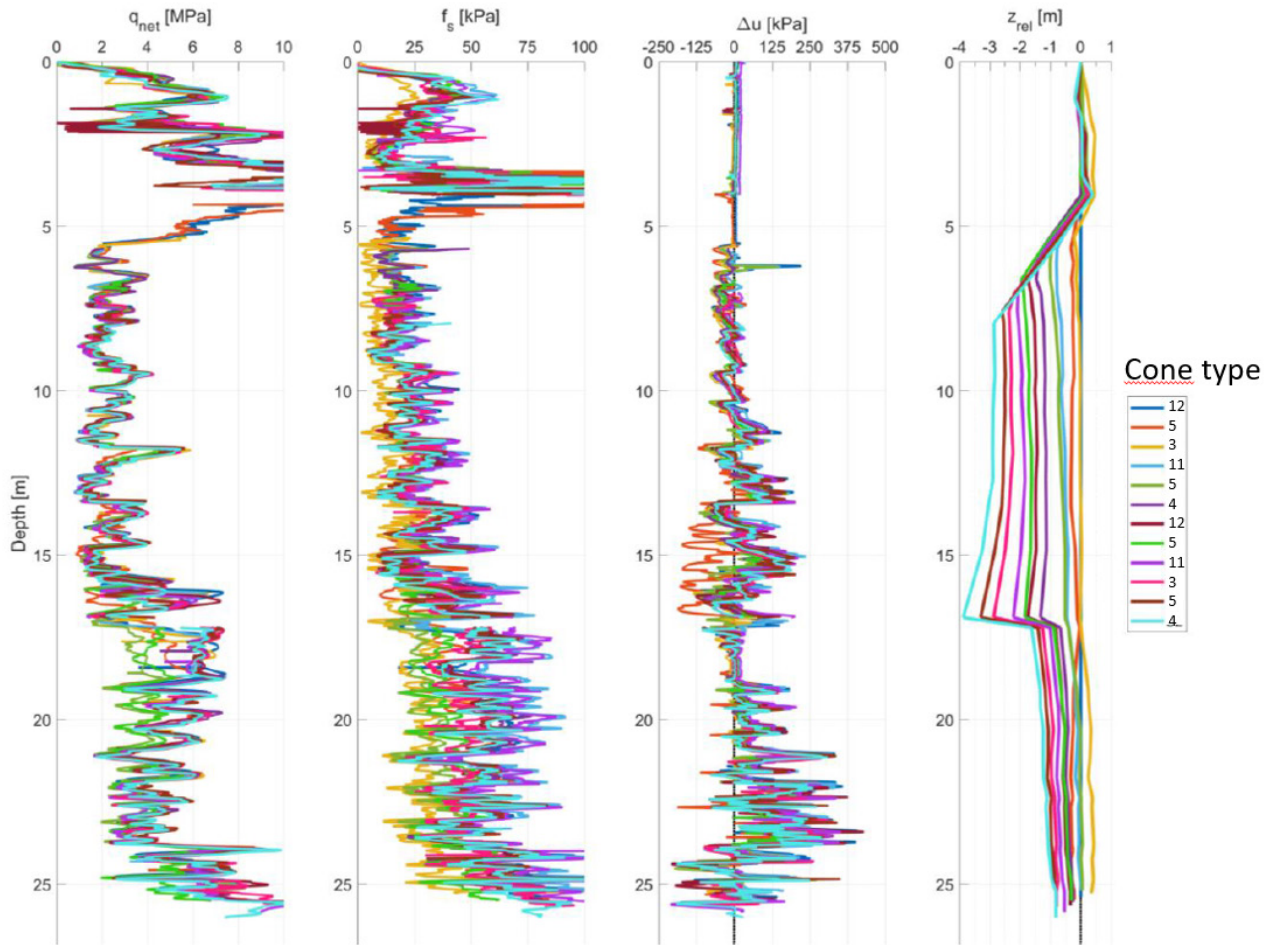


Figure 7.3.3. Comparison of derived CPTU parameters for all cone types at Øysand after depth adjustment (from Hammer, 2019).

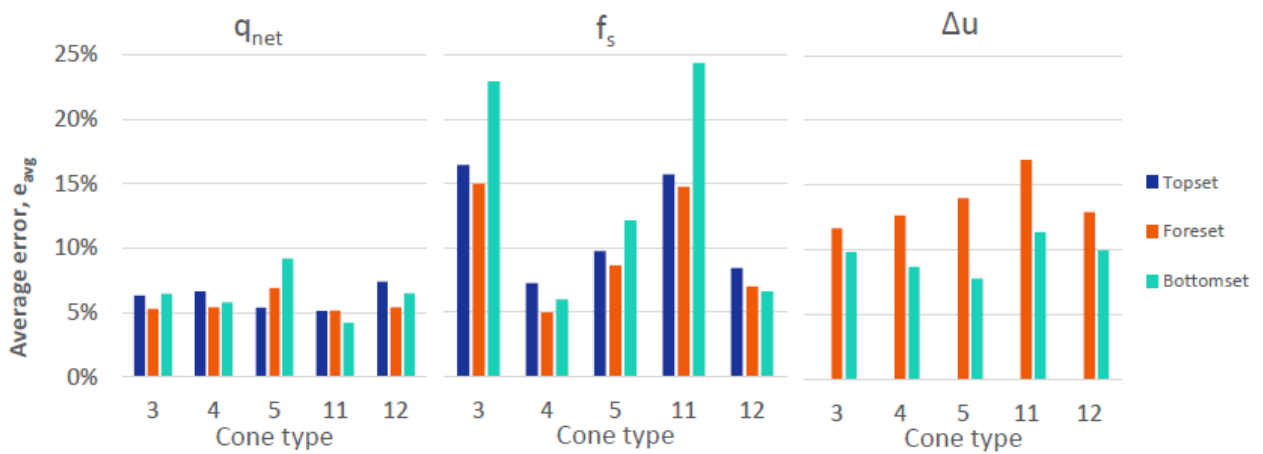


Figure 7.3.4. Average error for derived CPTU parameters for given cone types.

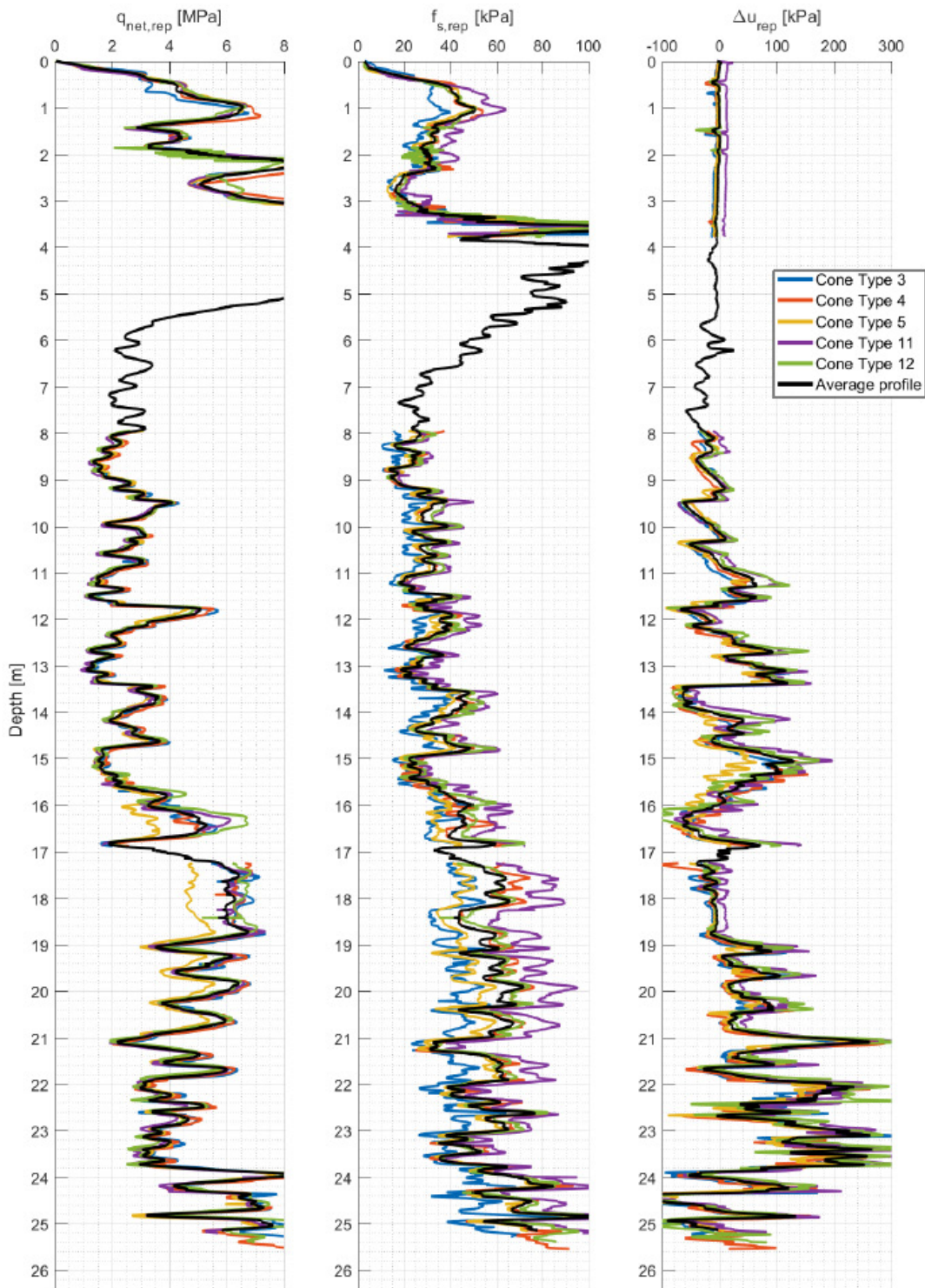


Figure 7.3.5. Comparison of representative profiles for cone types 3, 4, 5, 11 and 12 at Øysand (from Hammer, 2019).

7.4 Quick clay site – Tiller-Flotten

The representative average profiles for all cones studied at the quick clay site are illustrated in Figure 7.4.1. The results suggest that the pore pressure is more repeatable than the remaining two parameters. The cone resistance also shows good comparison between the different cone types while the sleeve friction shows a rather large range of values throughout the soil profile.

From Figure 7.4.1 cone resistance from cone 6 is generally in the upper range of the measurements. The difference between the highest and lowest representative values are relatively constant with depth and approximately around 200 kPa. Cone type 8 predicts lower values than the remaining cones with depth.

After testing of cone types 7 and 8, the calibration was controlled by the manufacturer. The results indicated problems with the cone resistance and sleeve friction calibration for cone 8. The calibration error of the sleeve friction was inconsistent and attempts to correct the measurements only resulted in more scatter. Correcting the cone resistance according to the new calibration values would lead to higher values for cone type 8, and thus bringing the values closer to the average of the other cones.

The sleeve friction varies significantly with cone type. Cone type 12 represents the very low estimate and cone type 3 the high estimate. Cone type 3 is a subtraction cone and can be susceptible to erroneous measurements in cone resistance. Cone type 12 has a 15 cm² cone tip area with a proportionally larger sleeve area compared to all of the other cone types, which are 10 cm² cones. In the quick clay layer (below ca. 8 m depth) cone type 12 shows the lowest measurements of f_s . Cone 8 demonstrates different results compared to the remaining tests around 5 m bgl.

Figure 7.4.1 shows that the pore pressure is less dependent on cone type. Most of the cones display less responsive pore pressure results in the upper 4 m of testing. Even though cone type 6 shows relatively good repeatability for the pore pressure measurements, the average for cone type 6 is quite a bit lower than for the other cone types between approximately 4 and 8 m depth. This may be due to poor saturation in this depth interval. Another explanation may be that the tests with cone type 6 have penetration speed 12 mm/s, while all the other tests have 20-24 mm/s. Lower speed will generally yield a small decrease in measured u_2 . However, below 8 m depth cone type 6 records values similar to the other cones. Cone type 6 is the only cone using a slot (filter) instead of a filter, and this may be a possible explanation why u_2 is lower. On the other hand, Lunne et al. (2018) report that the cone with slot filter gave consistently higher u_2 values compared to the other cones at Onsøy. Cone type 6 has relatively large inclination at the end of the soundings (22-23 degrees) compared to all of the other tests (0-6 degrees). The depths of the results have been corrected for inclination, but it is unknown if the high inclination affects the measured results in any other way. The scatter in the u_2 measurements generally increases with depth.

Cone type 12 gives relatively low values of u_2 compared to the average for all of the cones below 10 m depth. It is unknown whether or not this may be due to the larger diameter of the cone.

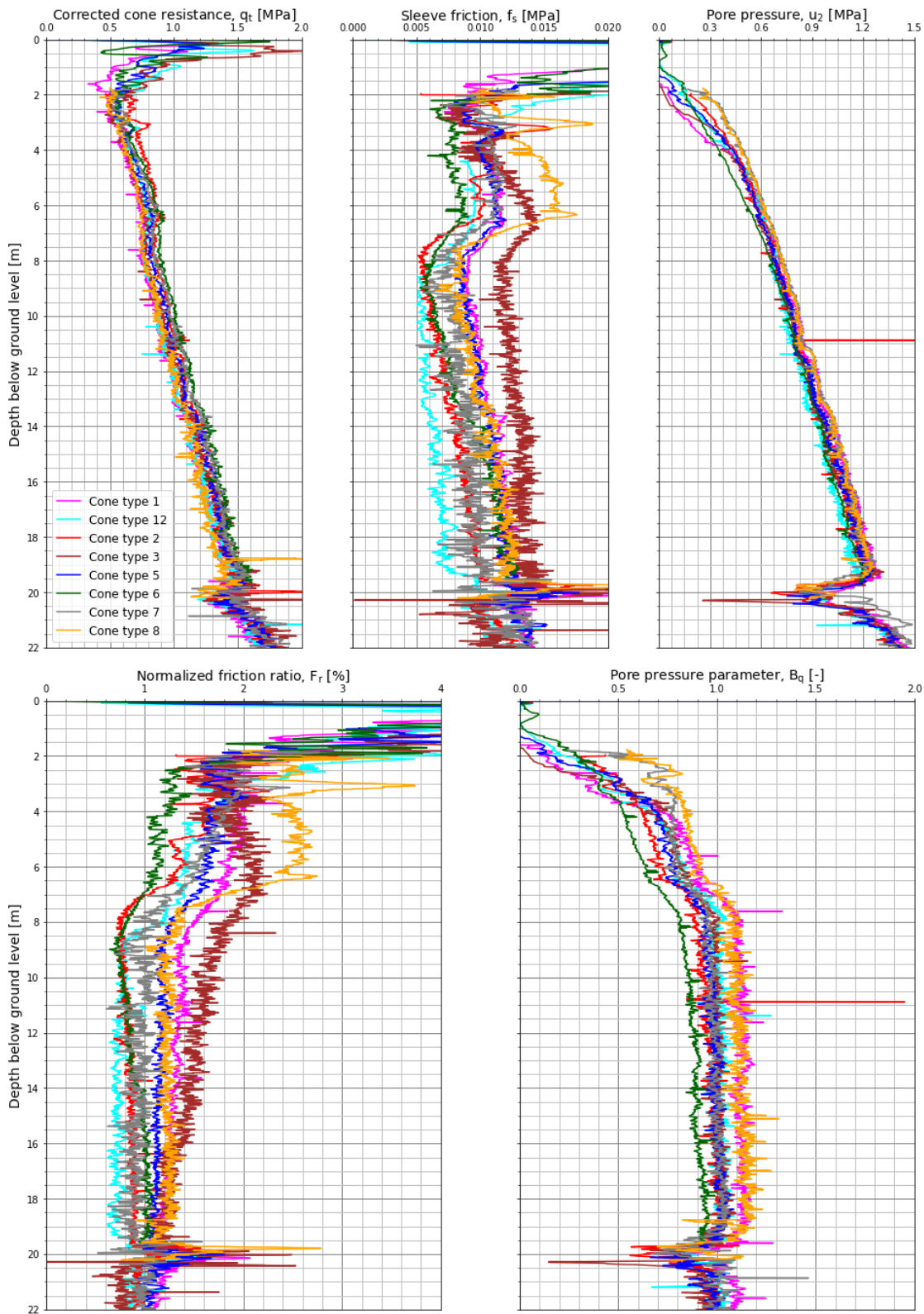


Figure 7.4.1 Measured and derived CPTU parameters. All cone types used at quick clay site.

7.5 Overall evaluation of differences

It is a challenging task to summarize the results at the four sites with a large number of cone penetrometers and soil conditions. As discussed above, temperature effects are very important and will be commented on first. We have received temperature calibration for cone types 1, 2, 3 and 7. It was assumed that the temperature effects for cone types 4, 5, 11 and 12 are the same as for cone type 3 since all these cone types have been made by the same manufacturer. It was also assumed that cone type 8 has the same dependency on temperature as cone type 7 because these have the same manufacturer.

Table 7.5-1 shows the correction of pressures per 1°C change in temperature. It also gives the air temperature at the time of testing at Tiller-Flotten and Onsøy, as well as the maximum pressure correction for each cone in kPa. Last, the table gives the potential error due to temperature change as percent of typical values at 10 m depth for Tiller ($q_c = 800$ kPa, $f_s = 8$ kPa, $u_2 = 800$ kPa) and Onsøy ($q_c = 430$, $f_s = 8$ kPa and $u_2 = 300$ kPa). The assumed ground temperatures for Tiller and Onsøy are 5° and 8°C respectively. The table clearly shows that the relative error due to temperature change may be large, especially for f_s . u_2 is less influenced than q_c by temperature change. Cone type 2 is relatively little influenced by changes in temperature compared to the other cones. For cone type 6 no temperature calibration has been available.

Table 7.5-1 Overview of temperature corrections – Tiller and Onsøy

Cone type	Representative air temperature	Pressure rate of change [kPa/1°C]			Maximum temperature correction [kPa (% error)]						
		Tiller/Onsøy	q_c	f_s	u_2	Cone resistance, q_c		Sleeve friction, f_s		Pore pressure, u_2	
						Tiller	Onsøy	Tiller	Onsøy	Tiller	Onsøy
1	17°C/15°C	11.70	0.120	0.120	140 (17.6 %)	81.9 (19 %)	1.4 (18 %)	0.8 (10.5 %)	1.4 (0.2 %)	0.8 (0.3 %)	
2	16°C/6°C	0.6	0.011	0.021	7 (0.8 %)	-1.2 (-0.3 %)	0.1 (1.5 %)	-0.02 (-0.3 %)	0.2 (0 %)	0 (0 %)	
3	14°C/15°C	5.5	0.49	-0.8	50 (6.2 %)	38.5 (9 %)	4.4 (55.1 %)	3.4 (42.9 %)	-7.2 (-0.9 %)	-5.6 (-1.9 %)	
4	-°C/15°C	5.5	0.49	-0.8	-	38.5 (9 %)	-	3.4 (42.9 %)	-	-5.6 (-1.9 %)	
5	14°C/15°C	5.5	0.49	-0.8	50 (6.2 %)	38.5 (9 %)	4.4 (55.1 %)	3.4 (42.9 %)	-7.2 (-0.9 %)	-5.6 (-1.9 %)	
6	18°C/0°C	NA	NA	NA	-	-	-	-	-	-	
7	19°C/0°C	2.1	0.04	0.68	29 (3.7 %)	-16.8 (-3.9 %)	0.6 (7 %)	-0.3 (-4 %)	9.5 (1.2 %)	-5.4 (-1.8 %)	
8	19°C/-°C	2.1	0.04	0.68	29 (3.7 %)	-	0.6 (7 %)	-	9.5 (1.2 %)	-	
12	14°C/-°C	5.5	0.49	-0.8	50 (6.2 %)	-	4.4 (55.1 %)	-	-7.2 (-0.9 %)	-	

ISO 22476-1:2012 (and Norwegian Geotechnical Society (NGF), Guideline No. 5, 2010) gives requirements for minimum allowable accuracy in terms of a specific value or percentage of the measured value. If a requirement for minimum allowable accuracy of 5 % of measured q_c is used as a criterion, cone type 1 does not meet the accuracy level at Tiller-Flotten. For Onsøy, no cone types meet this criterion except cone type 2. If, for f_s , a requirement of 10 % minimum allowable accuracy is used, four cones do not meet the requirement at both Tiller-Flotten and Onsøy sites. For the pore pressure, the effect of temperature change is very small compared to q_c and f_s .

Figures in Section 6 showed the variation in measured q_c , f_s and u_2 for all cone types at the 4 sites. For illustration purposes Table 7.5-2 gives the variations in ranges for ten of the cone types in absolute values in kPa and in % of the average reading at 8 m at the Tiller-Flotten, Onsøy and Halden sites. The number of tests carried out with one cone type at any of the sites vary from 2 to 4, and not all cone types have been used at all sites, therefore only some general trends will be commented upon. Red color indicates the range of measured values do not meet criteria for application class 1 in ISO 22476-1:2012.

For the two clay sites the variation in measured u_2 values are smaller than the variation in q_c , and the variation in f_s is largest. For the Halden silt site the variation in f_s values are about the same as the variation in q_c and u_2 . The reasons for this difference may be that the lateral variation is larger at this site and possibly also that the penetration is partially drained. For the sand site it is difficult to assess the level of accuracy given the lateral variability in soil behaviour. Higher cone resistance and sleeve friction were measured, and the observed scatter is of less significance compared to the clay sites.

Table 7.5-2 Ranges in measured values for the three sensor types at Tiller-Flotten, Onsøy and Halden

Cone type	Site	1	2	3	4	5	6	7	8	9	12	Unit		
q_c	Tiller-Flotten	130 (4)*	10 (3)	20 (2)	N/A	50 (4)	40 (4)	80 (3)	95 (3)	N/A	50 (2)	kPa		
		22.0	1.3	11.8	N/A	7.6	5.7	11.8	15.8	N/A	7.7	%		
	Onsøy	45 (4)	60 (3)	60 (2)	50 (4)	30 (4)	10 (3)	30 (2)	N/A	N/A	N/A	N/A	kPa	
		15	20	22	21	10	3.3	10	N/A	N/A	N/A	N/A	%	
	Halden	150 (3)	N/A	N/A	N/A	150 (3)	200 (2)	210 (3)	N/A	N/A	N/A	110 (2)	kPa	
		19.2	N/A	N/A	N/A	19	20	26	N/A	N/A	N/A	15	%	
	f_s	Tiller-Flotten	1.3	2.1	0.1	N/A	2.0	2.7	1.6	1.5	N/A	0.5	kPa	
			17.1	3.9	1.3	N/A	48.0	42.9	21.5	8.6	N/A	8.3	%	
		Onsøy	2	3	2.5	0.7	2	0.6	3	N/A	N/A	N/A	N/A	kPa
			31	41	31	11.1	21	16.2	33	N/A	N/A	N/A	N/A	%
		Halden	4	N/A	N/A	N/A	2.0	2.5	4	N/A	2	N/A	N/A	kPa
			22	N/A	N/A	N/A	20	25	24	N/A	22	N/A	N/A	%
u_2		Tiller-Flotten	21.0	63.0	4.0	N/A	51.0	21.0	6.0	20	N/A	40	kPa	
			3.0	9.1	0.6	N/A	7.5	3.2	0.8	3.1	N/A	5.7	%	
		Onsøy	30	10	25	15	10	35	5	N/A	N/A	N/A	N/A	kPa
			6.7	4.0	10	6.0	4.0	12.5	2.5	N/A	N/A	N/A	N/A	%
		Halden	45	N/A	N/A	N/A	50	50	45	N/A	10	N/A	N/A	kPa
			30	N/A	N/A	N/A	4.2	29	26	N/A	5.6	N/A	N/A	%

Notes: Number in bracket gives number of tests.

The figures in Section 7 illustrate the differences in average representative values for each cone type at all 4 sites covered in this report. In general, measured u_2 shows less variation for one cone type to another, while the corrected cone resistance shows somewhat larger variation. The sleeve friction, f_s , shows the largest variation. The friction ratio, F_r , shows much larger variation compared to the pore pressure parameter B_q .

Due to the large uncertainties with the f_s readings one should be careful using this parameter, and the friction ratio, when interpreting soil parameters for design. Since the measured u_2 values appear to frequently be the most reliable parameter it should be used in addition to q_t for deriving soil parameters.

Some major contributing factors to the uncertainties are reproduced from Lunne and Andersen (2007):

- ↗ Pore pressures acting on the ends of the friction sleeve. The effect depends on the actual areas at each end of the sleeve and the difference in pore pressure at top (u_3) and bottom (u_2) of cone. Normally u_3 is not measured, so correction can only be made by assuming the u_3/u_2 ratio.
- ↗ Distribution of the side friction behind the cone tip.
- ↗ Roughness of the sleeve surface.
- ↗ Amount of remoulding as a function of distance behind the cone tip.

8 Zero readings as function of time

Taking correct zero readings is an important part of CPTU in soft clays, since they are basic reference values for the rest of the tests. Since cone penetrometers are sensitive to temperature changes, the ideal procedure is to take the zero readings at the same temperature as in the ground. This may be done by taking the reference readings in a bucket with water of the same temperature as the ground. Unfortunately, taking zero reading in water with temperature like in situ temperature was only done for cone types 2, 9 and 10 at all the sites, as well as cone types 7 and 8 at the sand and quick clay sites. For the other cone types zero readings were taken at air temperature. Regardless of zero readings in water or air, all results except those from cone type 6 are corrected for temperature effects based on representative air temperature as discussed in Section 5.1.2.

To investigate the effect with time of temperature change on the zero readings, a study was performed in connection with tests done at the sand and quick clay sites with cone types 7 and 8. Before and after the tests, zero measurements in both air and water were frequently noted. At the quick clay site the measurements were noted for 15 minutes. At the sand site, the readings were generally noted until they stabilized, but for some tests the time to equilibrium was too long. The measurements were taken in air before they were made in water, both before and after the tests, except for TILC22 where the measurements after the test were performed in water before air.

The water should ideally have the same temperature as the in-situ ground temperature, but for some tests it was quite a bit higher. Table 8-1 shows the recorded air and water temperatures for all the tests. "-" indicates that no data was recorded. The in-situ temperature was assumed to be 5 °C for Tiller-Flotten and 6 °C at Øysand.

Table 8-1 Temperatures in water and air at calibration before and after tests. "-" indicates that no data was recorded.

Test ID	Before test		After test	
	Air temp.	Water temp.	Air temp.	Water temp.
TILC22	8	7	-	7
TILC23	22	11	24	-
TILC24	23	12	20	13
TILC25	20	11	-	9
TILC26	17	9	19	11
TILC27	21	11	26	11
OYSC43	14	7	13	7
Extra OYSC43	14	7		
OYSC44	7	7	-	-
Extra OYSC44	8	-		
OYSC45	14	8	16	7

Figures B1.1 to B1.18 in Appendix B show how the zero measurements stabilize with time. To fit all the tests into the same figures, results are shown as changes with respect to the first measurement in each series. For some of the tests the first measurement was either 20 or 40 seconds after the defined time zero. If the measurements are stable, the inclination of the graph should be zero.

Some stabilization measurements did not proceed a successful sounding, but the results are still valid. The graph "Extra OYSC43" in Figures B1.3 and B1.4 is the stabilization before a test which was unsuccessful due to no predrilling, but the zero-measurement stabilization before the test is still valid. "Extra OYSC44" shows stabilization in water. Since the time to stabilization seemed to be too long, the test was terminated before the start of the sounding. The whole process was restarted, and the subsequent sounding is OYSC44.

Some important observations may be noted from evaluating Figures B1.1 – B1.18. One is that not all zero readings have stabilized during the recorded period. Another is that some tests show relatively large change in readings during stabilization.

For the measurements of q_c it may be noted that in Figure B1.1 (air before test) TILC23 changes about 30 kPa until a relatively stable value is obtained after approximately 10 minutes. In Figure B1.3 (water before test) TILC23 stabilizes faster, but the change is about 90 kPa. In the same figure TILC25, OYSC43 and "Extra OYSC43" show a relatively large shift. TILC24 shows relatively large shift and has not stabilized after 15 minutes. In Figure B1.5 (air after test) TILC 23 has a shift of approximately 50 kPa until stabilizing after about 10 minutes. TILC25 has large shift and is not stable after 15 minutes. Figure B1.7 (water after test) indicate that the measurements are relatively stable after 3 minutes, and that the maximum shift is lower than for the other q_c graphs.

For the measurements of u_2 Figures B1.13 and B1.14 (air before test) show that the measurements generally have not stabilized within 15 minutes. The changes in values are however much smaller than for q_c . OYSC45 exhibits large shift in the first measurements, but then it stabilizes more smoothly. Figure B1.15 (water before test) show that most of the measurements have stabilized after 15 minutes. "Extra OYSC44" and OYSC45 have not stabilized after that time. Figures B1.16 and B1.17 (air after test) indicate relatively little stabilization after 15 minutes. TILC25 shows relatively large shift and no stabilization, while TILC23 is relatively stable but with quite much shift in the zero measurement. Figure B1.18 (water after test) show that all the measurements are relatively stable after 15 minutes, and the drift in the measurements are relatively small.

Figures B1.9 – B1.12 indicate that the zero measurements for sleeve friction are relatively constant with time and with change in temperature for the cone type tested.

The observations in the previous paragraphs show the importance of good procedures for taking zero readings. They indicate that the temperature of the cone may seriously

affect the readings. Also, they highlight the importance of waiting for the readings to stabilize at ground temperature. It is also clear that cone type 7 is less temperature stable compared to cone 8. It can also be seen that stabilization is quicker and more uniform when taking readings in water compared to taking readings in air.

9 Recommendations for future testing

The most important recommendation for future testing is that the requirements and recommendations given in ISO 22476-1:2012 (Geotechnical investigation and testing – Field testing – Part 1: Electrical cone and piezocone testing) and Norwegian Geotechnical Society (NGF) Guideline No. 5 (2010) are followed. Some key issues from these two documents are:

1. The thrust machine shall push the rods so that the axis of the pushing force is as close to vertical as possible. The deviation from the intended axis of the cone should be less than 2° .
2. The pore pressure measurement system shall be saturated to give good pore pressure response during penetration.
3. Especially for deep CPTUs it is important to correct the penetration length for inclination effects.
4. Recommended minimum distance between a CPT and adjacent boreholes is 2 m.

It is of course important to also follow the other requirements and recommendations given in the ISO standard (or NGF Guideline).

Other recommendations for testing in soft clays as have been confirmed in this study:

- a. The measured sleeve frictions are very small and vary significantly from one manufacturer to another. One should be careful with using the sleeve friction and friction ratio in design, unless local experience with one penetrometer type has given consistent correlations.
- b. Usually the penetration pore pressure is the most consistent measurement and it should be used for deriving soil parameters in addition to q_t
- c. If a soil investigation is planned as a follow up or continuation of a soil investigation carried out by a different contractor, it is recommended to plan 1 or 2 new tests adjacent to tests from the previous investigation. In this way the effect of cone penetrometer type can be evaluated.

Zero readings are to be taken before and after each test with the cone penetrometer at a temperature as close as possible to ground temperature. It is important to wait until the readings have stabilized before taking zero readings. For future testing the following procedure is suggested when testing onshore in very soft clay where accurate readings are essential:

At the start of a testing campaign, place the cones to be used in a bucket of water with temperature as in the ground. Monitor zero readings with time to check the time needed to fulfil the following criteria:

- ↗ *Change in $q_c < 5$ kPa in last 5 min period*
- ↗ *Change in $f_s < 0.5$ kPa in last 5 min period*
- ↗ *Change in $u_2 < 1$ kPa in last 5 min period*

Use the longest stabilizing time for q_c , f_s and u_2 to take zero readings before the start of each new test. After each test, place the cone in a bucket of water again and take zero readings until the criteria listed above is satisfied.

10 Summary and conclusions

Using cone penetrometers from different manufacturers may yield different results even if the equipment complies with international standards. The establishment of five new test sites in Norway, each with characteristic material type, has given the opportunity to revisit the problem of uncertainties in CPTU test results. Twelve different penetrometers from five manufacturers were tested at the soft clay site, silt site, quick clay site and sand site. A total of eighty-seven cone penetration tests have been included in this study. Three cone manufacturers carried out the testing themselves while NGI or NPRA carried out the remaining tests.

The initial plan was that at least 3 tests should be carried out no closer than 2 m apart with each penetrometer at each of the test sites. Not all the tests were carried out in accordance with the initial plan and the results are described and analyses as performed at each site.

For the soft clay and quick clay sites, some cone types showed significantly lower q_c and f_s values compared to other tests. Based on previous experience it was suspected that zero shift due to temperature difference between air and soil could contribute significantly to this scatter. Based on that, the results from all four sites were corrected for temperature effects. This significantly decreased the scatter in the data. To eliminate this uncertainty, it is recommended to take zero readings with the cone penetrometer at a temperature as close as possible to ground temperature as recommended by ISO 22476-1:2012. If this is not the case, it is recommended to use cone specific temperature calibration to correct for temperature effects.

Regarding tests with the same cone type, this study suggests that the penetration pore pressure, u_2 , provides the most repeatable results. The corrected cone resistance, q_t , generally varies somewhat more than u_2 . Some of the cone types give good repeatability for sleeve friction, f_s , while some show relatively large variation. These conclusions are valid for all test sites. Comparing results from different cone types reveal that the penetration pore pressure generally produces less scatter compared to the corrected cone resistance and sleeve friction. The measured sleeve frictions are very small for soft soils and vary significantly from one cone type to another, which is in line with previous experience. Hence one should be careful using sleeve friction, and the friction ratio, when interpreting soil parameters for design in soft soils. Since the measured u_2 appears to be the most reliable parameter, it should be used in addition to q_t for deriving soil parameters.

One of the tested cones use a slot filter. It should be noted that this cone gives different u_2 values compared to the remaining cones for the soft clay site, the silt site and the quick clay site. The results show that filter saturation is poor in the start of some tests and this could be improved as emphasized by ISO 22476-1:2012. Following the ISO code it is recommended to carry out the testing with a minimum distance between a CPT and adjacent boreholes of 2 m. The thrust machine should push the rods so that the axis

of the pushing force is as close to vertical as possible. The deviation from the intended axis of the cone should be less than 2° .

For some of the tests at the soft clay sites, measured sleeve friction, not corrected for temperature, can be as low as zero. For subtraction cones, the measured values may be this low due to the way the sleeve friction is calculated. A small offset in the measured cone resistance may lead to erroneous values of sleeve friction. As remedy it is suggested to correct the cone resistance and resistance behind sleeve for temperature effects before doing the subtraction.

The early results from this study showed the importance of taking correct zero readings, especially in soft soils. Some cone penetrometers are sensitive to temperature changes and it was decided to study the time necessary to get stable readings of the cone resistance, sleeve friction and penetration pore pressure. Zero readings with time were monitored before and after eleven cone penetration tests at the quick clay site and the sand site. The penetrometers were placed in a bucket of water and in free air.

The results show the importance of good procedures for taking zero readings and indicate that cone temperature may seriously affect the readings. The importance of waiting for the readings to stabilize at ground temperature is evident from the results. It was also observed that stabilization is quicker and more uniform when taking readings in water compared to taking readings in air. To obtain stable zero readings close to ground temperature, the following procedure is recommended when testing onshore in very soft clay where accurate readings are essential:

At the start of a testing campaign, place the cones to be used in a bucket of water with temperature as in the ground. Monitor zero readings with time to check the time needed to fulfil the following criteria:

- ↴ *Change in $q_c < 5$ kPa in last 5 min period*
- ↴ *Change in $f_s < 0.5$ kPa in last 5 min period*
- ↴ *Change in $u_2 < 1$ kPa in last 5 min period*

Use the longest stabilizing time for q_c , f_s and u_2 to take zero readings before the start of each new test. After each test, place the cone in a bucket of water again and take zero readings until the criteria listed above is satisfied.

11 Acknowledgements

Pagani, Geotech and Geomil contributed by performing the tests with their CPTU equipment. NPRA and NGI carried out the remaining tests using other CPTU equipment. The authors would like to acknowledge the Research Council of Norway (RCN) for funding the Norwegian GeoTest Site project (No. 245650/F50).

12 References

- Blaker, Ø., Carroll, R., & L'Heureux, J. S. (2016). Characterisation of the Halden silt.
- Blaker Ø, Carroll R, Paniagua Lopez AP, et al. (2019) Halden research site: geotechnical characterization of a post glacial silt. *AIMS Geosci* 5: 184–234.
- Cabal, K. & Robertson, P.K. (2014). Accuracy and Repeatability of CPT Sleeve Friction Measurements. Proc. CPT'14, Las Vegas, Nevada, USA.
- Gauer, P., Lunne, T., Mlynarek, Z., Wolynski, W. & Croll, M. (2002). Quality of CPTu -Statistical analyses of CPTu data from Onsøy. NGI Report No.: 20001099-2, Oslo.
- Gerland & Villing (1995). Nondestructive density determination on marine sediment cores from gamma-ray attenuation measurements. *Geo-Marine Lett.* 15: 111-118.018.
- Gundersen AS, Hansen RC, Lunne T, et al. (2019) Characterization and engineering properties of the NGTS Onsøy soft clay site. *AIMS Geosci* 5: 665–703.
- Hammer, H.B. (2019). Accuracy of CPTUs in deltaic sediments and the effect of cone penetrometer type. Project thesis—TBA4510. Norwegian University of Science and Technology. Trondheim, Norway.
- ISO 22476-1:2012. Geotechnical investigation and testing—Field testing—Part, 1.
- Jamiolkowski, M., Lo Presti, D. C. F., & Manassero, M. (2003). Evaluation of relative density and shear strength of sands from CPT and DMT. In *Soil behavior and soft ground construction* (pp. 201-238).
- L'Heureux, J.S. & Lunne, T. (2019): Characterization and Engineering properties of Natural Soils used for Geotesting. *AIMS Geosciences*, 5(4): 940-959.
- L'Heureux, J.S., Lindgård, A. & Emdal, A. (2019). The Tiller-Flotten research site: Geotechnical characterization of a sensitive clay deposit. *AIMS Geosci* 5: 831–867.
- Lindgård, A., Gundersen, A., Lunne, T., L'Heureux, J.S., Kåsin, K., Haugen, E., Emdal, A., Carlson, M., Veldhuijzen, A. & Siviero, M. (2018). Effect of cone type on measured CPTU results from Tiller-Flotten quick clay test site.
- Lunne, T., Eidsmoen, T., Gillespie, D., Howland, J.D. (1986). Laboratory and field evaluation of cone penetrometers. Use of In Situ Tests in Geotechnical Engineering: Proceedings of In Situ '86, a specialty conference, American Society of Civil Engineers. Blacksburg, Va. 1986, pp. 714-729. Also publ. in: Norwegian Geotechnical Institute, Oslo. Publication, 171, 1988.
- Lunne T, Long M, Forsberg CF (2003). Characterisation and engineering properties of Onsøy clay. *Charact Eng Prop Nat Soils* 1: 395–427.
- Lunne, T. (2010). The CPT in offshore soil investigations; Keynote lecture. International Symposium on Cone Penetration Testing, 2. Huntington Beach, Ca. 2010. Proceedings, Vol. 1, pp. 71-113.
- Lunne, T., Strandvik, S. O., Kåsin, K., L'Heureux, J. S., Haugen, E., Uruci, E. & Kassner, M. (2018). Effect of cone penetrometer type on CPTU results at a soft clay test site in Norway. In *Cone Penetration Testing IV: Proceedings of the 4th International Symposium on Cone Penetration Testing (CPT 2018)*, June 21-22, 2018, Delft, The Netherlands.
- NGTS (2018a). Norwegian GeoTest Sites (NGTS) – Field and laboratory test results Halden. NGTS Report No. 20160154-04-R.
- NGTS (2018b). Norwegian GeoTest Sites (NGTS) – Factual report Øysand research site. NGTS Report No. 20160154-08-R
- NGTS (2018c). Norwegian GeoTest Sites (NGTS) – Field and laboratory test results, NGTS soft clay site – Onsøy. NGTS Report No. 20160154-10-R.

NGTS (2018d). Norwegian GeoTest Sites (NGTS) – Factual report Tiller research site. NGTS Report No. 20160154-19-R.

Powel, J.P. and Lunne, T. (2005). A comparison of different sized piezocones in UK clays. International Conference on Soil Mechanics and Foundation Engineering, 16. Osaka 2005. Proceedings, Vol. 2, pp. 531-536.

Tiggelman, L. & Beukema, H.J. (2008). Sounding ring investigation. Proc. ISC-3, Taiwan, pp. 757-762.

Appendix A

INDIVIDUAL CPTU RESULTS

Contents

A1	Soft clay site – Onsøy	2
A2	Silt site – Halden	25
A3	Sand site – Øysand	38
A4	Quick clay site – Tiller-Flotten	64

A1 Soft clay site – Onsøy

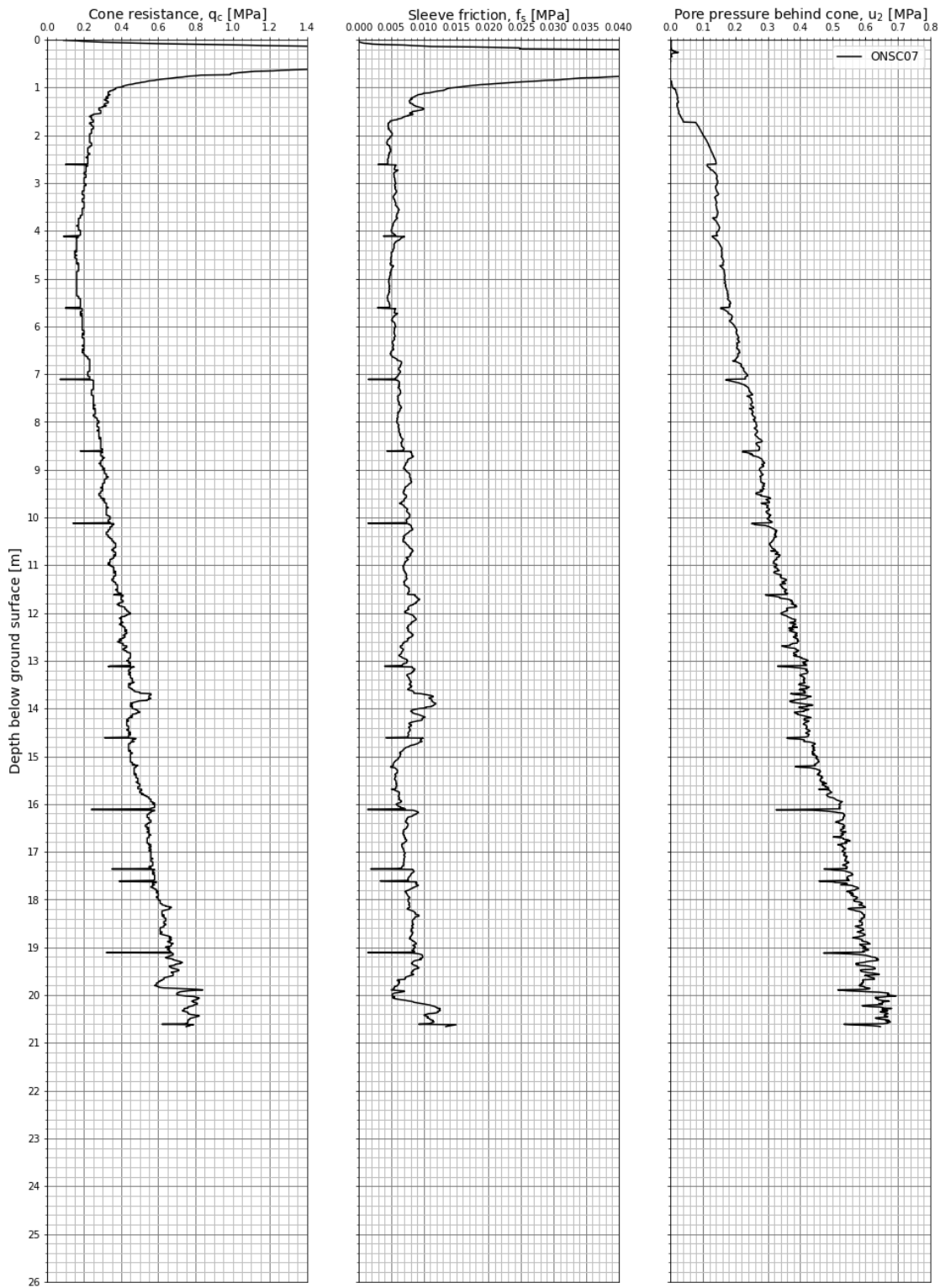


Figure A1.1 Measured cone resistance, sleeve friction and pore pressure – ONSC07.

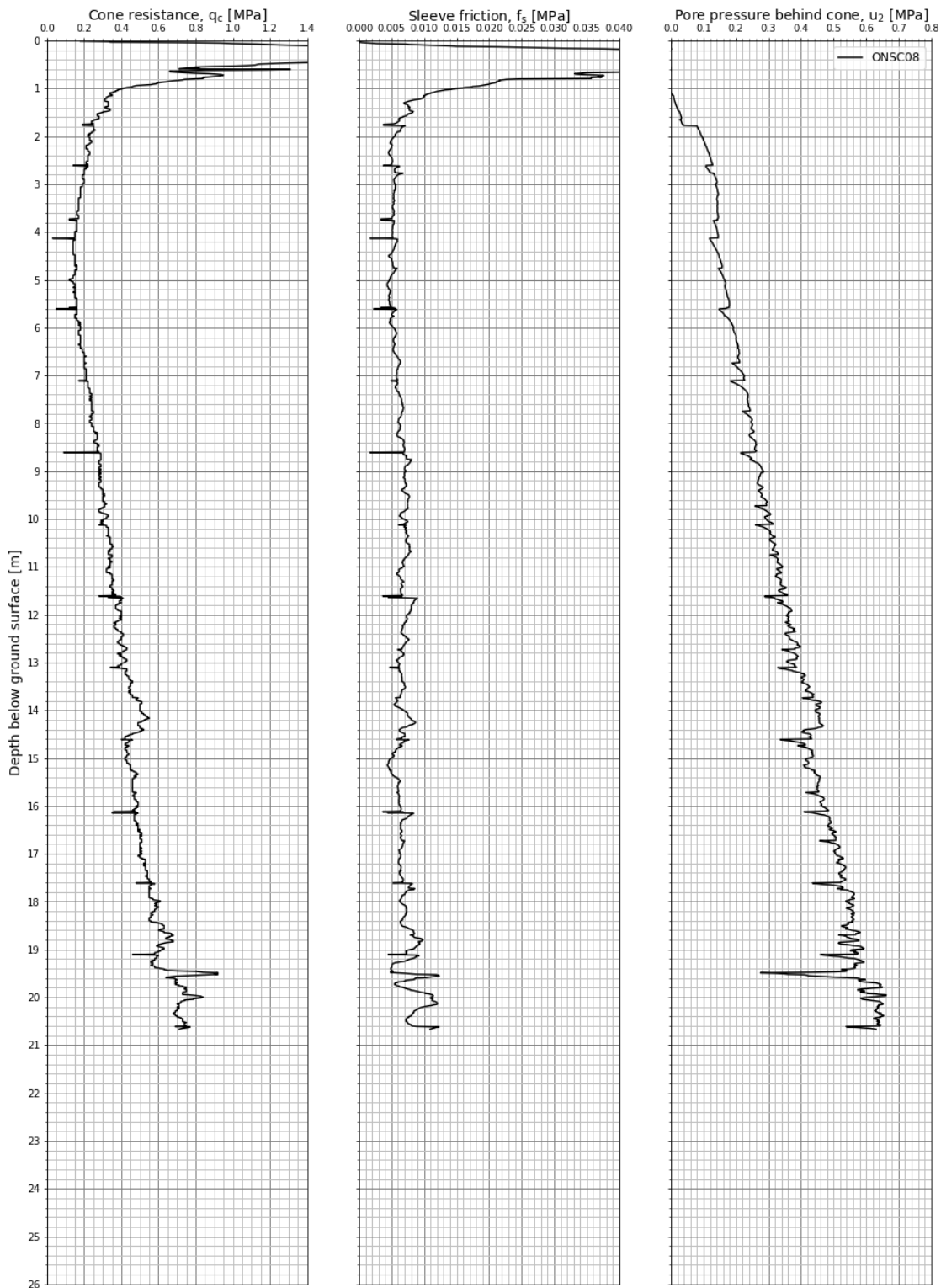


Figure A1.2 Measured cone resistance, sleeve friction and pore pressure – ONSC08.

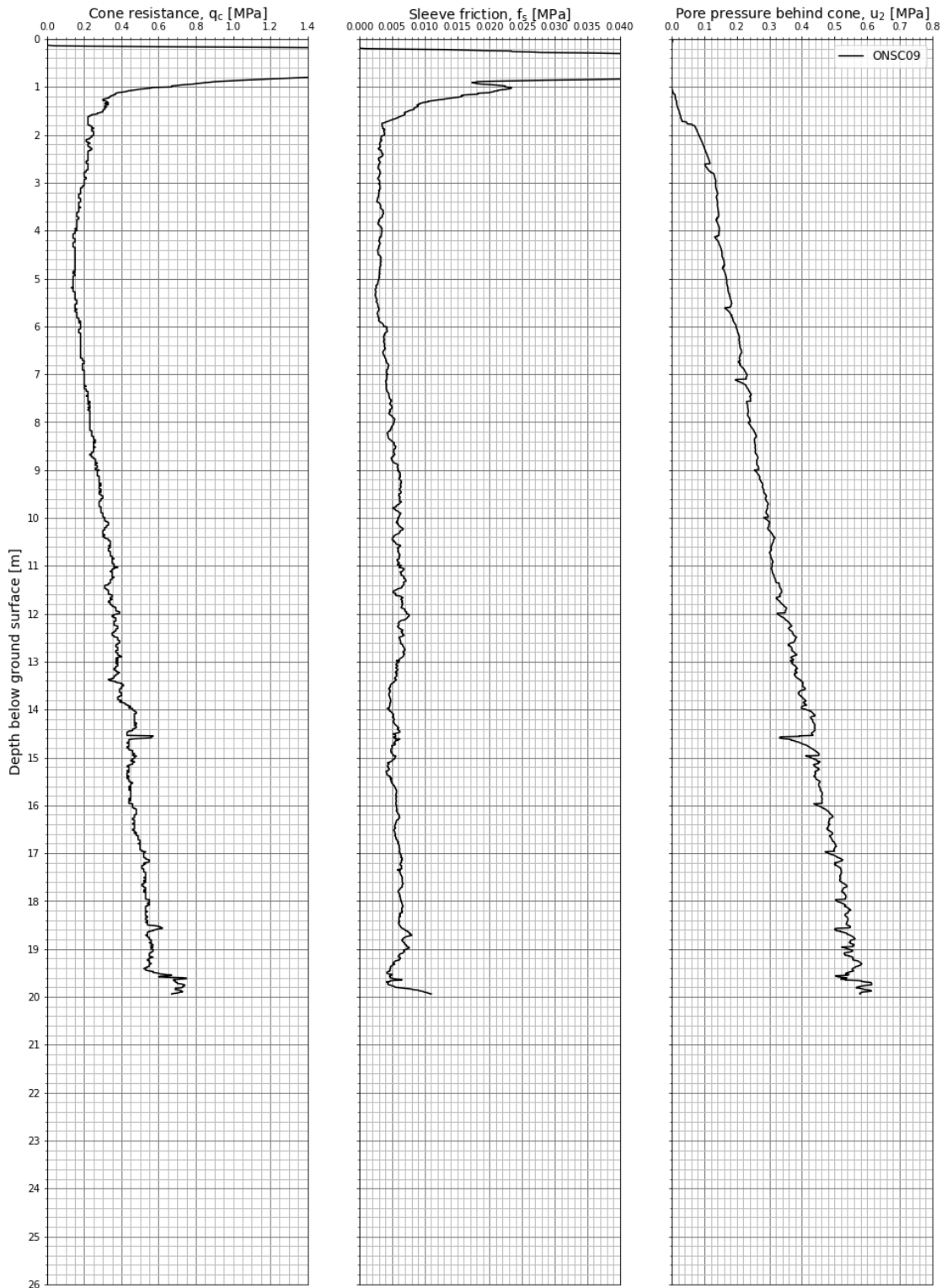


Figure A1.3 Measured cone resistance, sleeve friction and pore pressure – ONSC09.

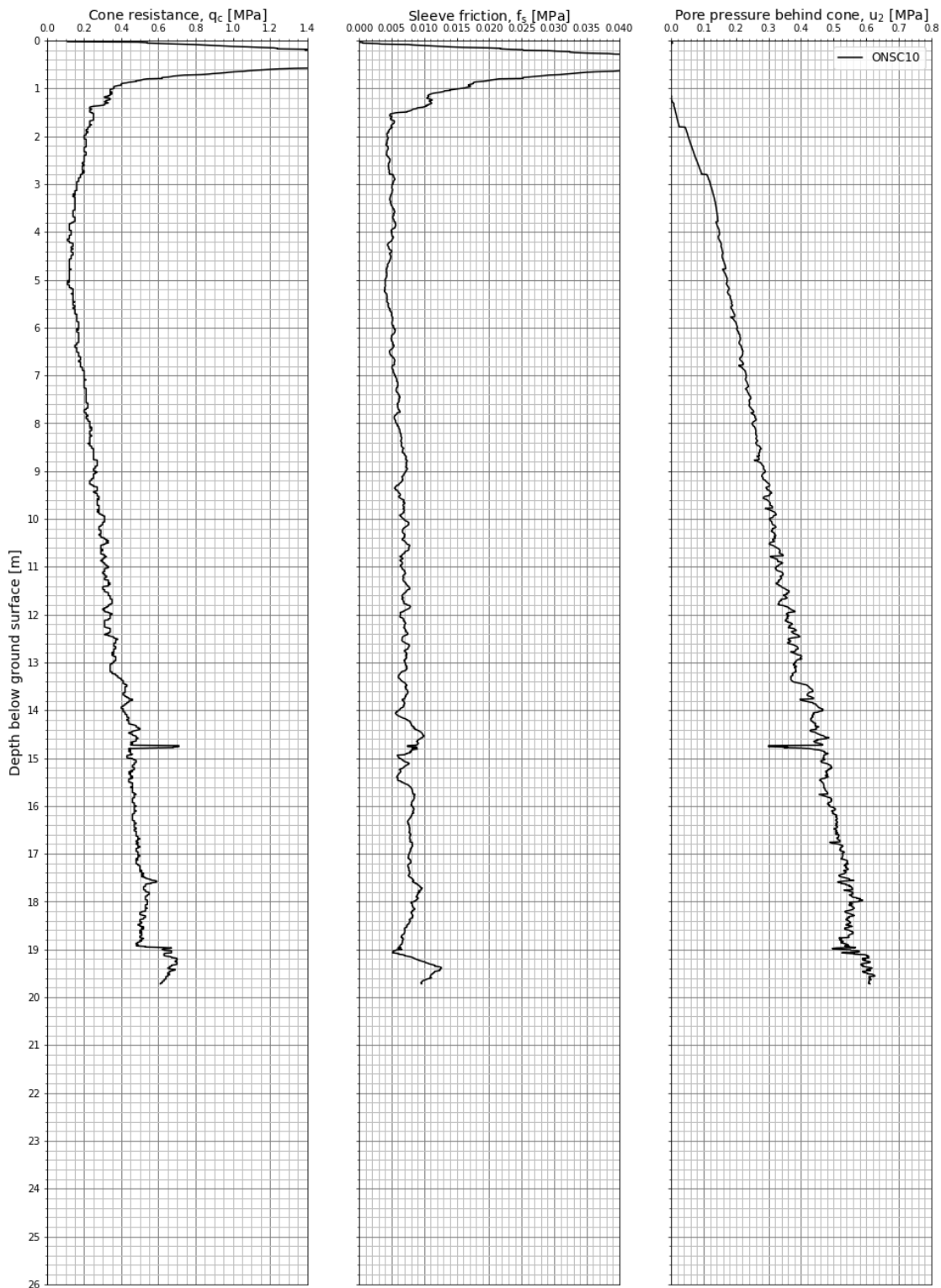


Figure A1.4 Measured cone resistance, sleeve friction and pore pressure – ONSC10.

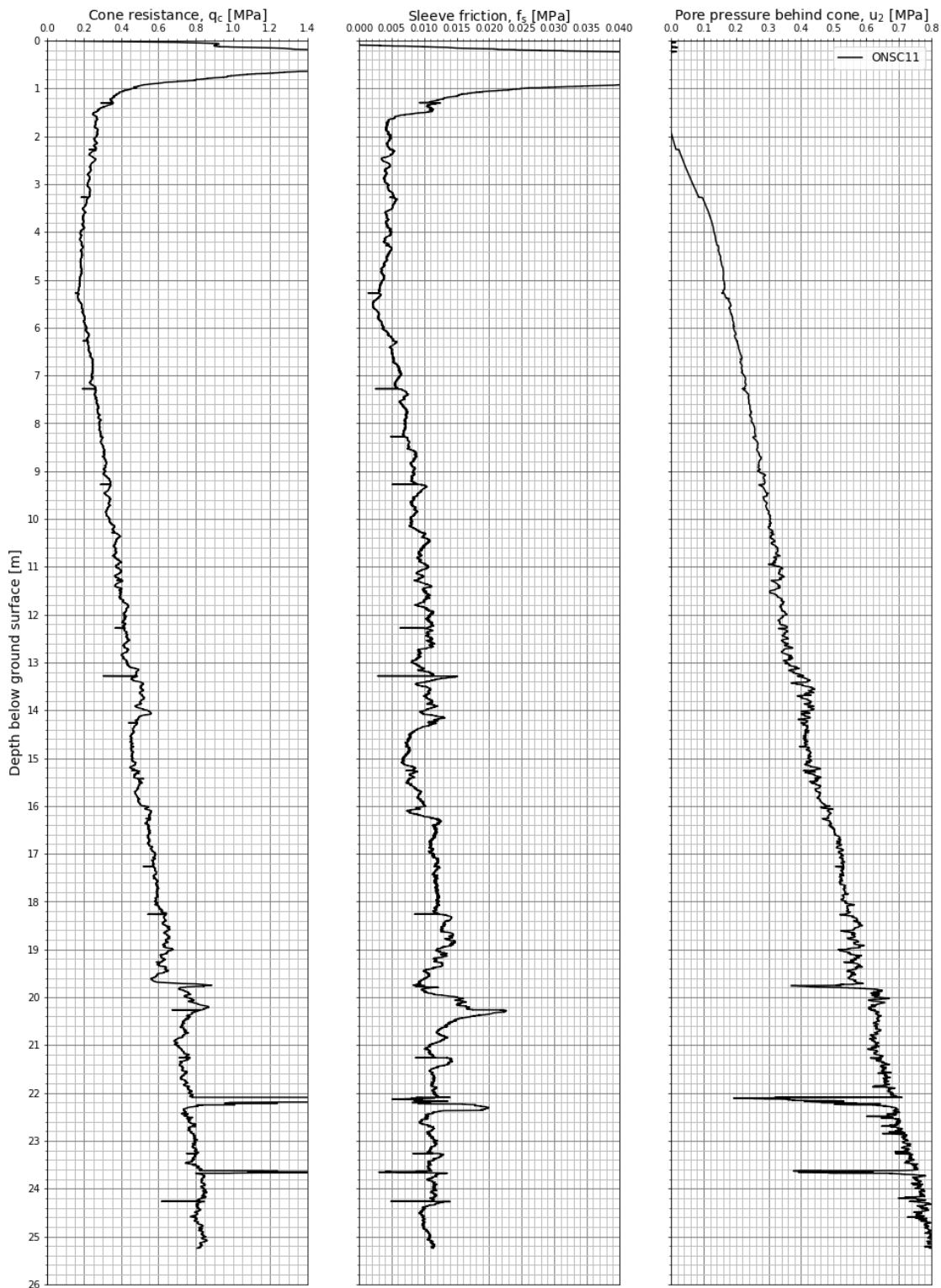


Figure A1.5 Measured cone resistance, sleeve friction and pore pressure – ONSC11.

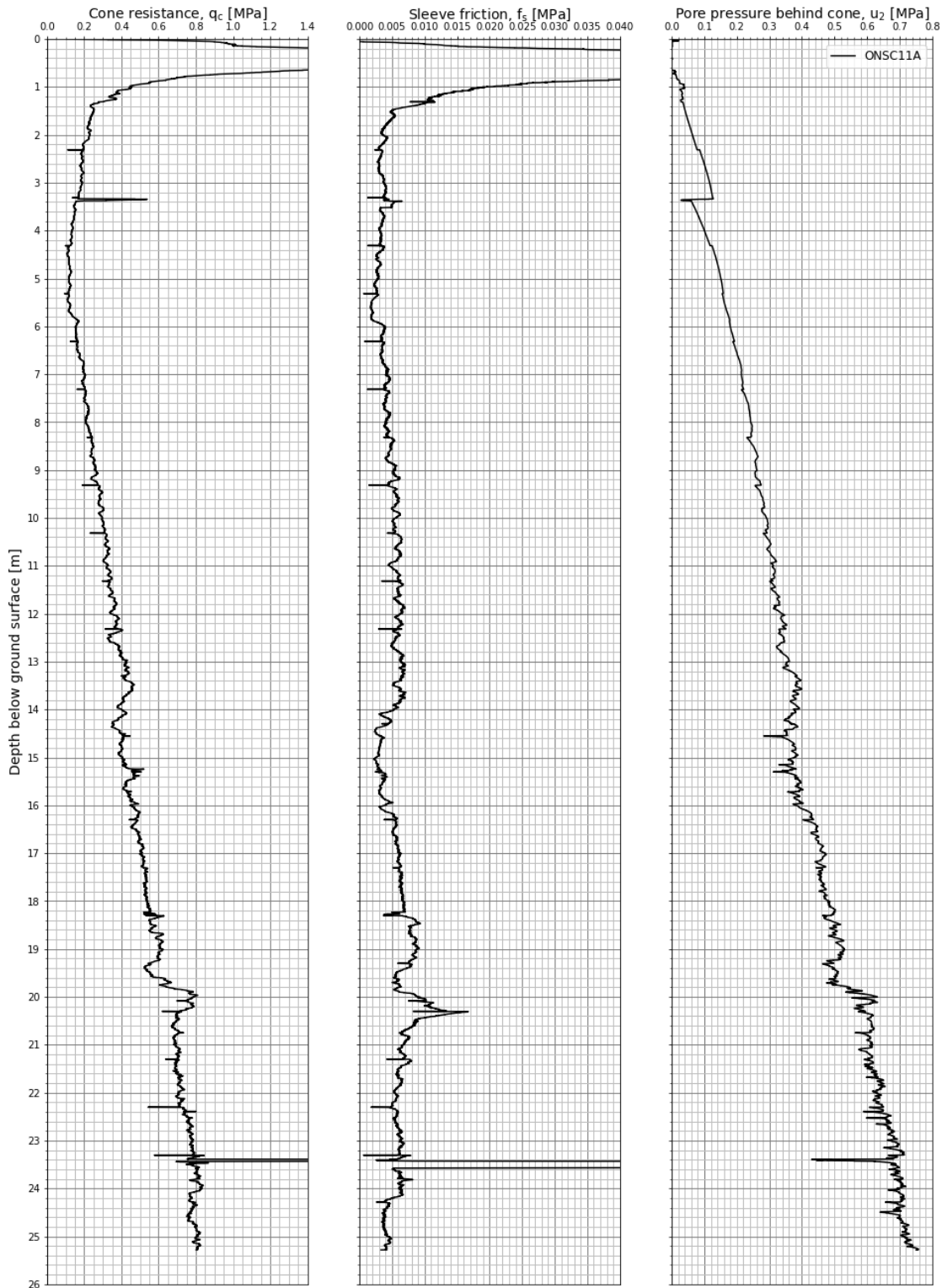


Figure A1.6 Measured cone resistance, sleeve friction and pore pressure – ONSC11A.

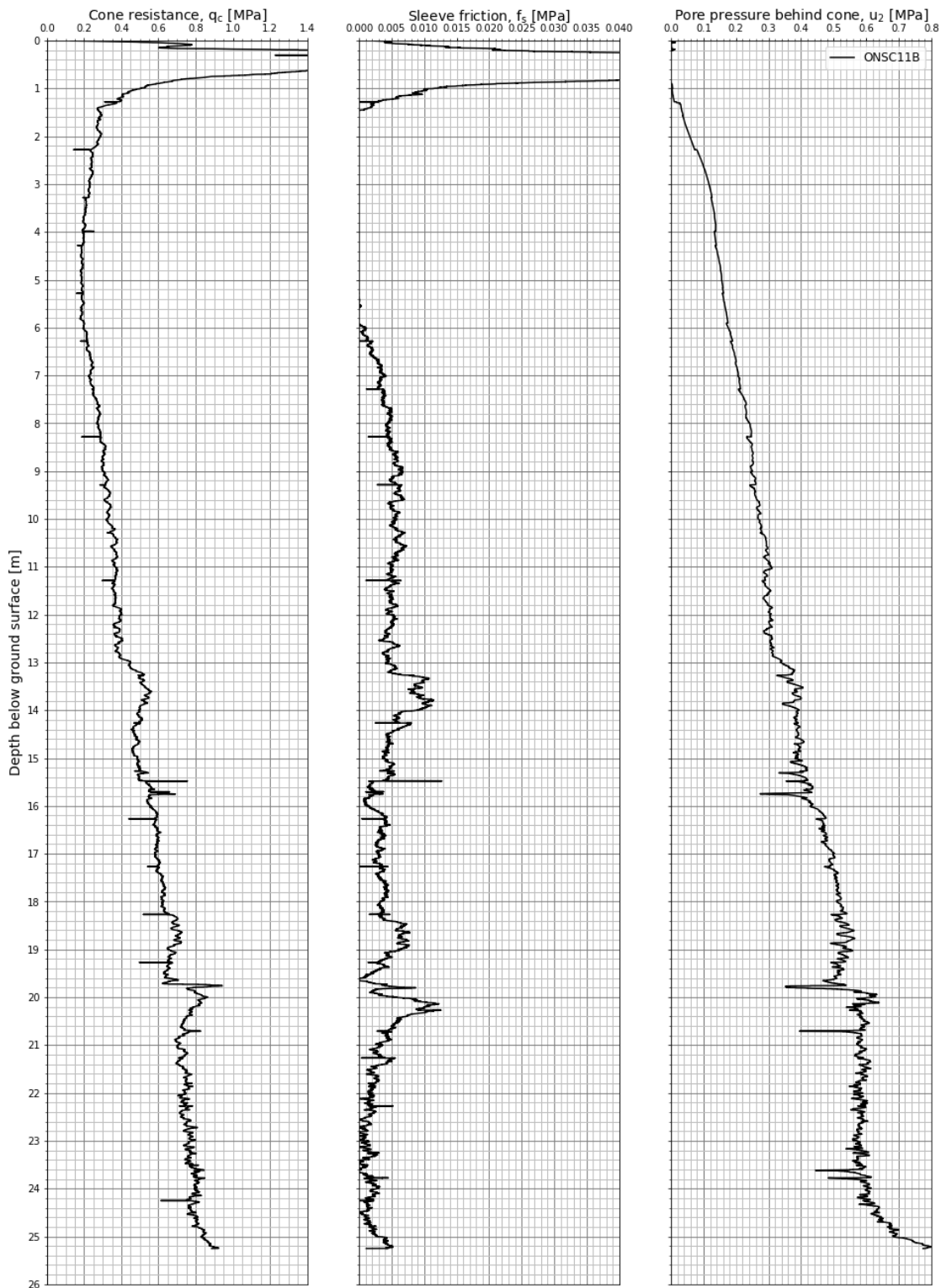


Figure A1.7 Measured cone resistance, sleeve friction and pore pressure – ONSC11B.

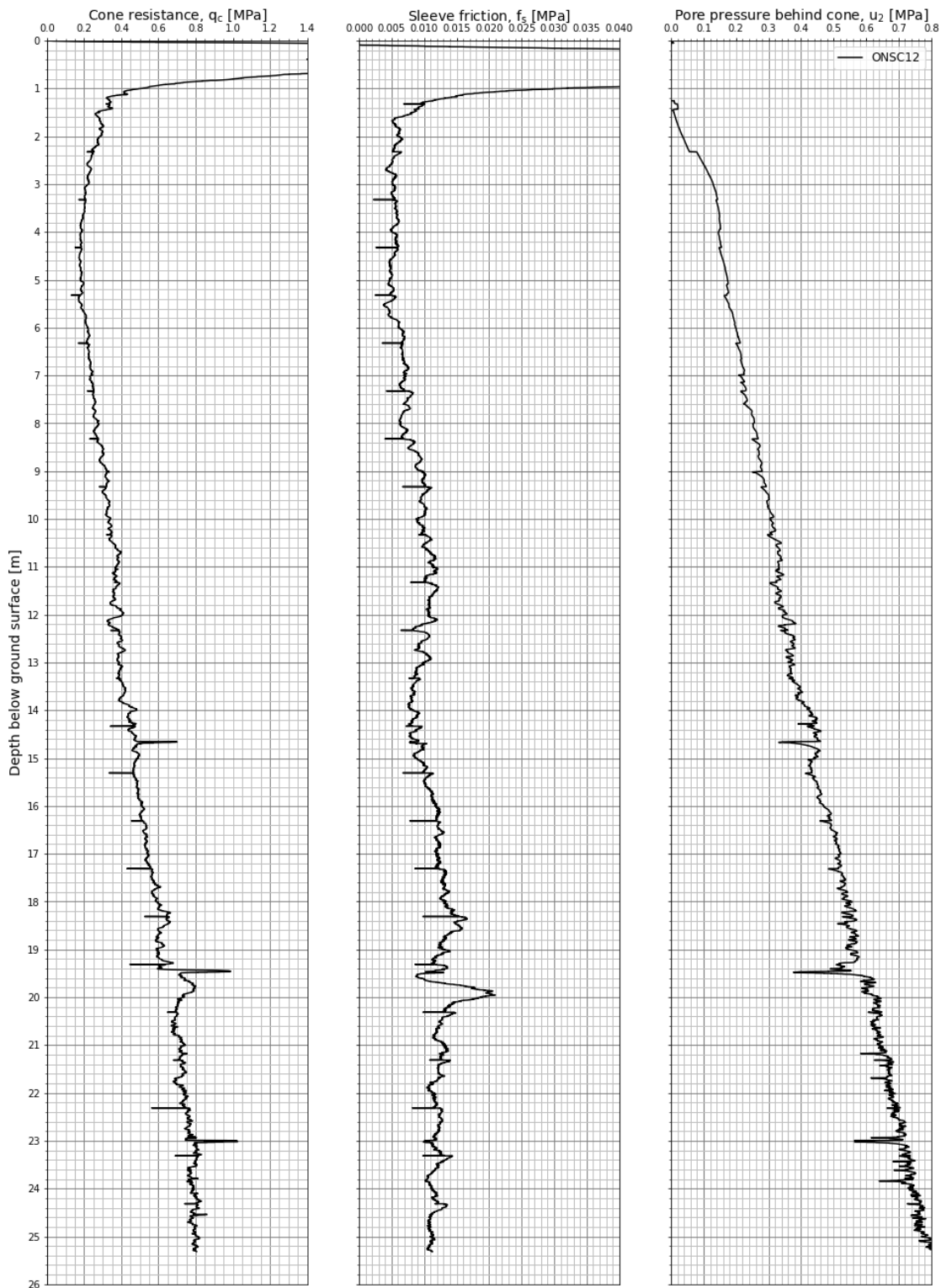


Figure A1.8 Measured cone resistance, sleeve friction and pore pressure – ONSC12.

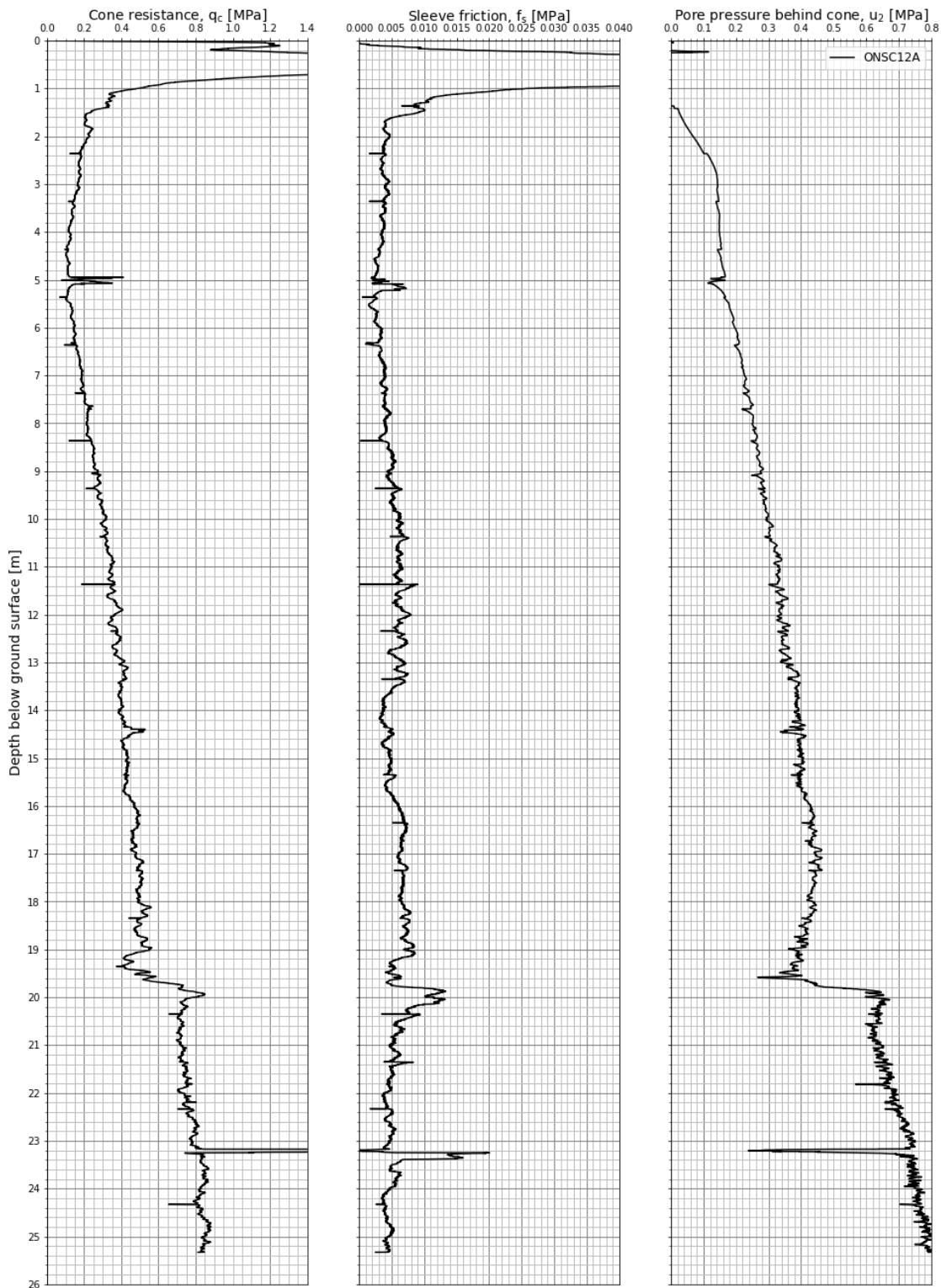


Figure A1.9 Measured cone resistance, sleeve friction and pore pressure – ONSC12A.

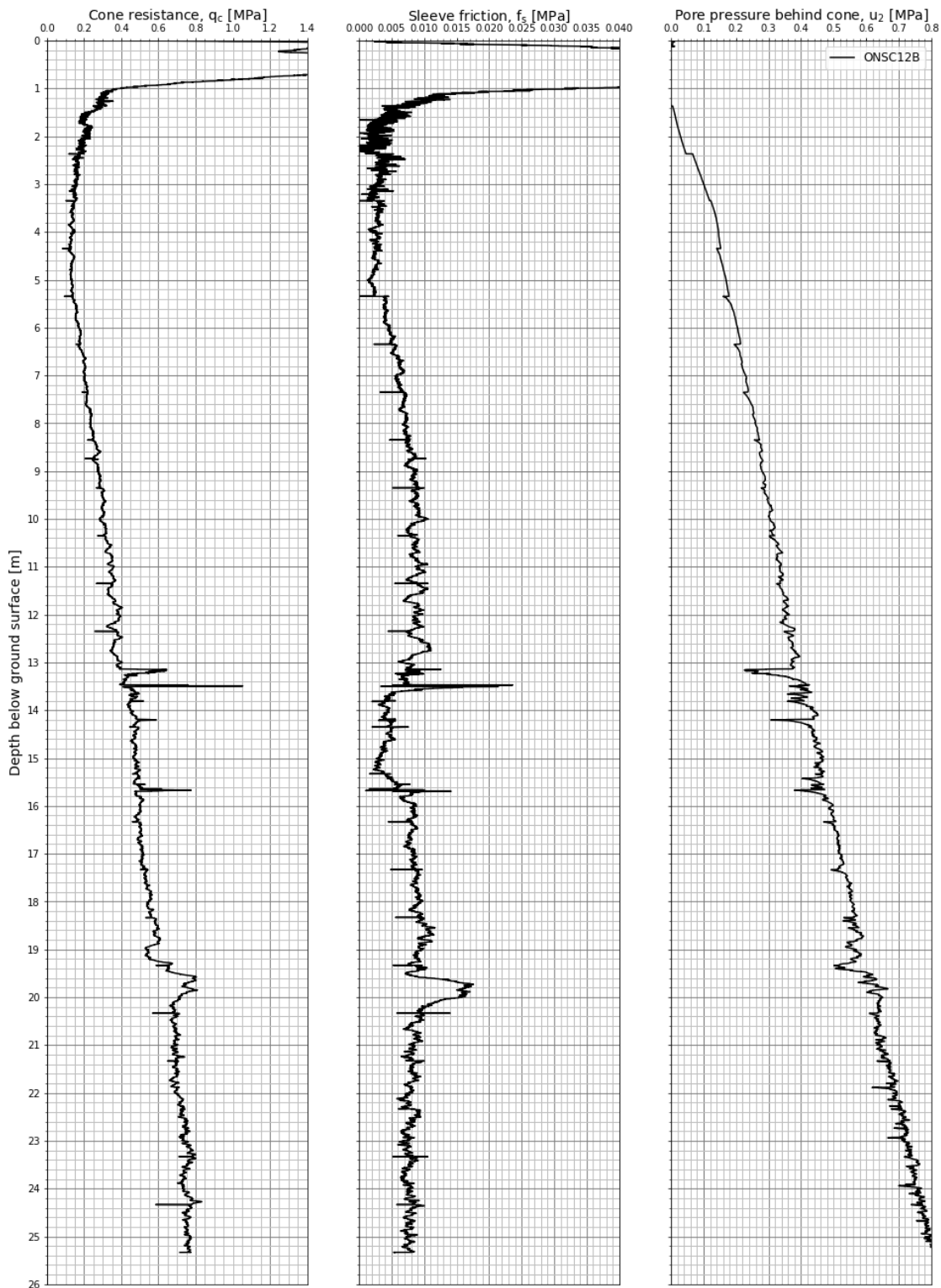


Figure A1.10 Measured cone resistance, sleeve friction and pore pressure – ONSC12B.

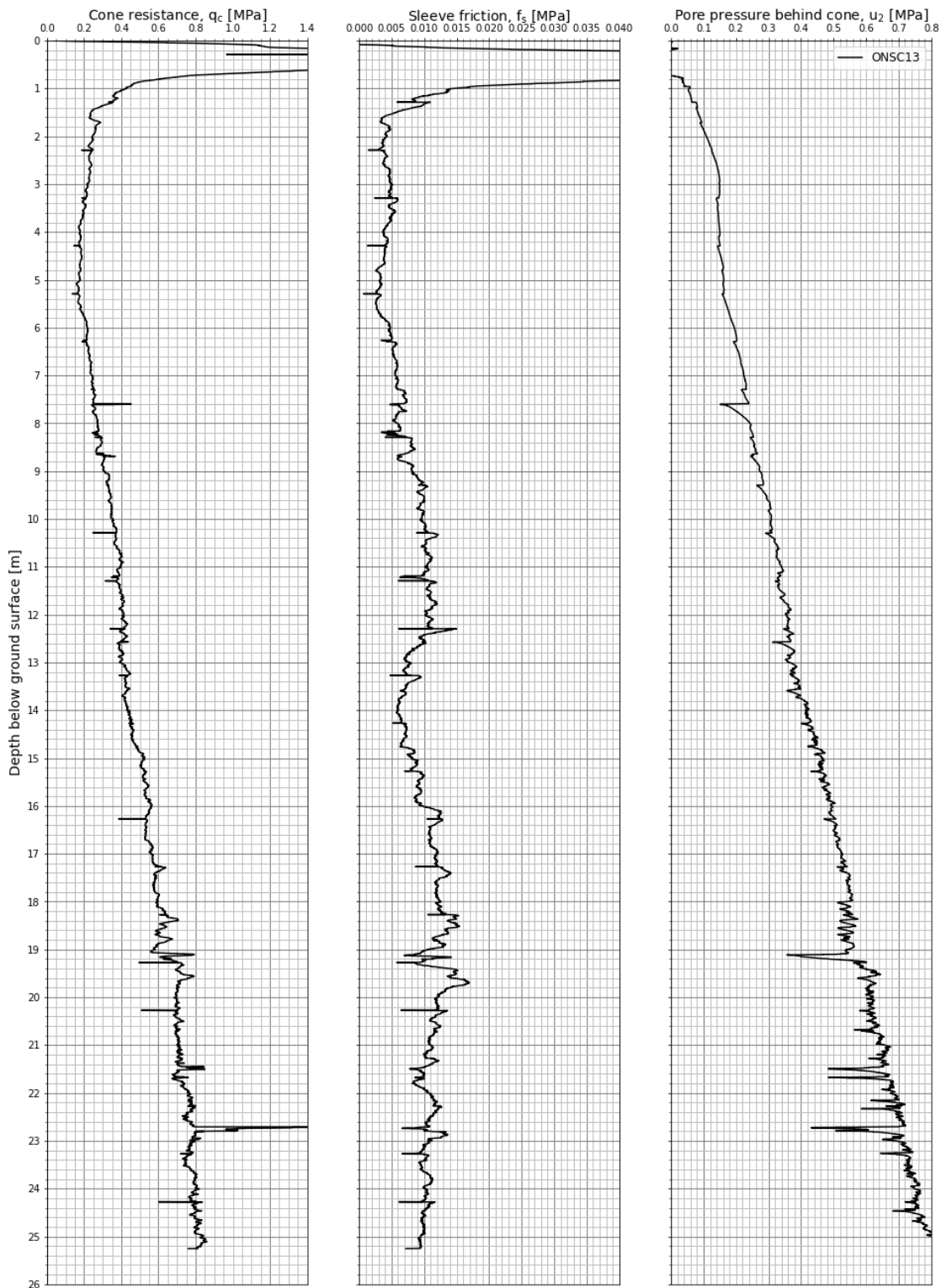


Figure A1.11 Measured cone resistance, sleeve friction and pore pressure – ONSC13.

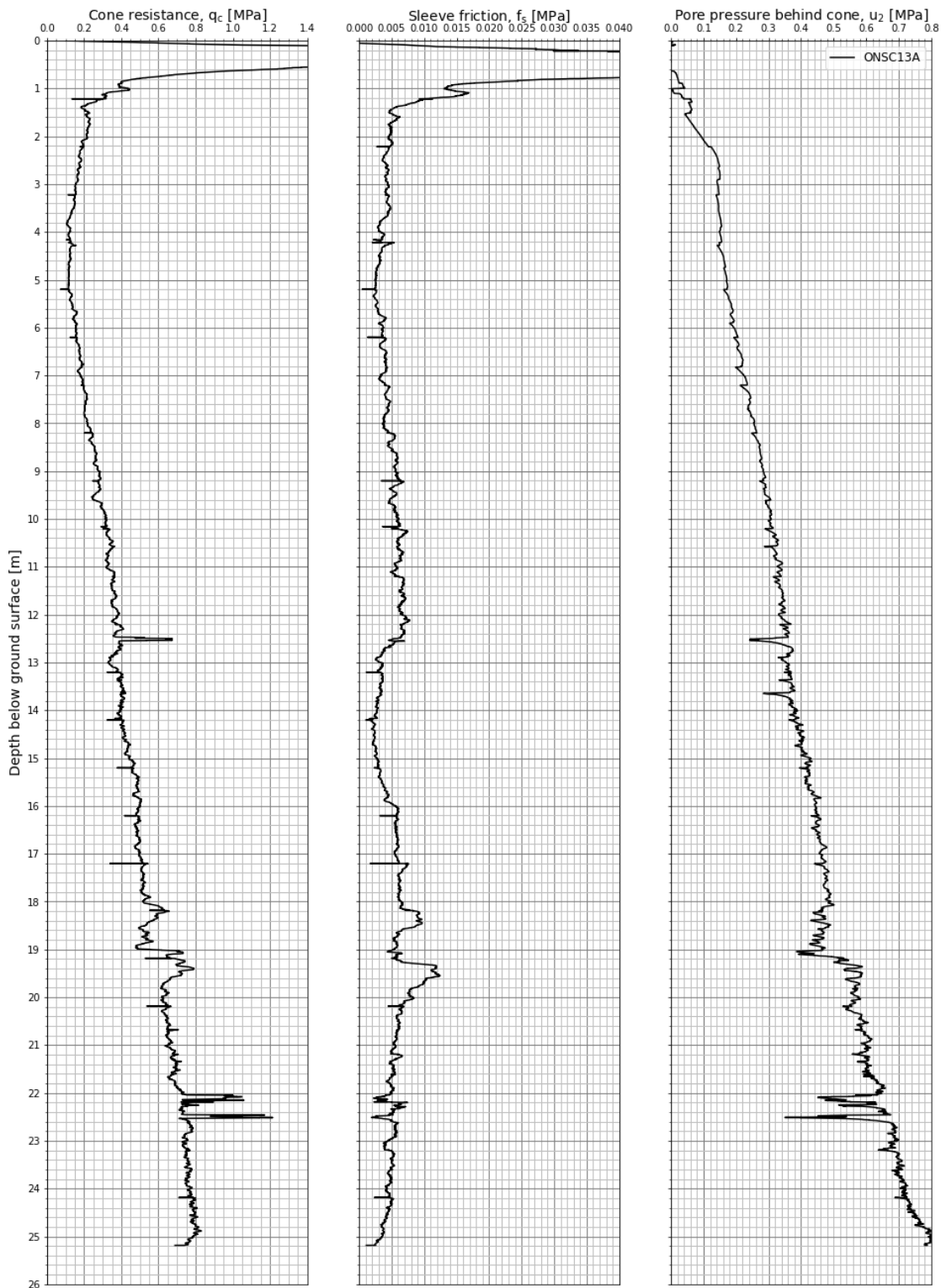


Figure A1.12 Measured cone resistance, sleeve friction and pore pressure – ONSC13A.

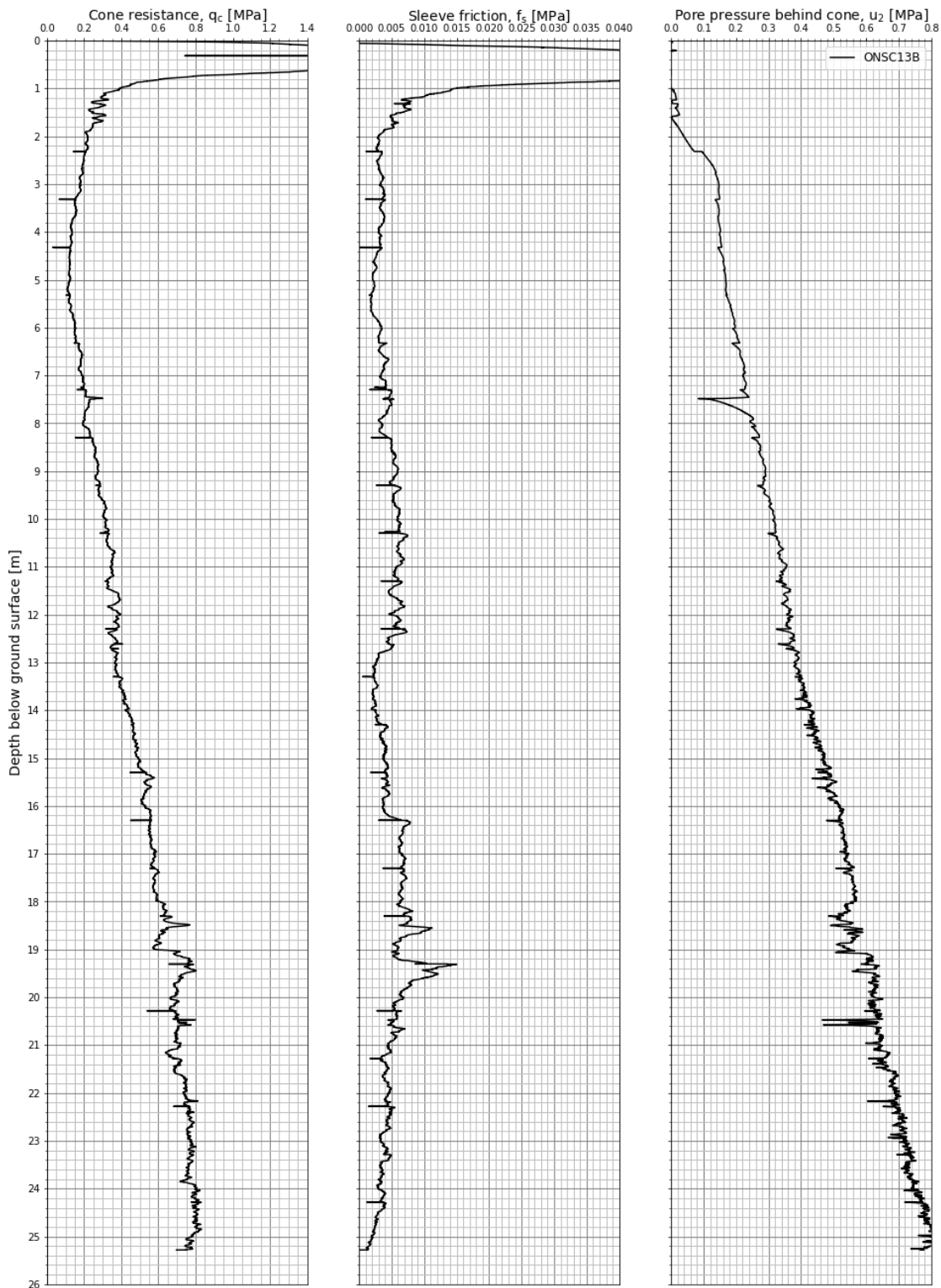


Figure A1.13 Measured cone resistance, sleeve friction and pore pressure – ONSC13B.

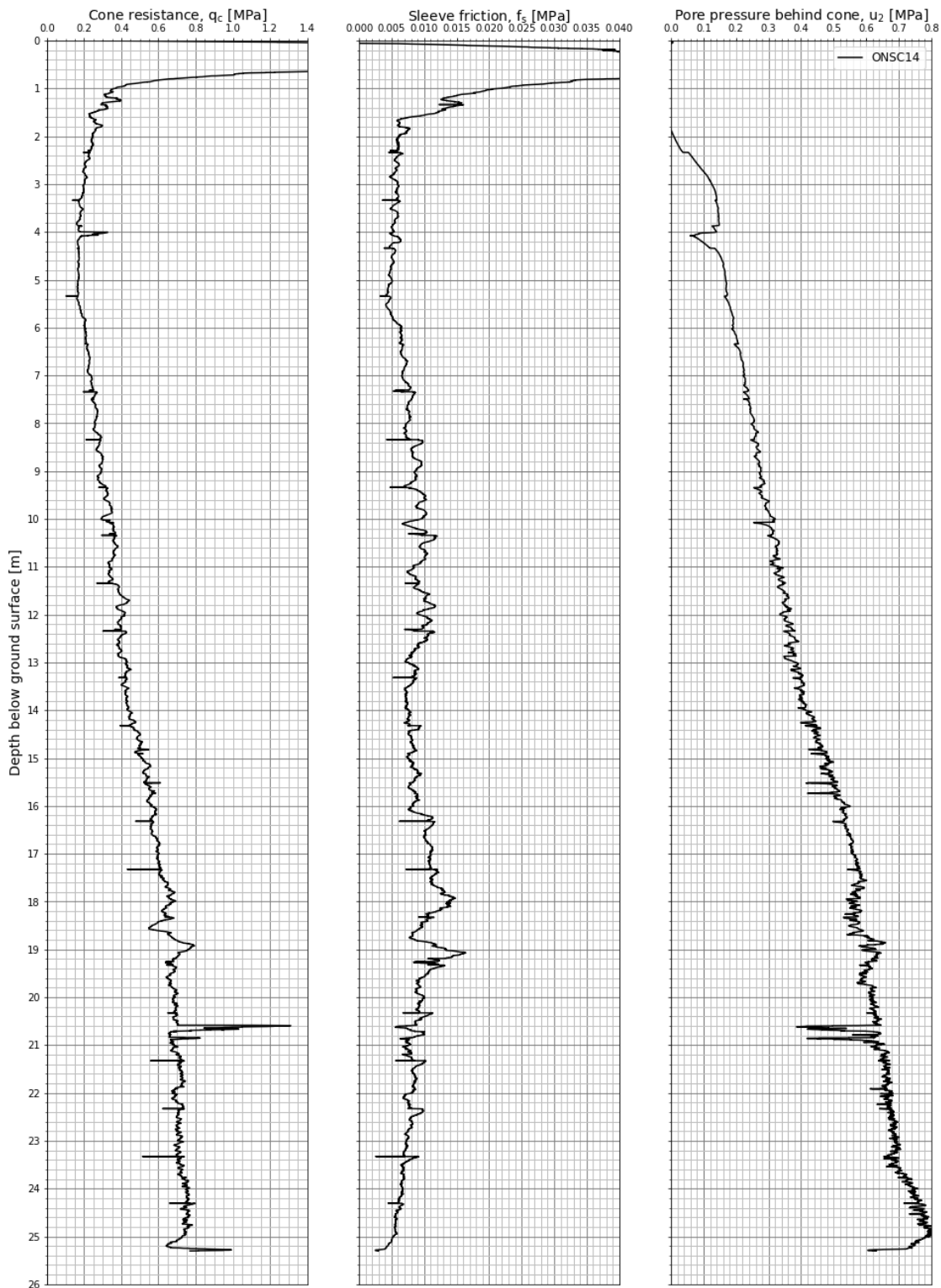


Figure A1.14 Measured cone resistance, sleeve friction and pore pressure – ONSC14.

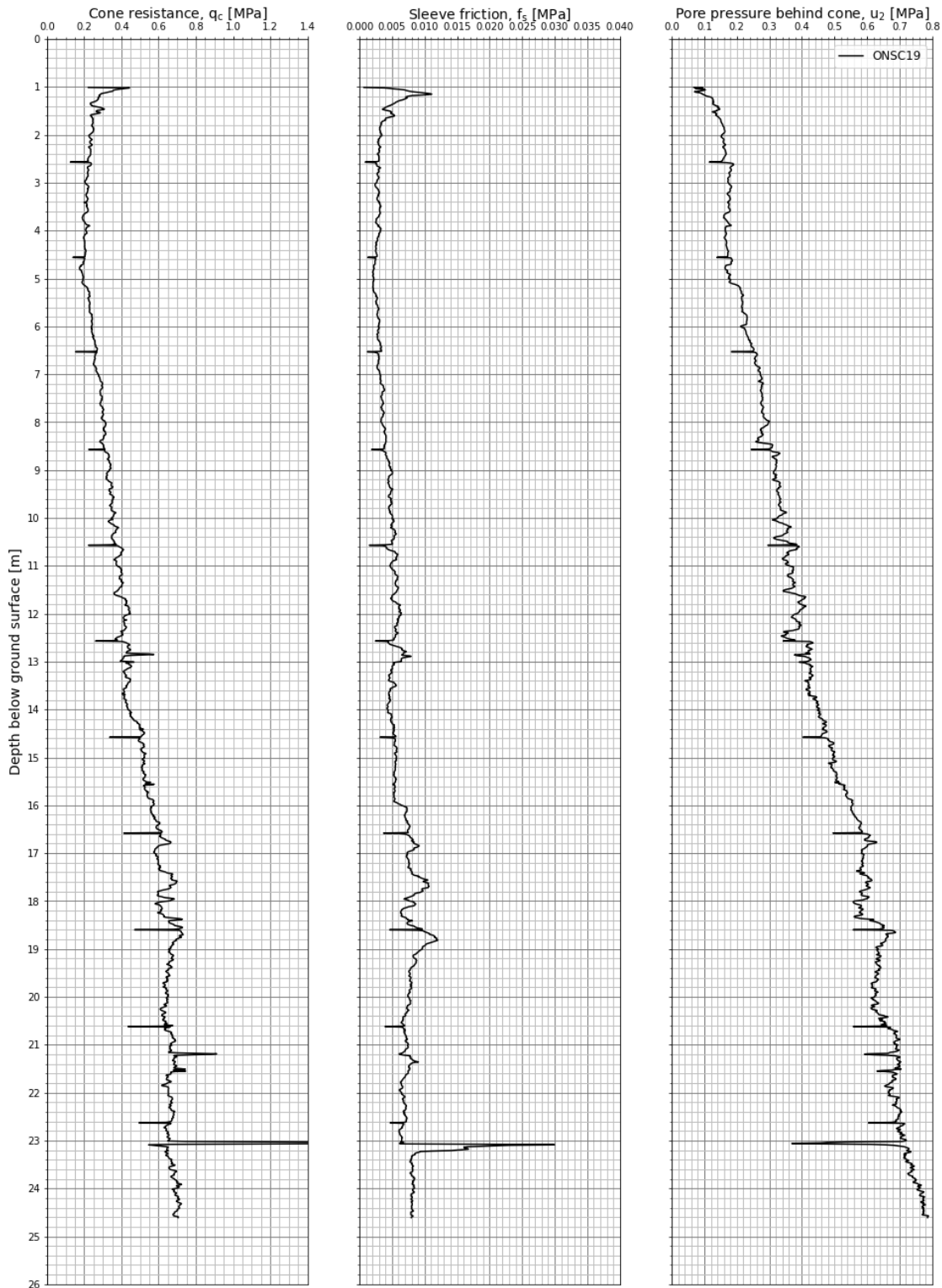


Figure A1.15 Measured cone resistance, sleeve friction and pore pressure – ONSC19.

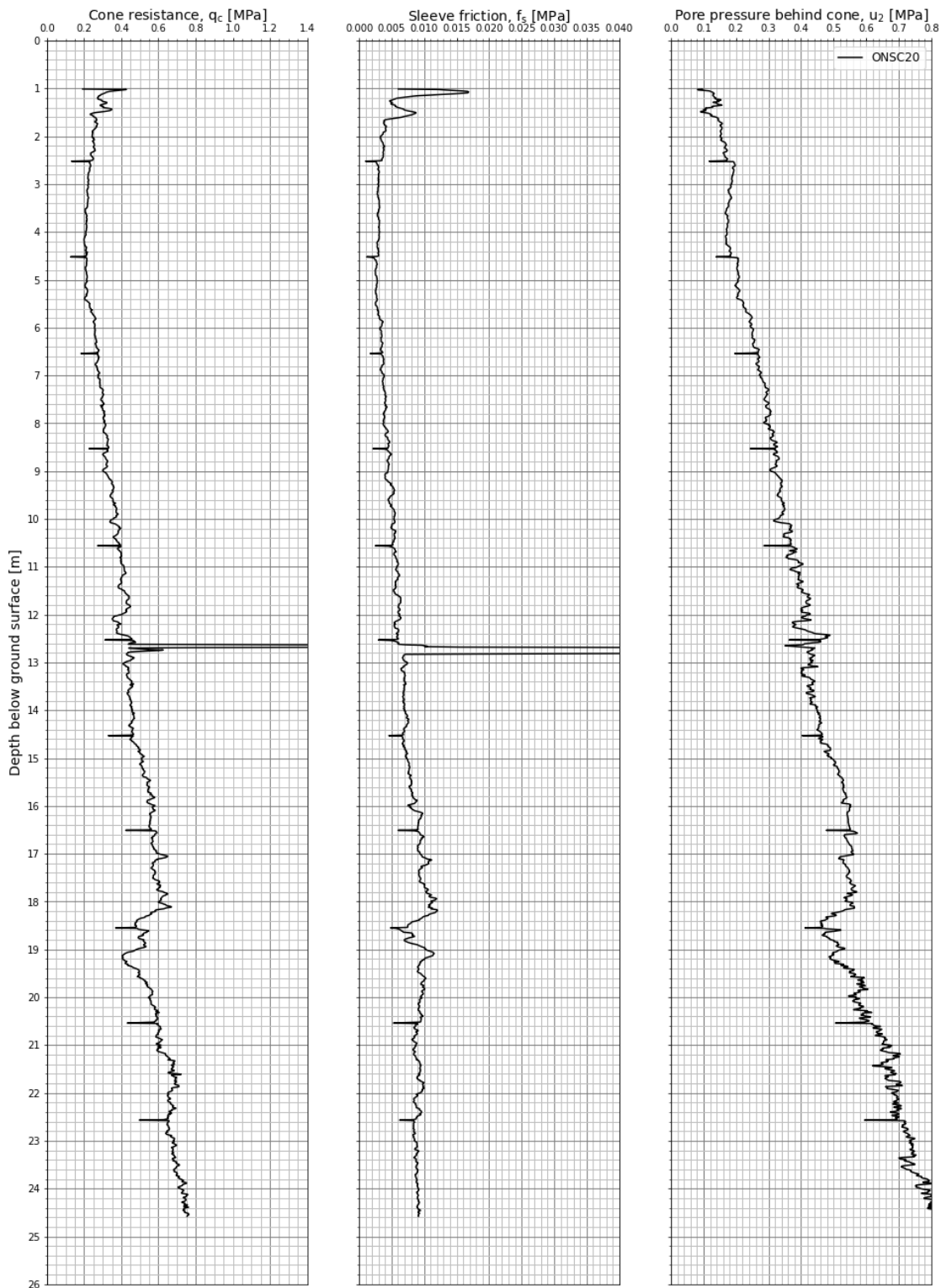


Figure A1.16 Measured cone resistance, sleeve friction and pore pressure – ONSC20.

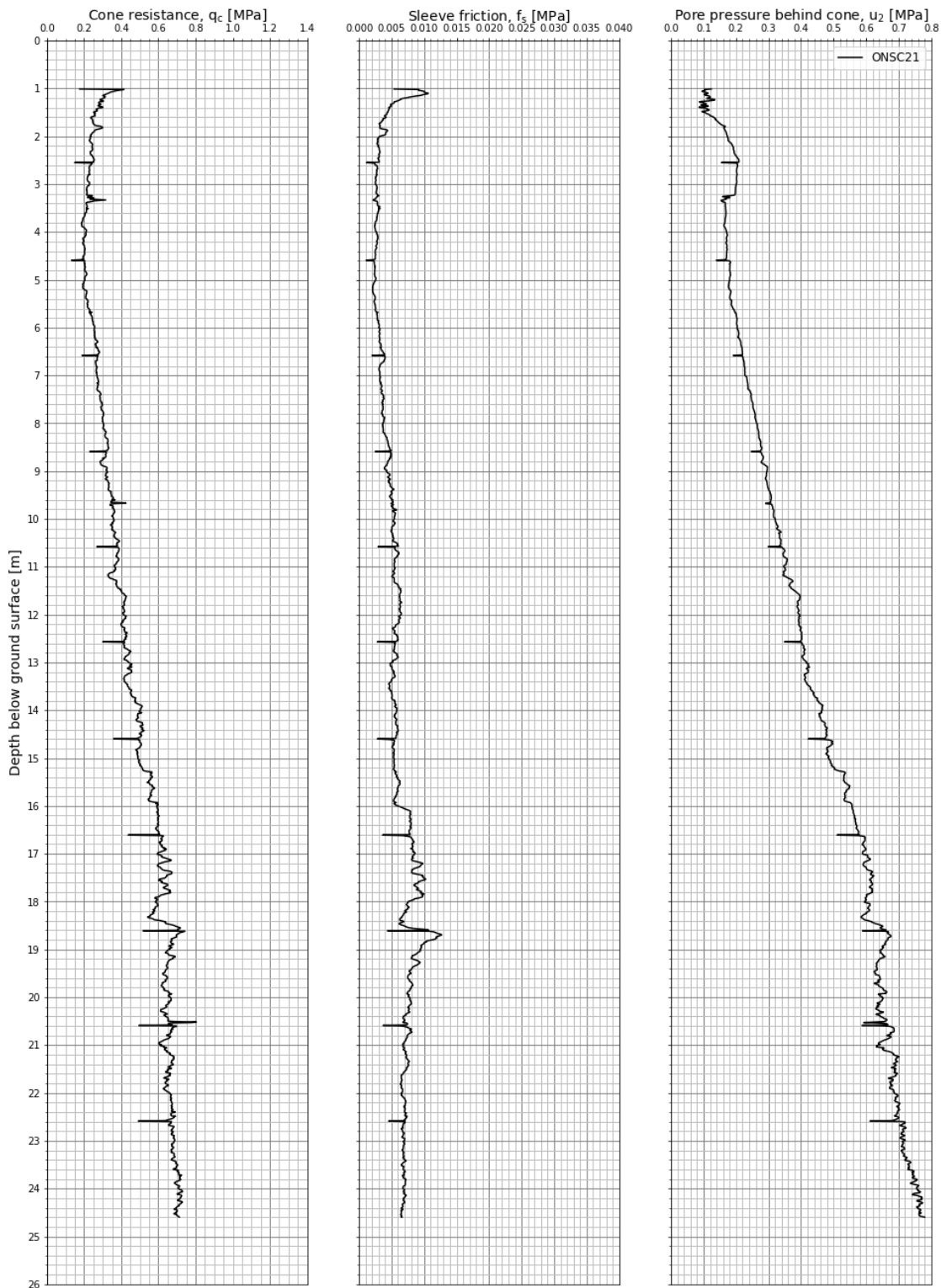


Figure A1.17 Measured cone resistance, sleeve friction and pore pressure – ONSC21.

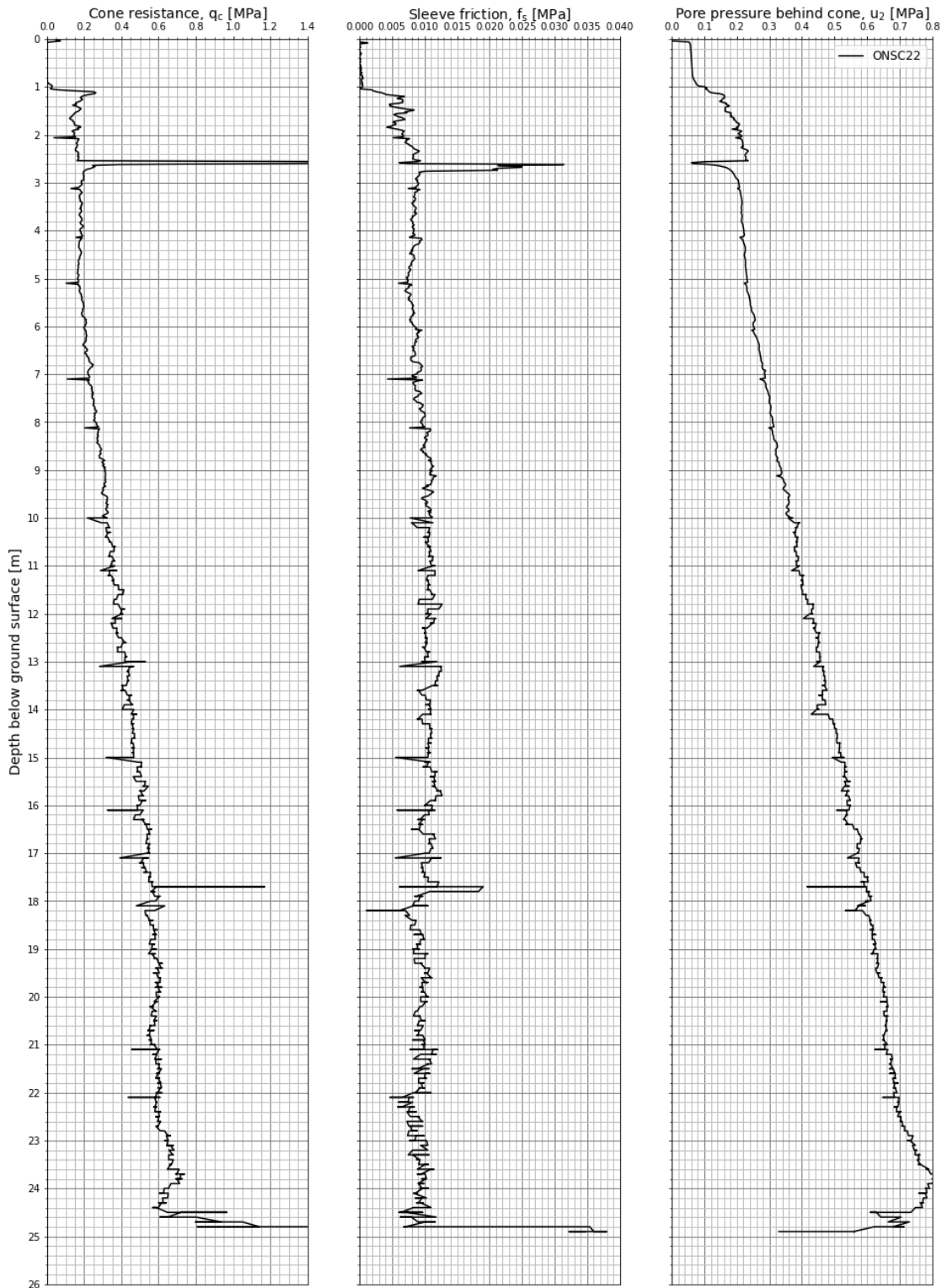


Figure A1.18 Measured cone resistance, sleeve friction and pore pressure – ONSC22.

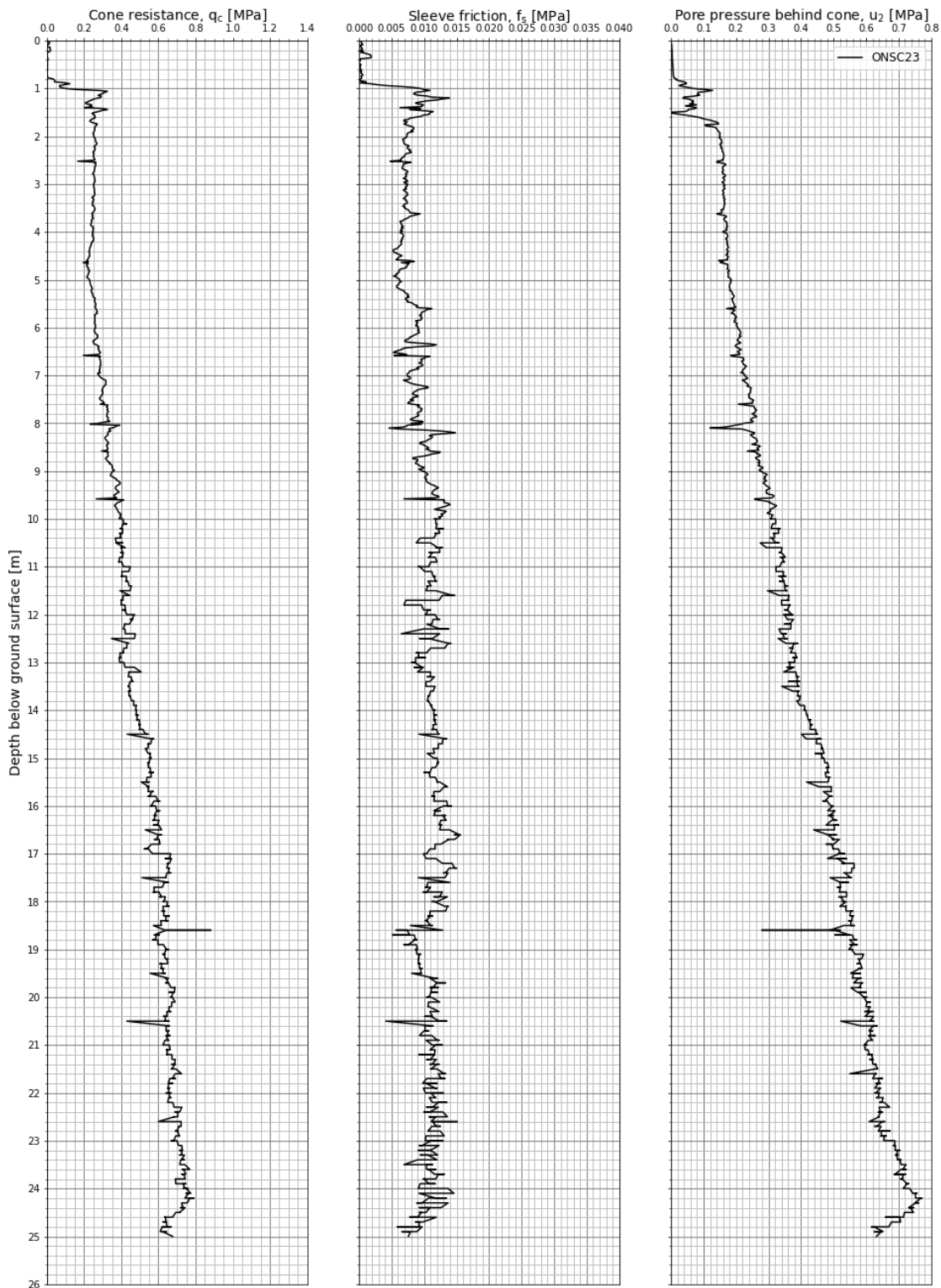


Figure A1.19 Measured cone resistance, sleeve friction and pore pressure – ONSC23.

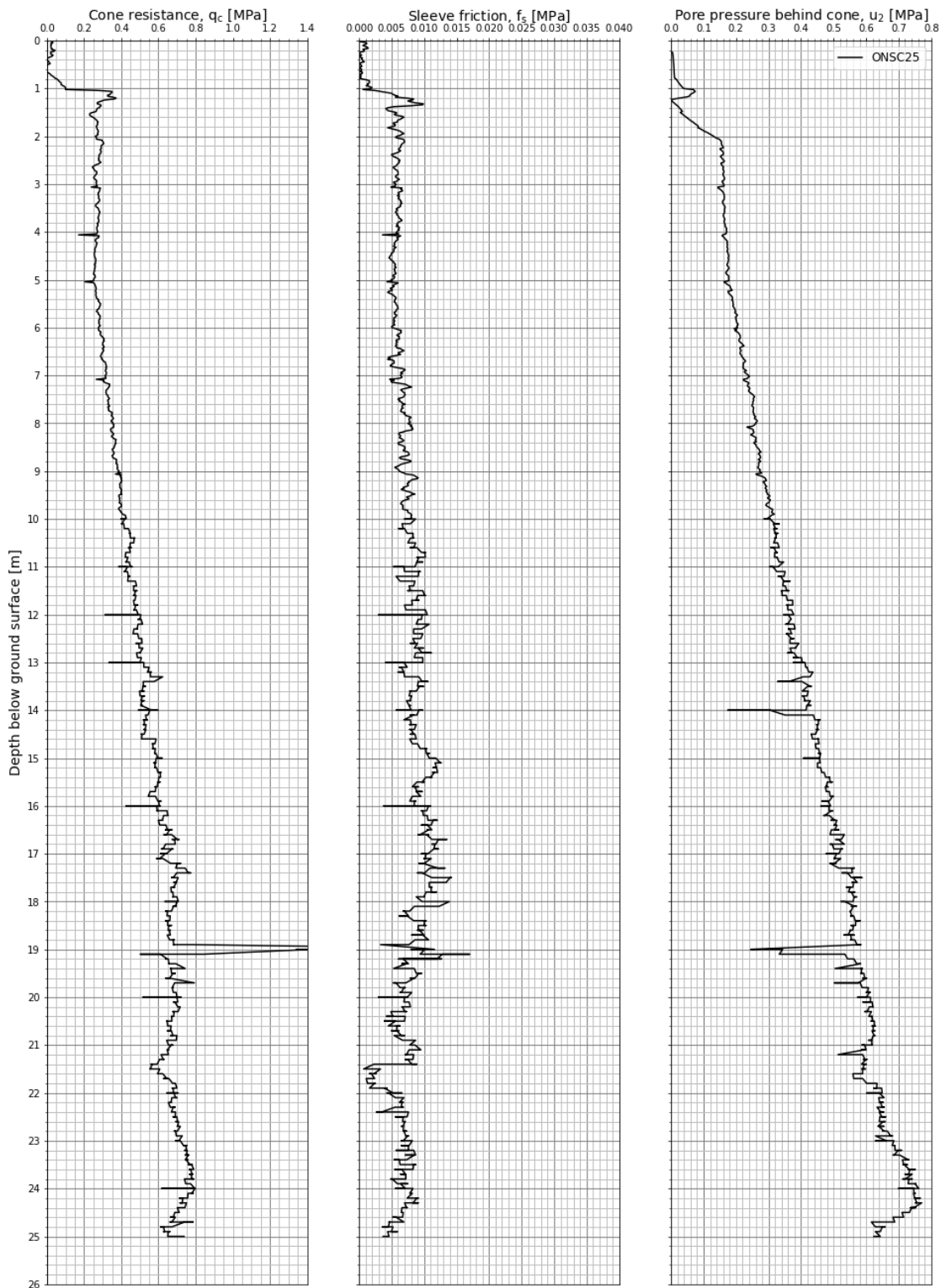


Figure A1.20 Measured cone resistance, sleeve friction and pore pressure – ONSC25.

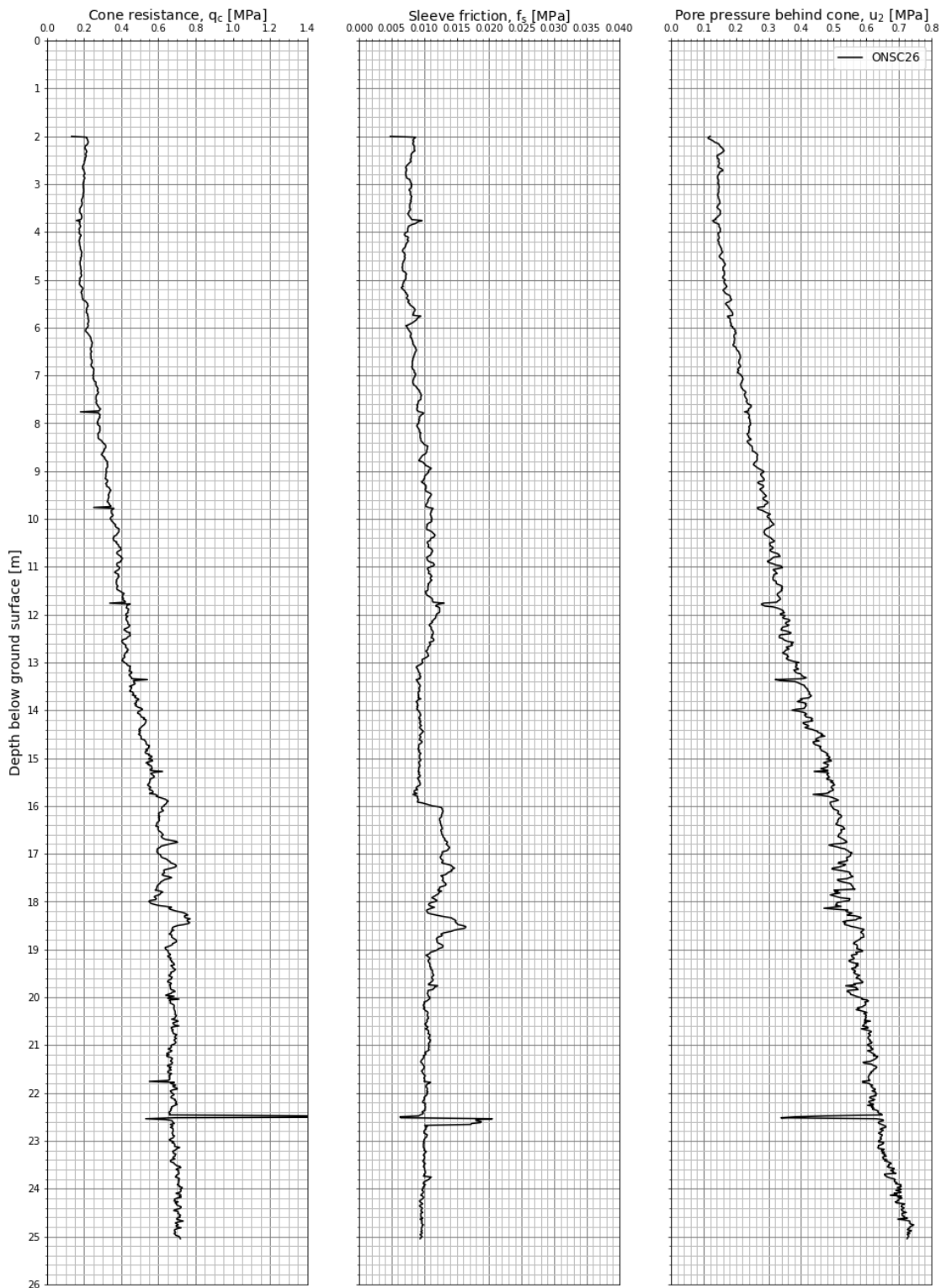


Figure A1.21 Measured cone resistance, sleeve friction and pore pressure – ONSC26.

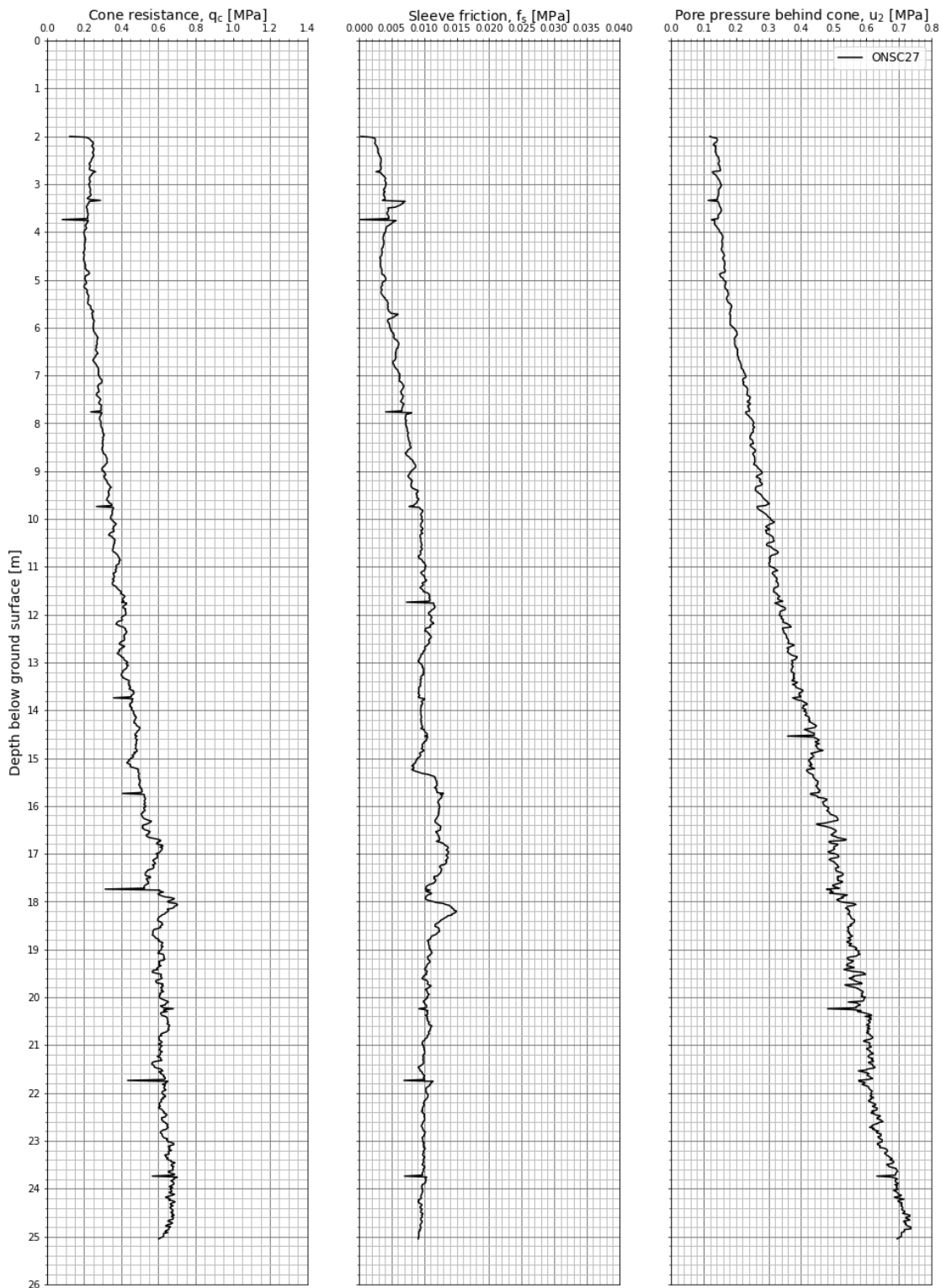


Figure A1.22 Measured cone resistance, sleeve friction and pore pressure – ONSC27.

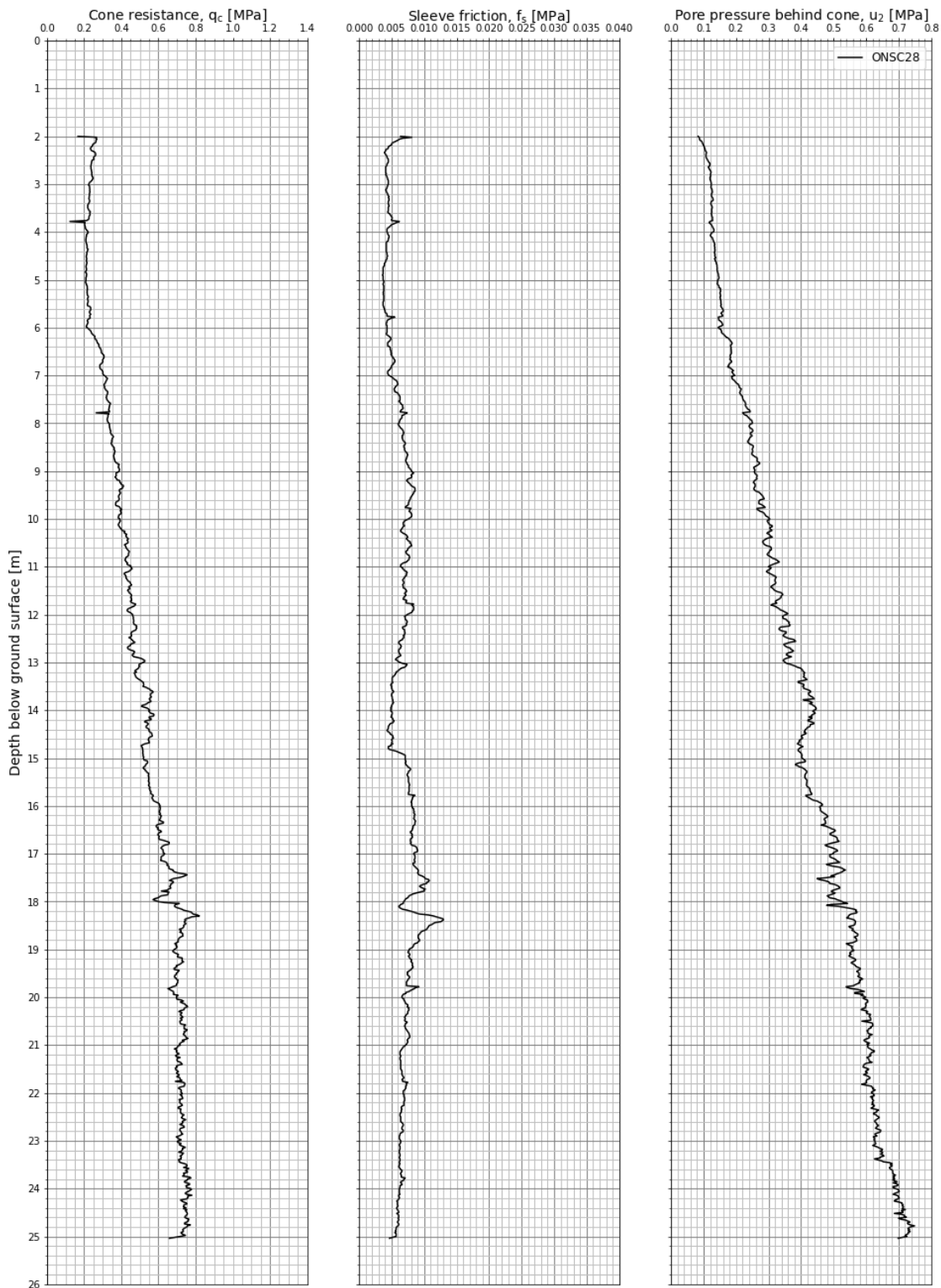


Figure A1.23 Measured cone resistance, sleeve friction and pore pressure – ONSC28.

A2 Silt site – Halden

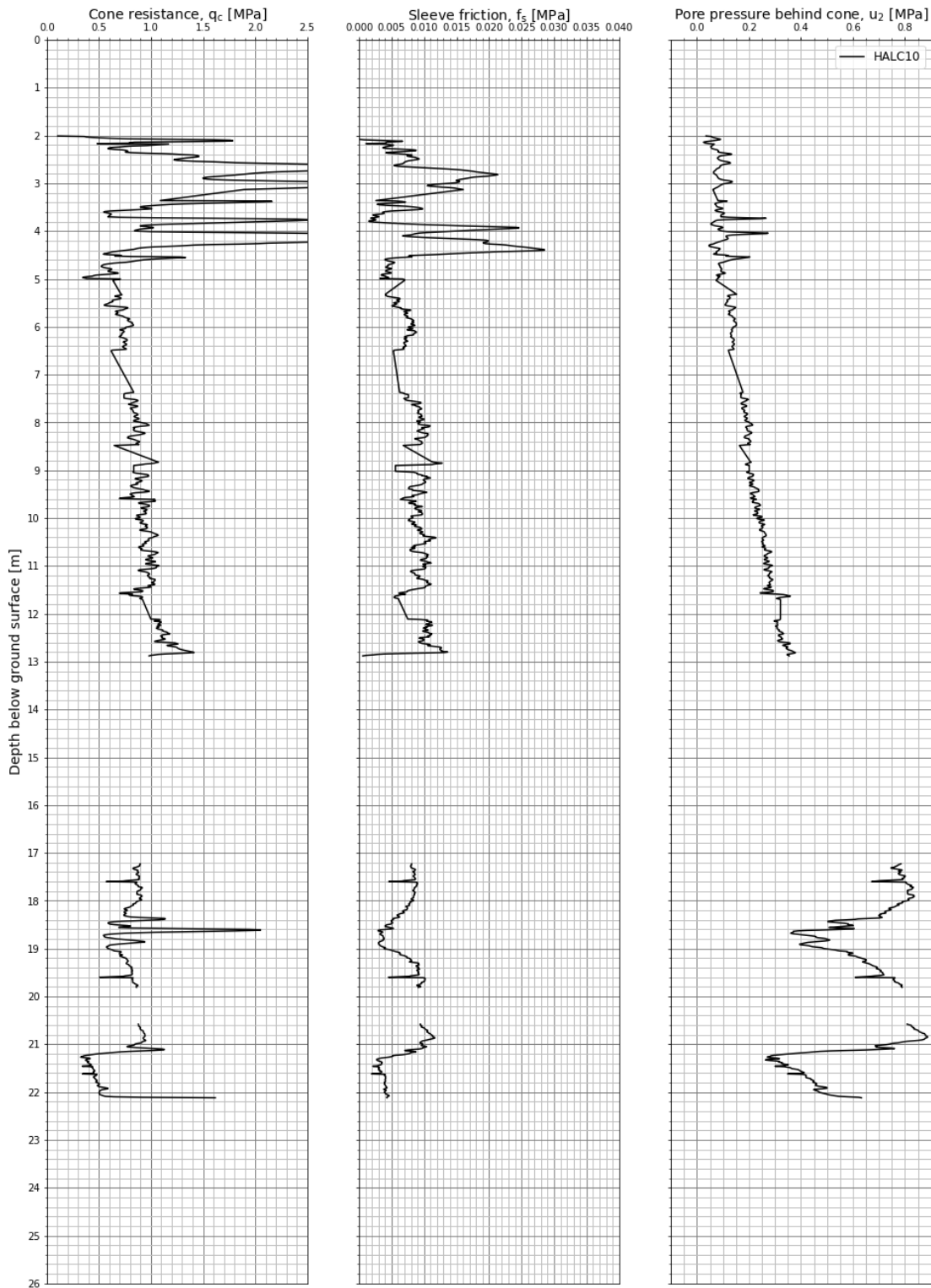


Figure A2.1 Measured cone resistance, sleeve friction and pore pressure – HALC10.

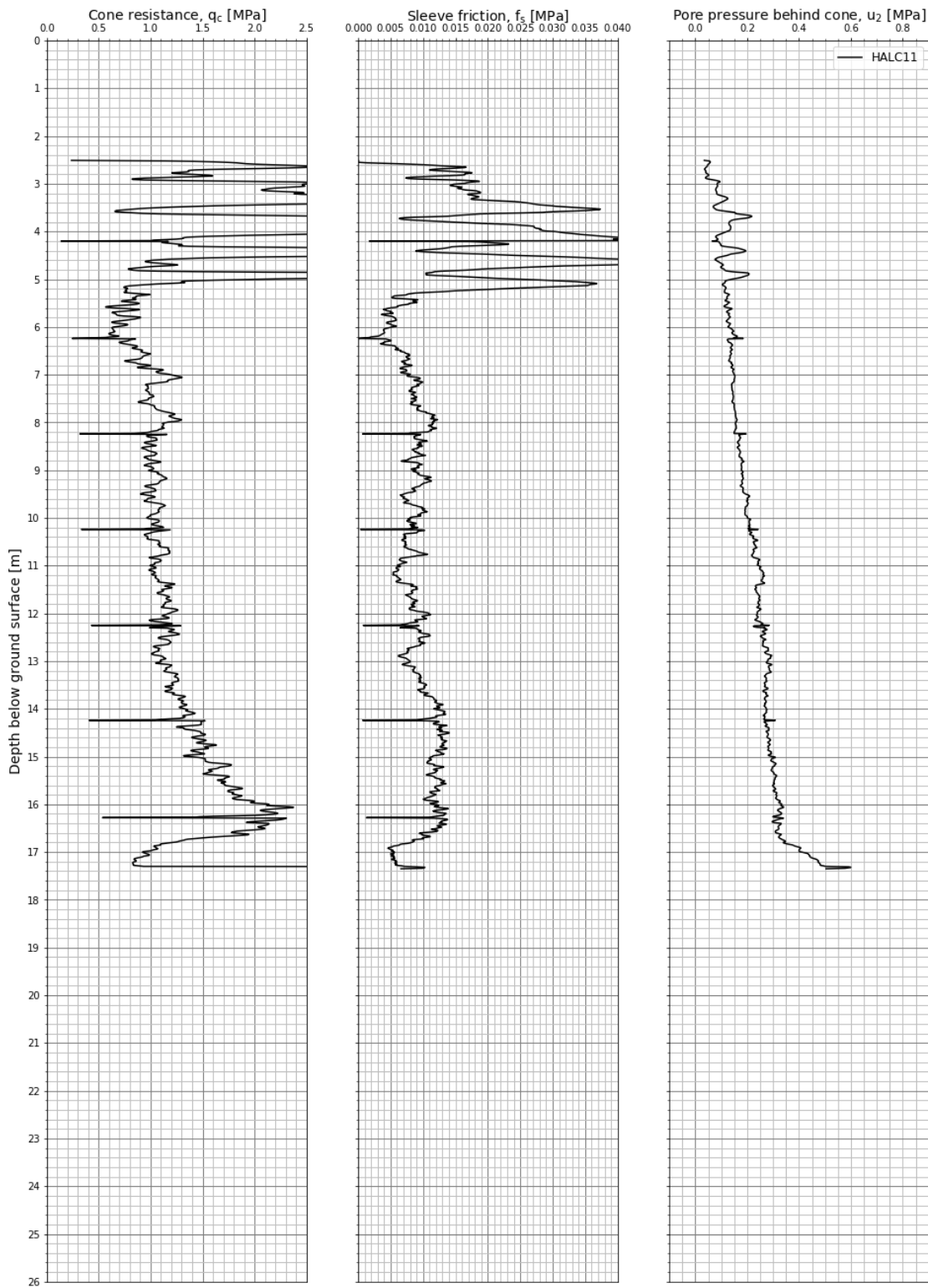


Figure A2.2 Measured cone resistance, sleeve friction and pore pressure – HALC11.

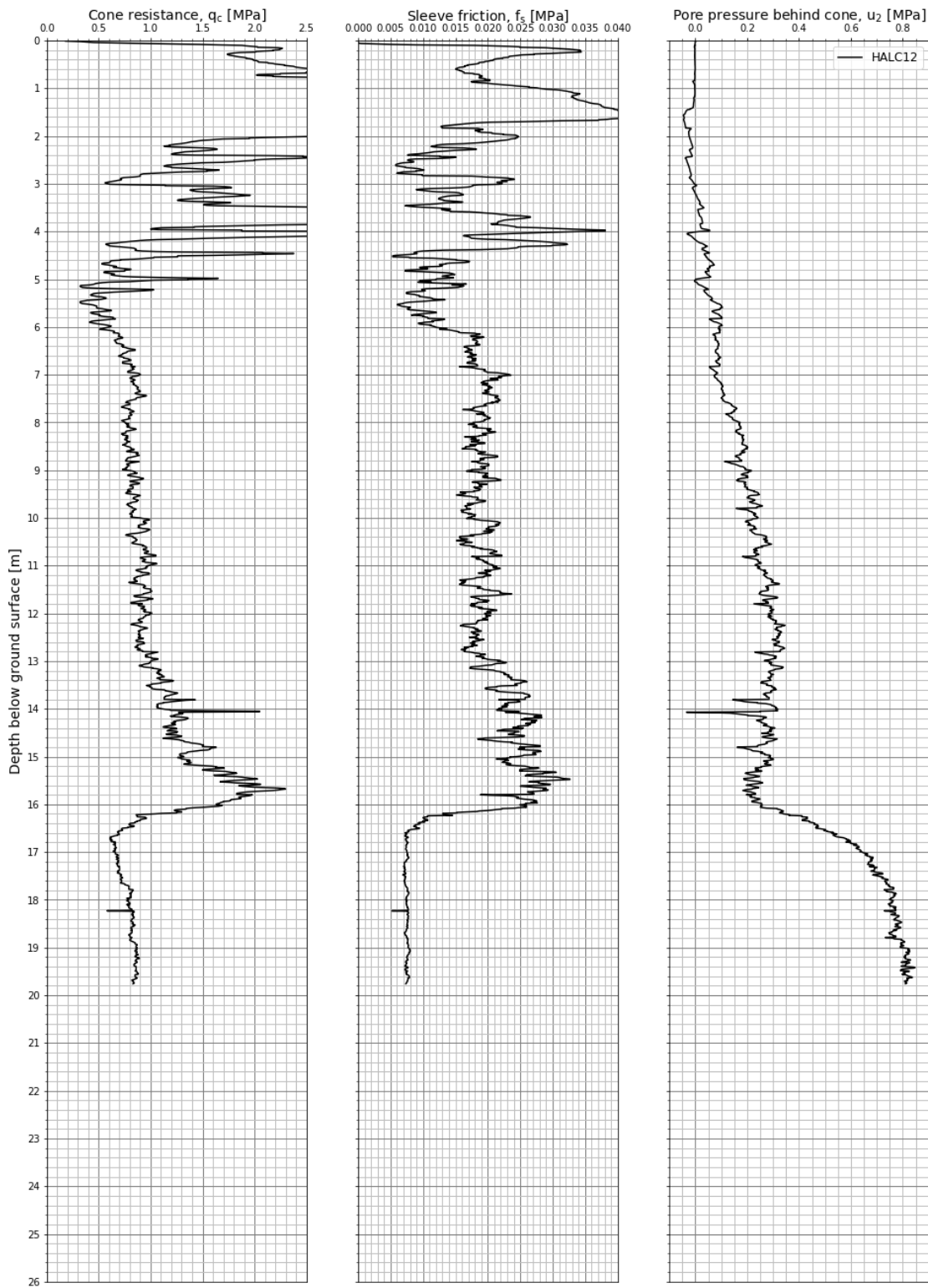


Figure A2.3 Measured cone resistance, sleeve friction and pore pressure – HALC12.

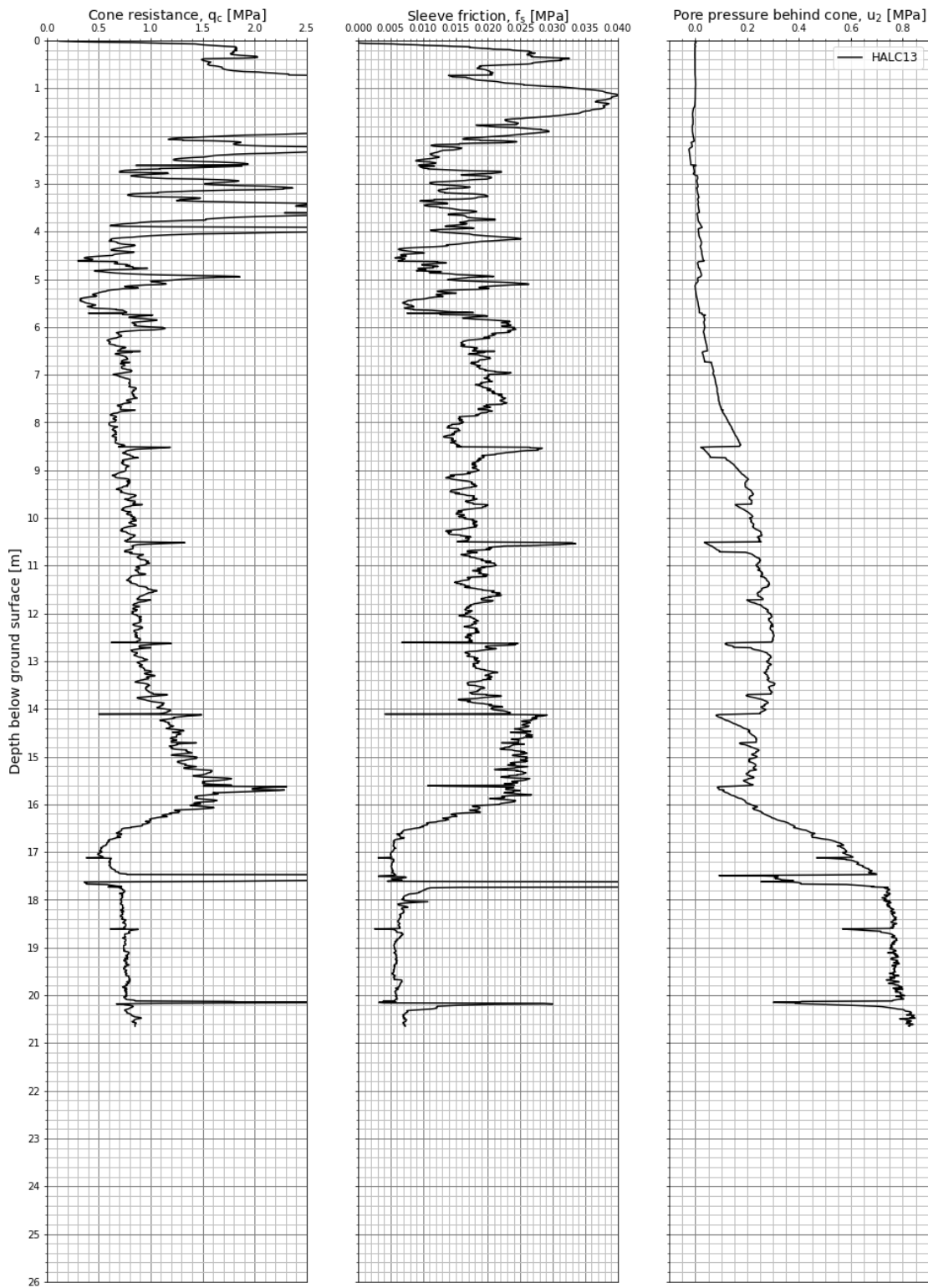


Figure A2.4 Measured cone resistance, sleeve friction and pore pressure – HALC13.

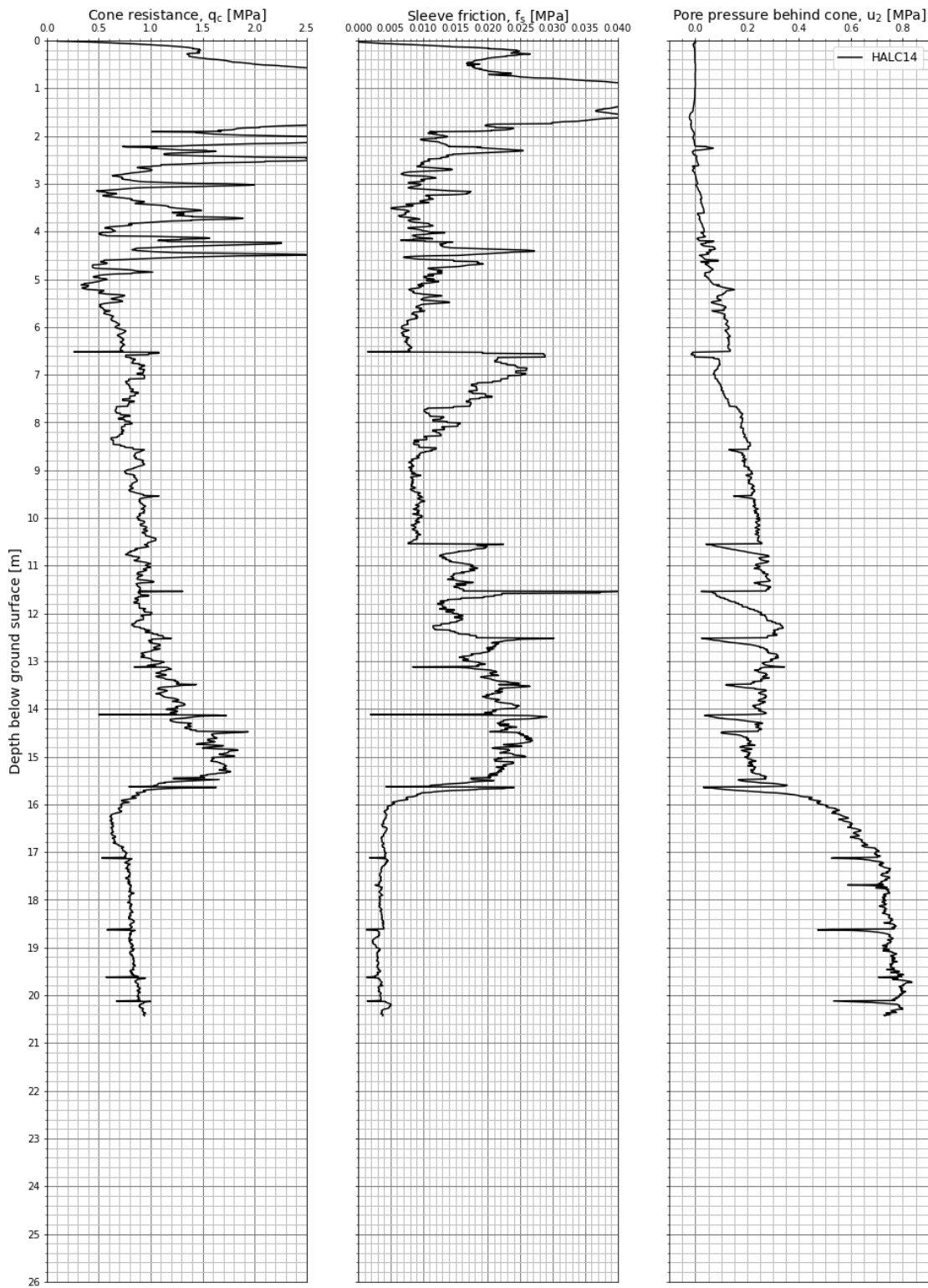


Figure A2.5 Measured cone resistance, sleeve friction and pore pressure – HALC14.

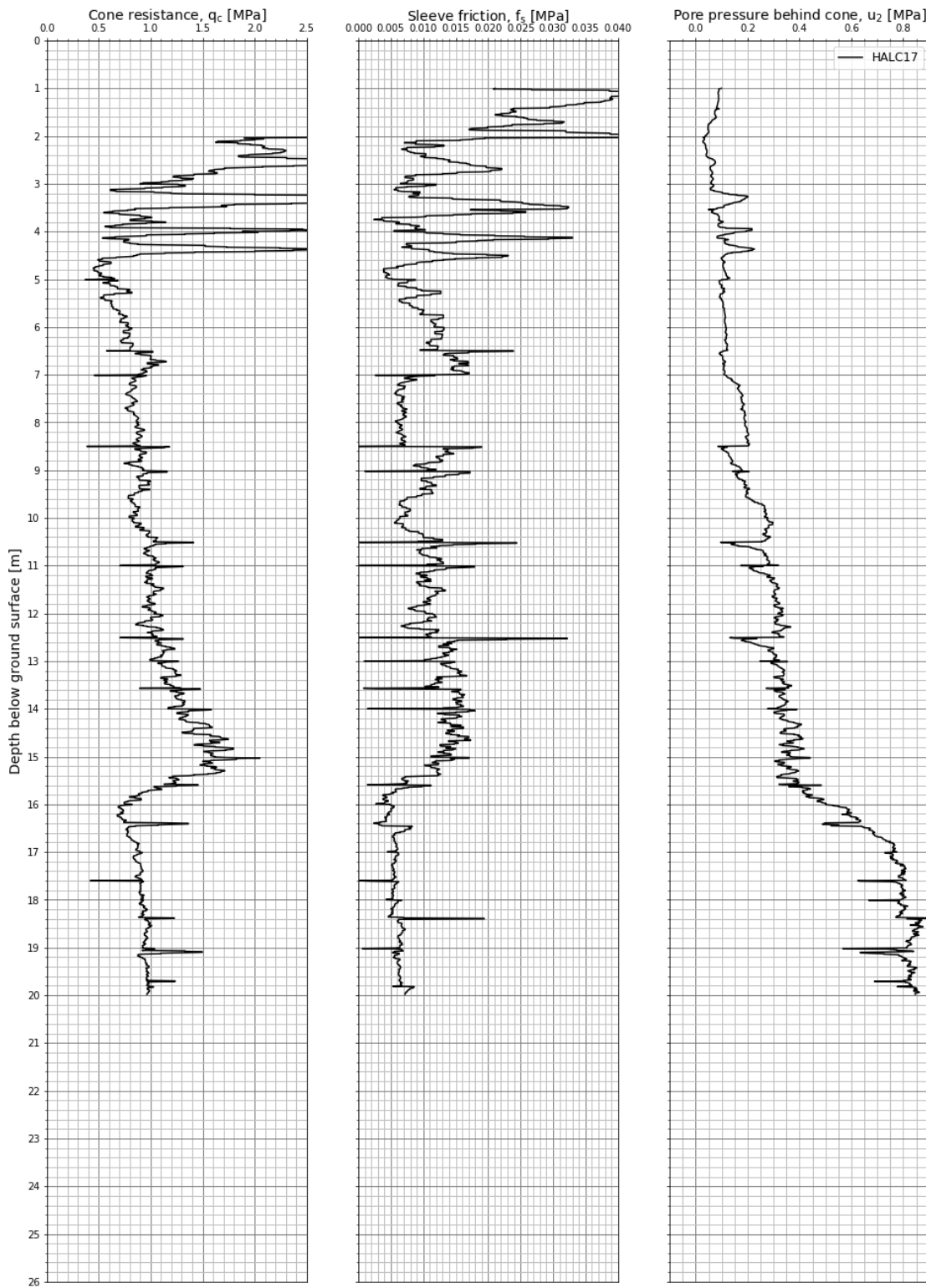


Figure A2.6 Measured cone resistance, sleeve friction and pore pressure – HALC17.

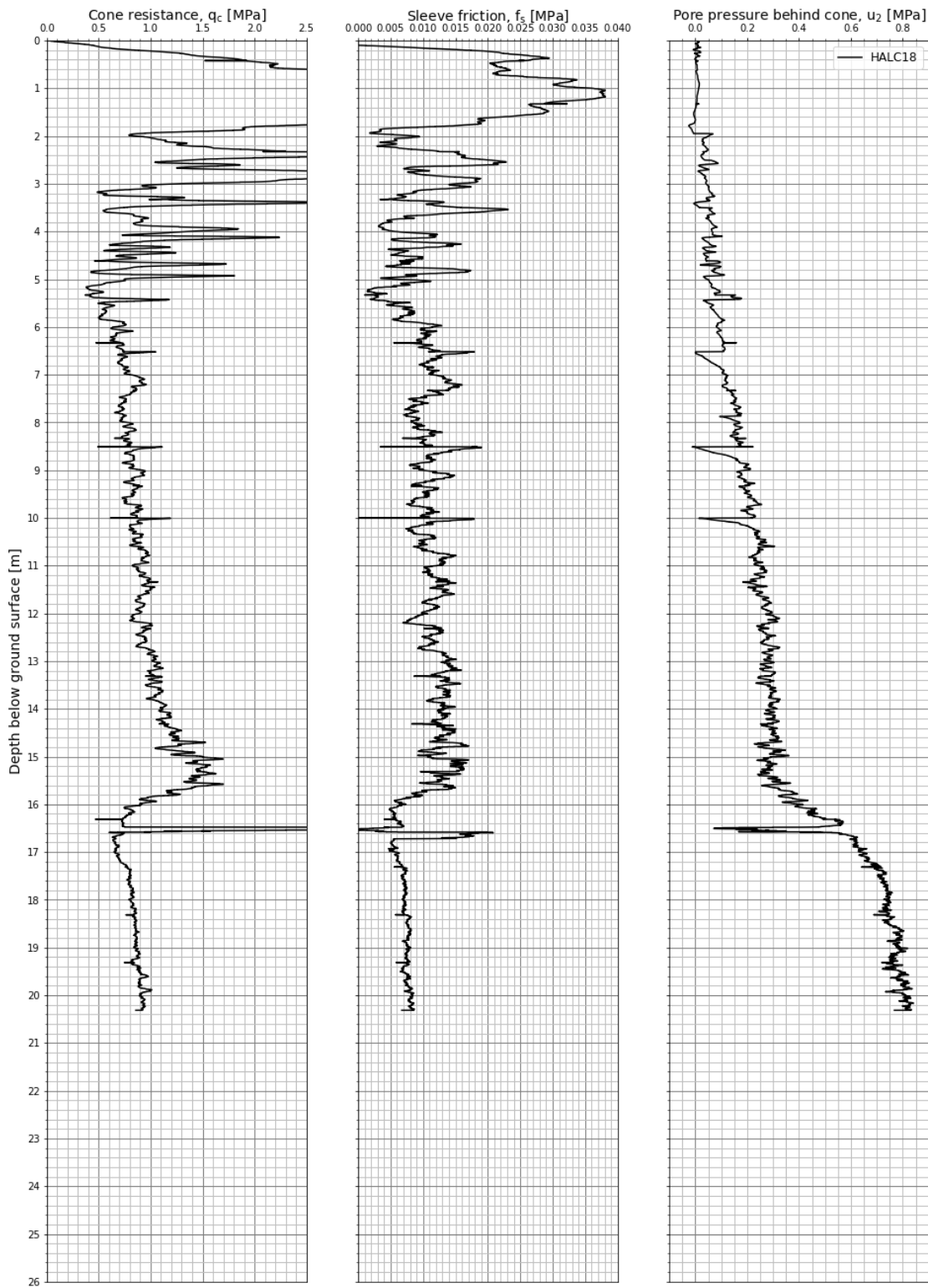


Figure A2.7 Measured cone resistance, sleeve friction and pore pressure – HALC18.

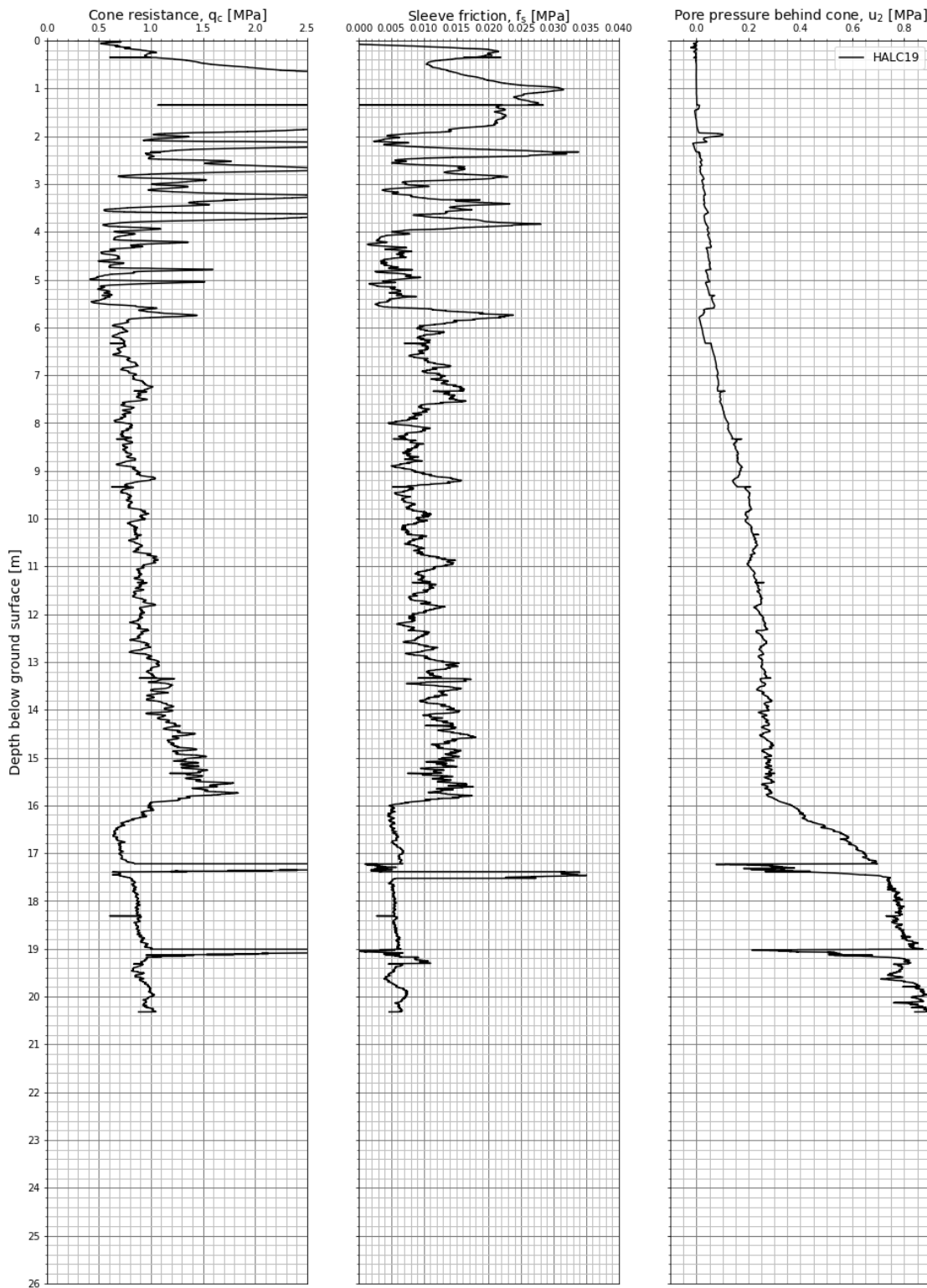


Figure A2.8 Measured cone resistance, sleeve friction and pore pressure – HALC19.

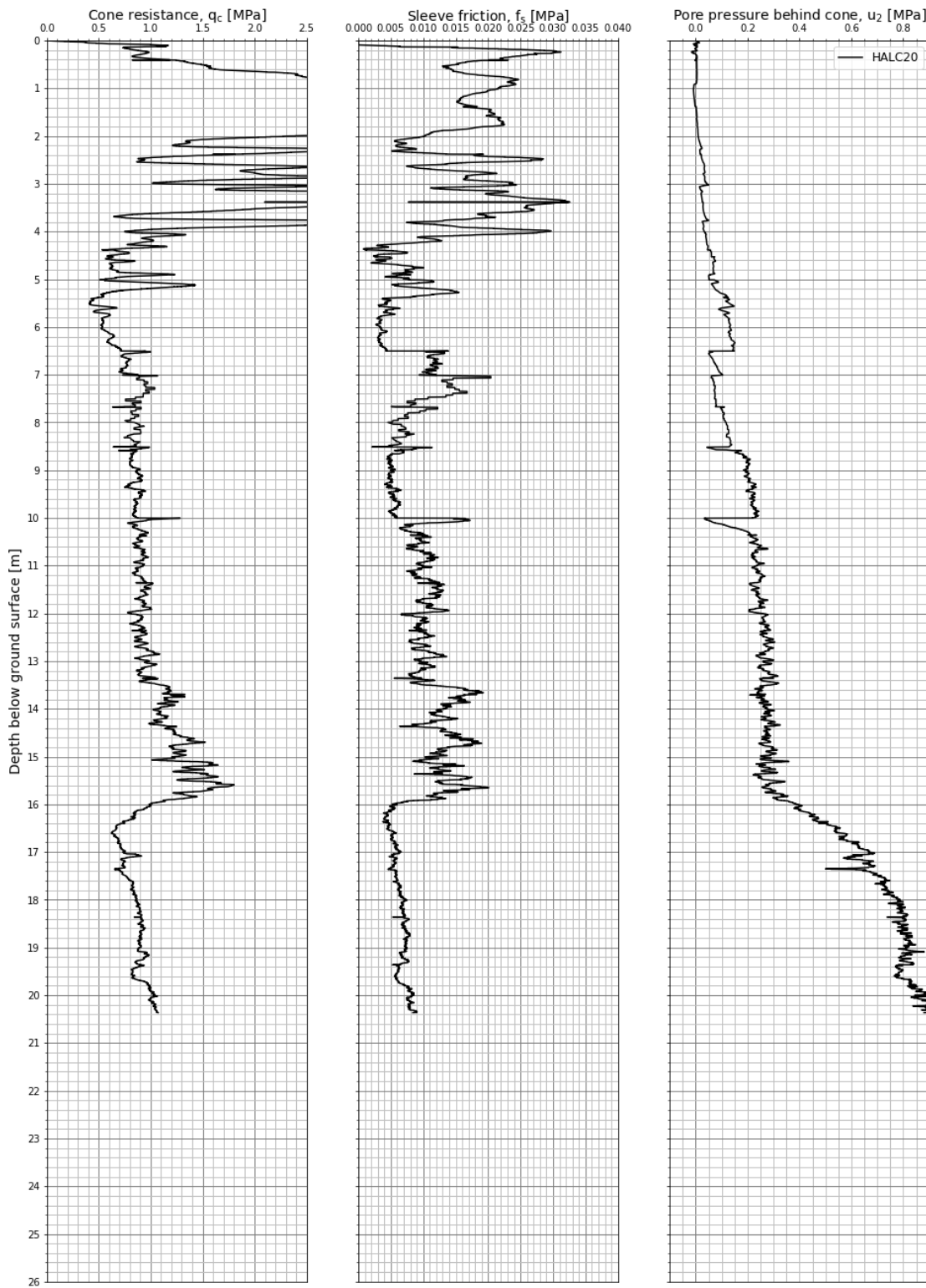


Figure A2.9 Measured cone resistance, sleeve friction and pore pressure – HALC20.

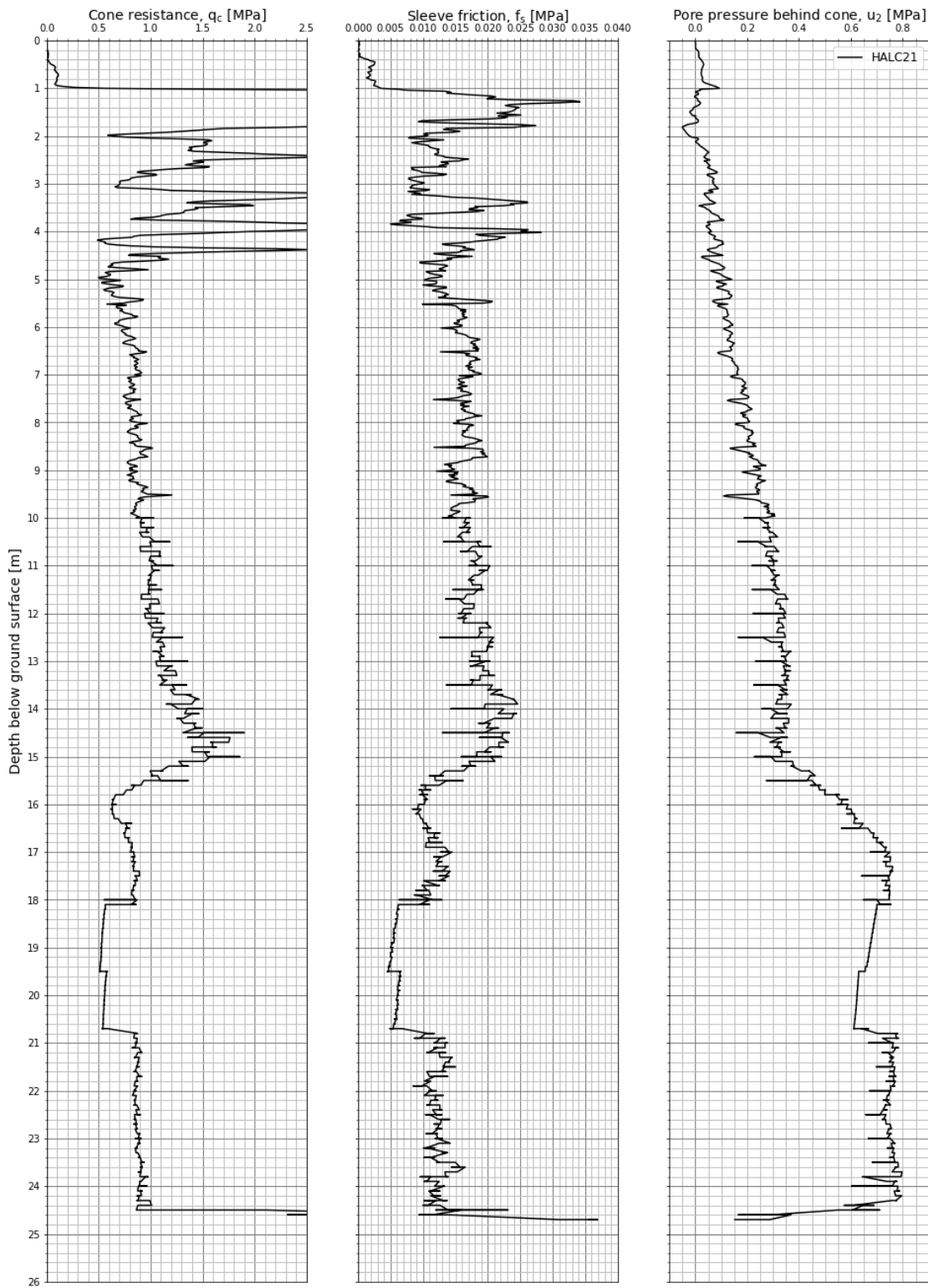


Figure A2.10 Measured cone resistance, sleeve friction and pore pressure – HALC20.

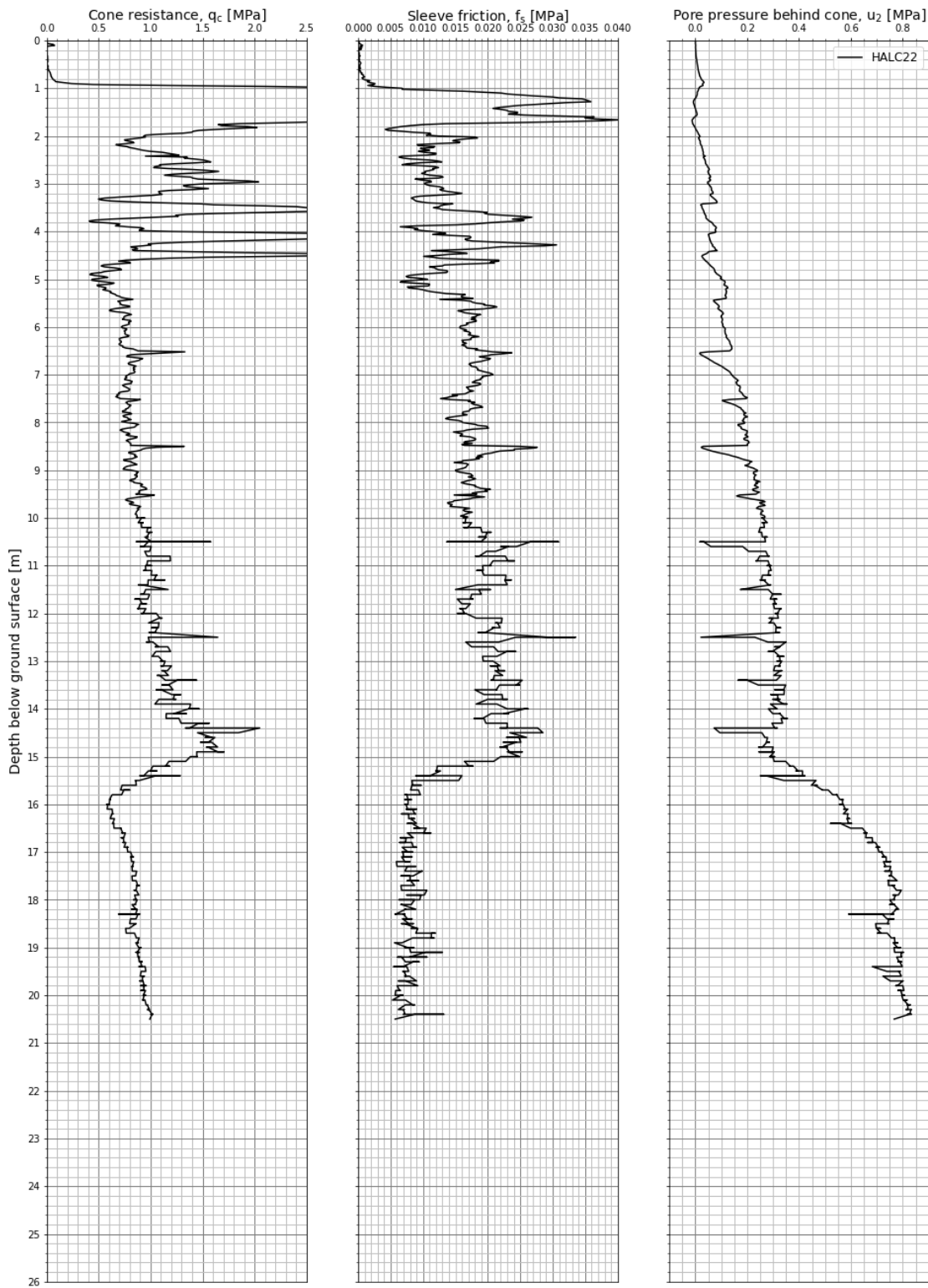


Figure A2.11 Measured cone resistance, sleeve friction and pore pressure – HALC22.

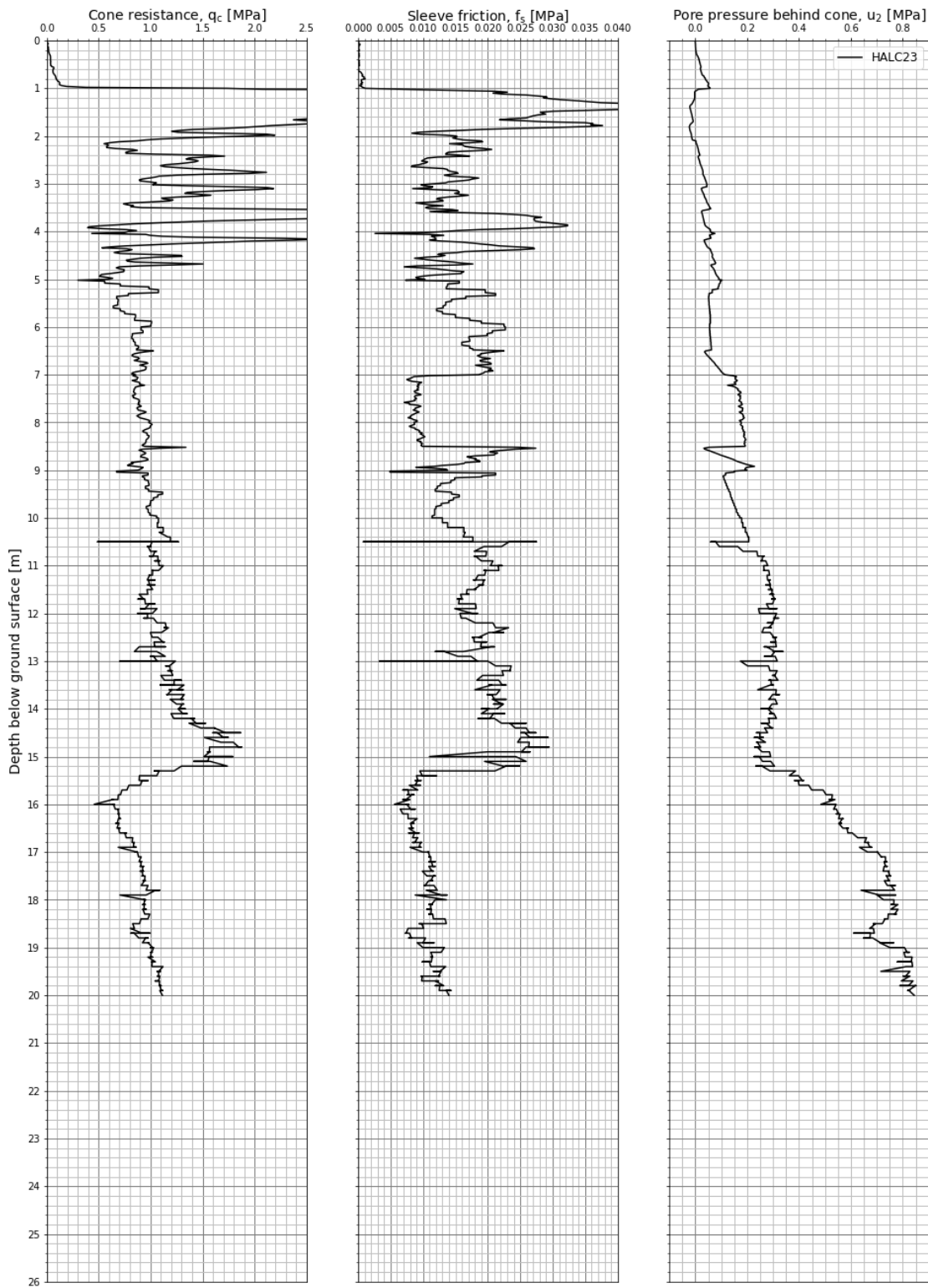


Figure A2.12 Measured cone resistance, sleeve friction and pore pressure – HALC23.

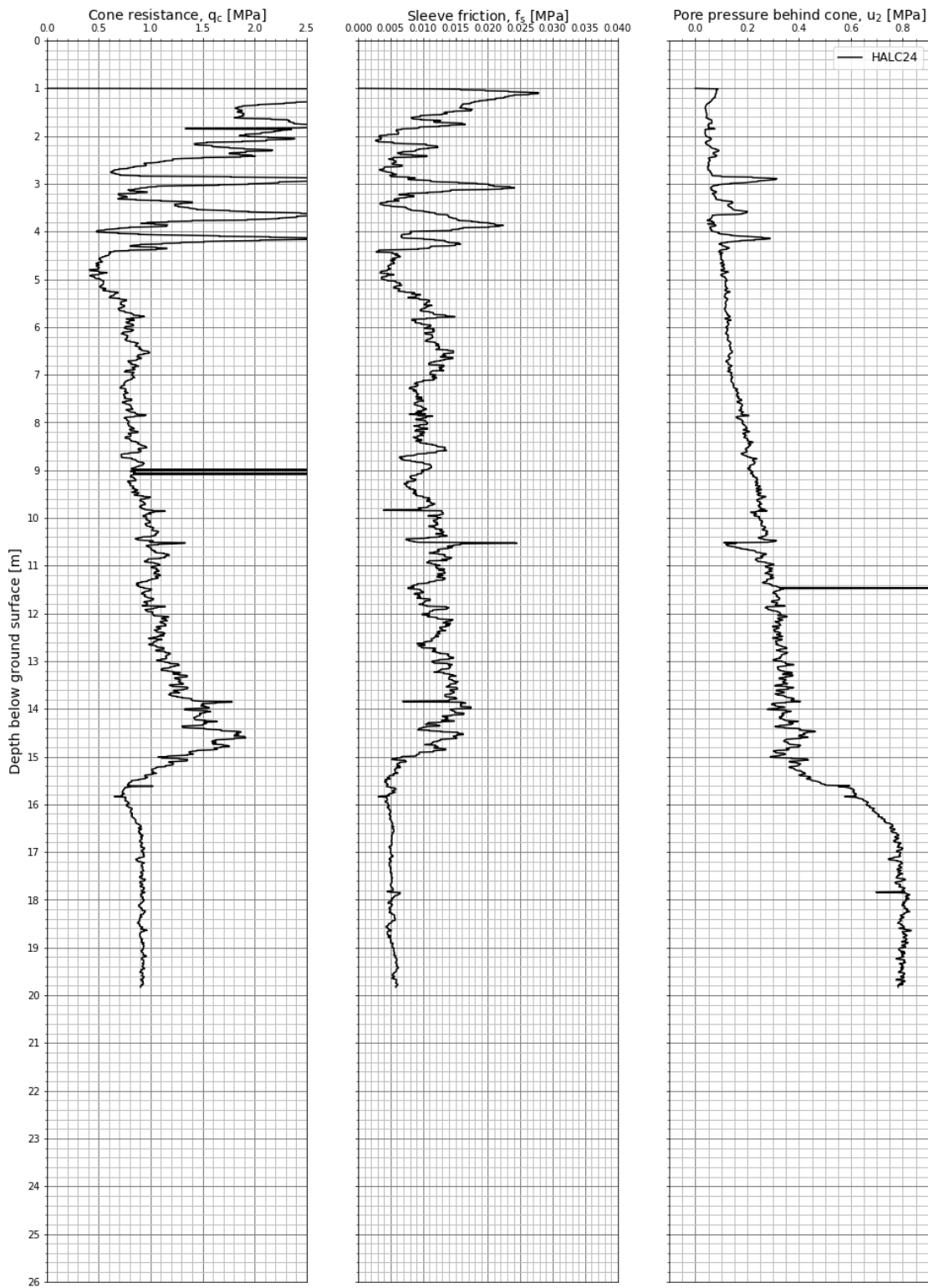


Figure A2.13 Measured cone resistance, sleeve friction and pore pressure – HALC24.

A3 Sand site – Øysand

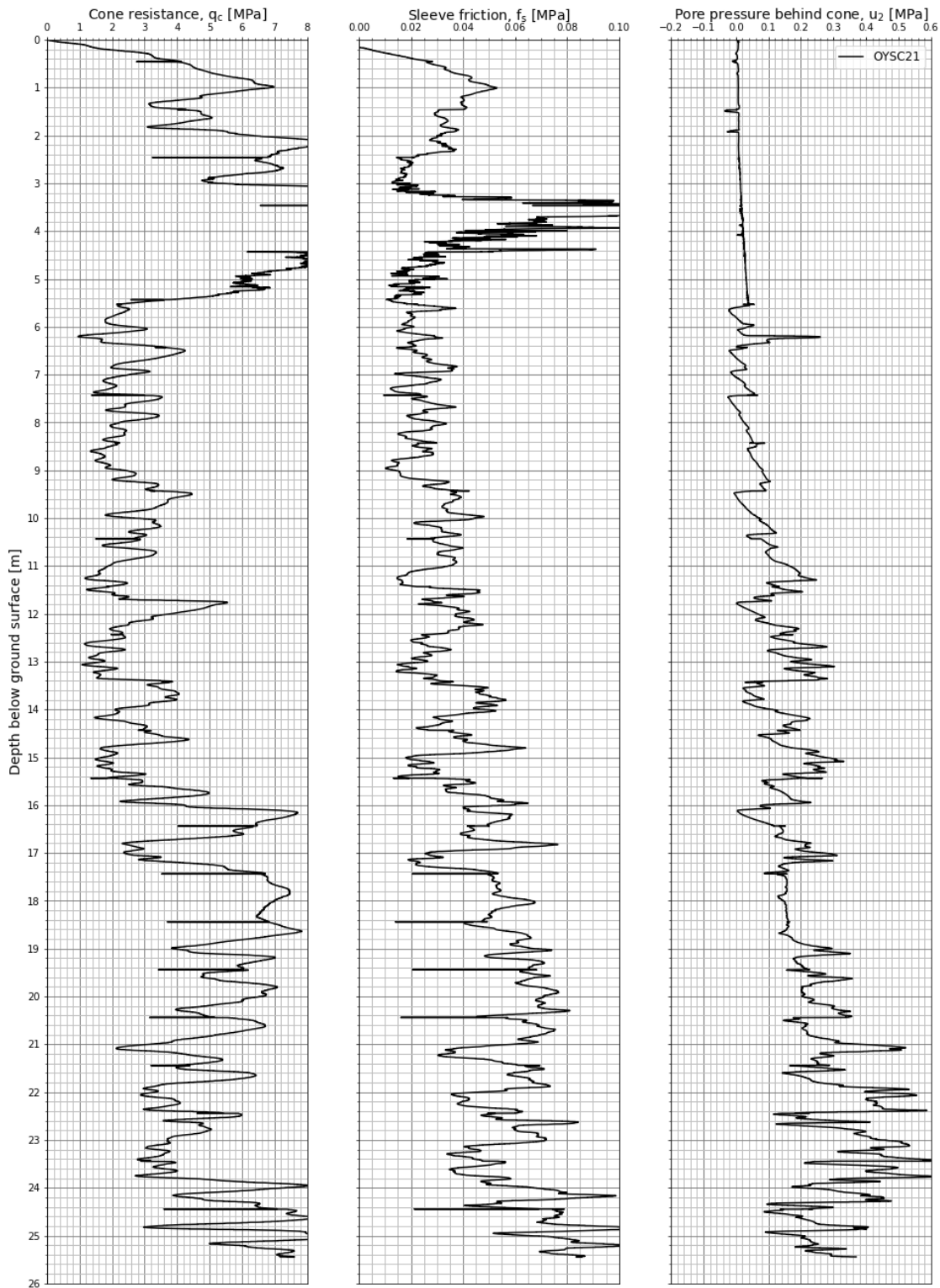


Figure A3.1 Measured cone resistance, sleeve friction and pore pressure – OYSC21.

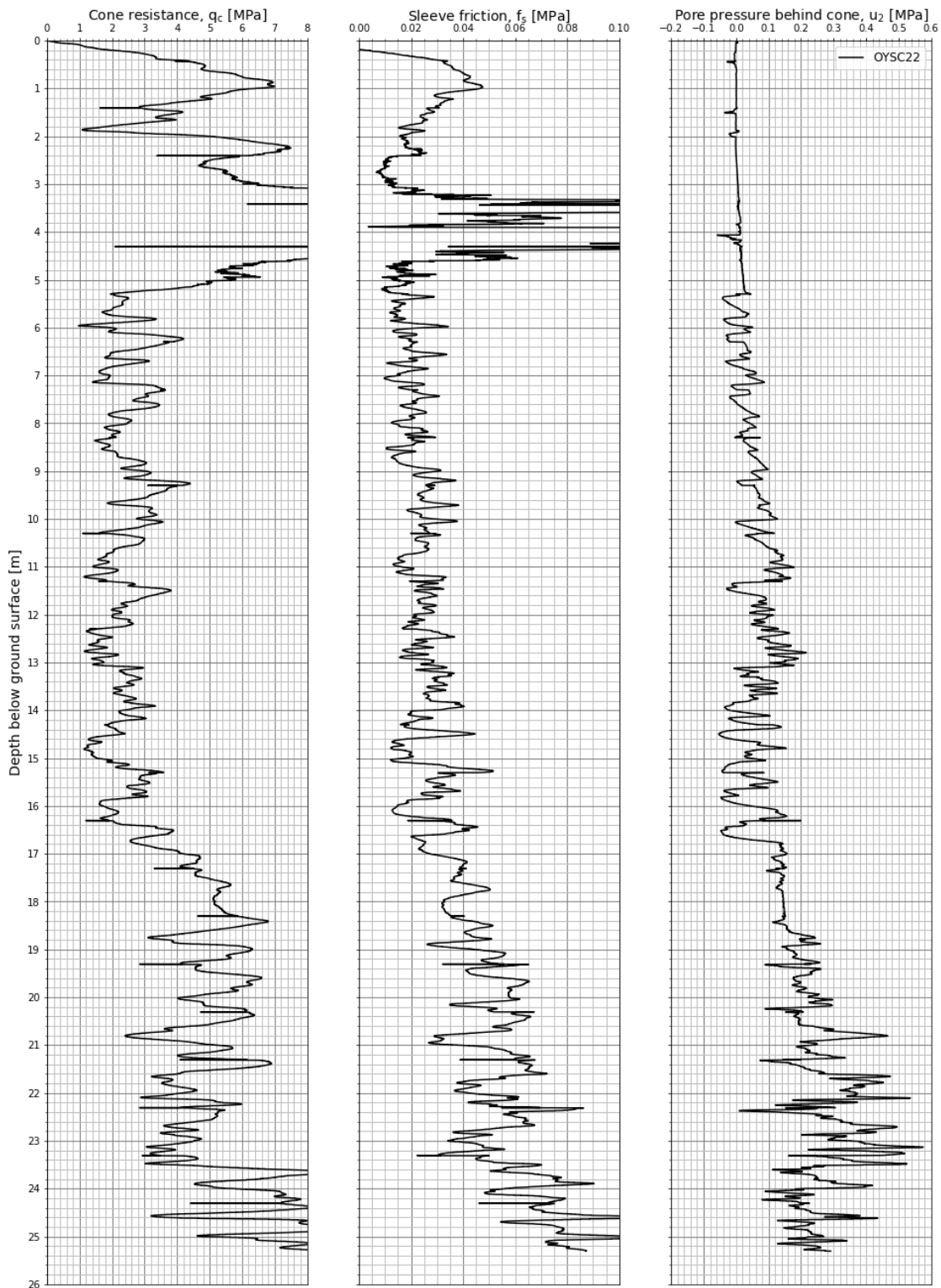


Figure A3.2 Measured cone resistance, sleeve friction and pore pressure – OYSC22.

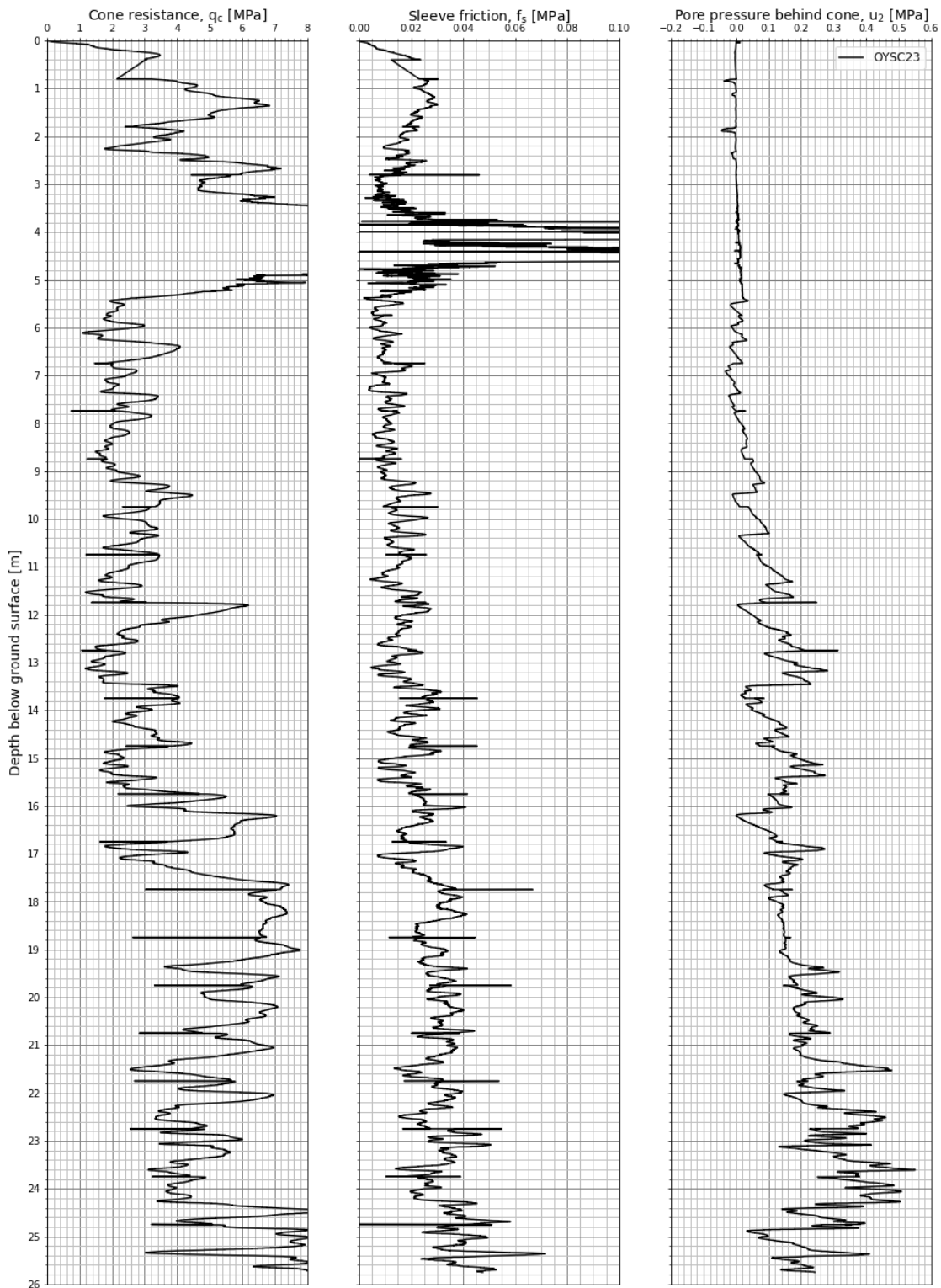


Figure A3.3 Measured cone resistance, sleeve friction and pore pressure – OYSC23.

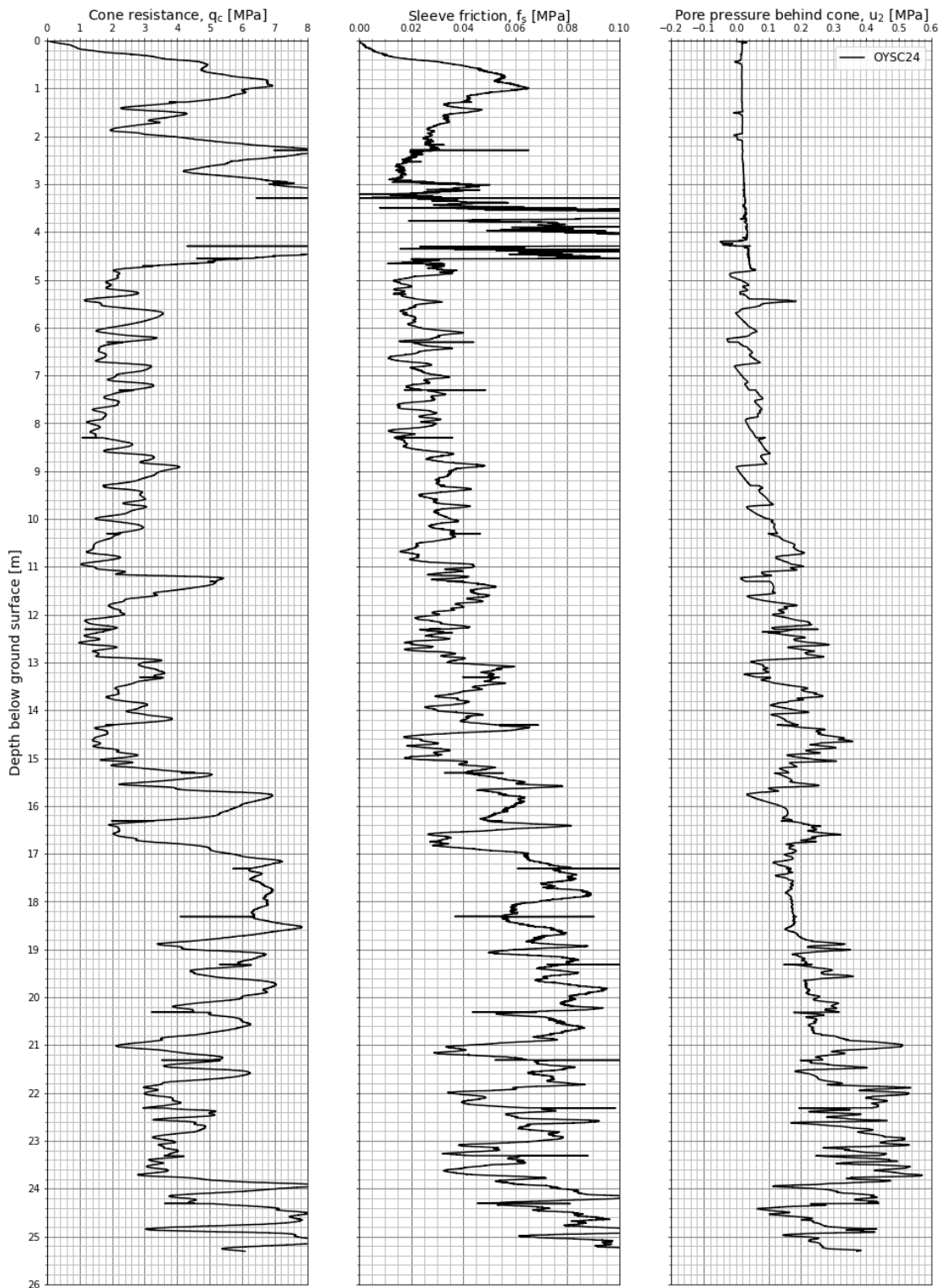


Figure A3.4 Measured cone resistance, sleeve friction and pore pressure – OYSC24.

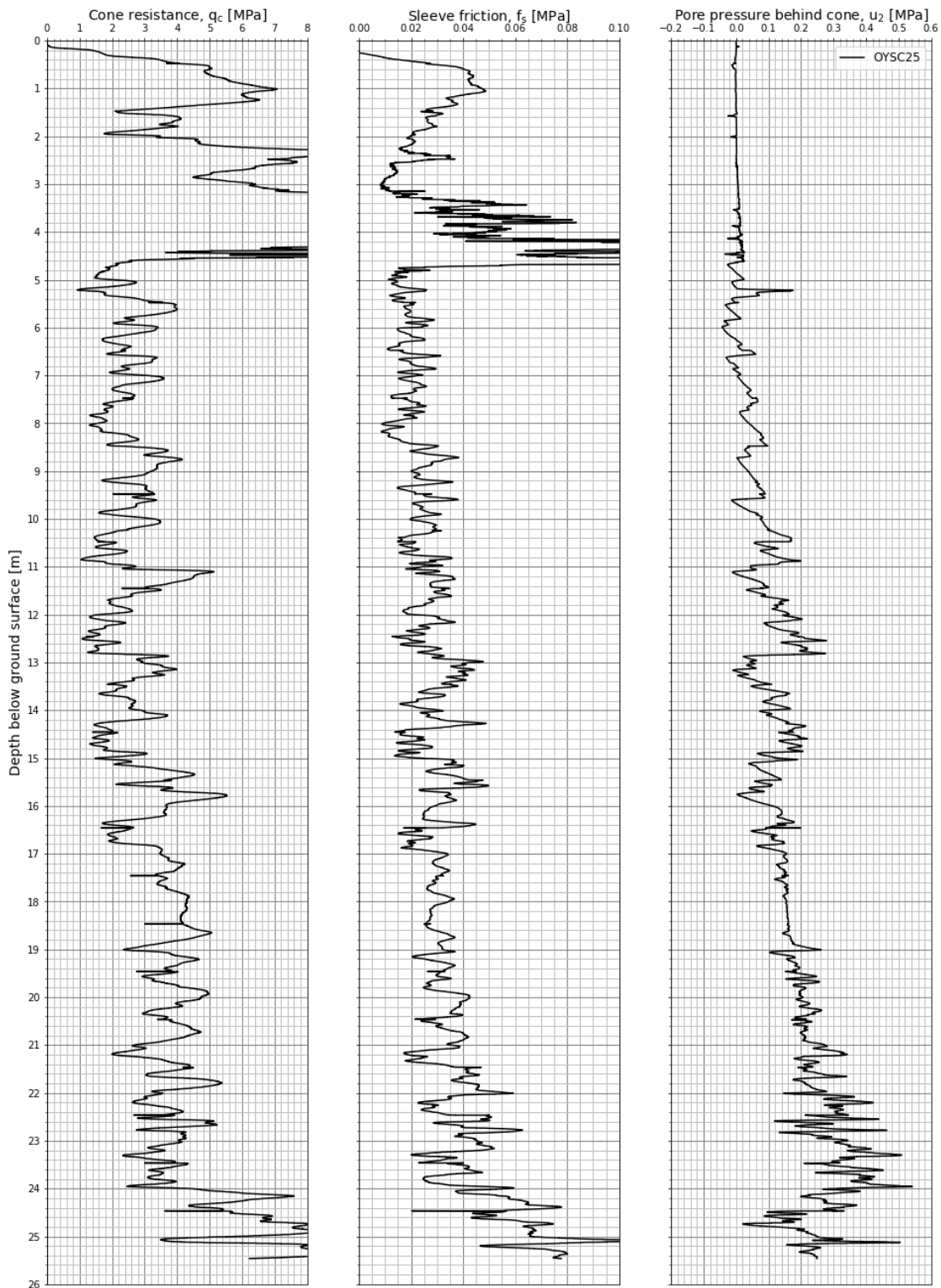


Figure A3.5 Measured cone resistance, sleeve friction and pore pressure – OYSC25.

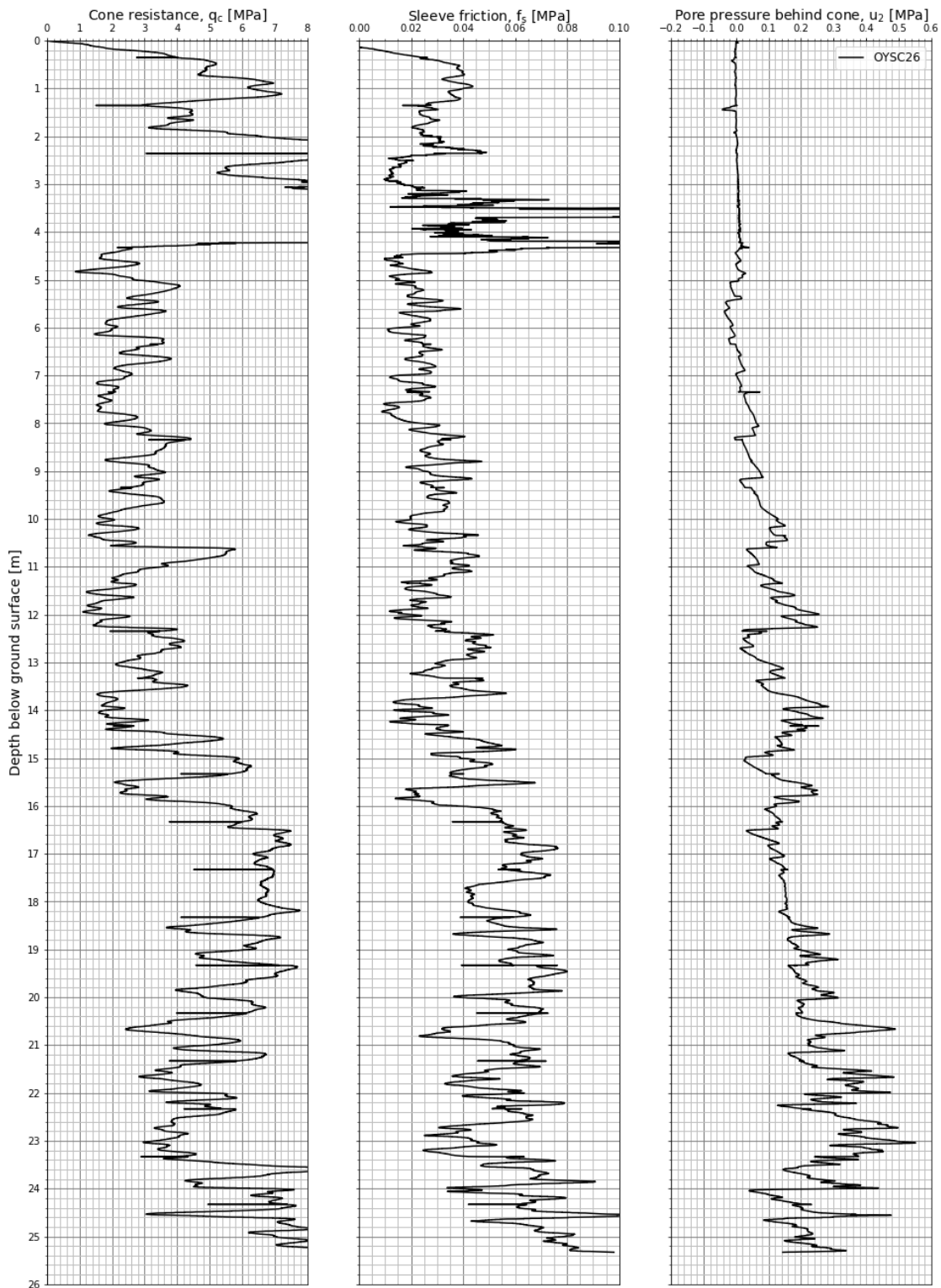


Figure A3.6 Measured cone resistance, sleeve friction and pore pressure – OYSC26.

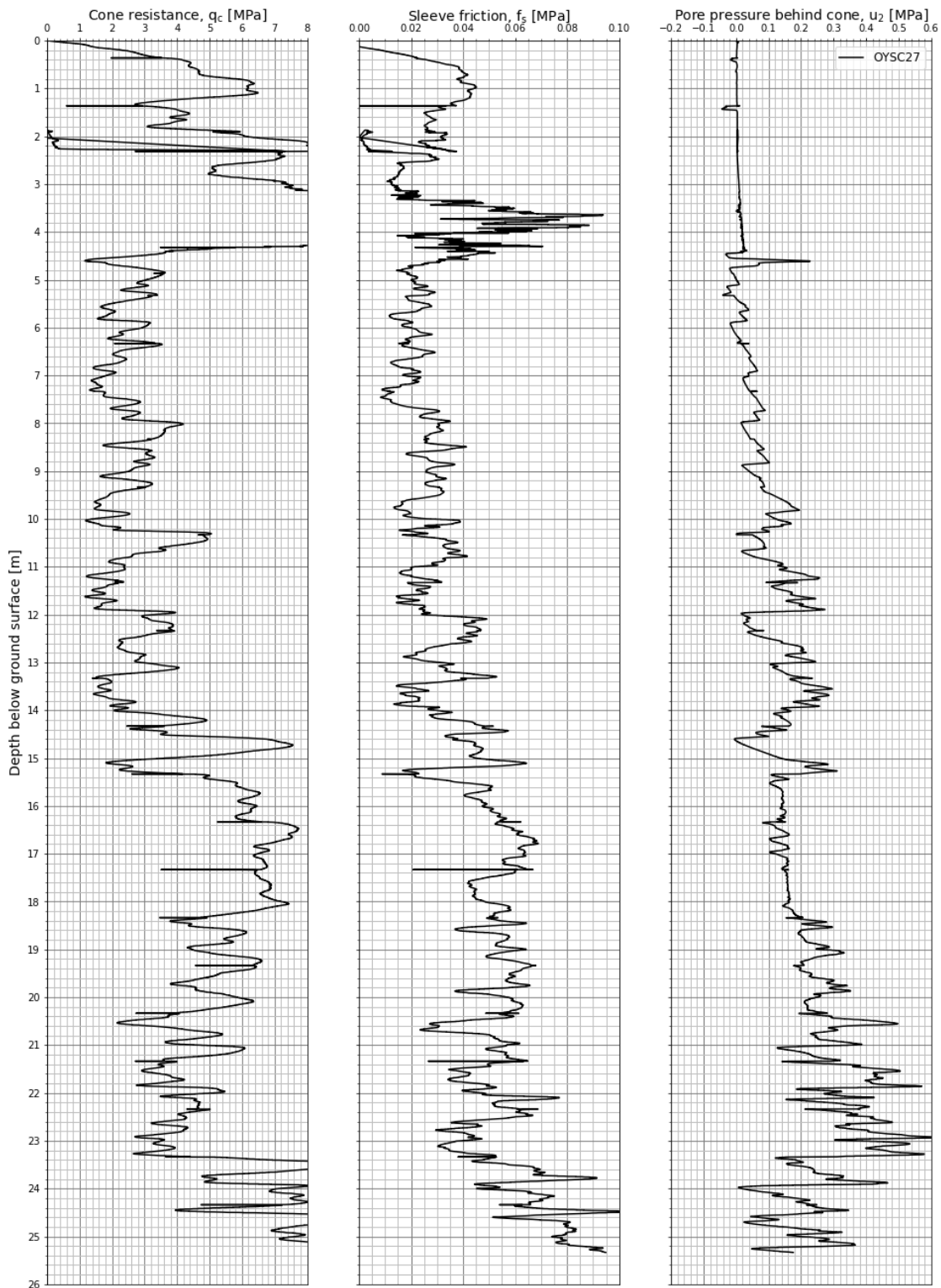


Figure A3.7 Measured cone resistance, sleeve friction and pore pressure – OYSC27.

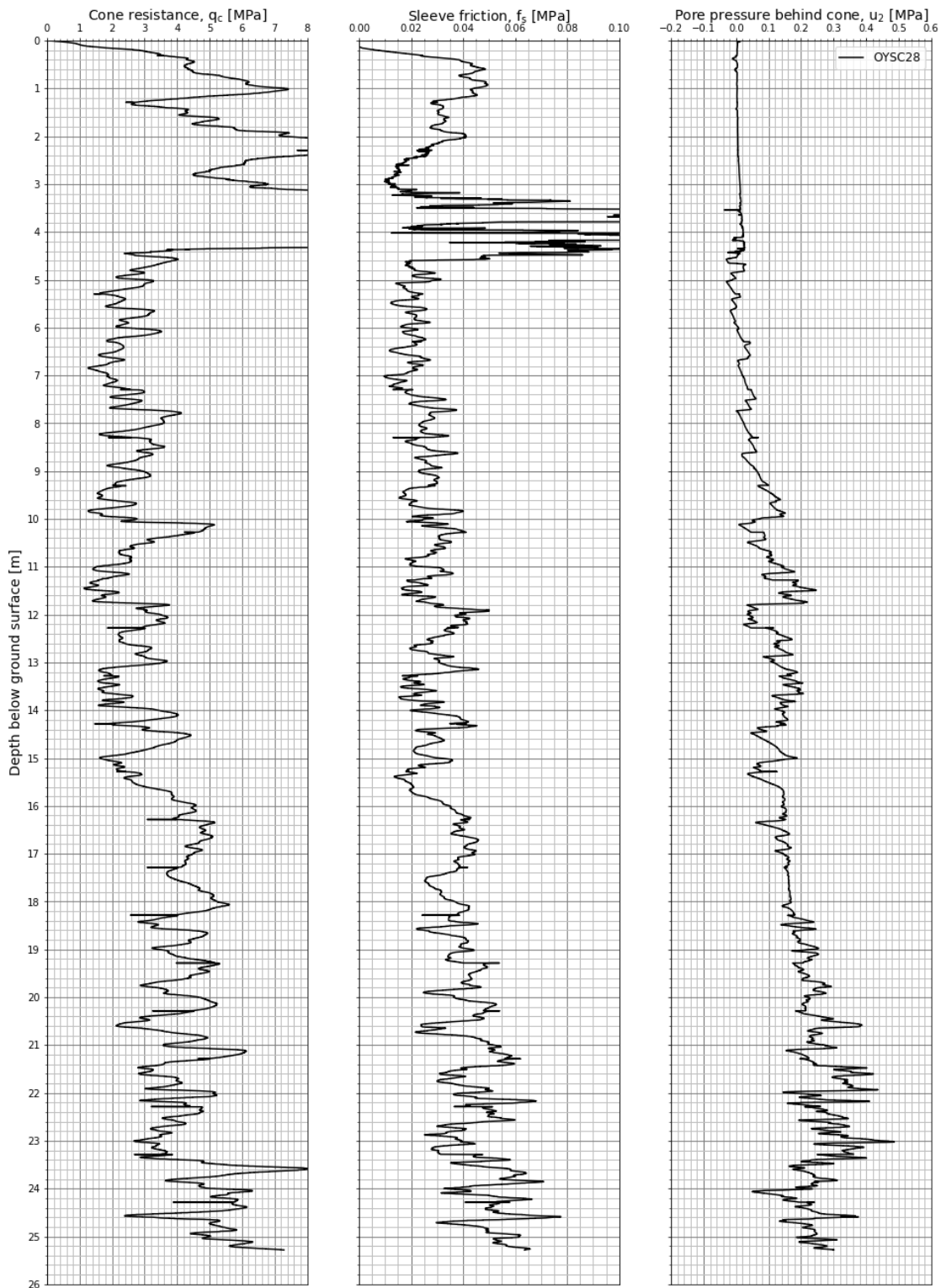


Figure A3.8 Measured cone resistance, sleeve friction and pore pressure – OYSC28.

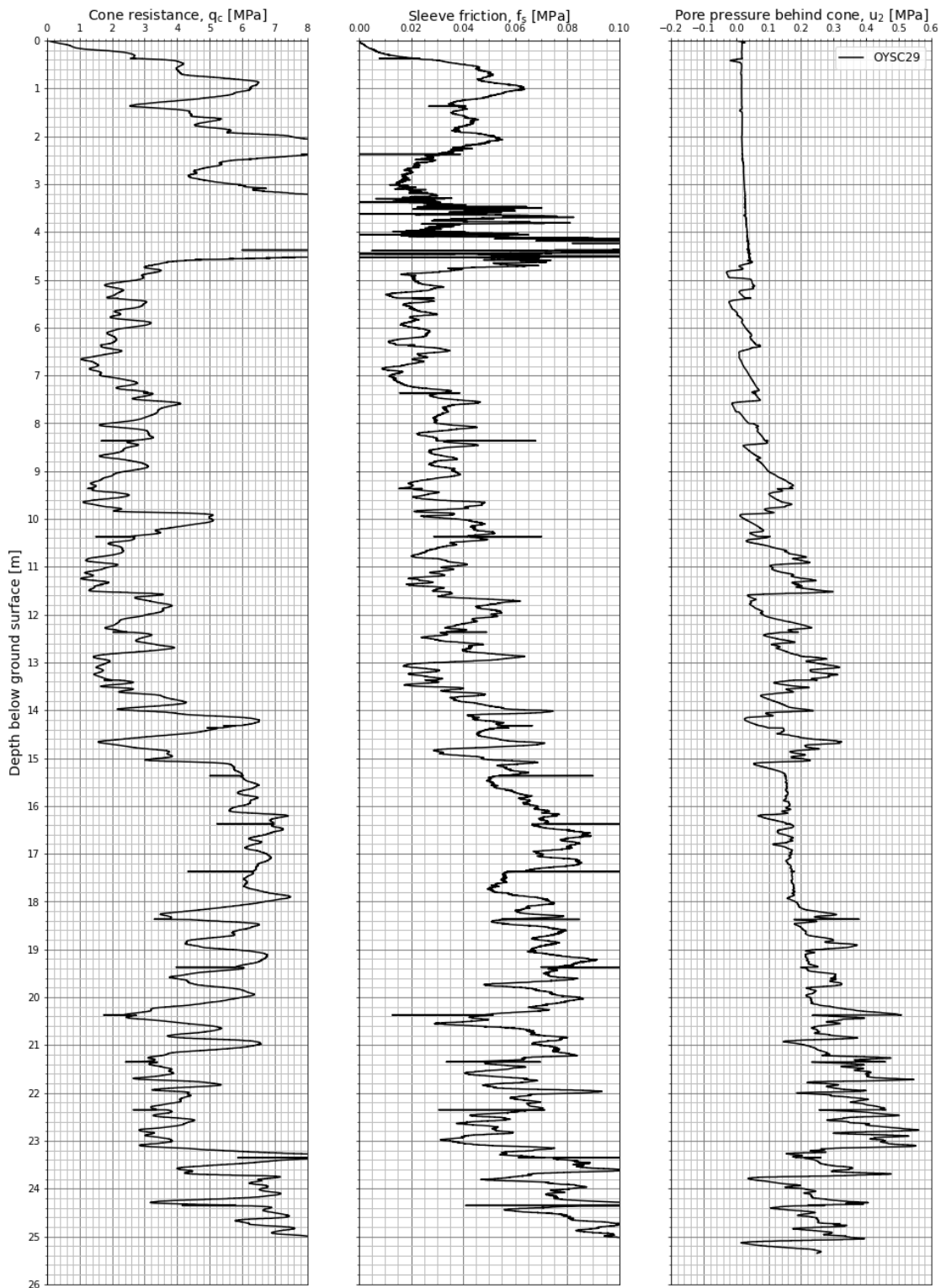


Figure A3.9 Measured cone resistance, sleeve friction and pore pressure – OYSC29.

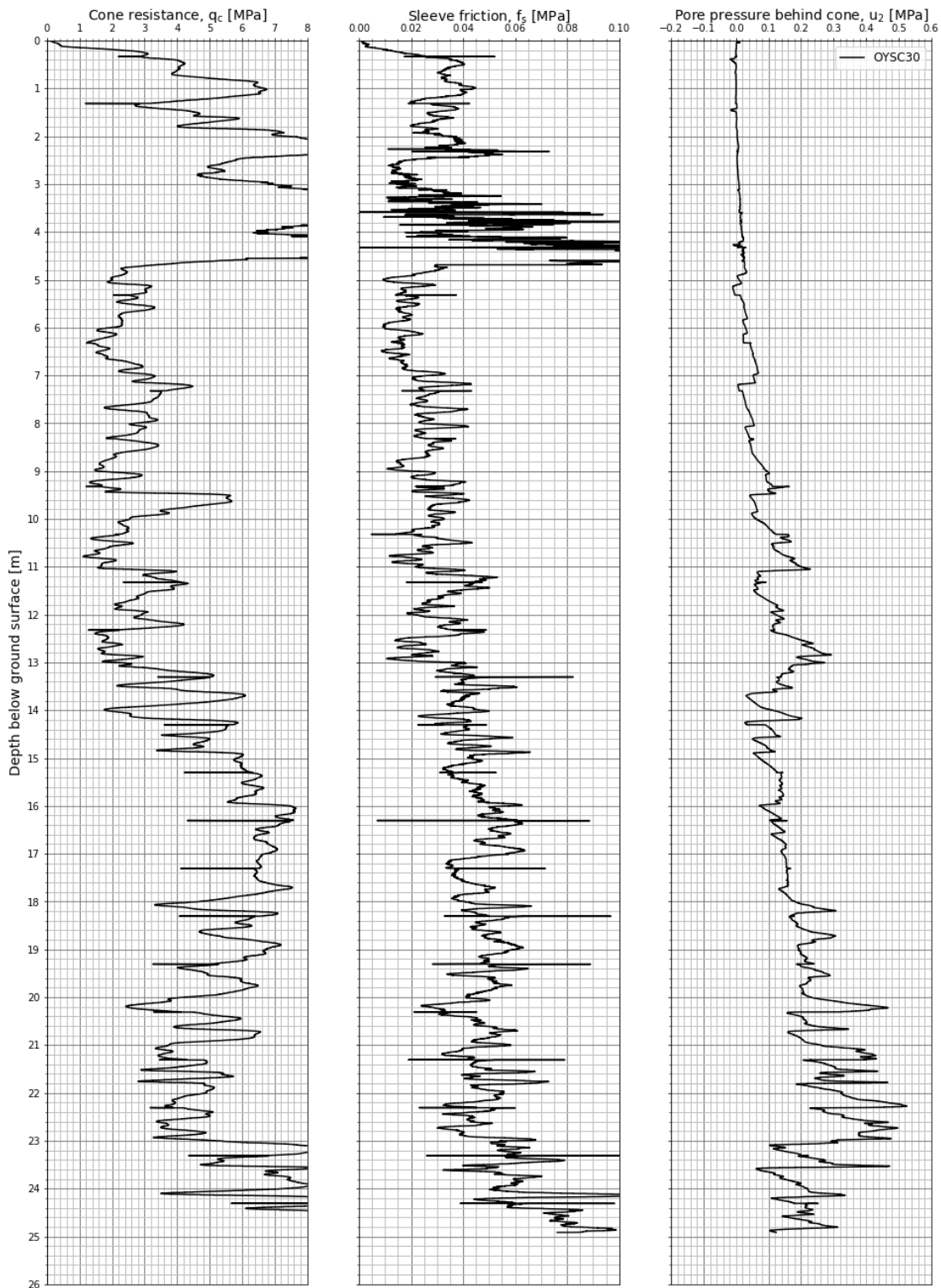


Figure A3.10 Measured cone resistance, sleeve friction and pore pressure – OYSC30.

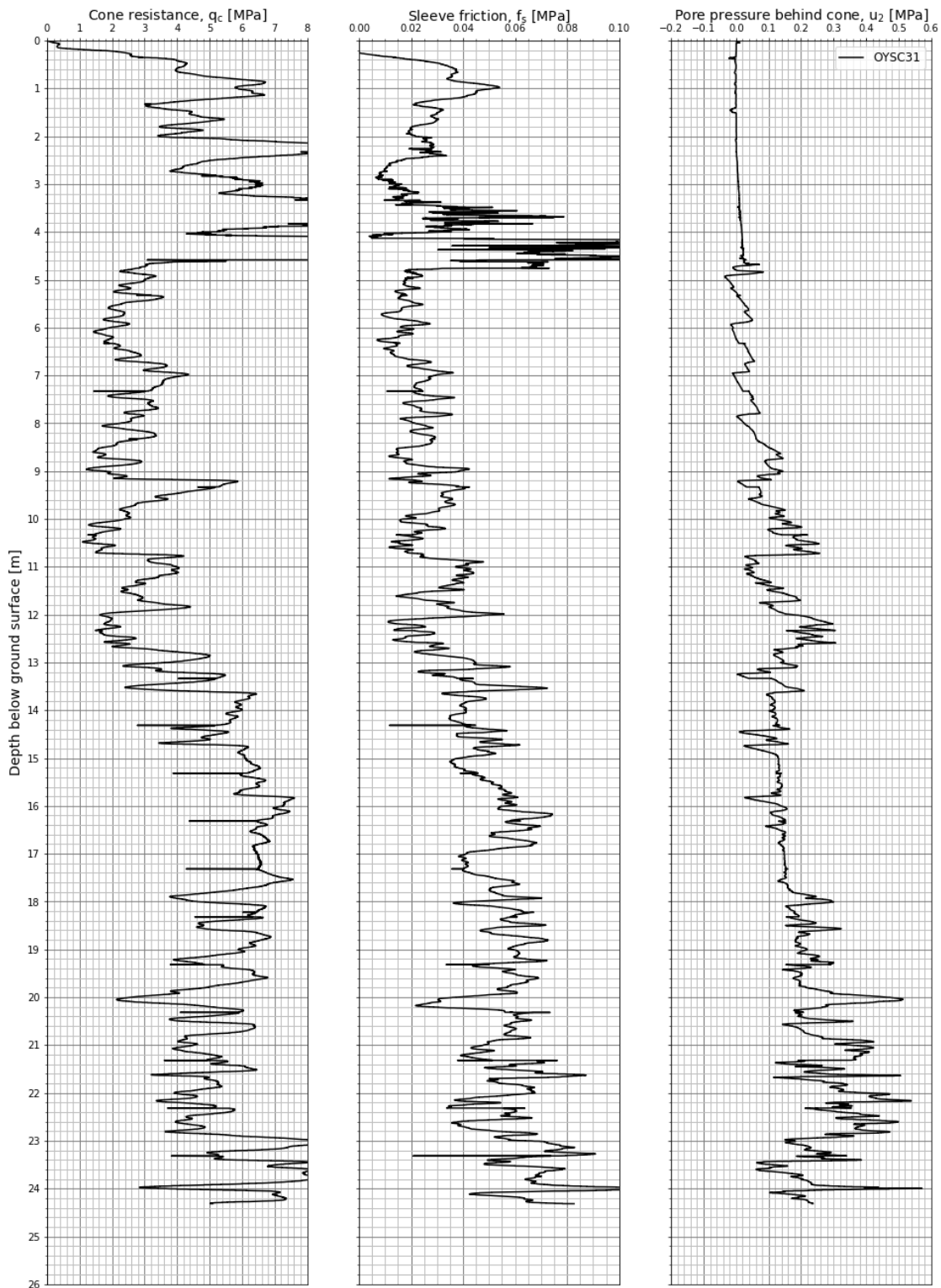


Figure A3.11 Measured cone resistance, sleeve friction and pore pressure – OYSC31.

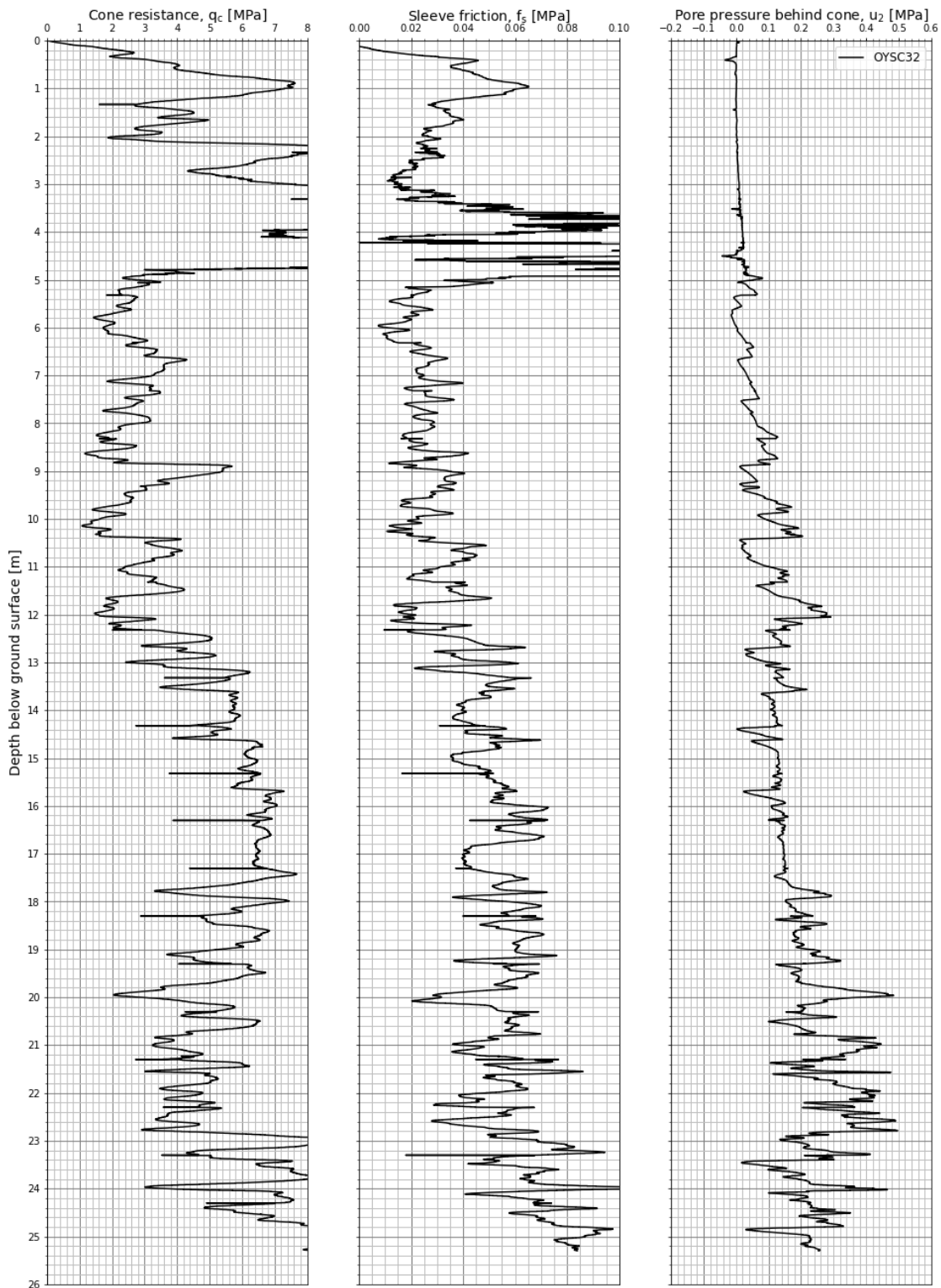


Figure A3.12 Measured cone resistance, sleeve friction and pore pressure – OYSC32.

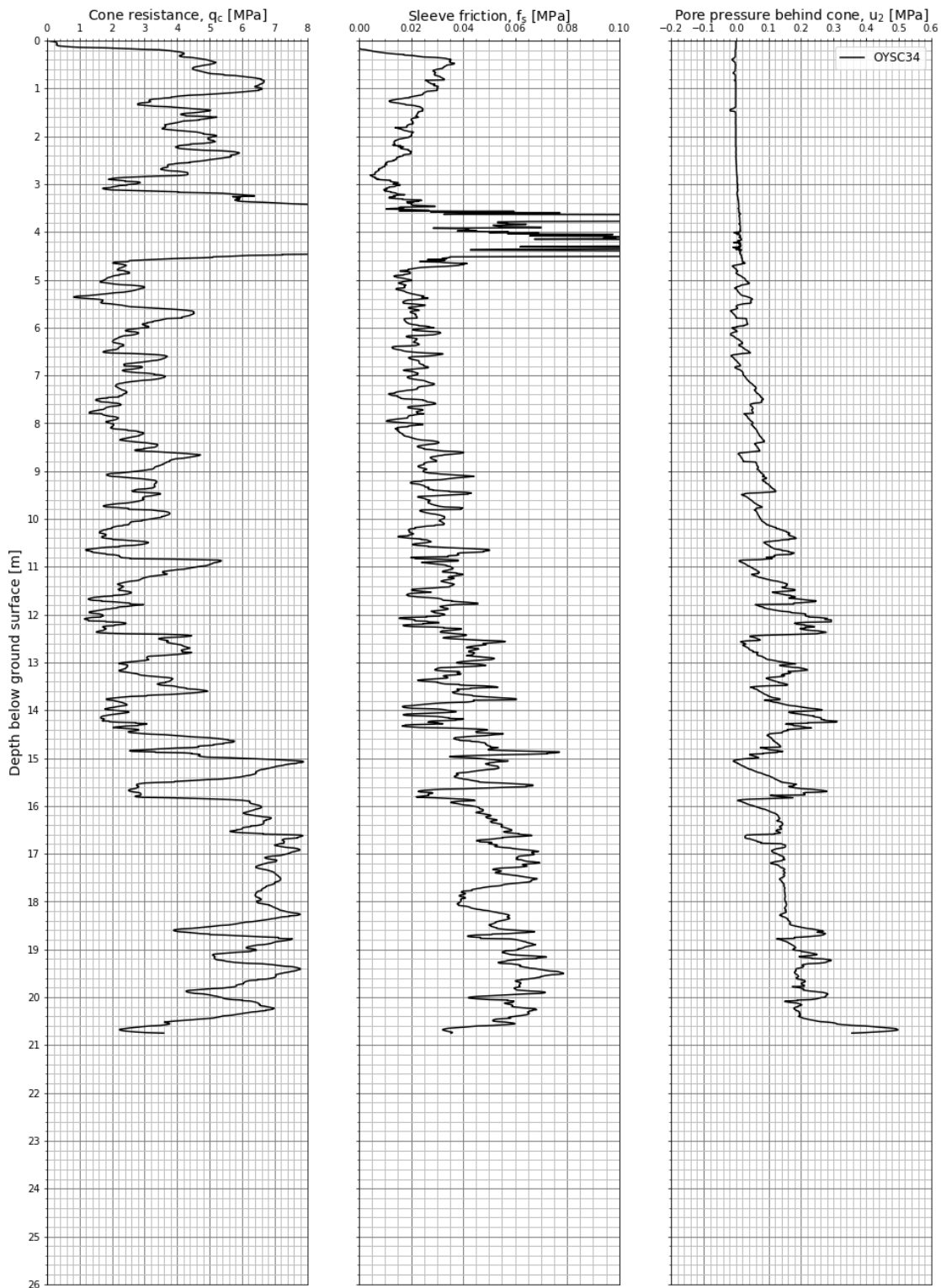


Figure A3.13 Measured cone resistance, sleeve friction and pore pressure – OYSC34.

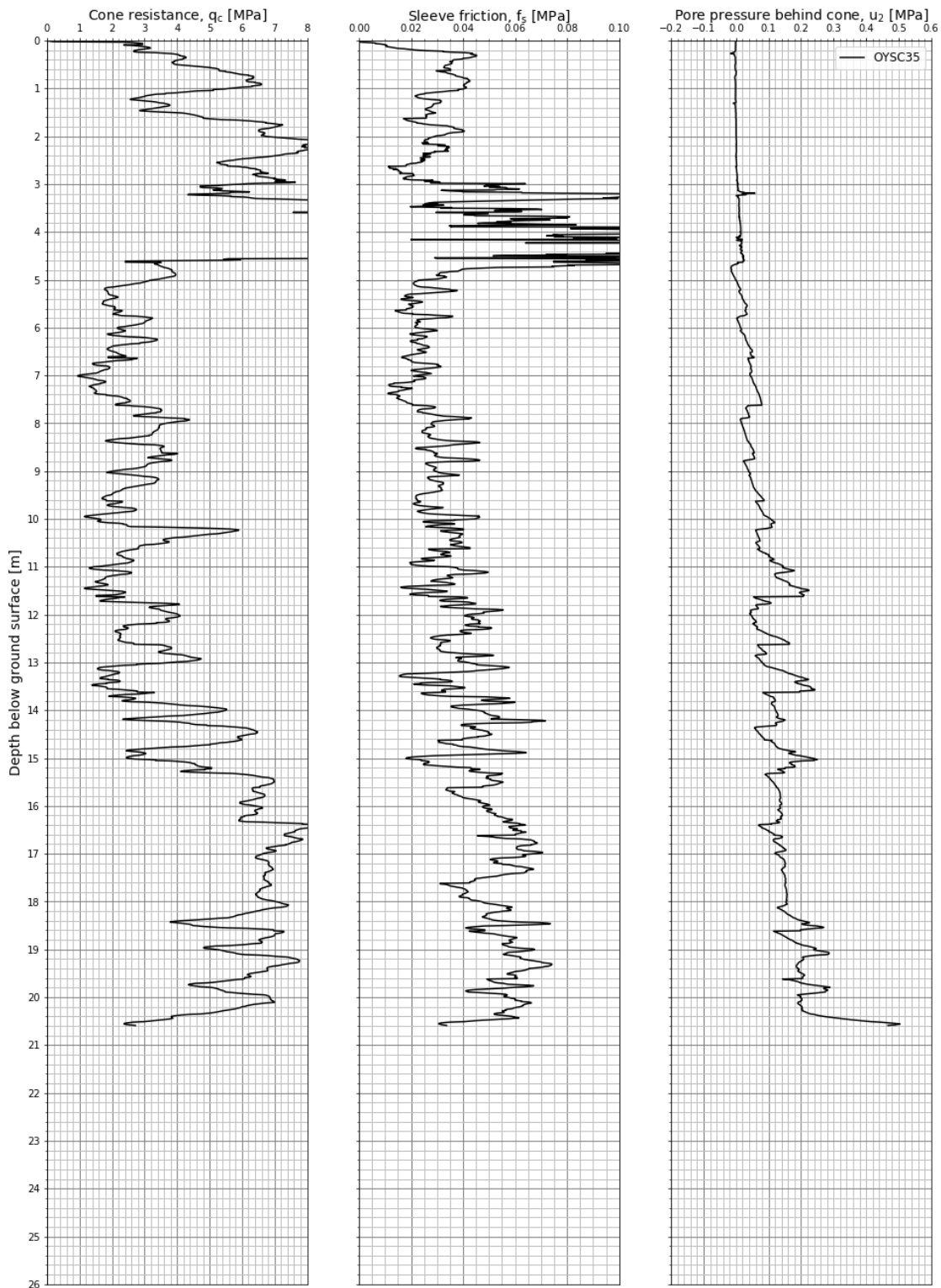


Figure A3.14 Measured cone resistance, sleeve friction and pore pressure – OYSC35.

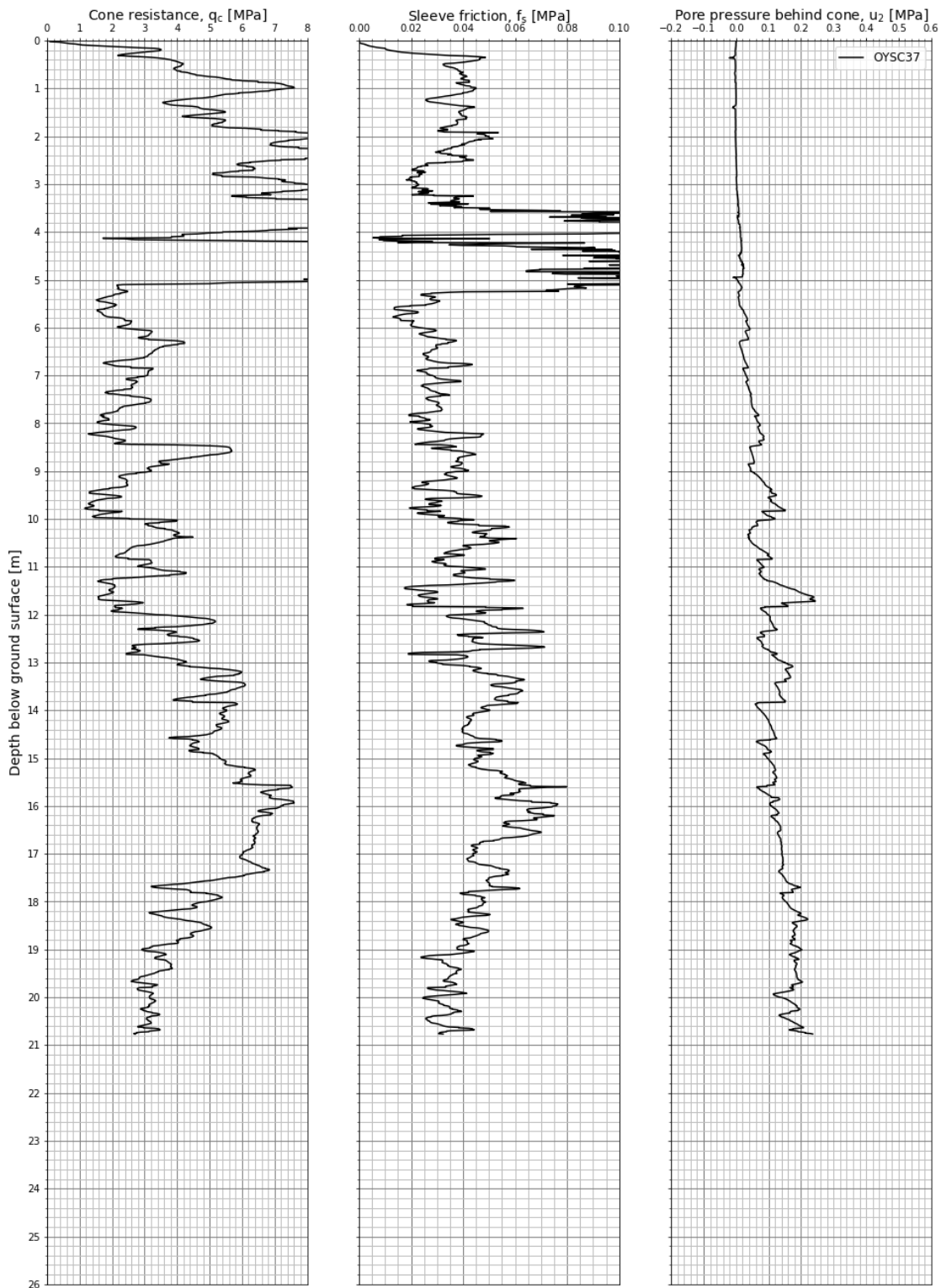


Figure A3.15 Measured cone resistance, sleeve friction and pore pressure – OYSC37.

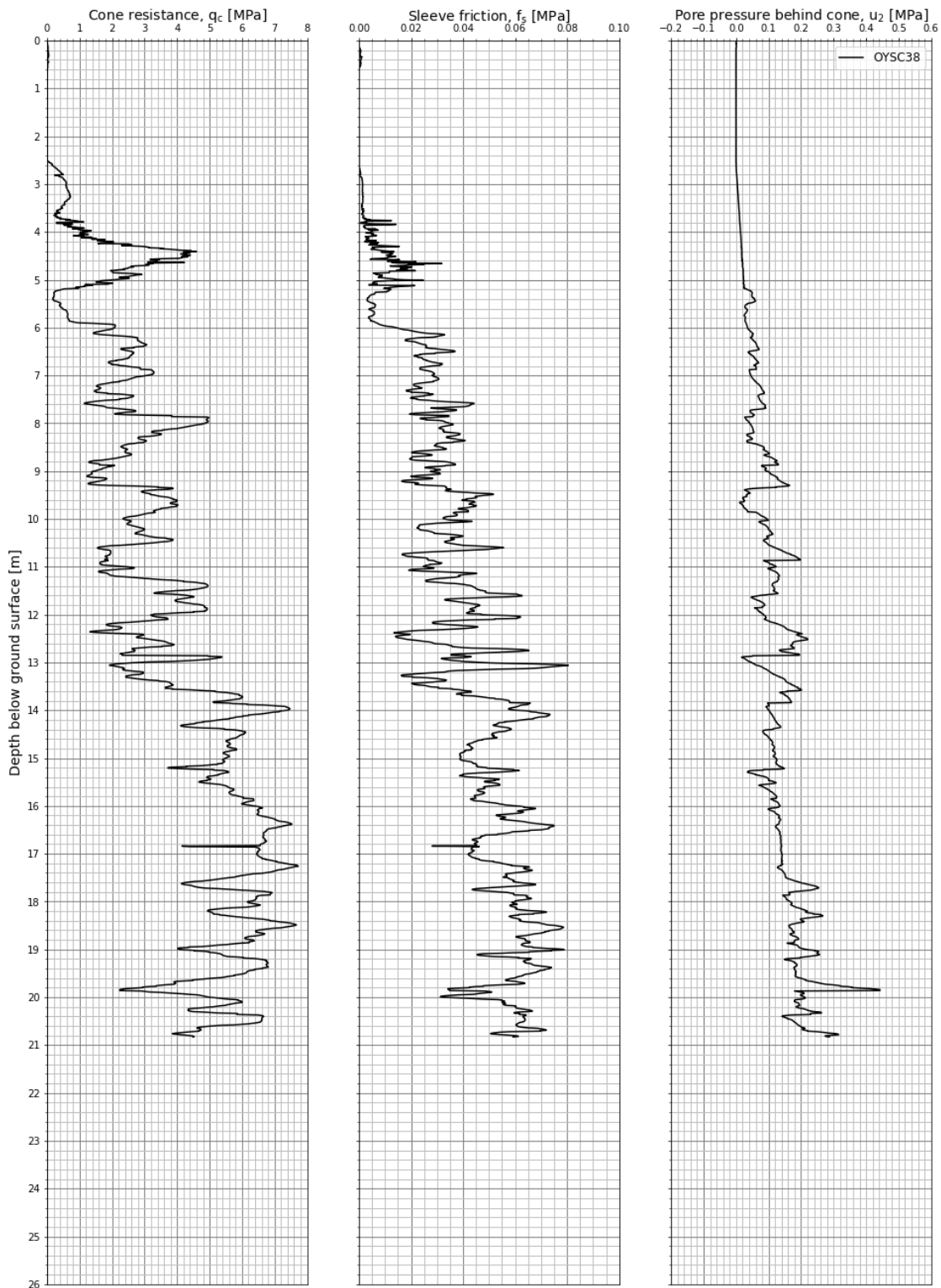


Figure A3.16 Measured cone resistance, sleeve friction and pore pressure – OYSC38.

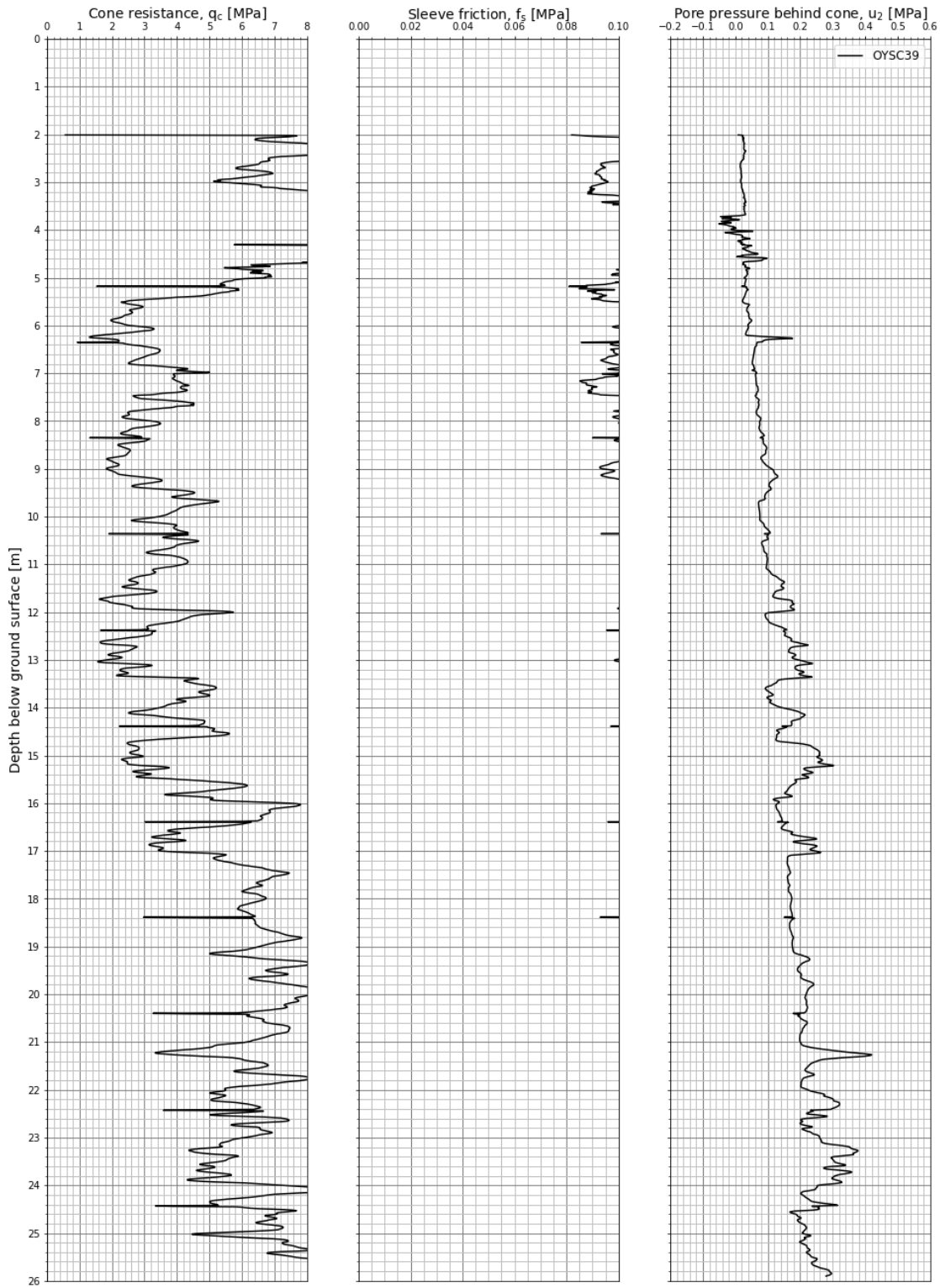


Figure A3.17 Measured cone resistance, sleeve friction and pore pressure – OYSC39.

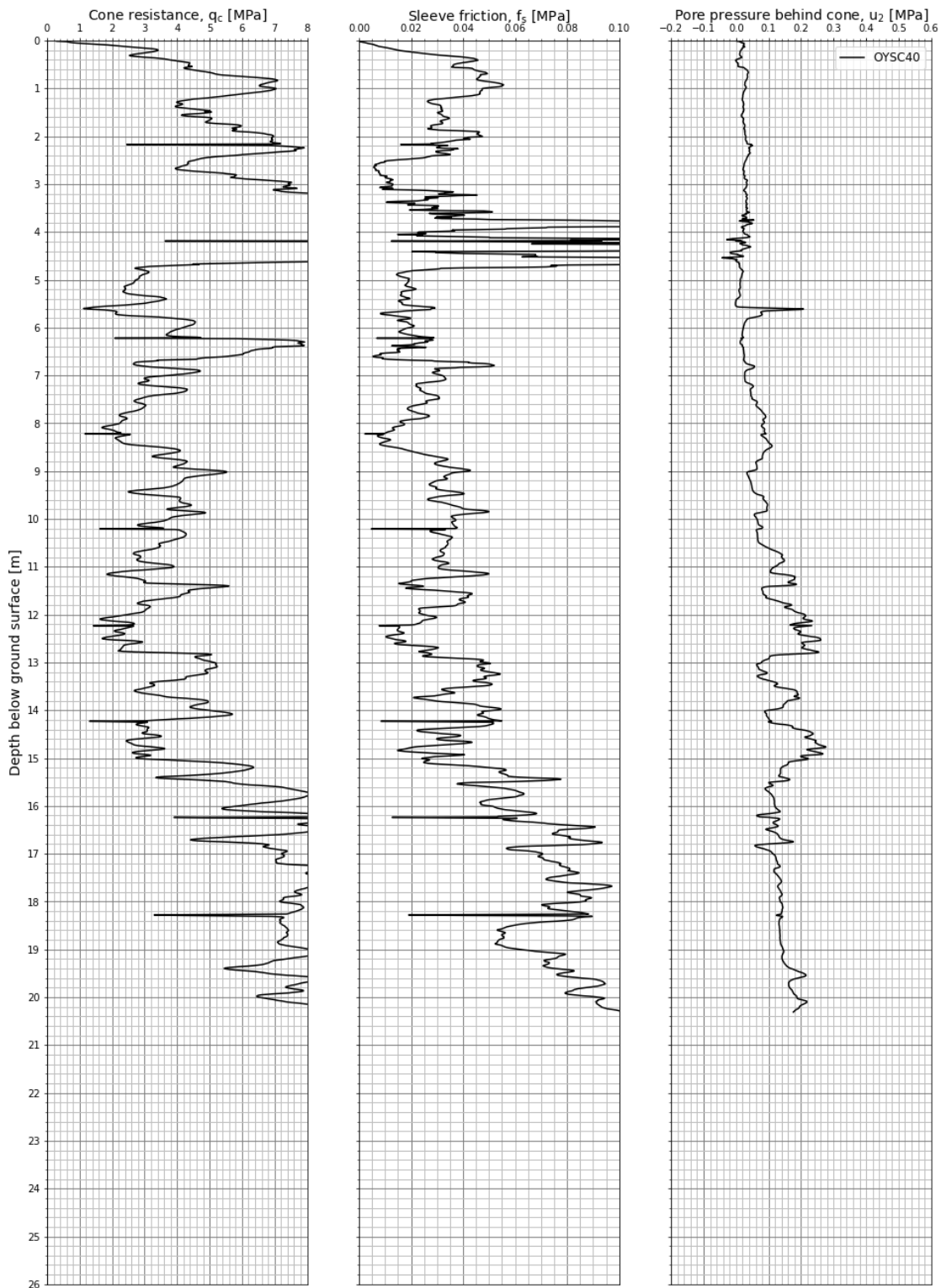


Figure A3.18 Measured cone resistance, sleeve friction and pore pressure – OYSC40.

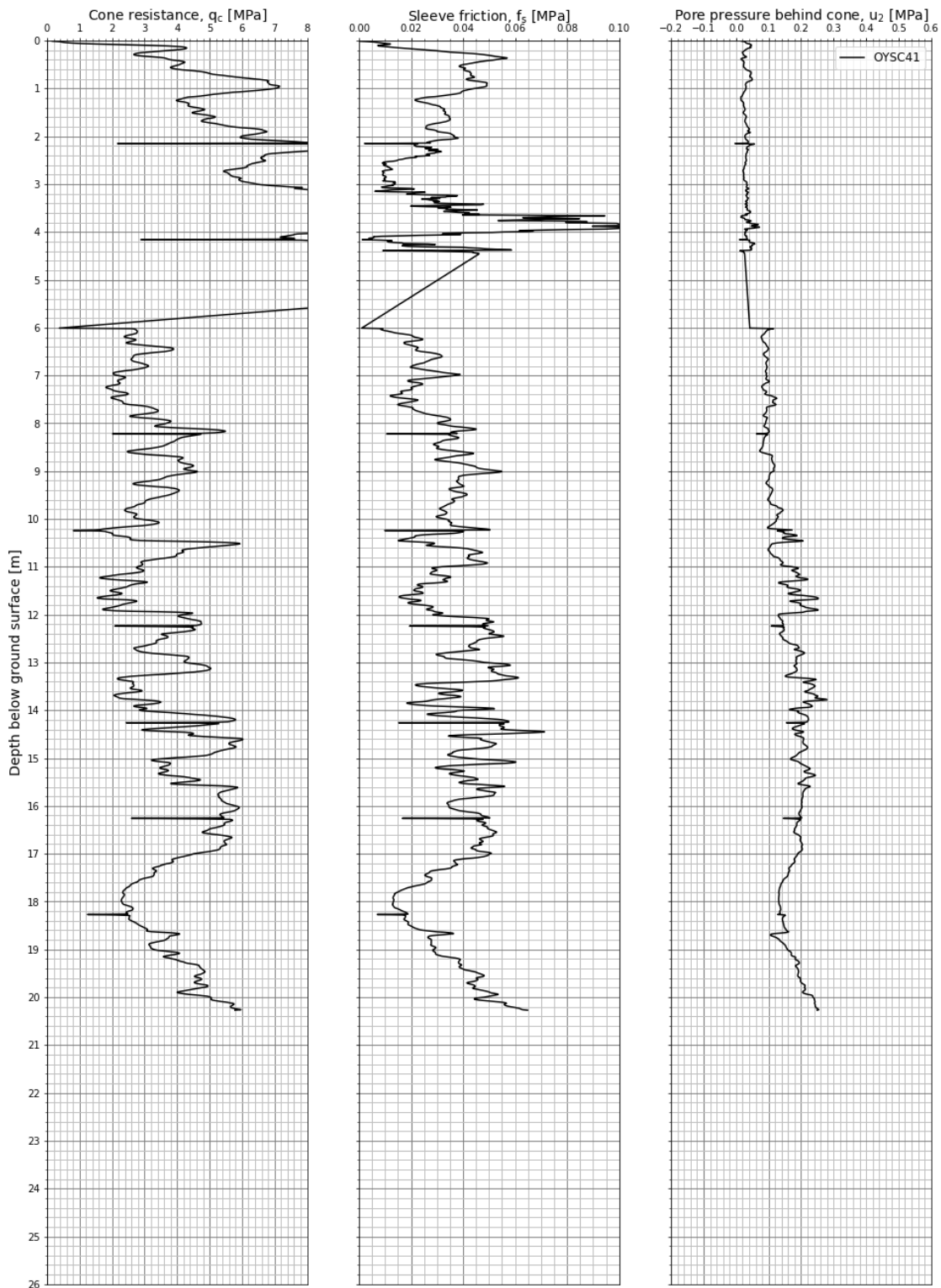


Figure A3.19 Measured cone resistance, sleeve friction and pore pressure – OYSC41.

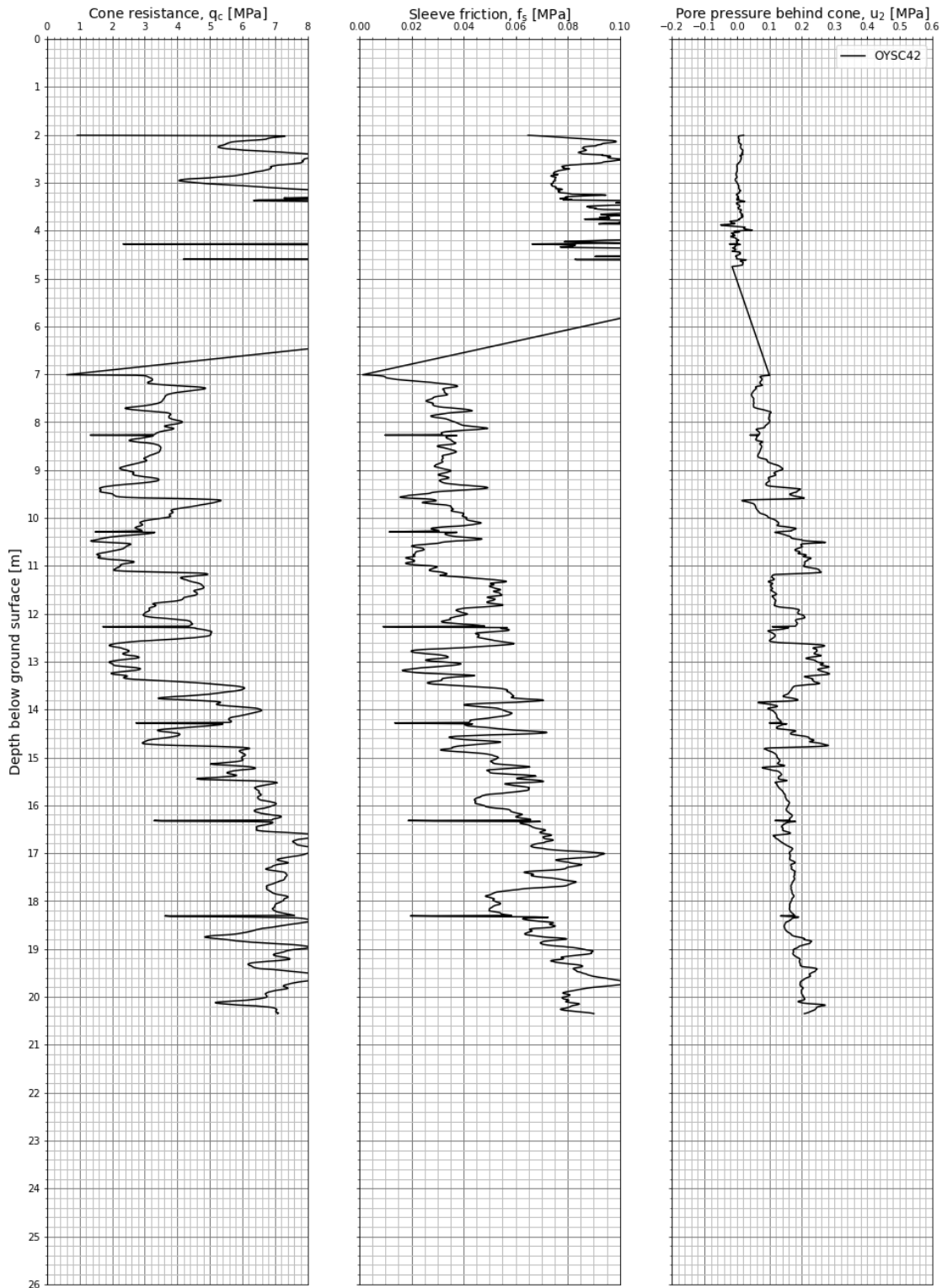


Figure A3.20 Measured cone resistance, sleeve friction and pore pressure – OYSC42.

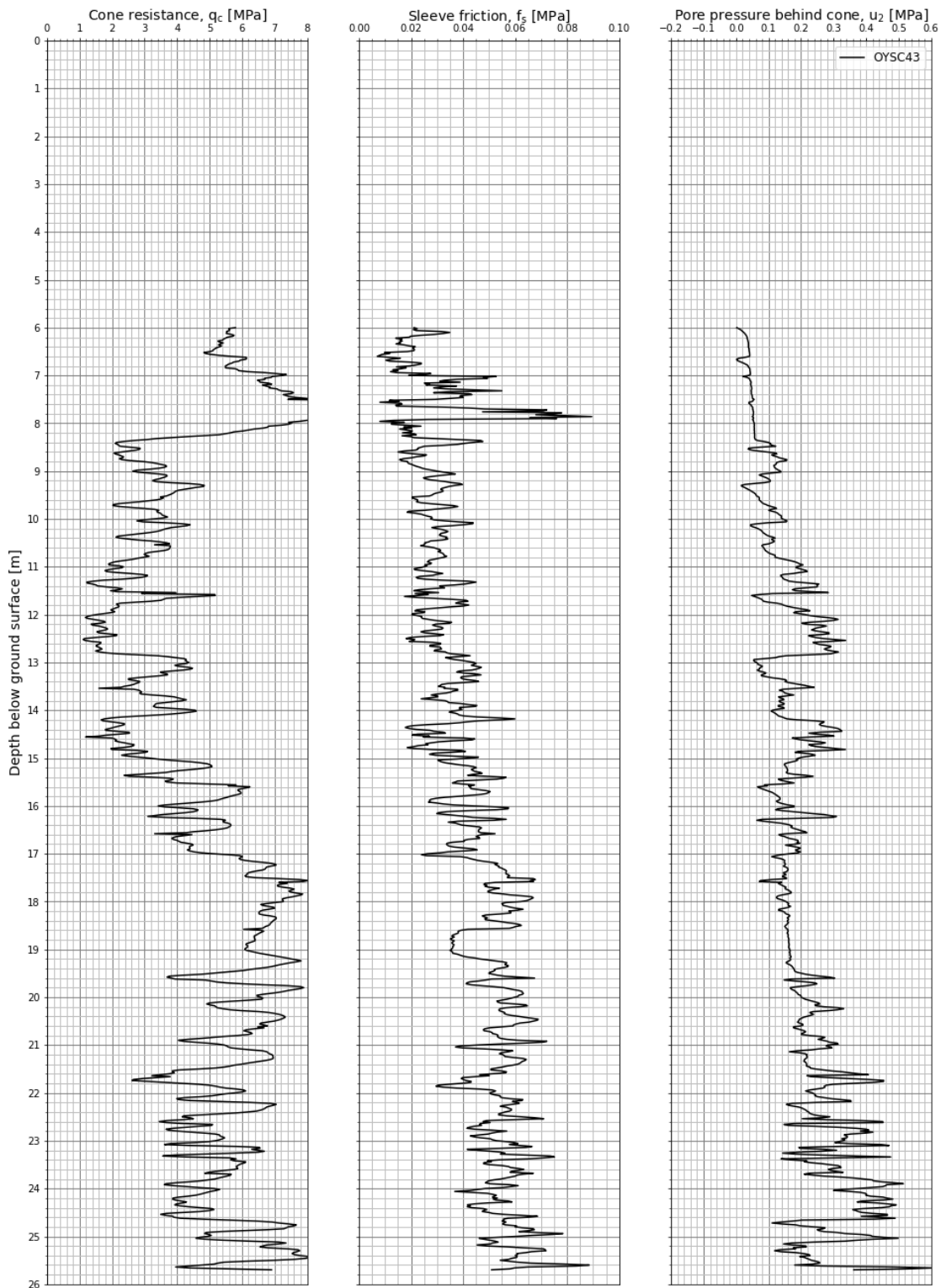


Figure A3.21 Measured cone resistance, sleeve friction and pore pressure – OYSC43.

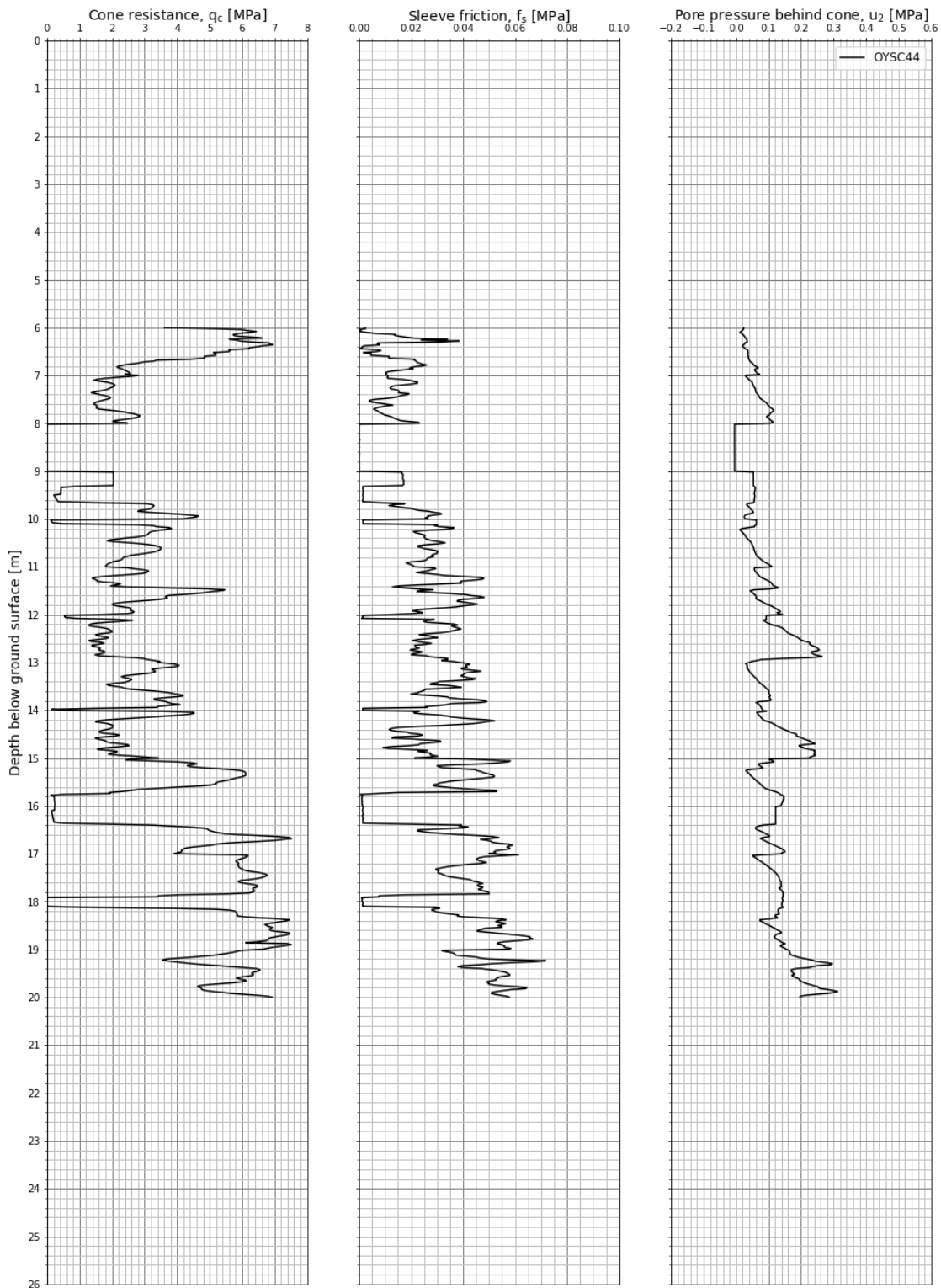


Figure A3.22 Measured cone resistance, sleeve friction and pore pressure – OYSC44.

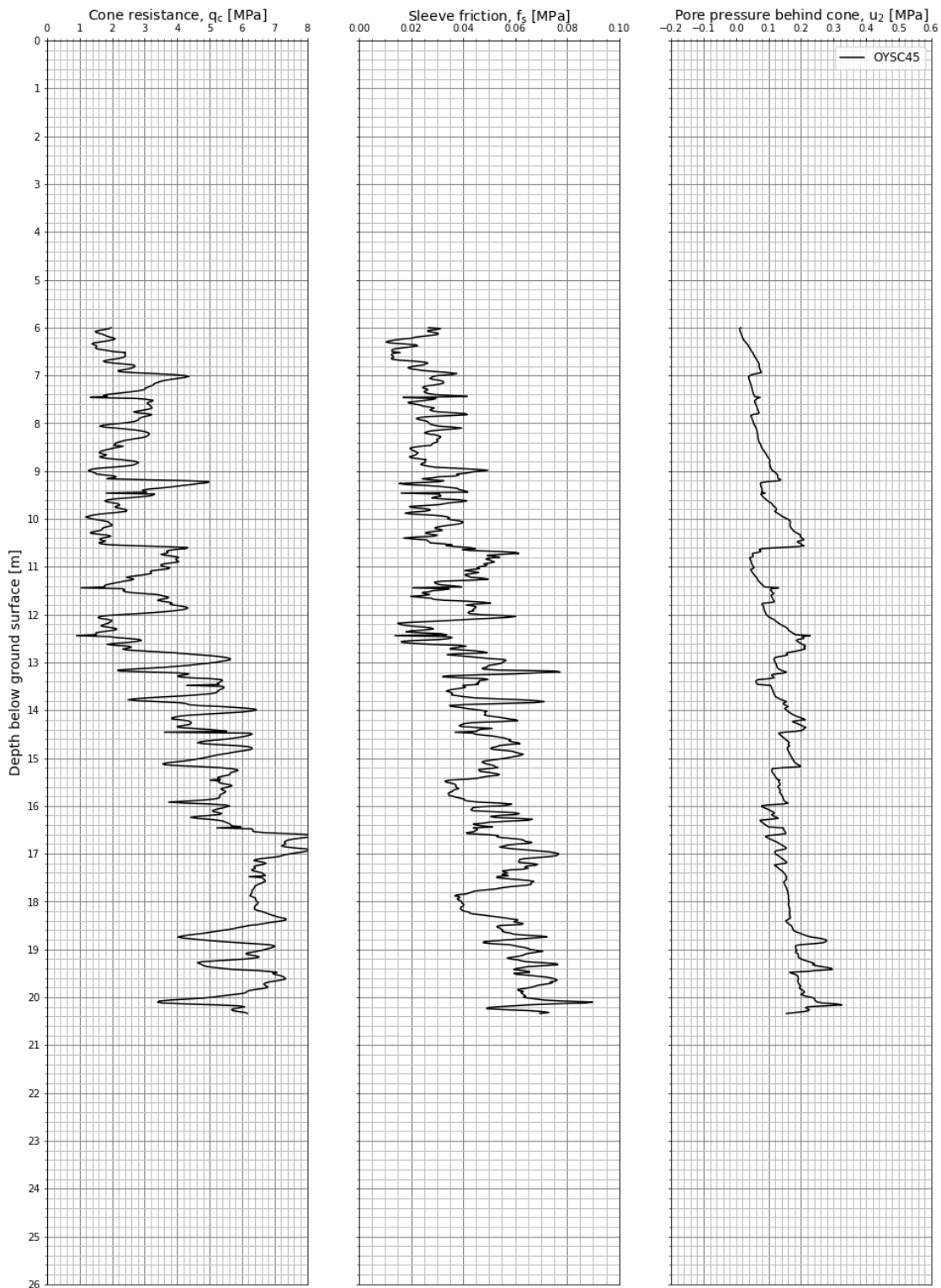


Figure A3.23 Measured cone resistance, sleeve friction and pore pressure – OYSC45.

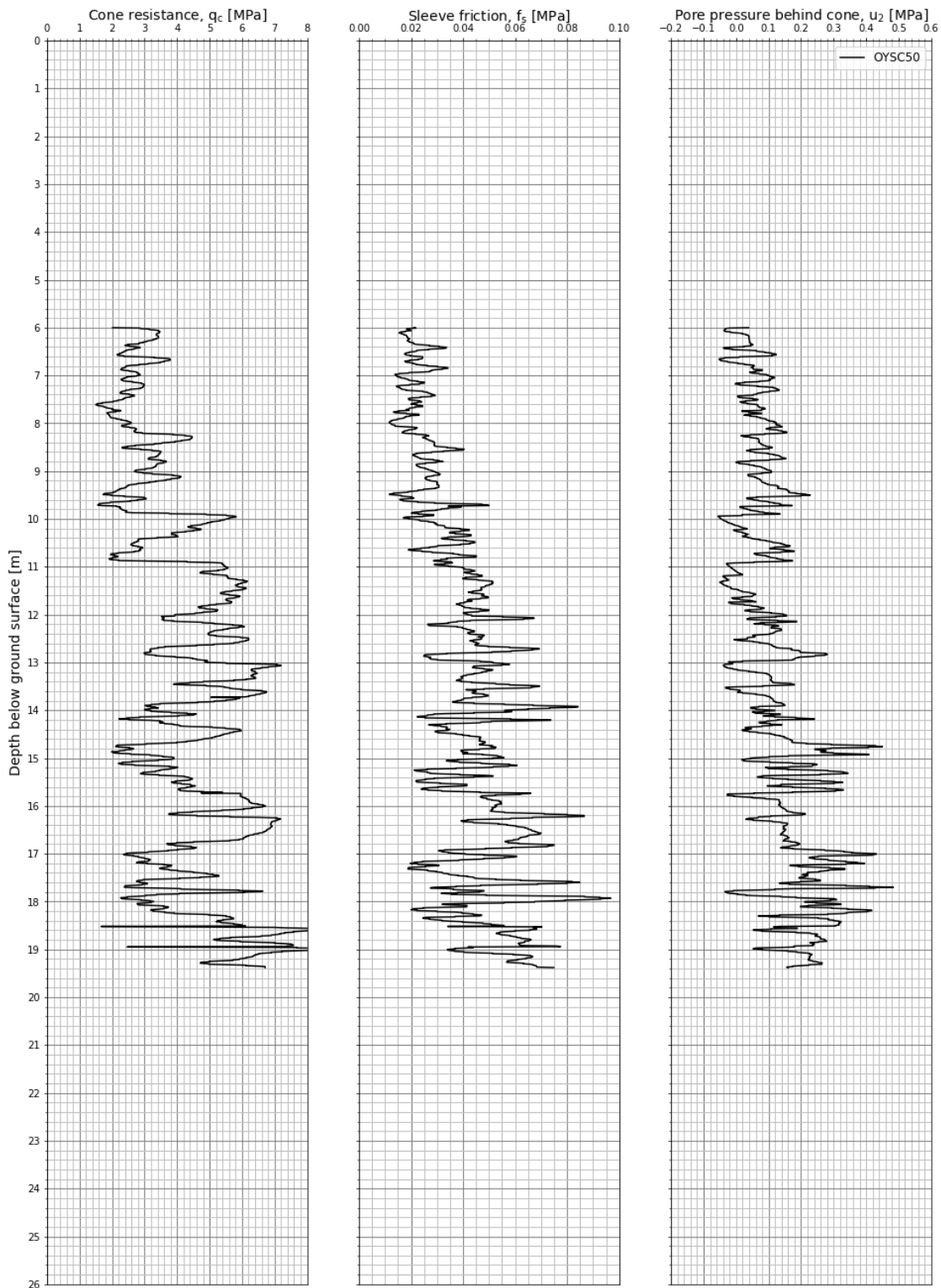


Figure A3.24 Measured cone resistance, sleeve friction and pore pressure – OYSC50.

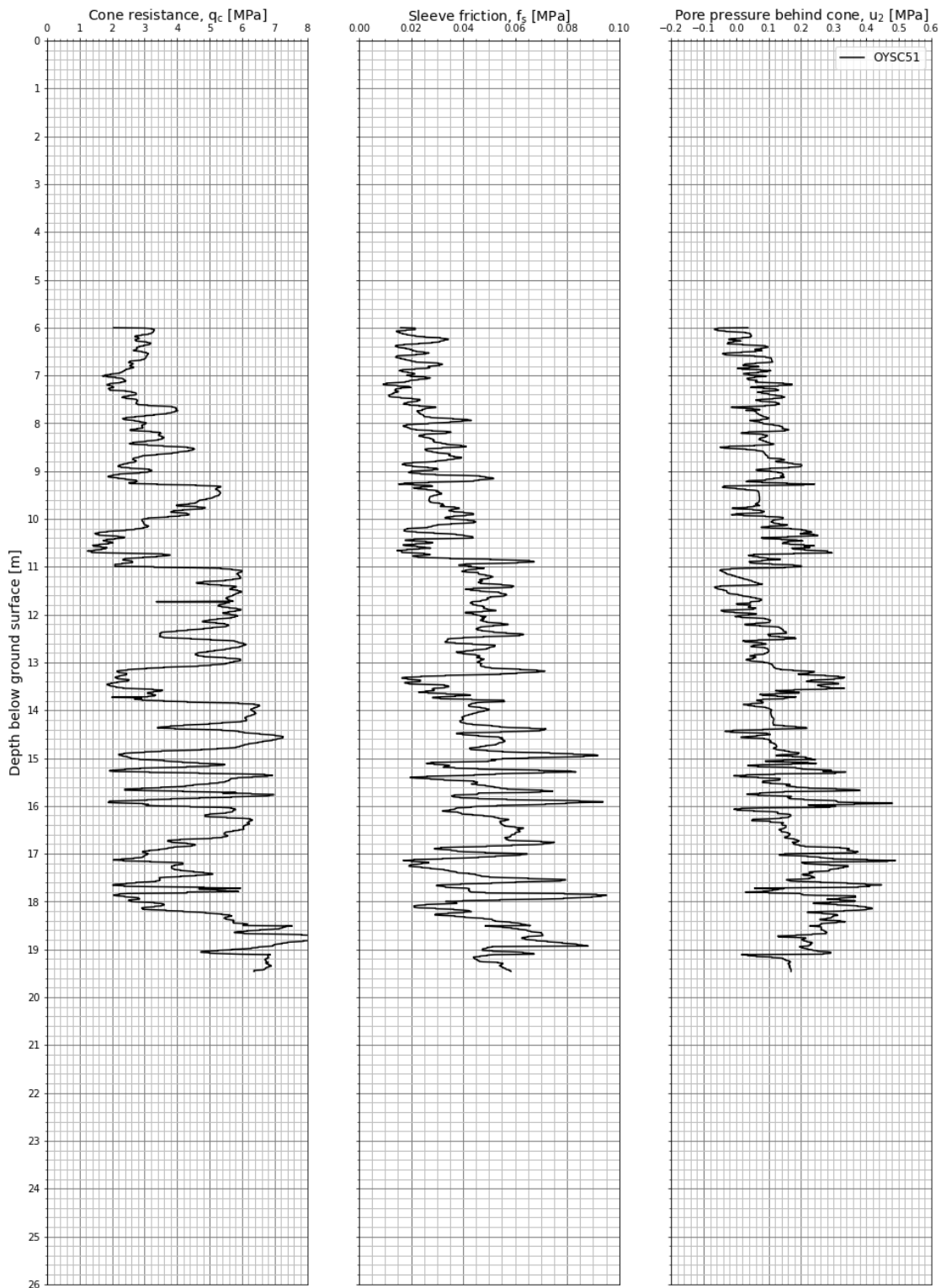


Figure A3.25 Measured cone resistance, sleeve friction and pore pressure – OYSC51.

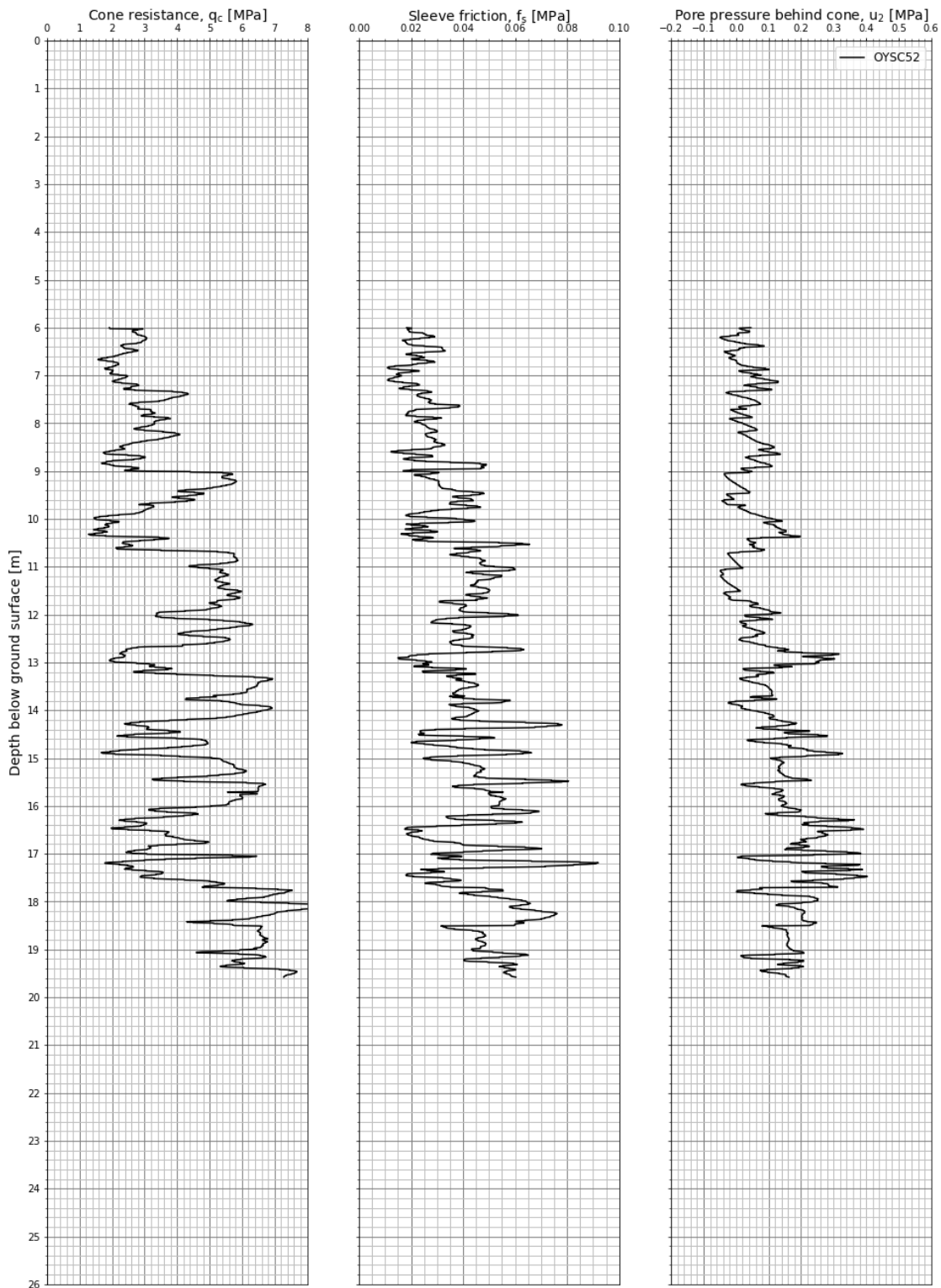


Figure A3.26 Measured cone resistance, sleeve friction and pore pressure – OYSC51.

A4 Quick clay site – Tiller-Flotten

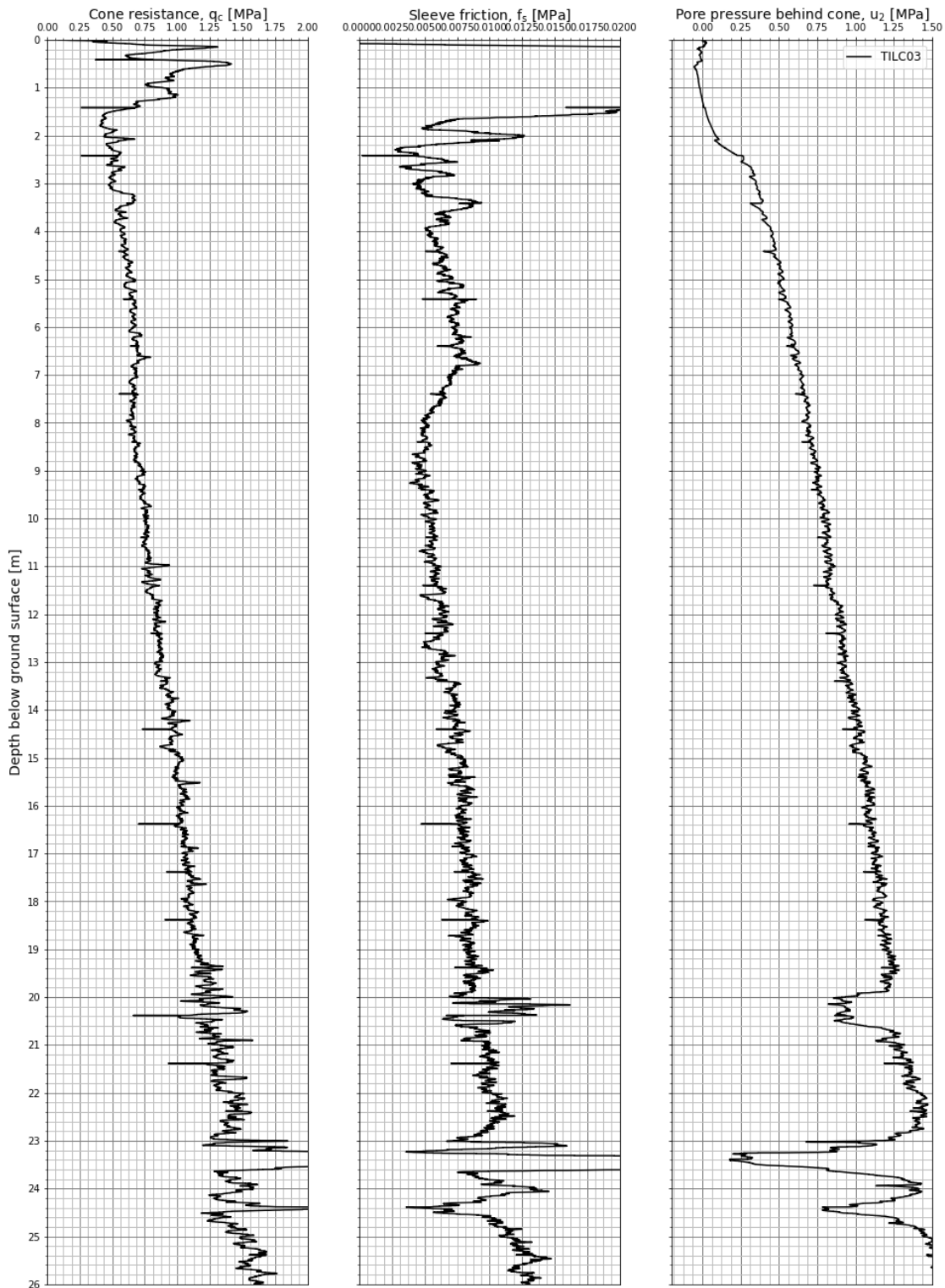


Figure A4.1 Measured cone resistance, sleeve friction and pore pressure – TILCO3.

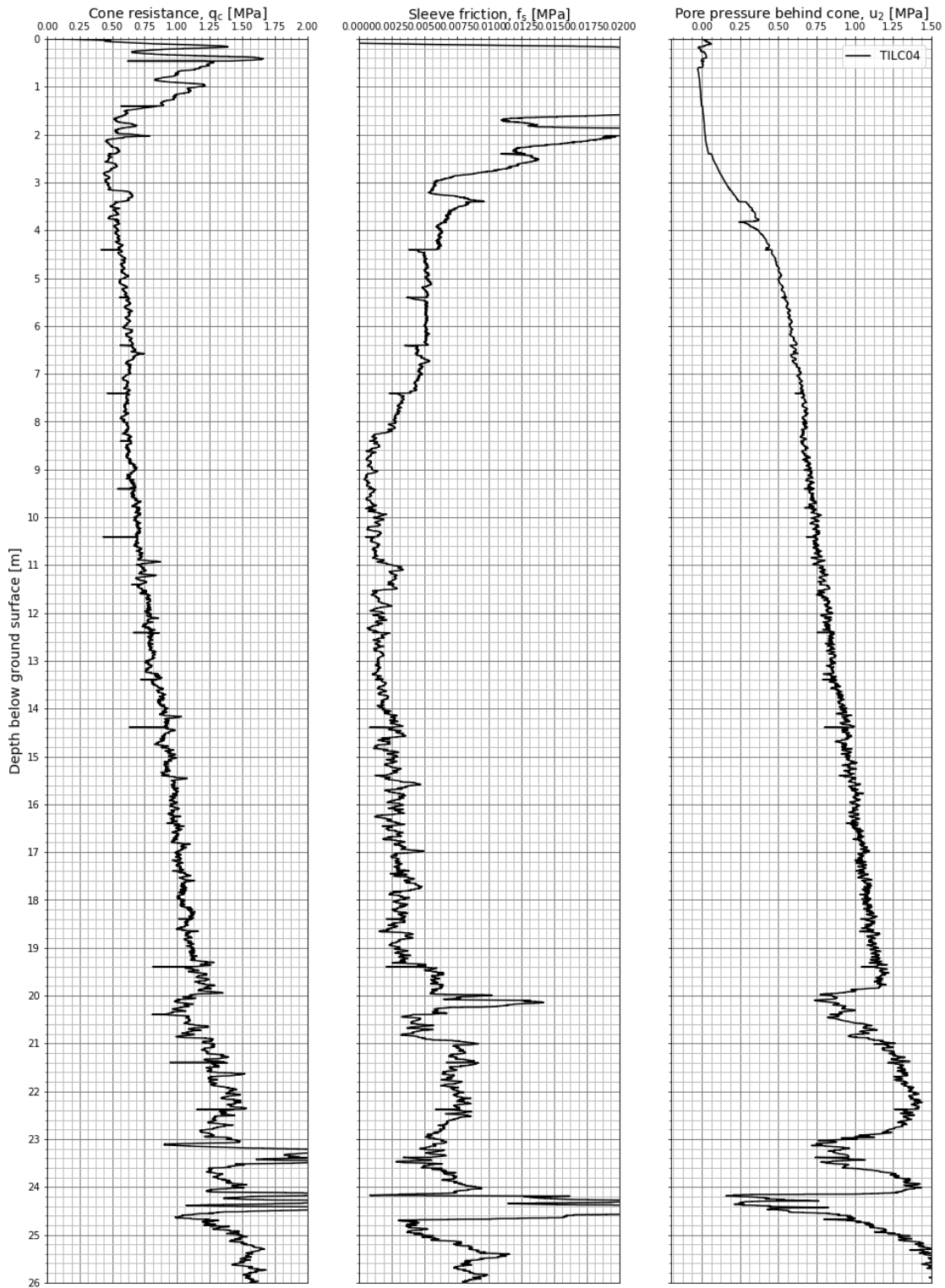


Figure A4.2 Measured cone resistance, sleeve friction and pore pressure – TILC04.

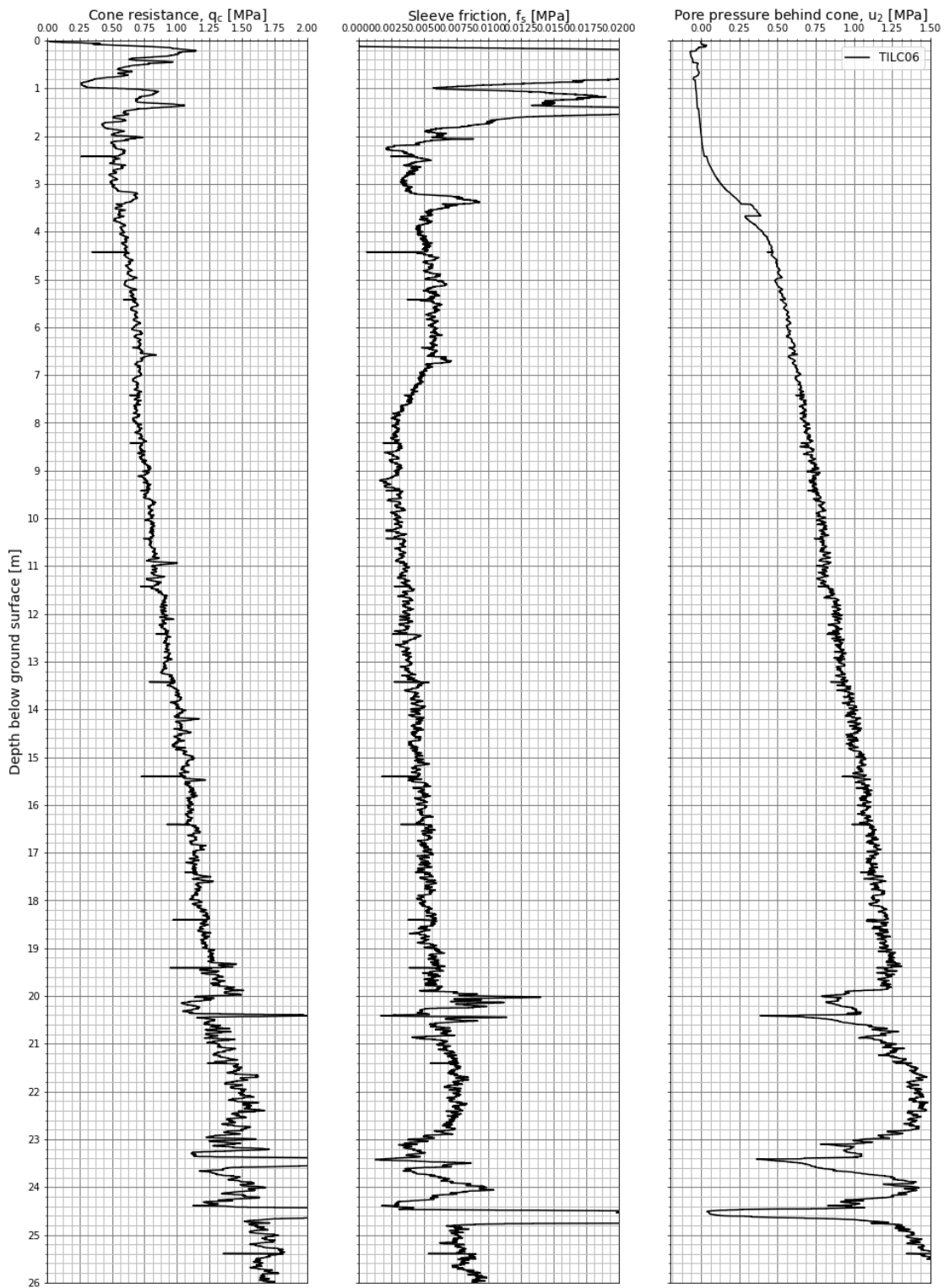


Figure A4.3 Measured cone resistance, sleeve friction and pore pressure – TILC06.

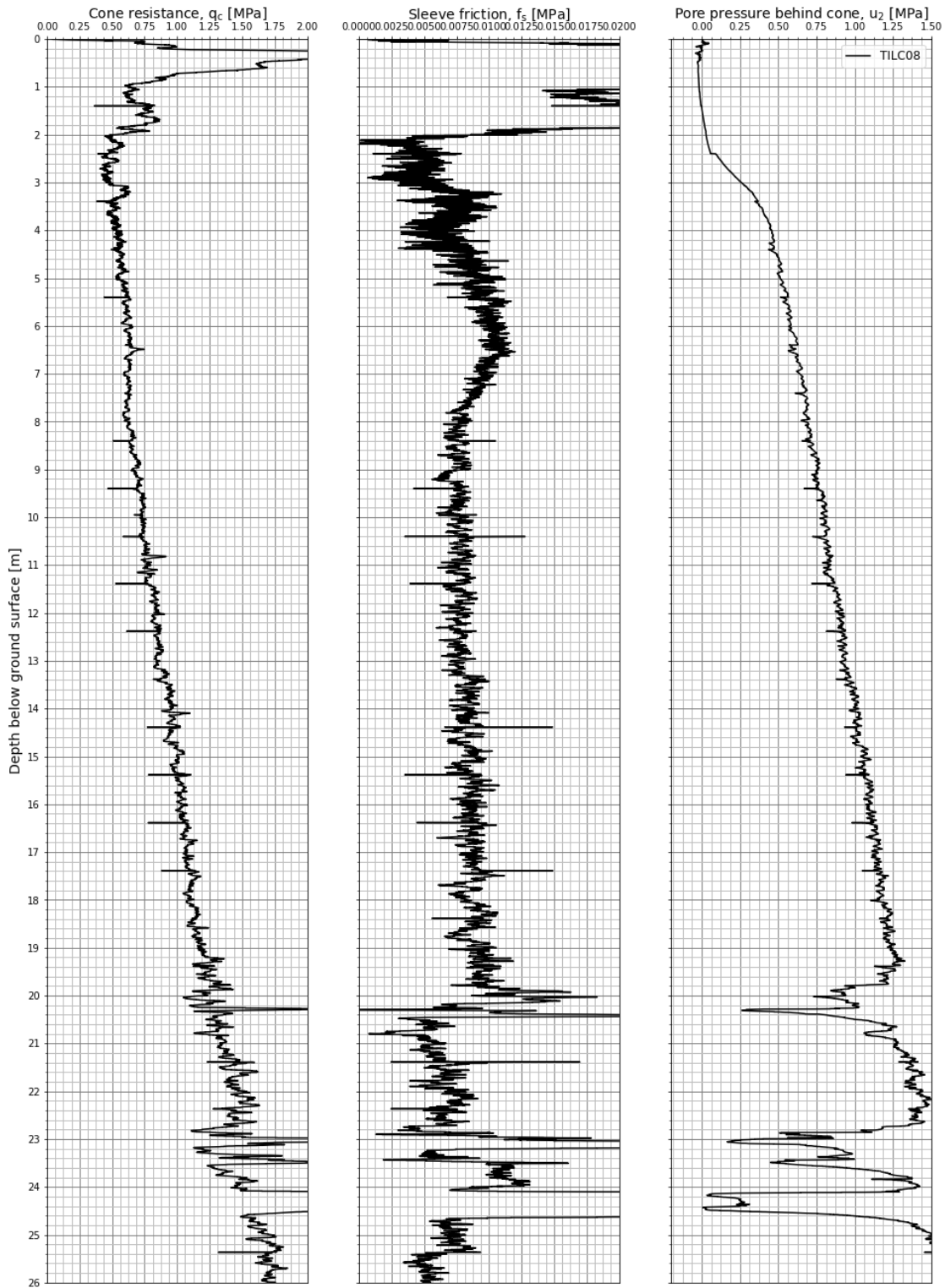


Figure A4.4 Measured cone resistance, sleeve friction and pore pressure – TILC08.

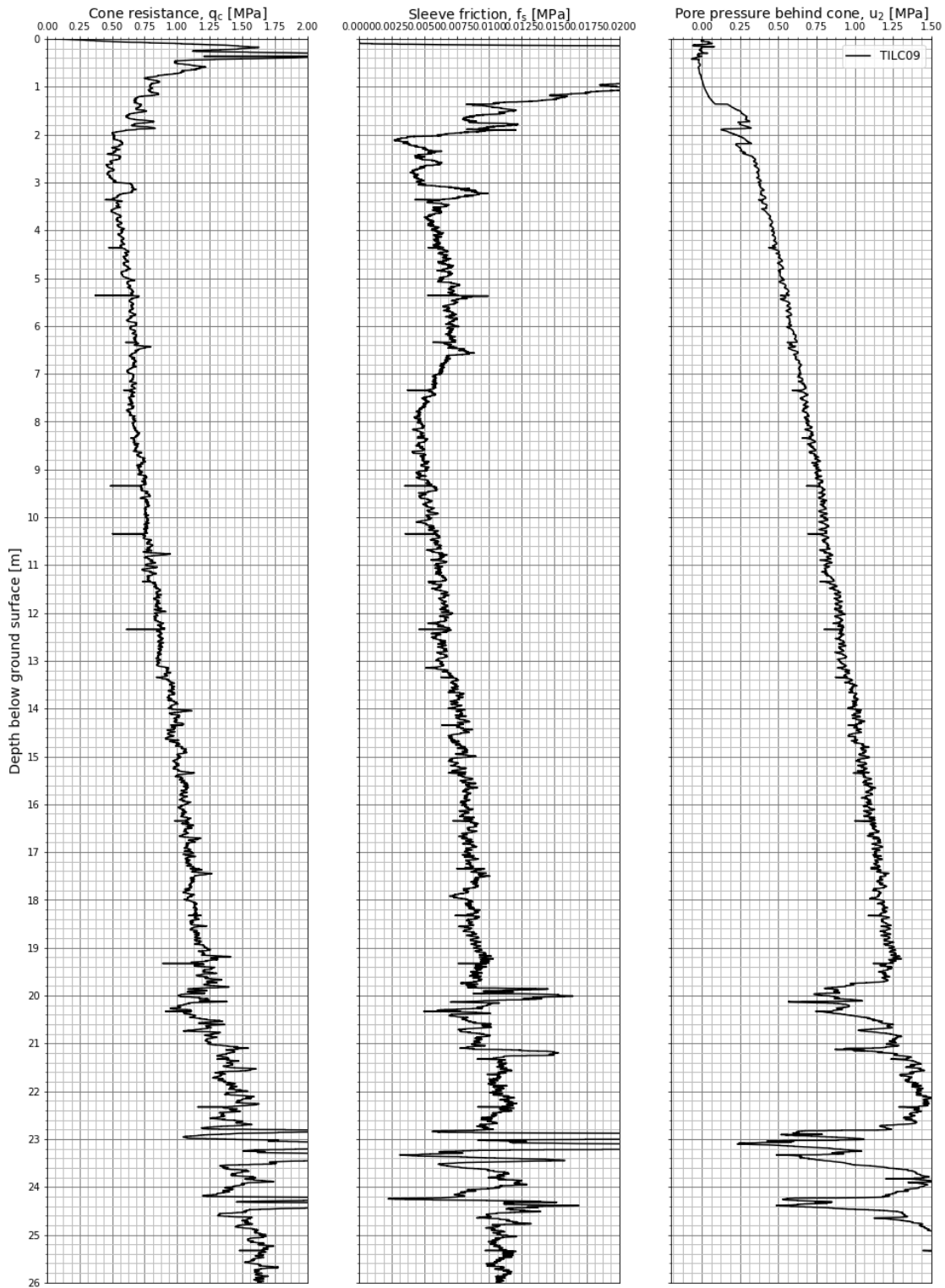


Figure A4.5 Measured cone resistance, sleeve friction and pore pressure – TILC09.

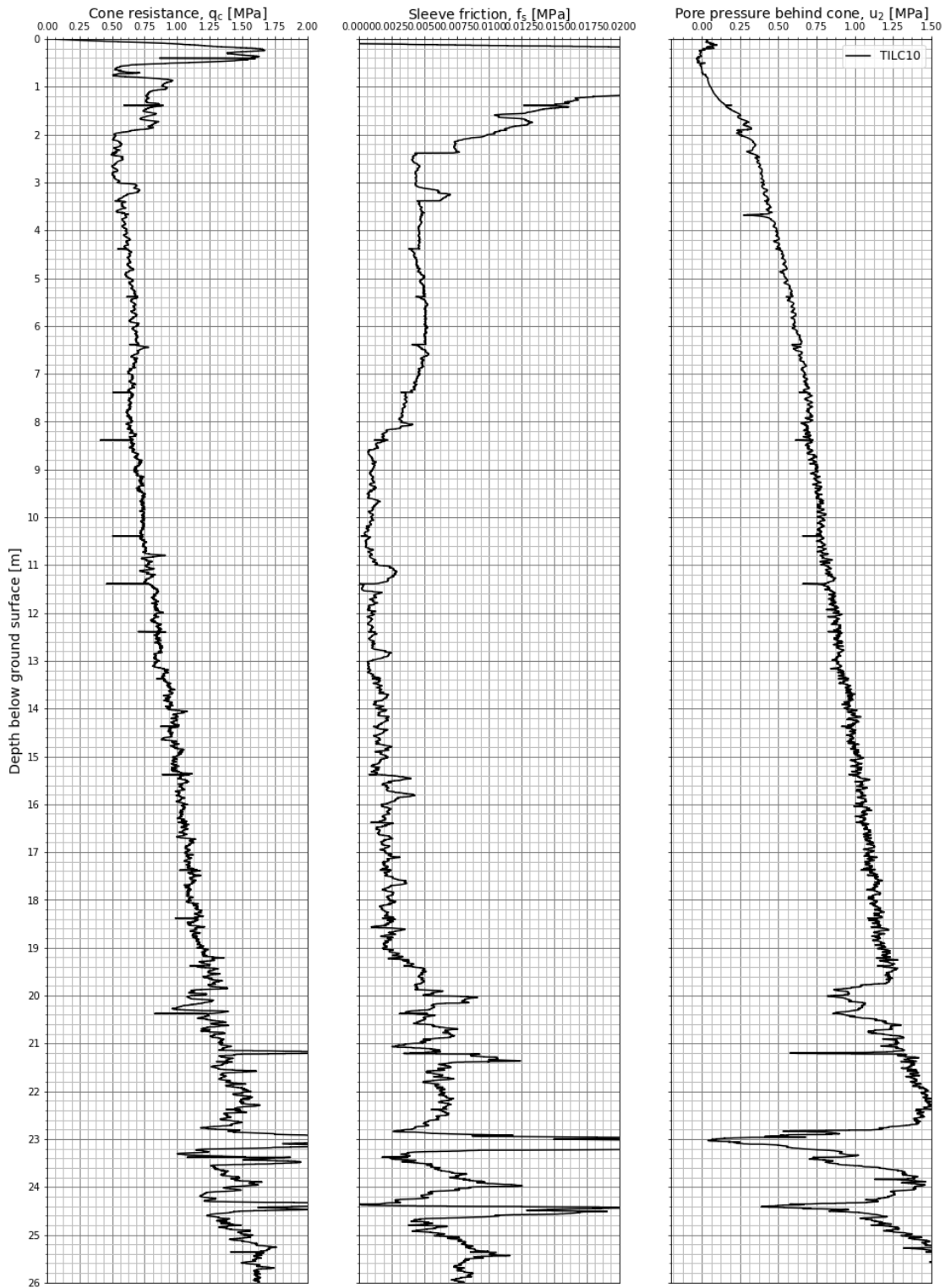


Figure A4.6 Measured cone resistance, sleeve friction and pore pressure – TILC10.

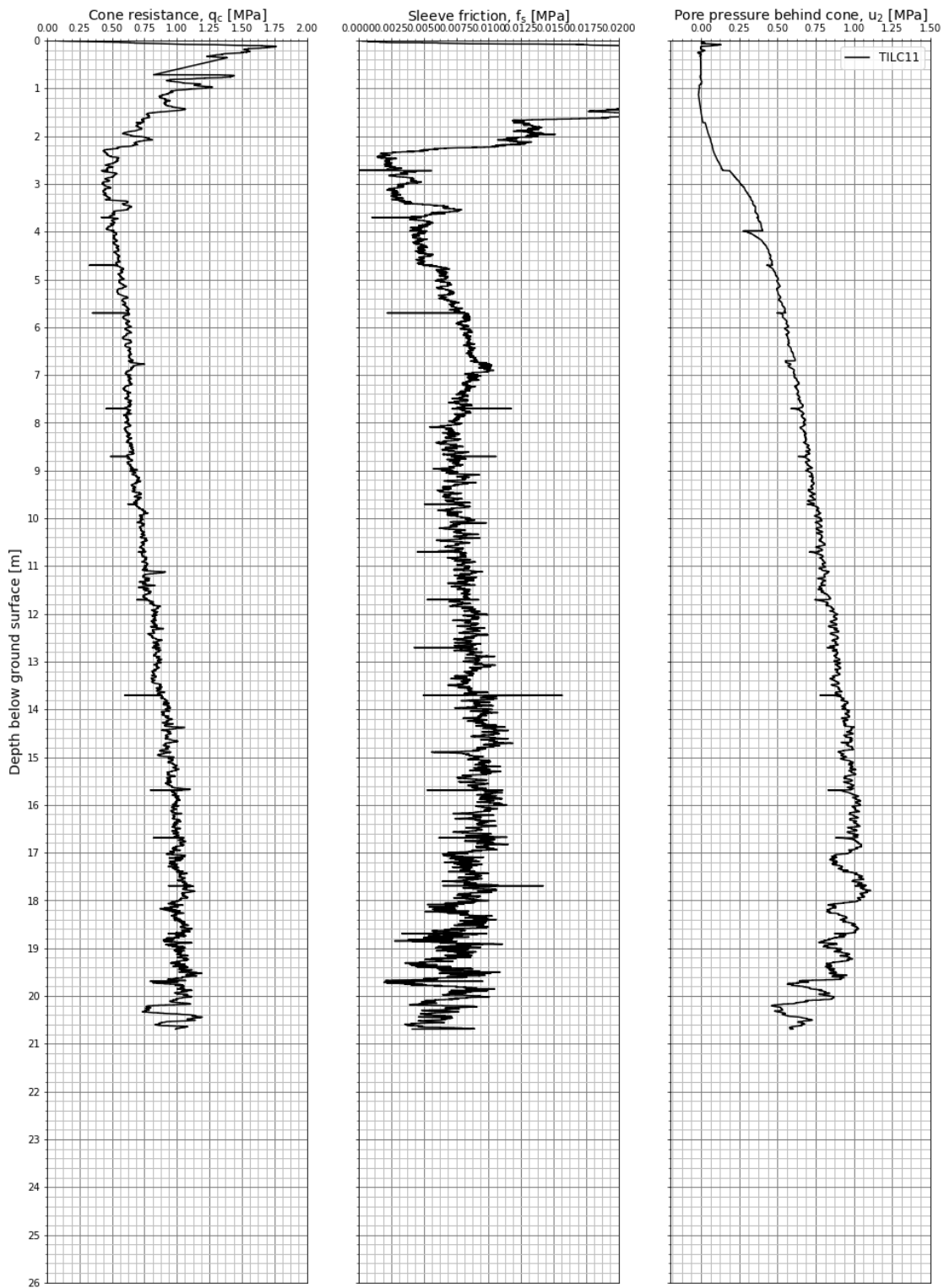


Figure A4.7 Measured cone resistance, sleeve friction and pore pressure – TILC11.

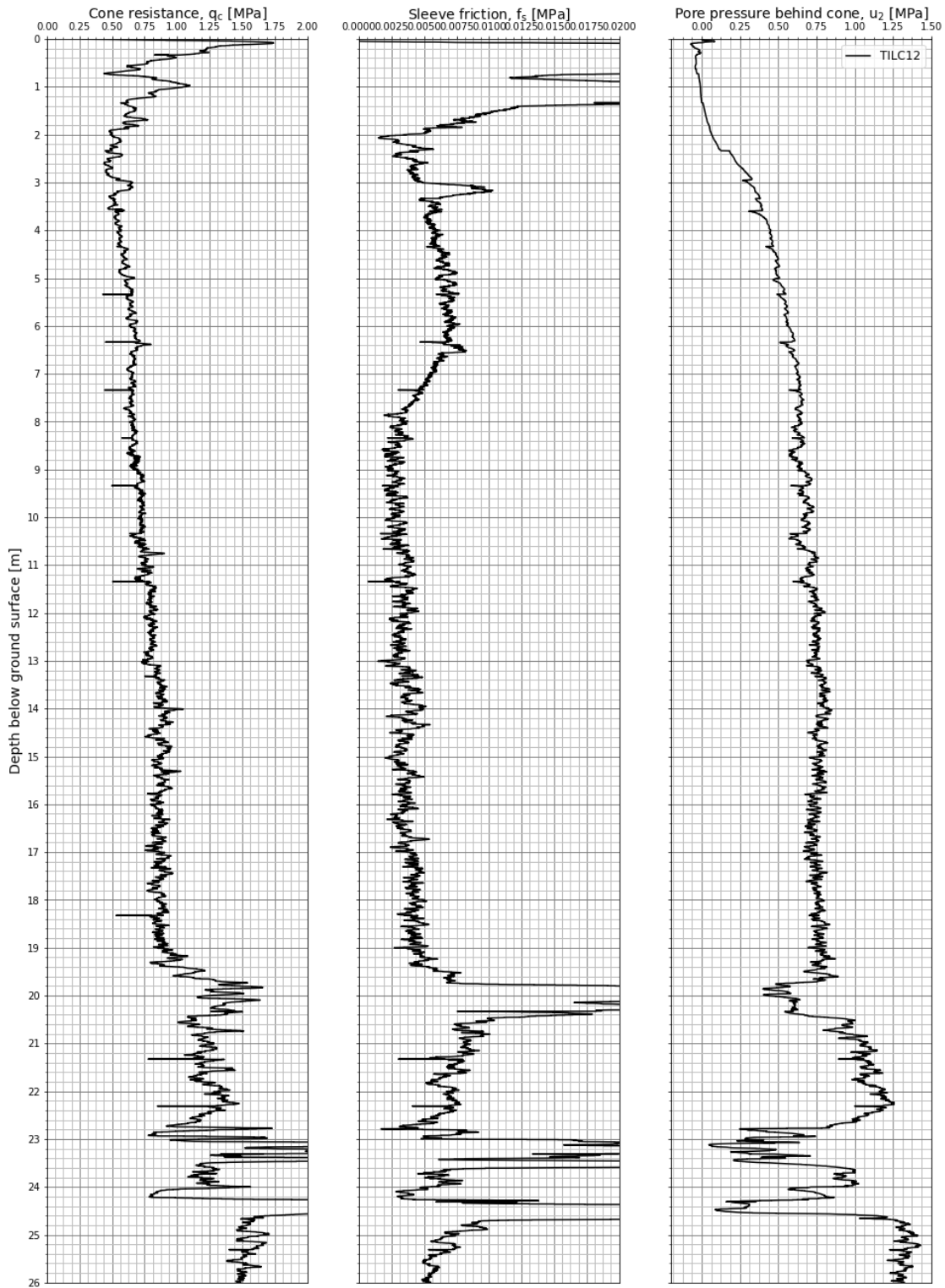


Figure A4.8 Measured cone resistance, sleeve friction and pore pressure – TILC12.

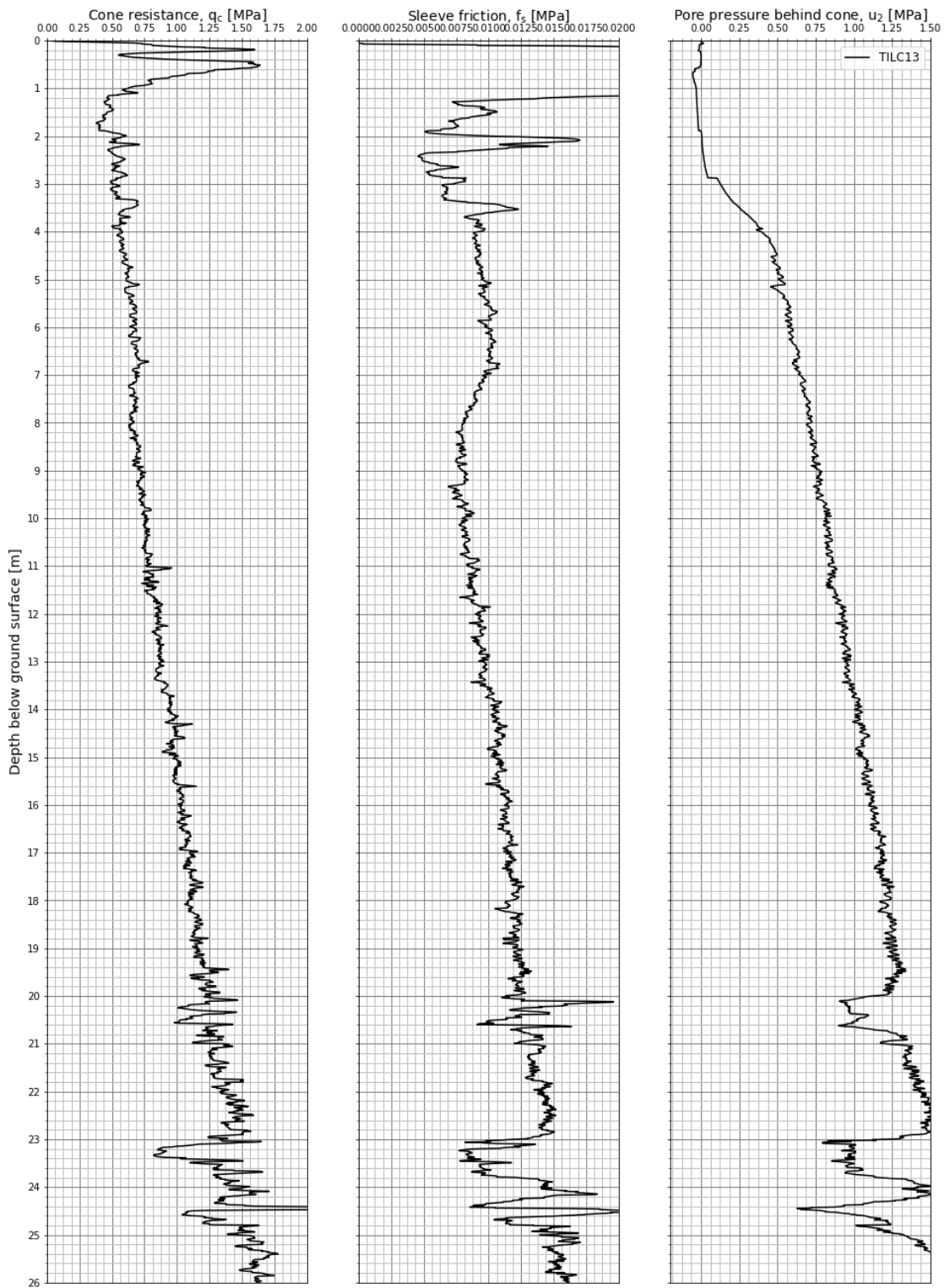


Figure A4.9 Measured cone resistance, sleeve friction and pore pressure – TILC13.

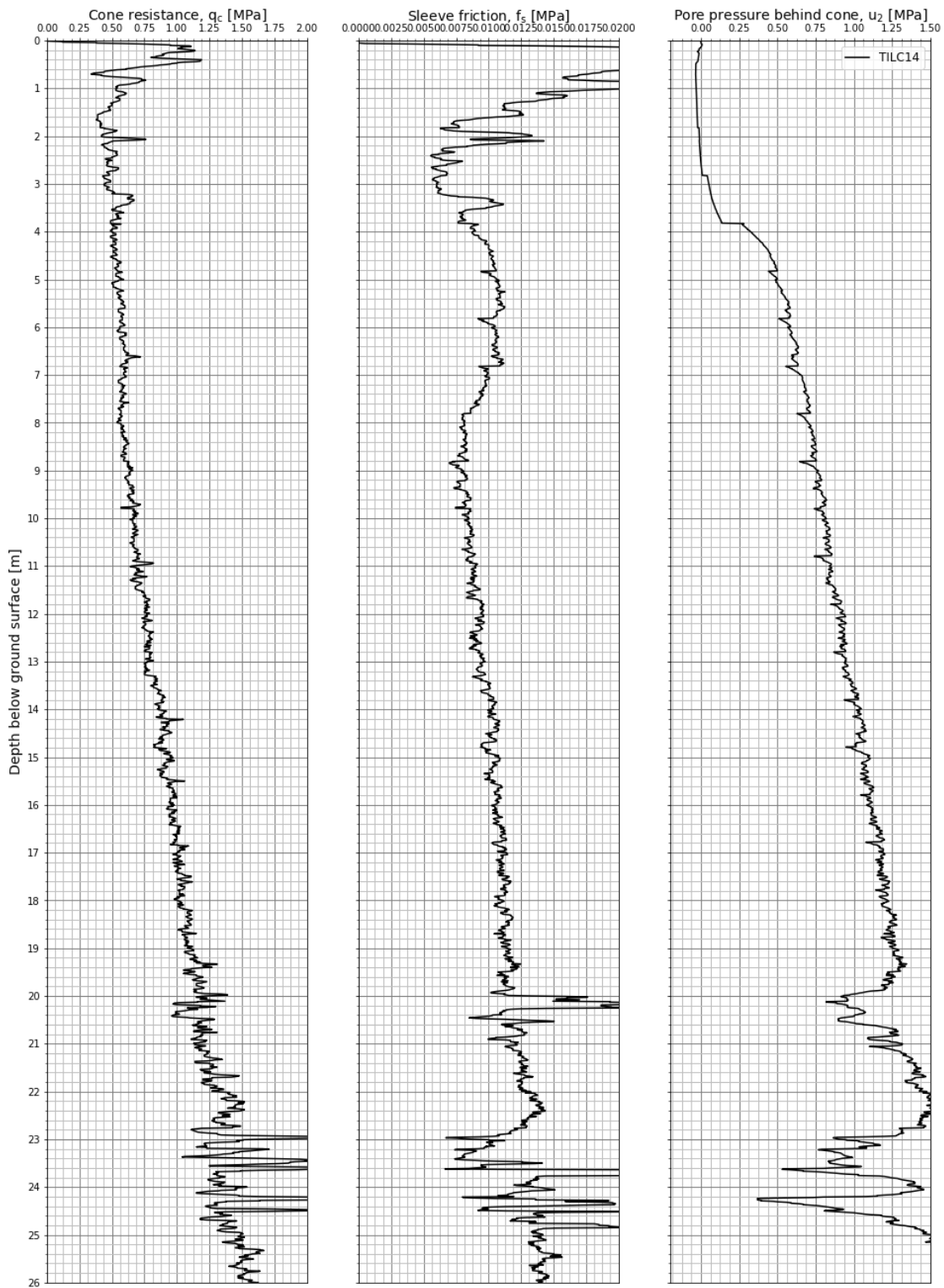


Figure A4.10 Measured cone resistance, sleeve friction and pore pressure – TILC14.

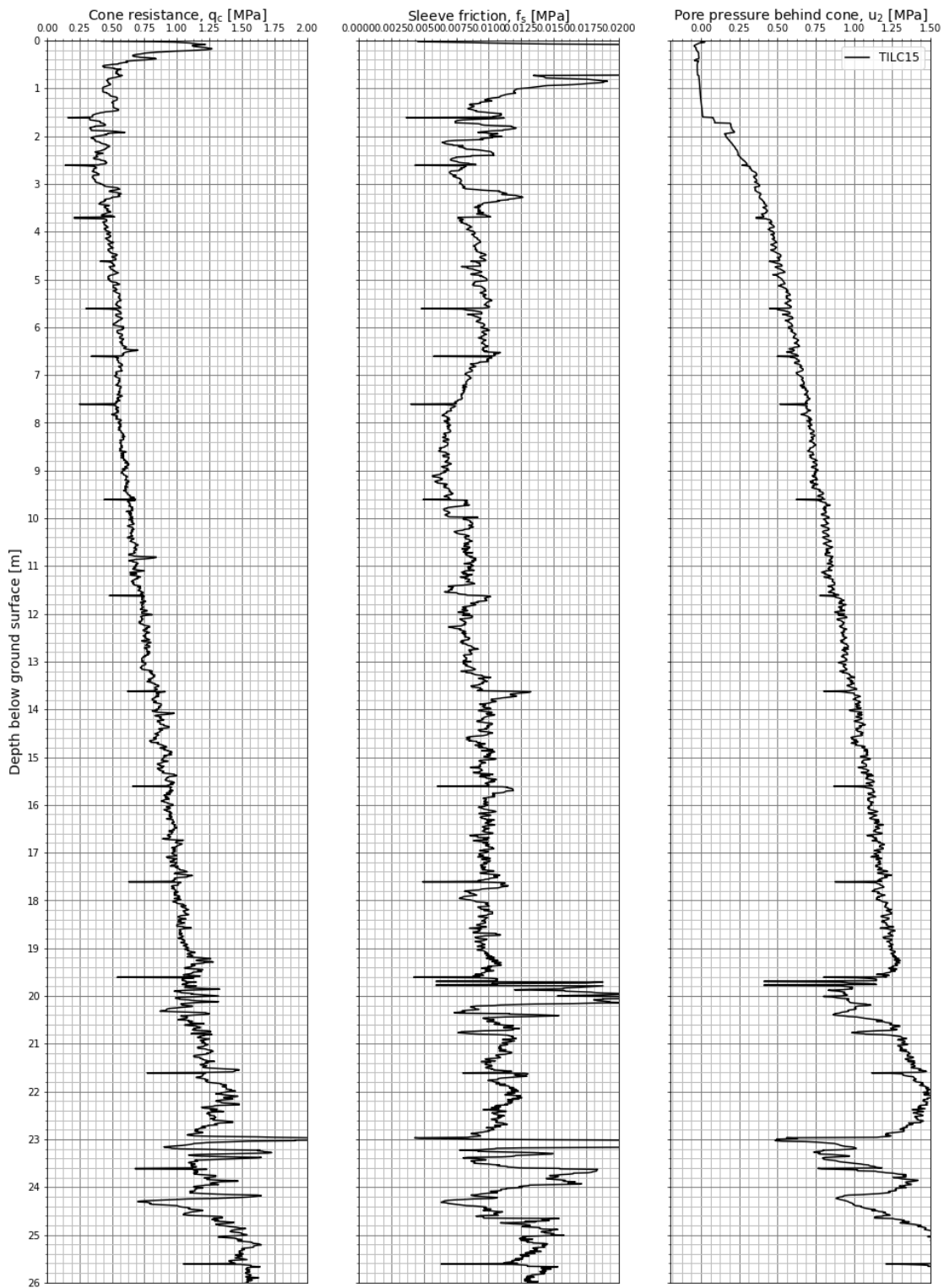


Figure A4.11 Measured cone resistance, sleeve friction and pore pressure – TILC15.

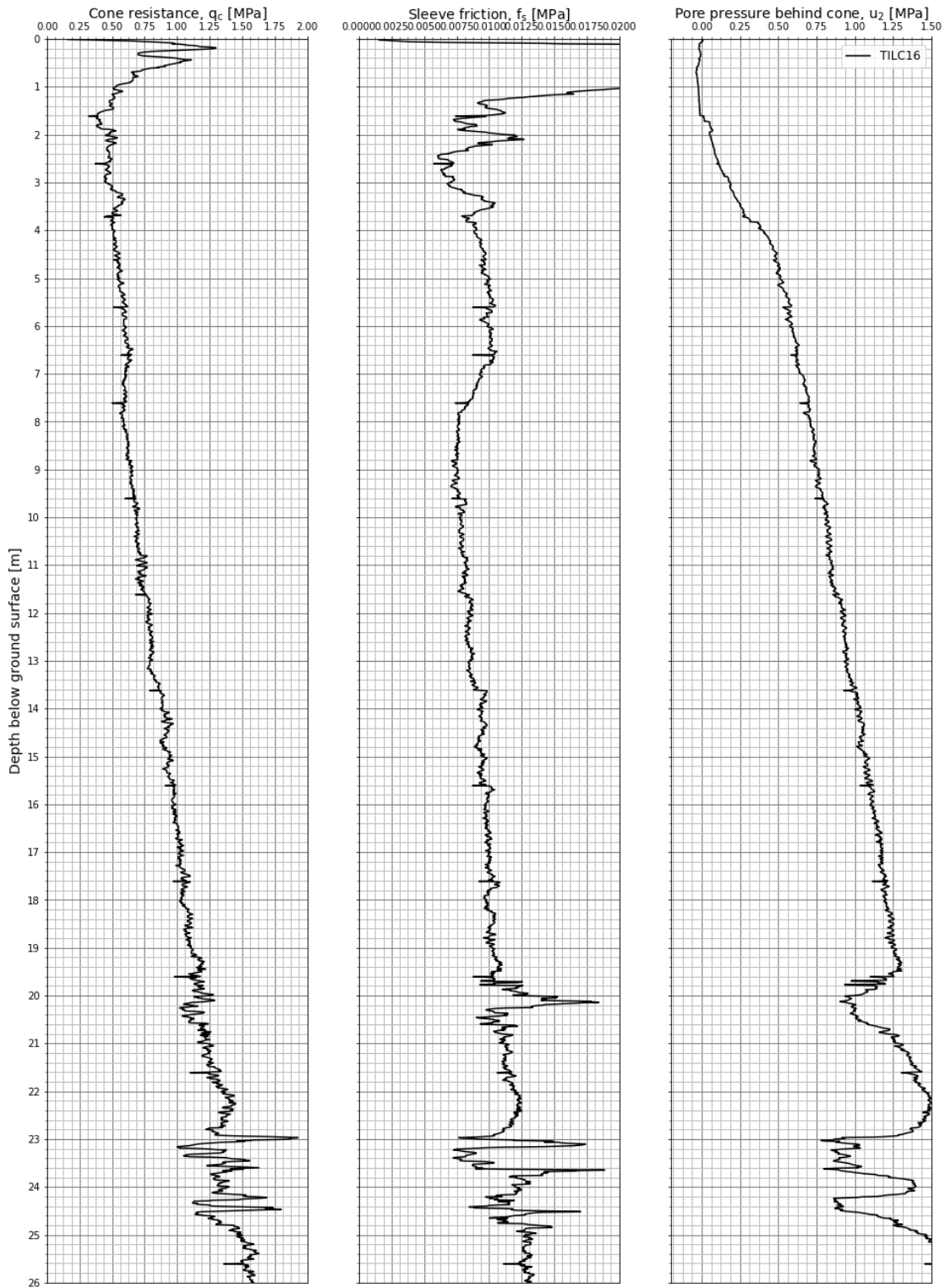


Figure A4.12 Measured cone resistance, sleeve friction and pore pressure – TILC16.

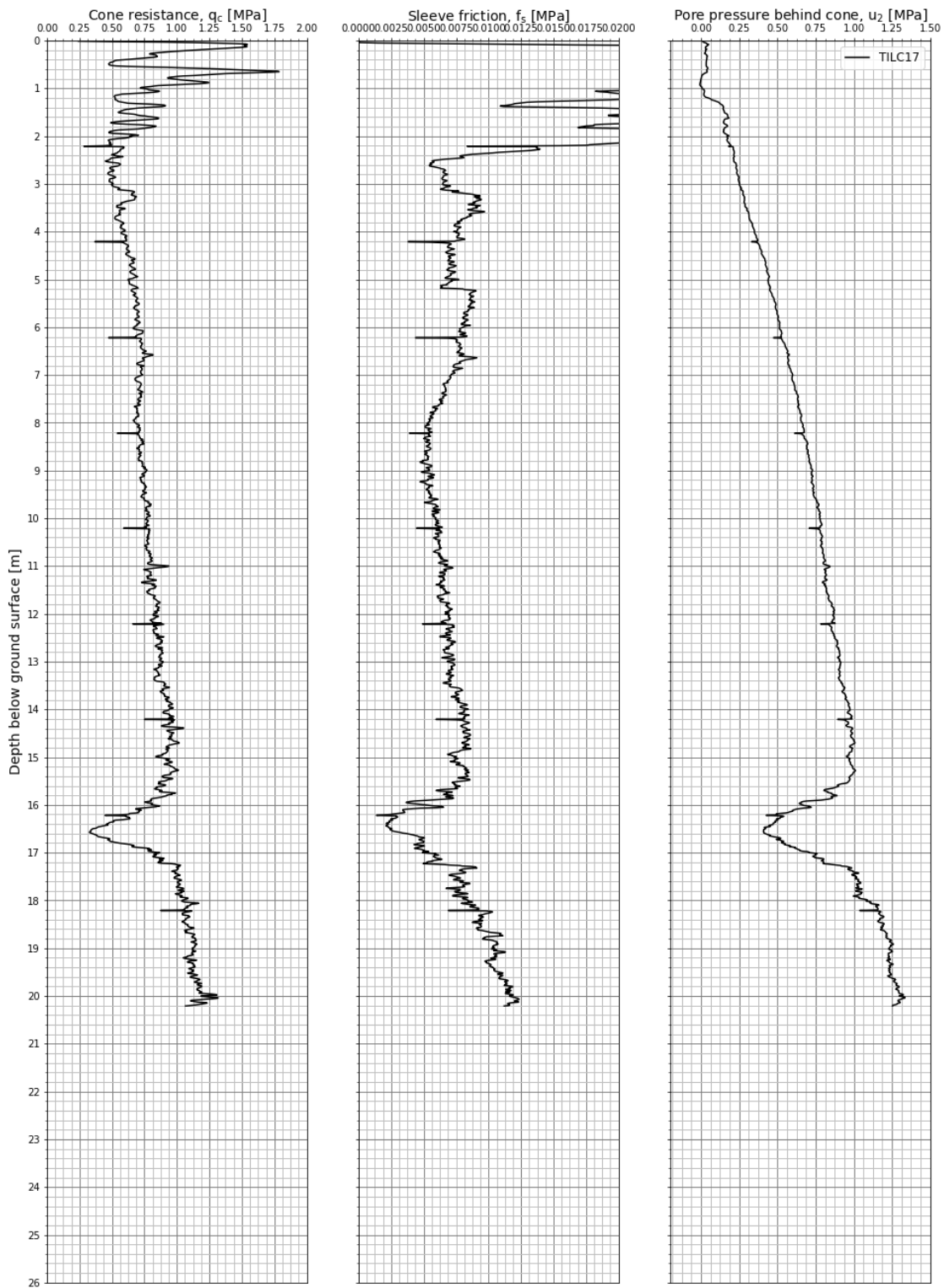


Figure A4.13 Measured cone resistance, sleeve friction and pore pressure – TILC17.

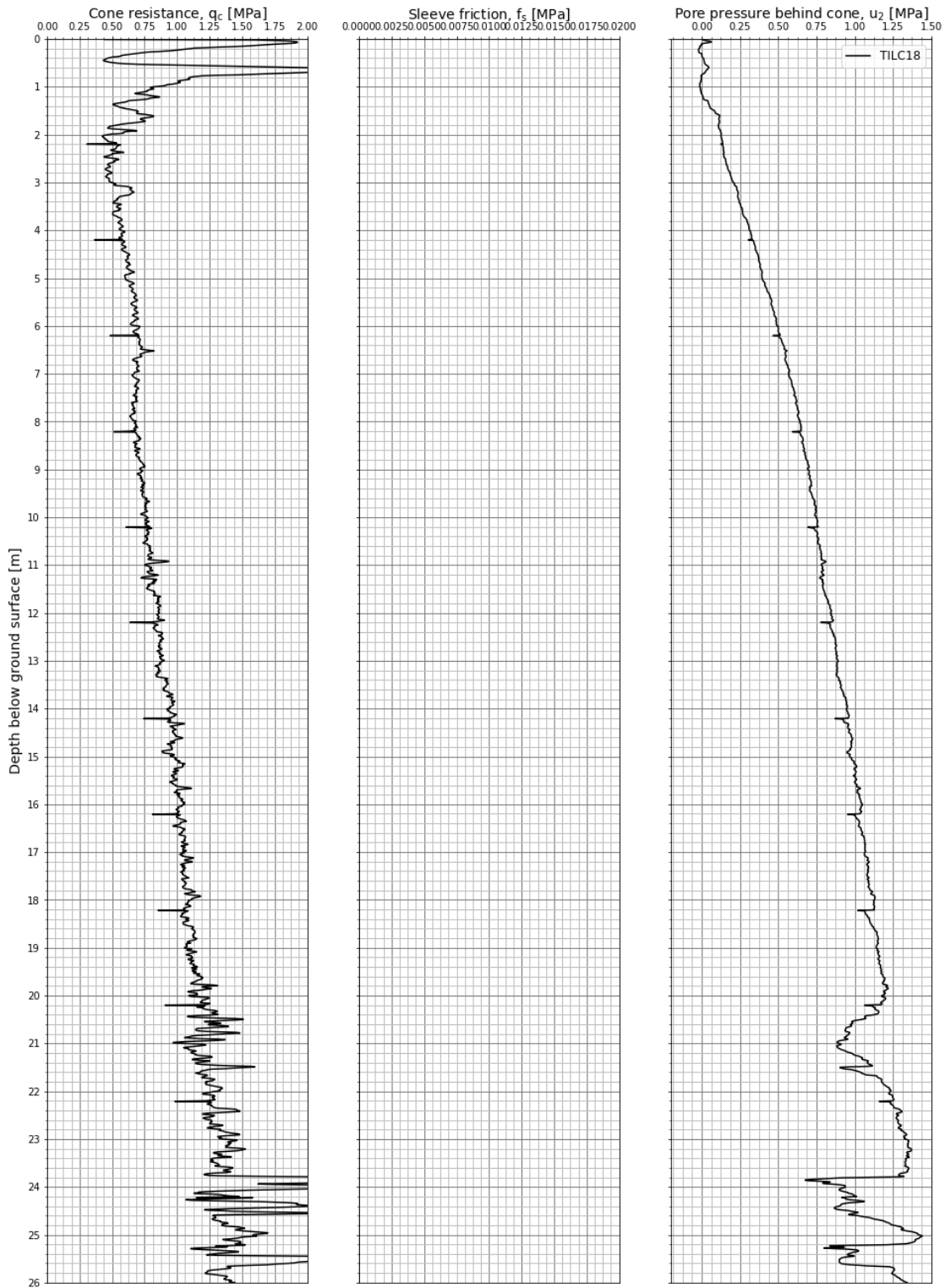


Figure A4.14 Measured cone resistance, sleeve friction and pore pressure – TILC18.

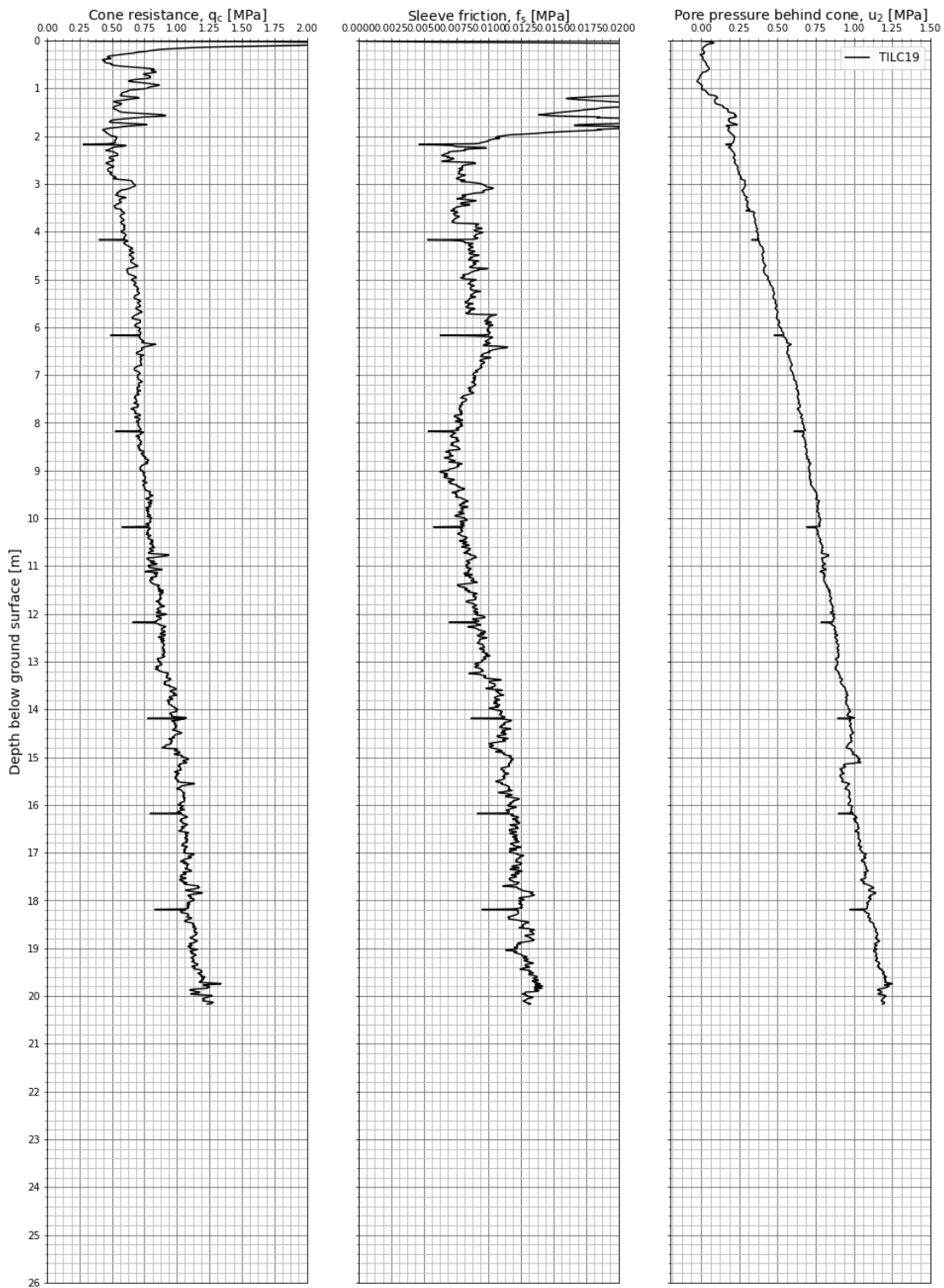


Figure A4.15 Measured cone resistance, sleeve friction and pore pressure – TILC19.

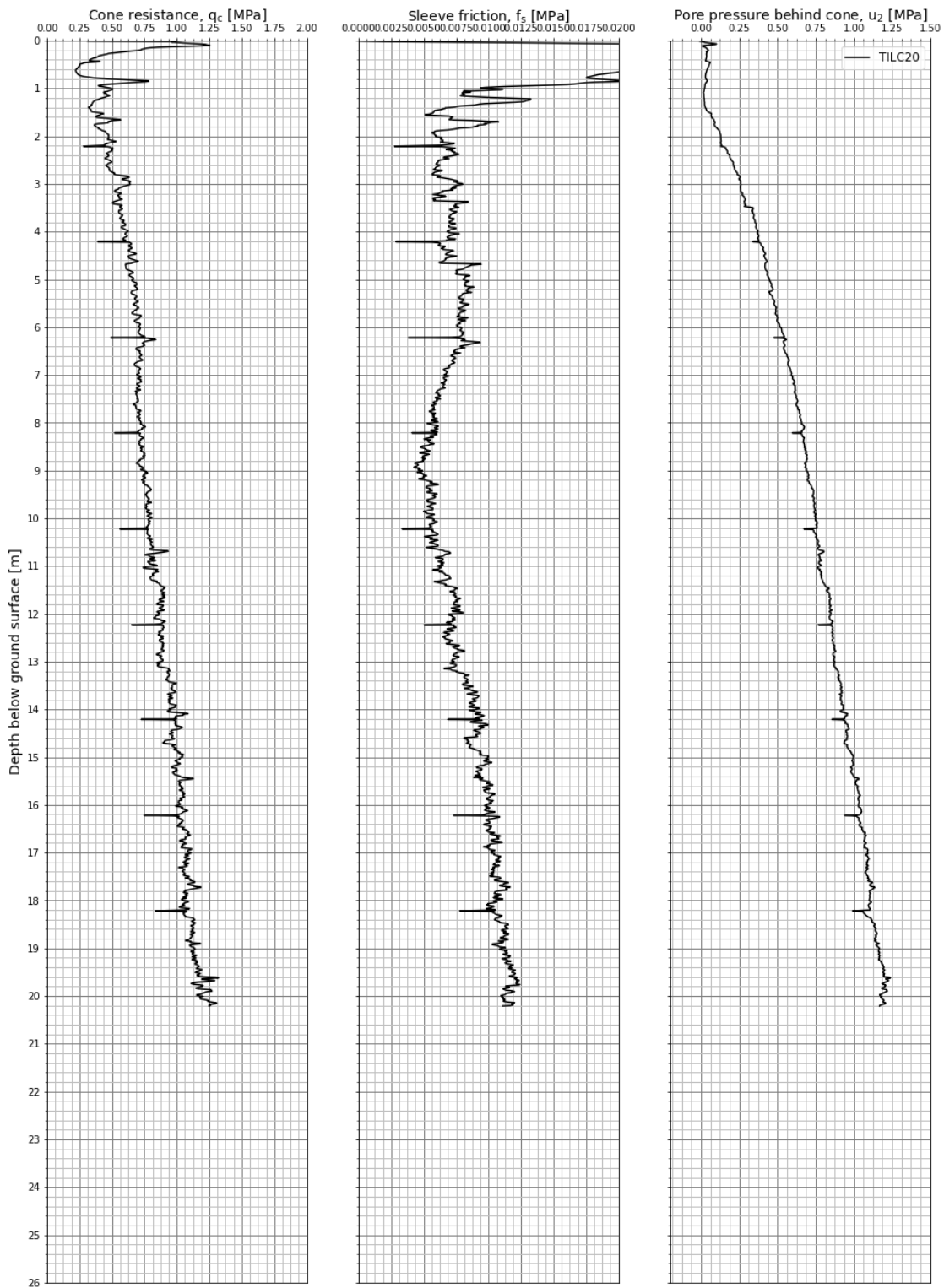


Figure A4.16 Measured cone resistance, sleeve friction and pore pressure – TILC20.

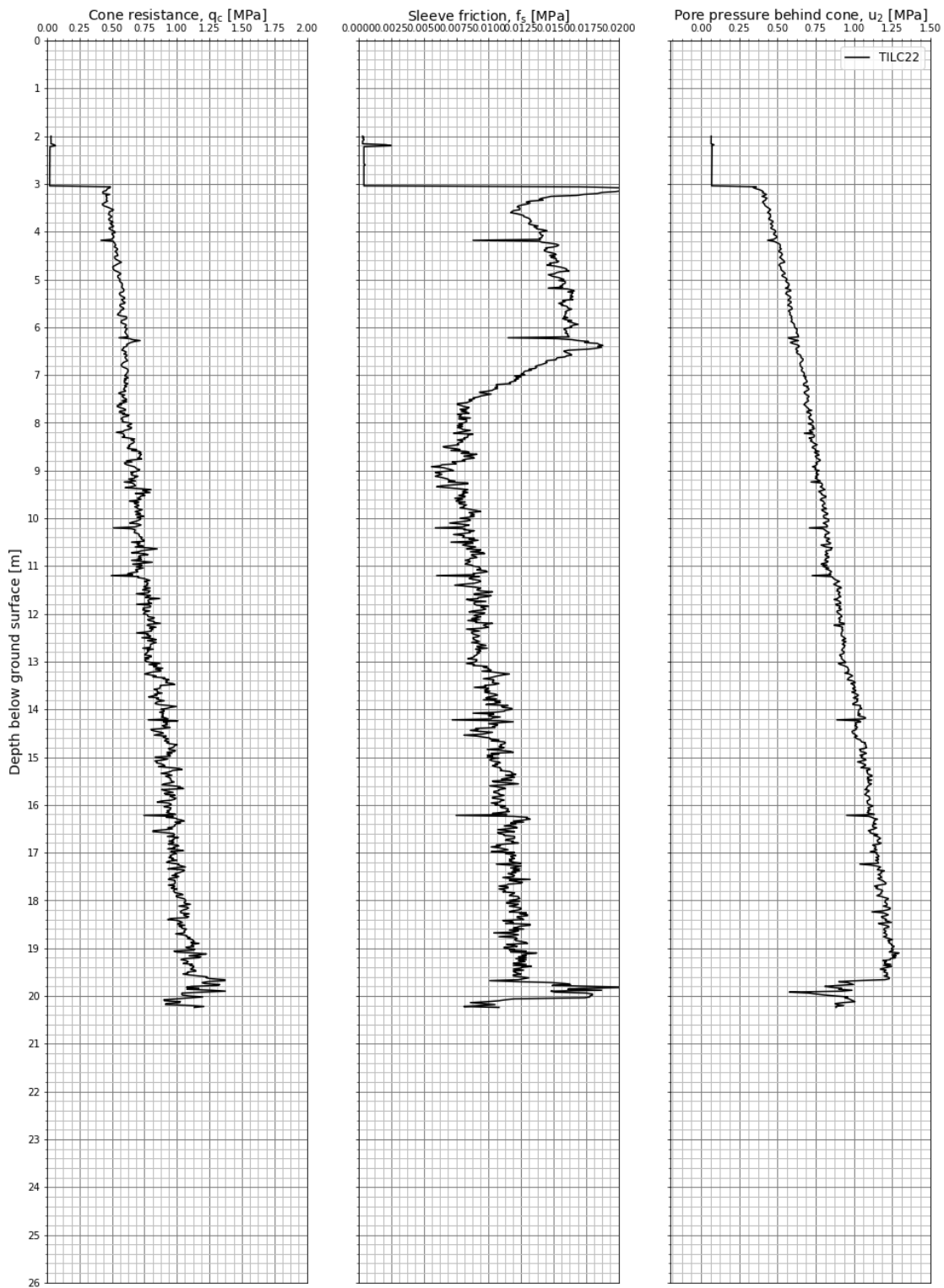


Figure A4.17 Measured cone resistance, sleeve friction and pore pressure – TILC22.

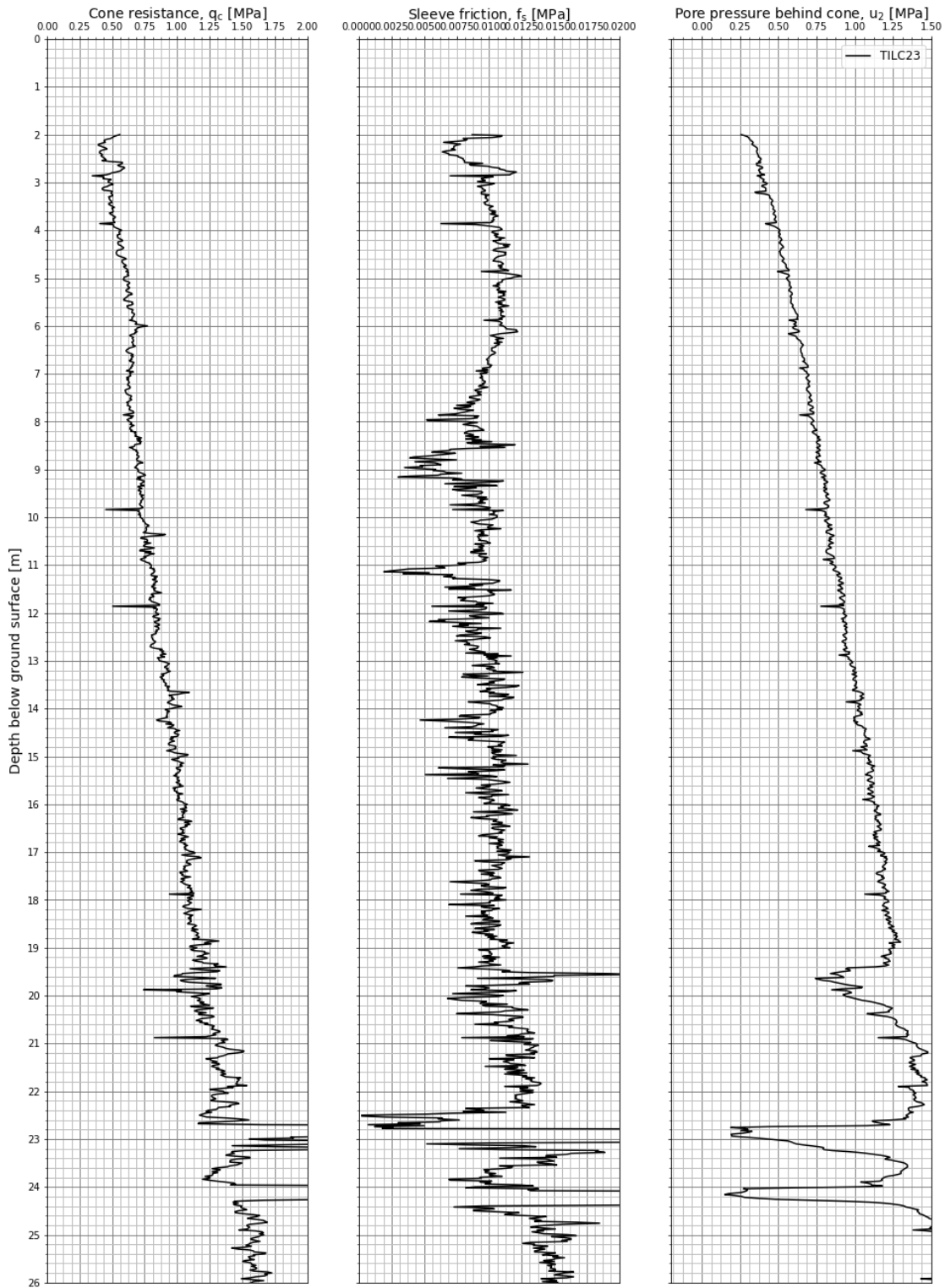


Figure A4.18 Measured cone resistance, sleeve friction and pore pressure – TILC23.

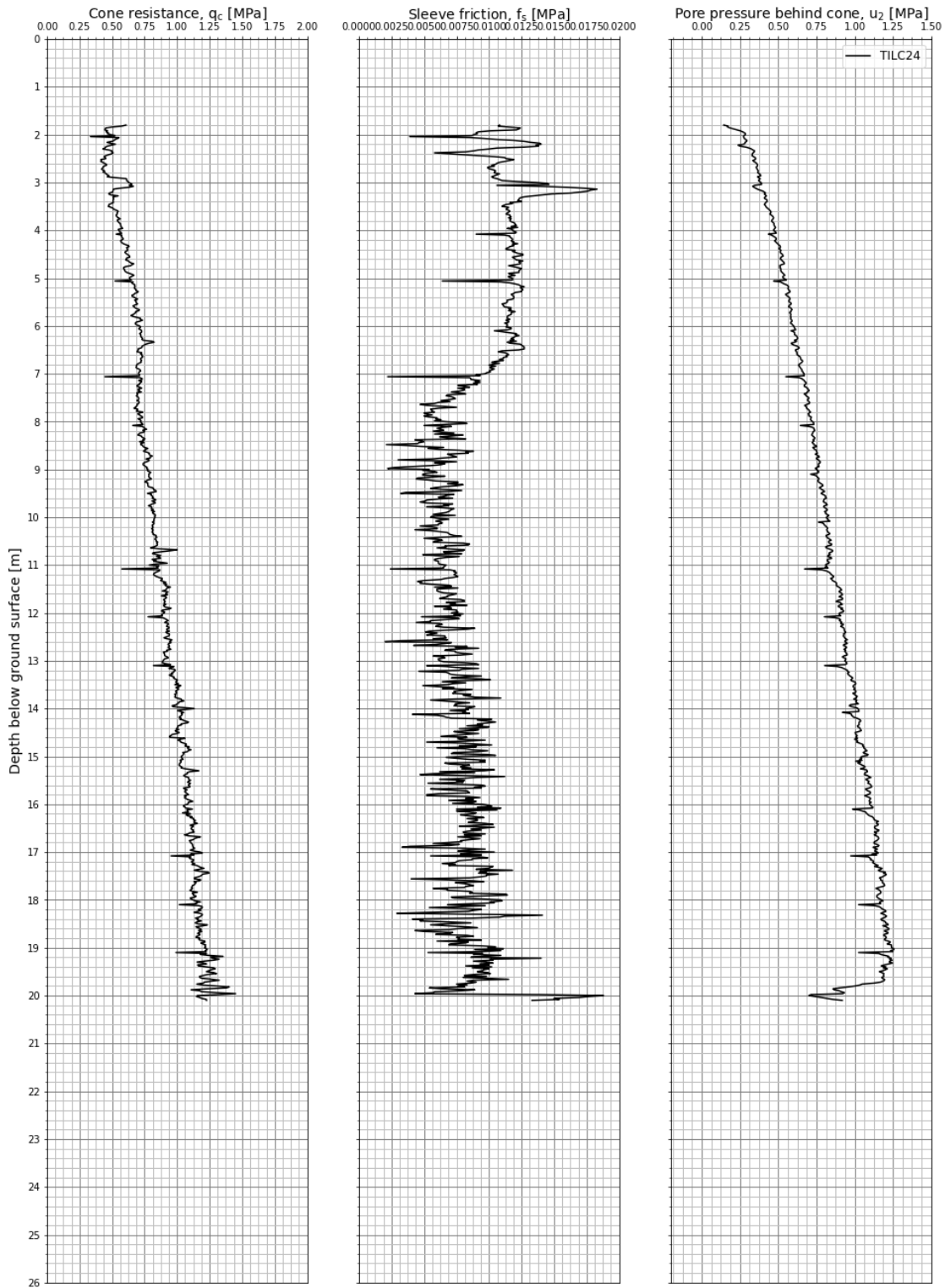


Figure A4.19 Measured cone resistance, sleeve friction and pore pressure – TILC24.

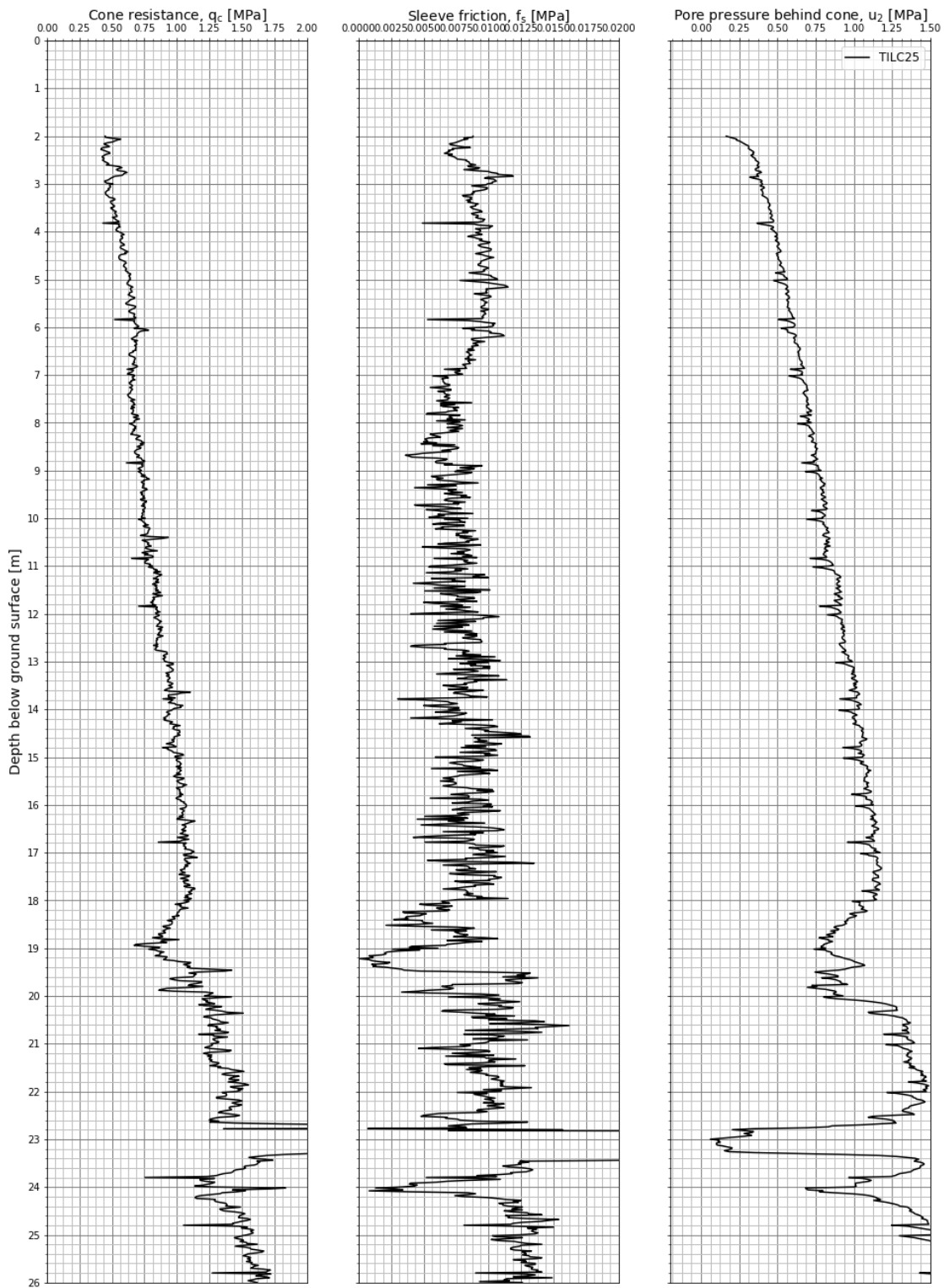


Figure A4.20 Measured cone resistance, sleeve friction and pore pressure – TILC25.

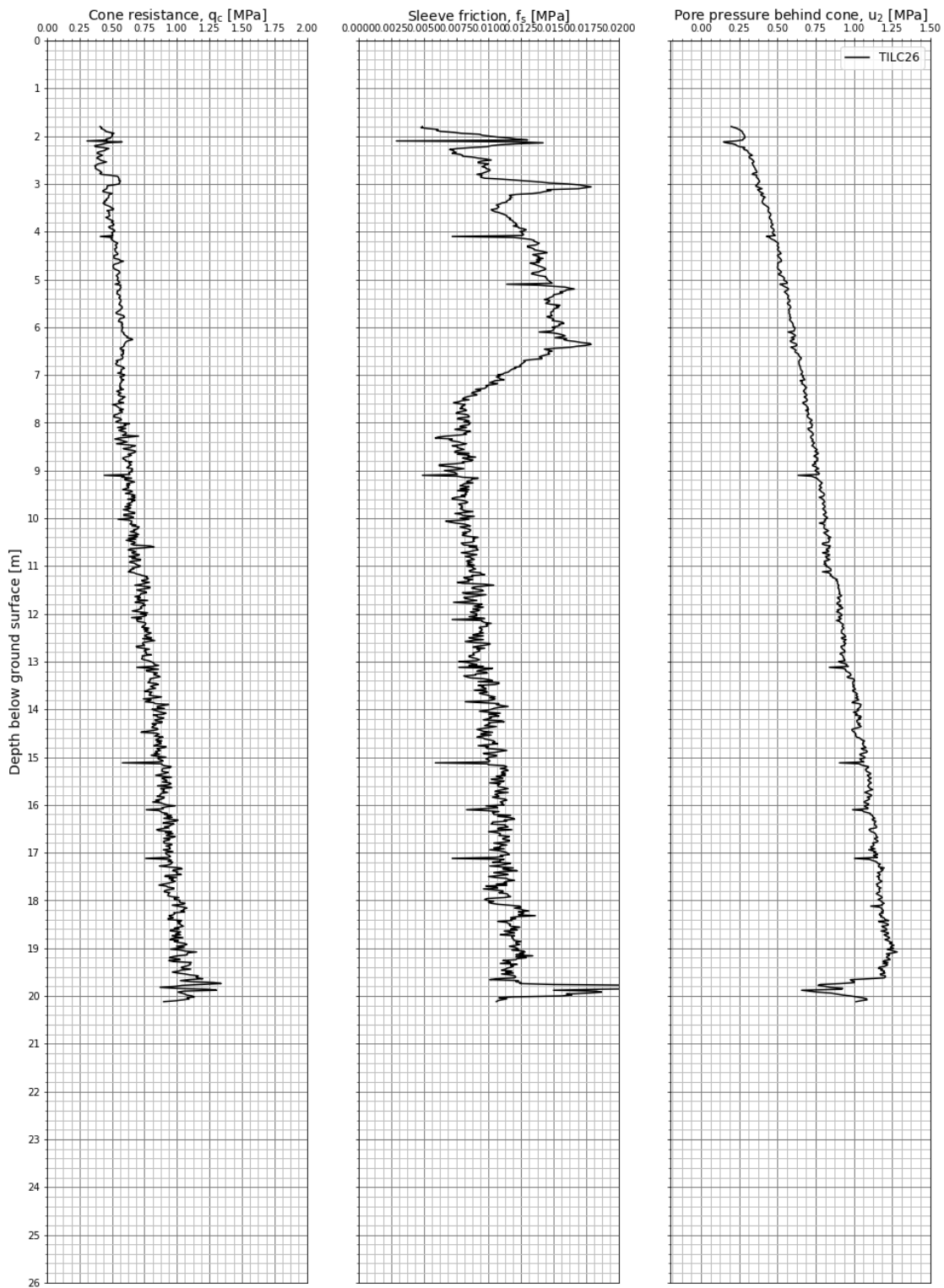


Figure A4.21 Measured cone resistance, sleeve friction and pore pressure – TILC25.

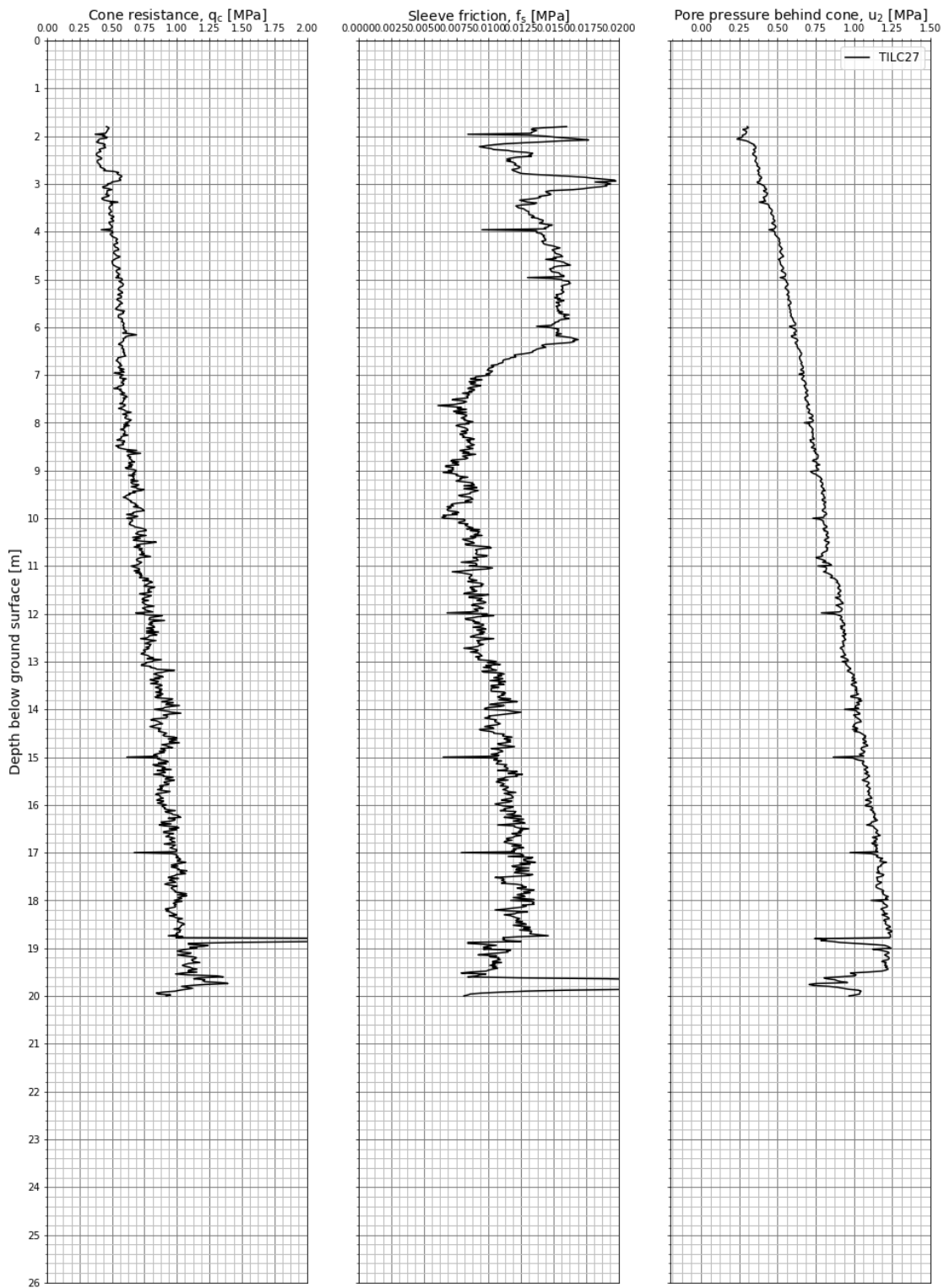


Figure A4.22 Measured cone resistance, sleeve friction and pore pressure – TILC27.

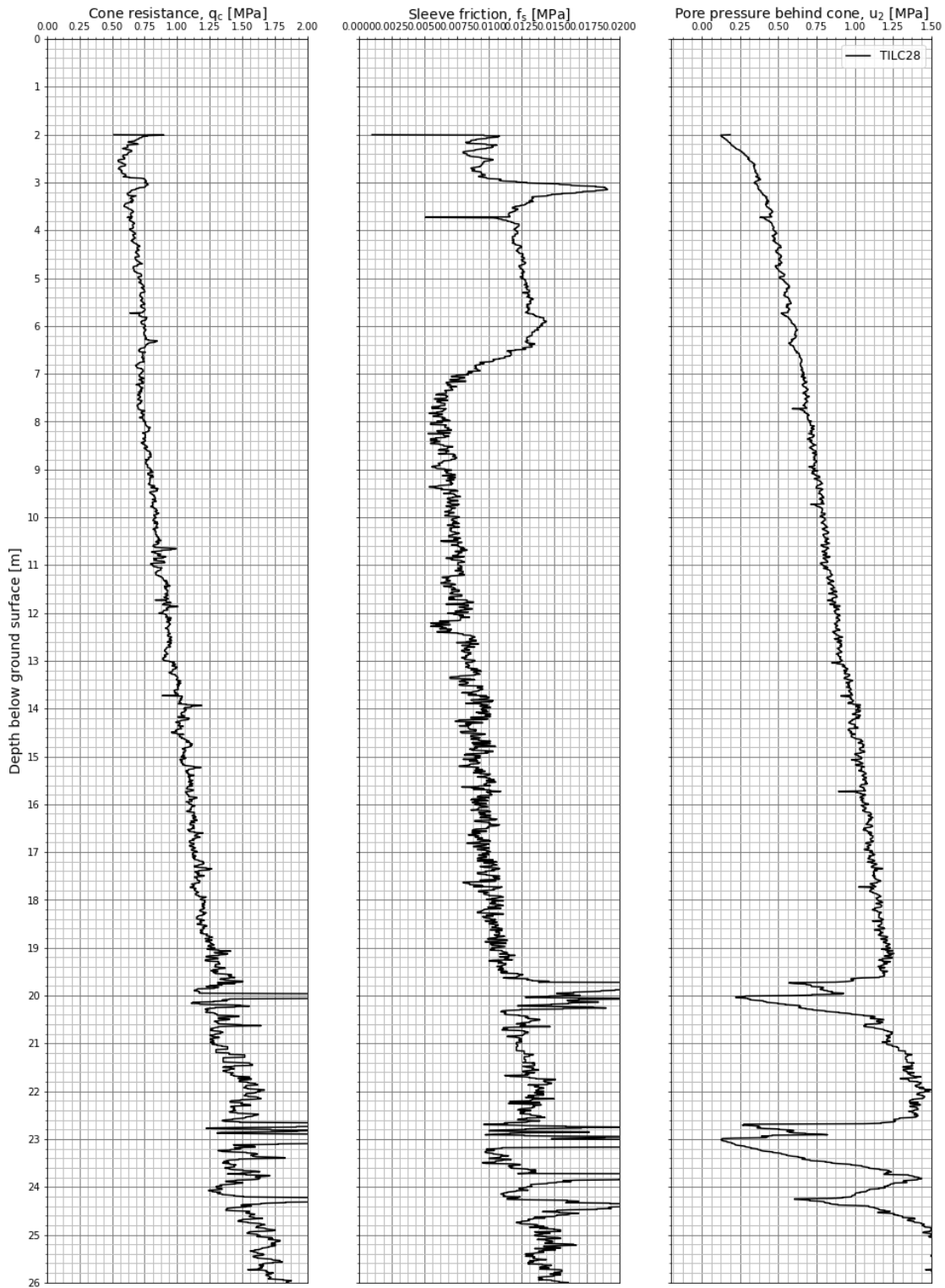


Figure A4.23 Measured cone resistance, sleeve friction and pore pressure – TILC28.

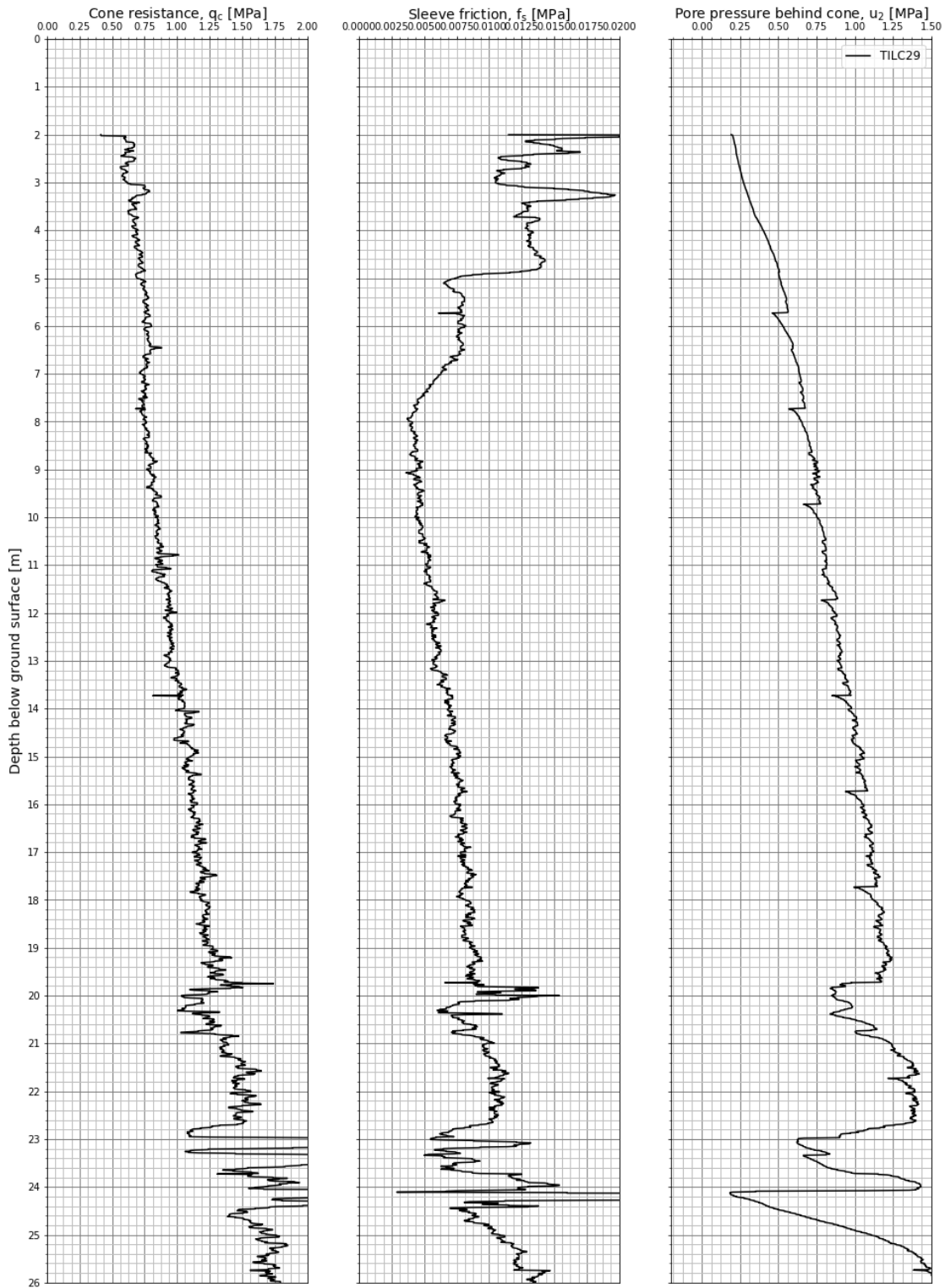


Figure A4.24 Measured cone resistance, sleeve friction and pore pressure – TILC29.

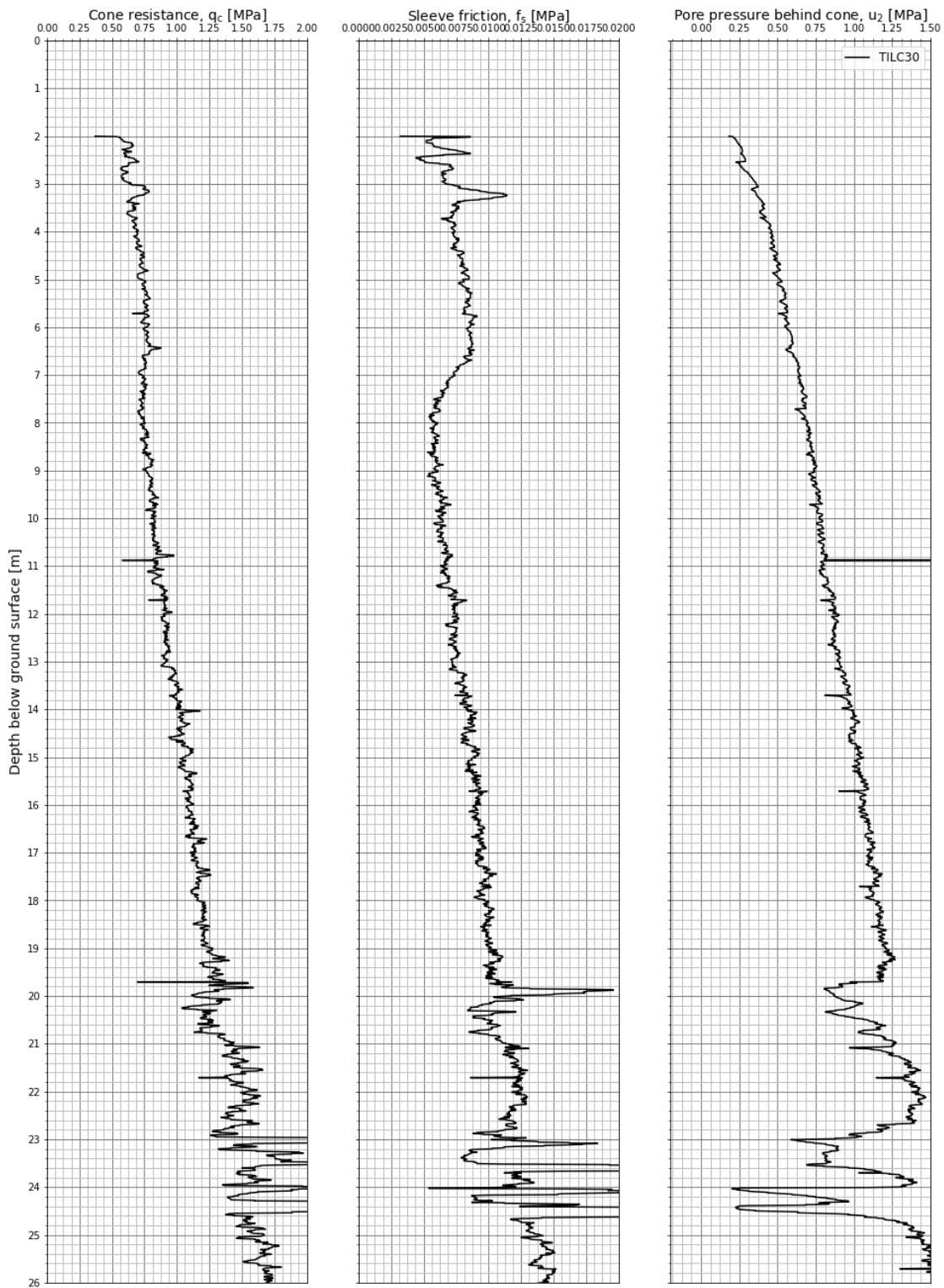


Figure A4.25 Measured cone resistance, sleeve friction and pore pressure – TILC30.

Appendix B

ZERO READING AS FUNCTION OF TIME – FIGURES

Contents

B1	Figures	2
-----------	----------------	----------

B1 Figures

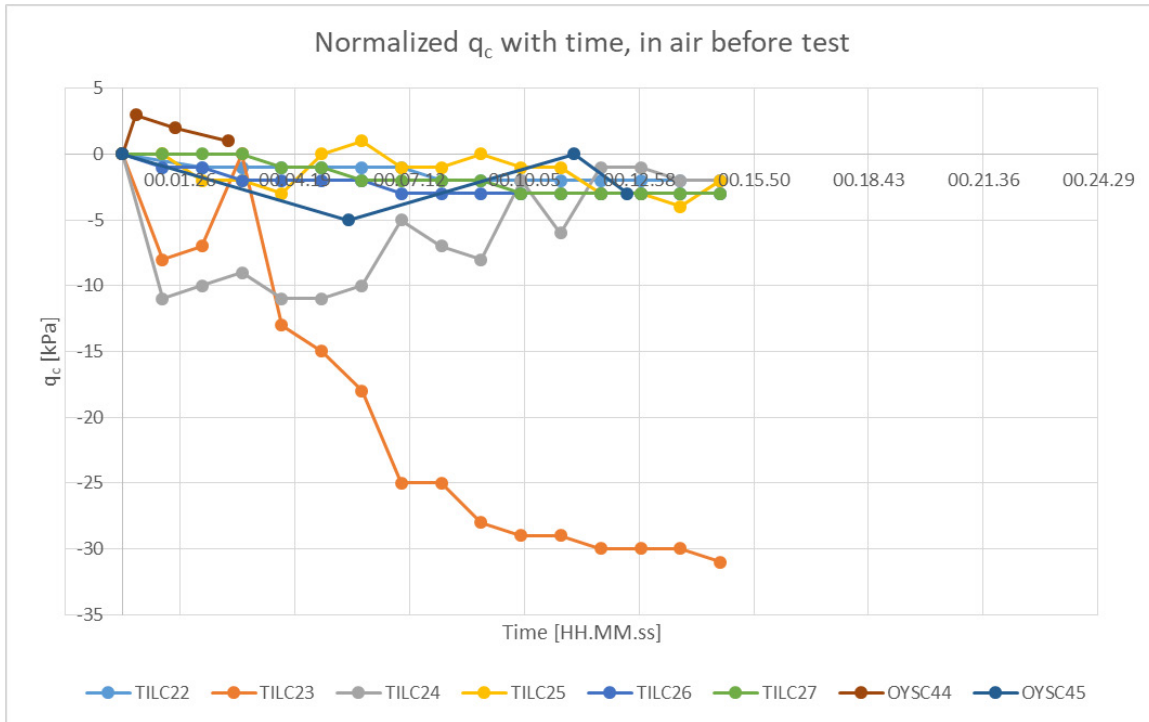


Figure B1.1 Stabilization of q_c with time in air before test.

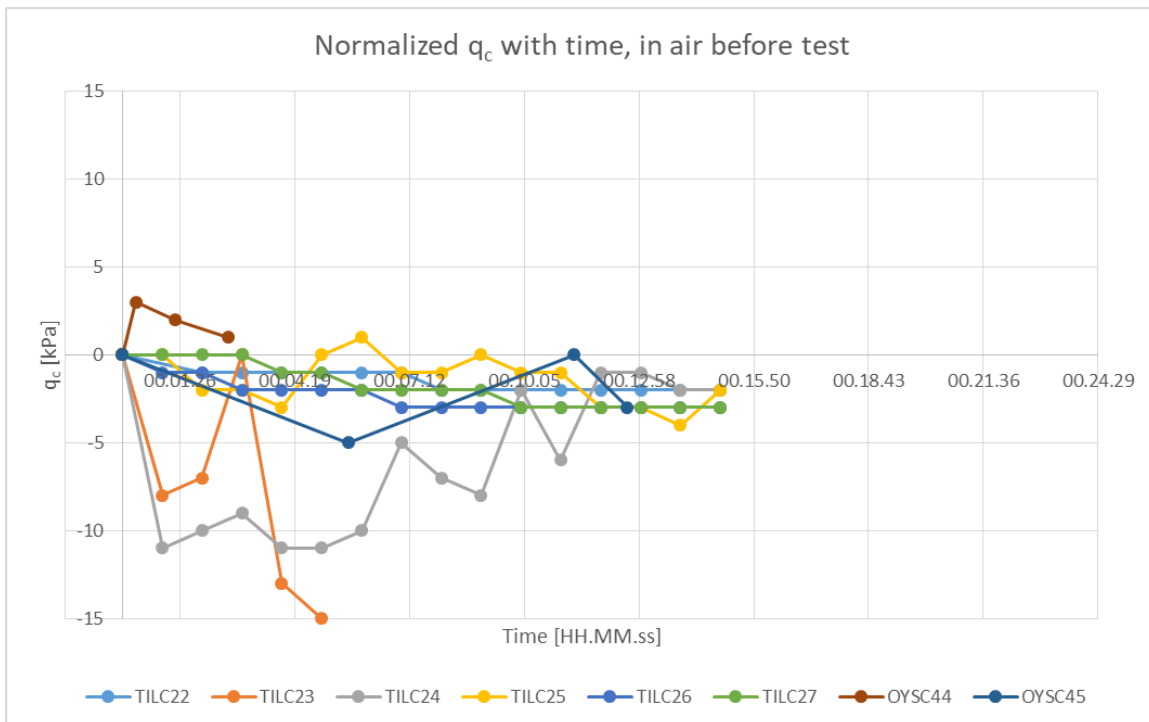


Figure B1.2 Stabilization of q_c with time in air before test. Equal scale for all q_c .

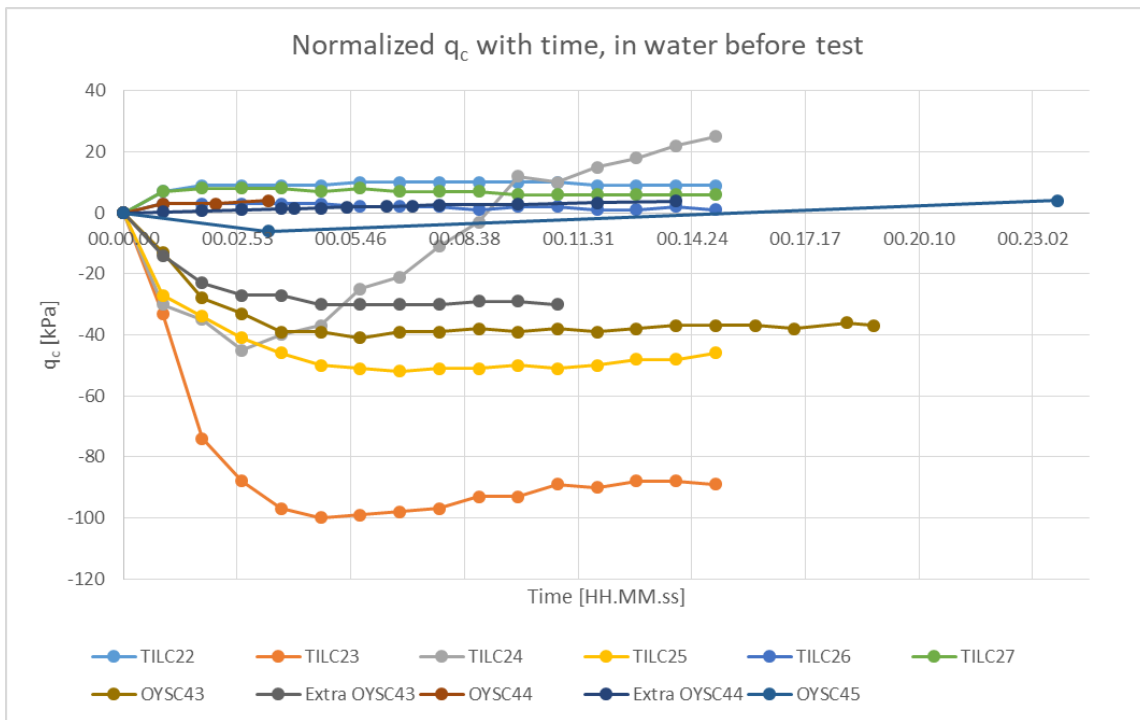


Figure B1.3 Stabilization of q_c with time in water before test.

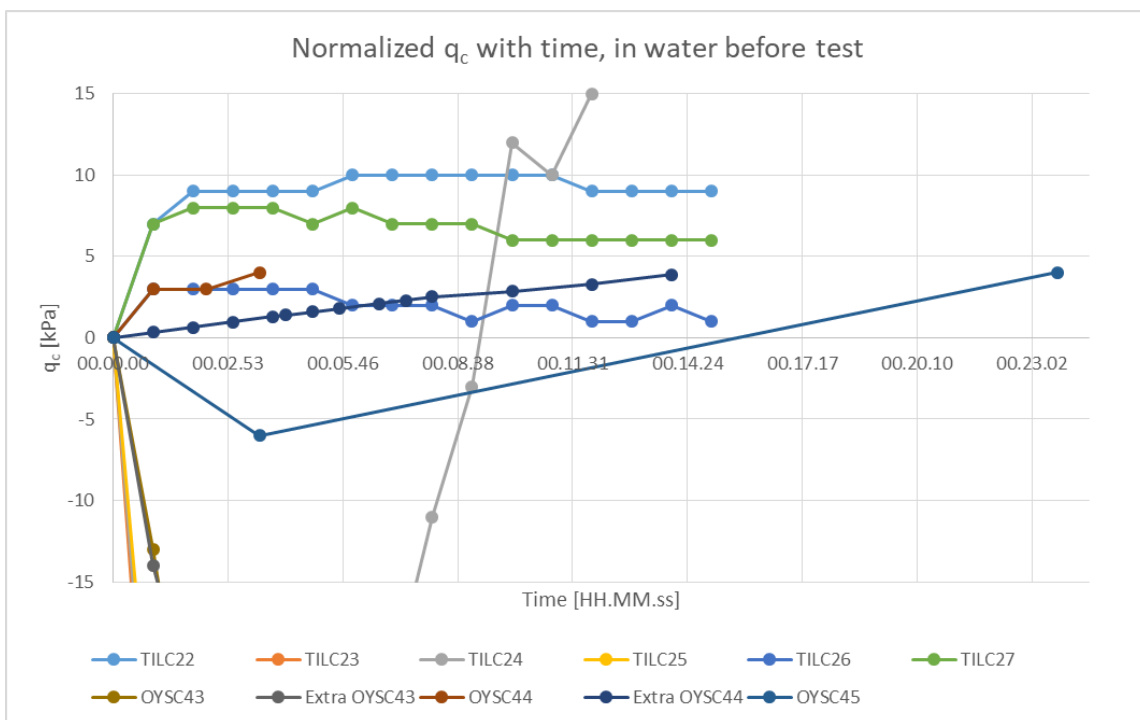


Figure B1.4 Stabilization of q_c with time in water before test. Equal scale for all q_c .

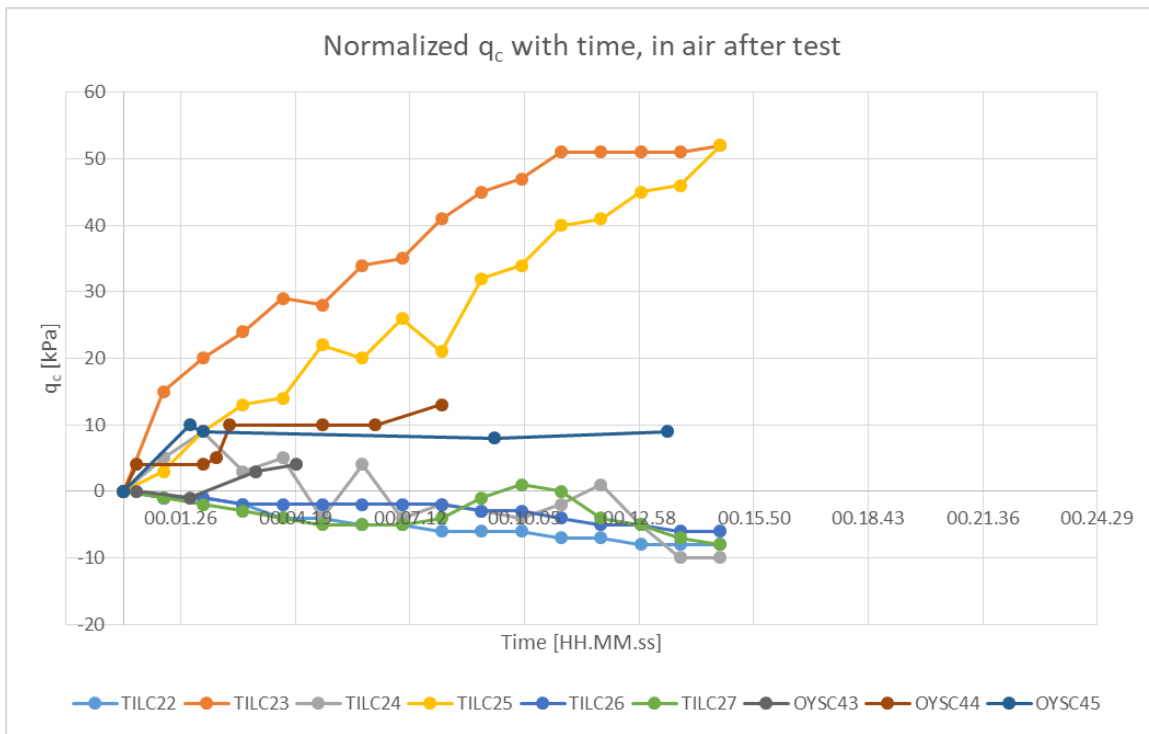


Figure B1.5 Stabilization of q_c with time in air after test.

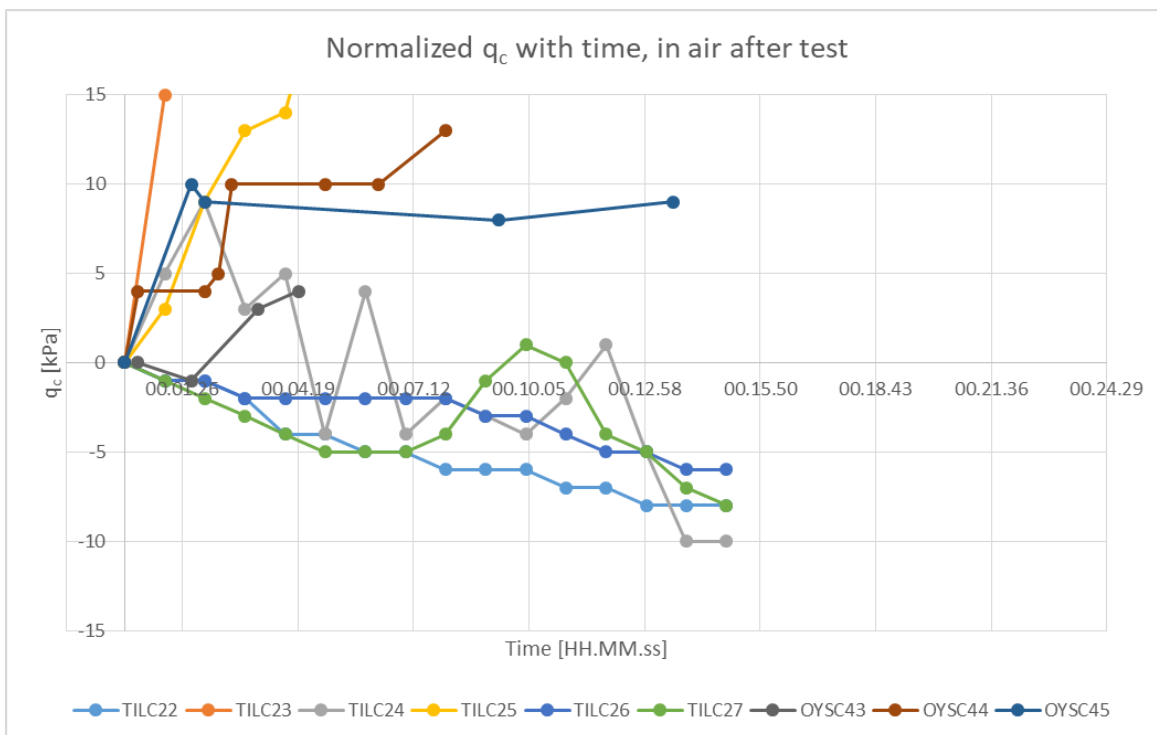


Figure B1.6 Stabilization of q_c with time in air after test. Equal scale for all q_c .

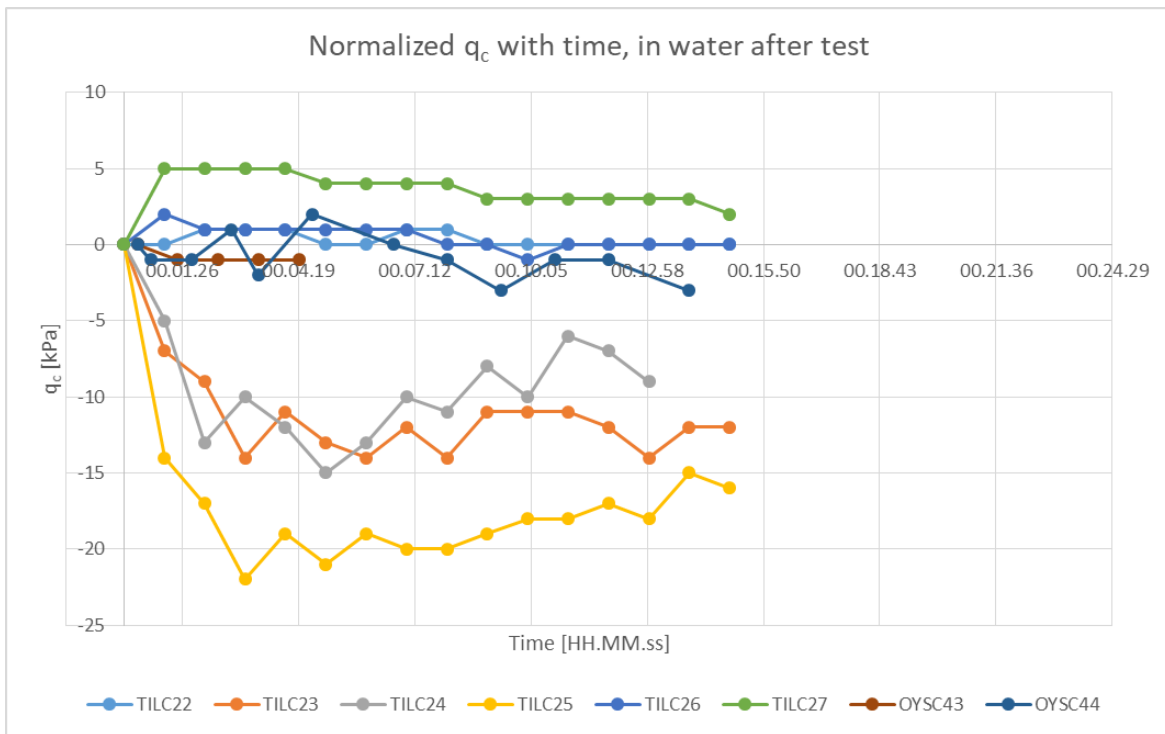


Figure B1.7 Stabilization of q_c with time in water after test.

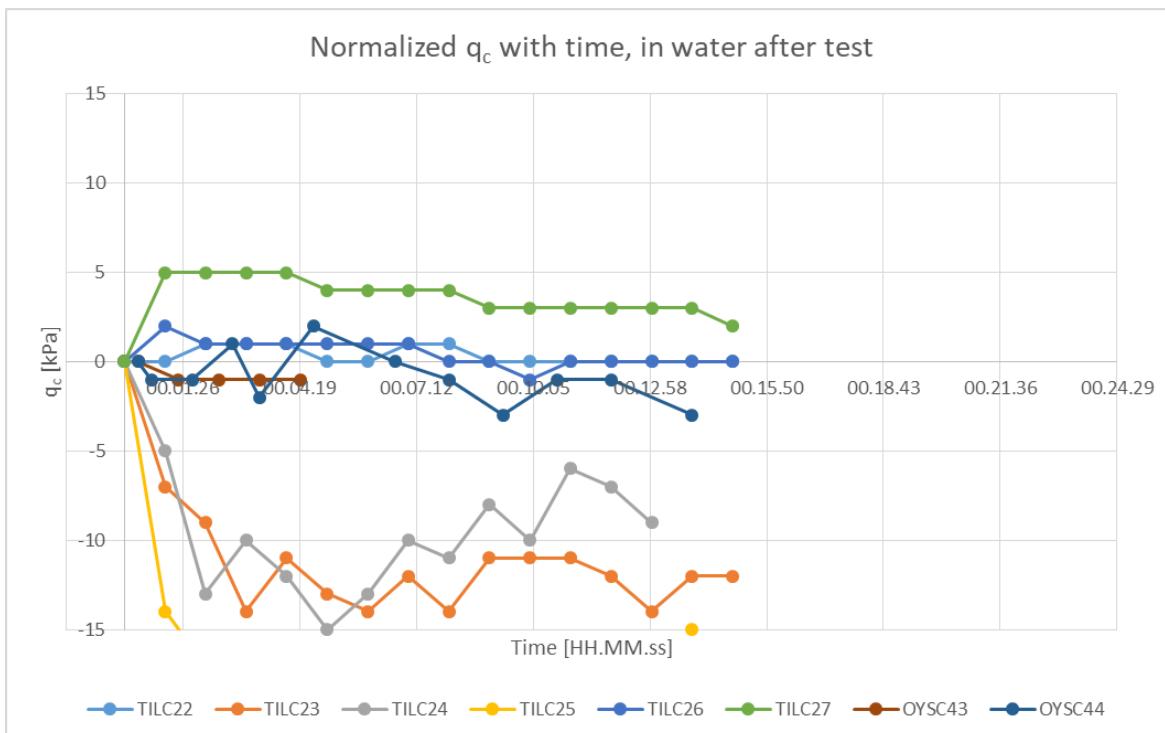


Figure B1.8 Stabilization of q_c with time in water after test. Equal scale for all q_c .

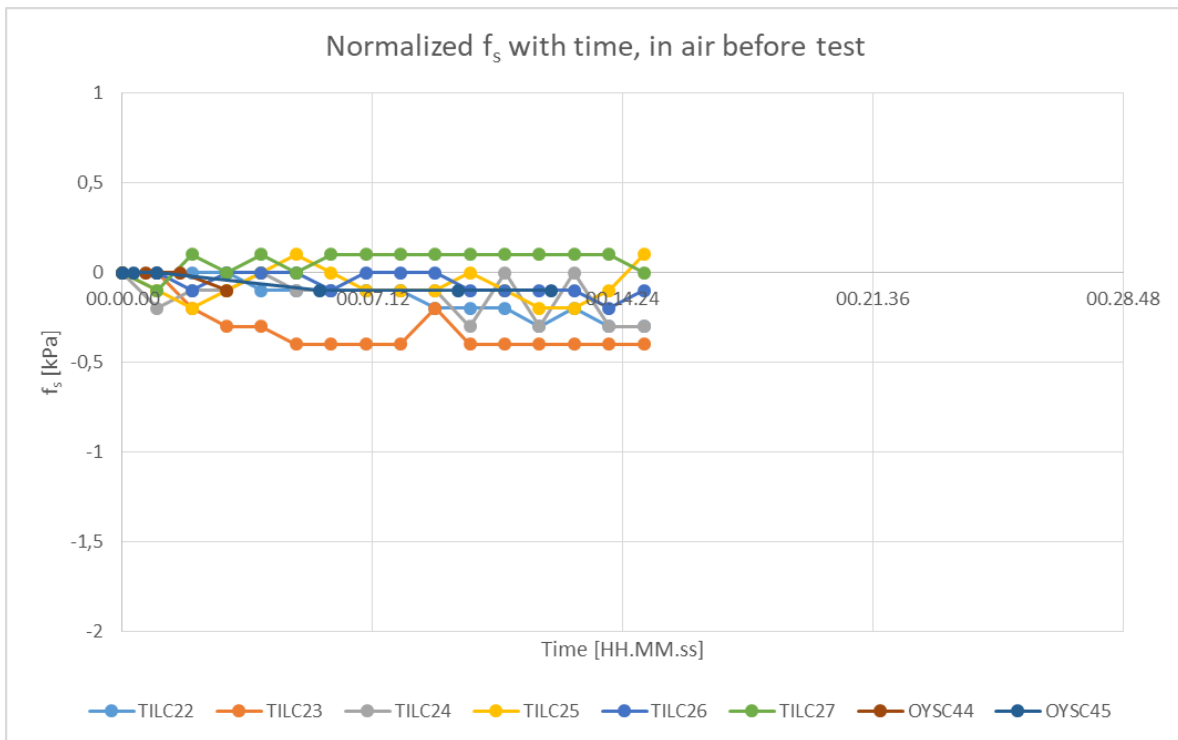


Figure B1.9 Stabilization of f_s with time in air before test. Equal scale for all f_s .

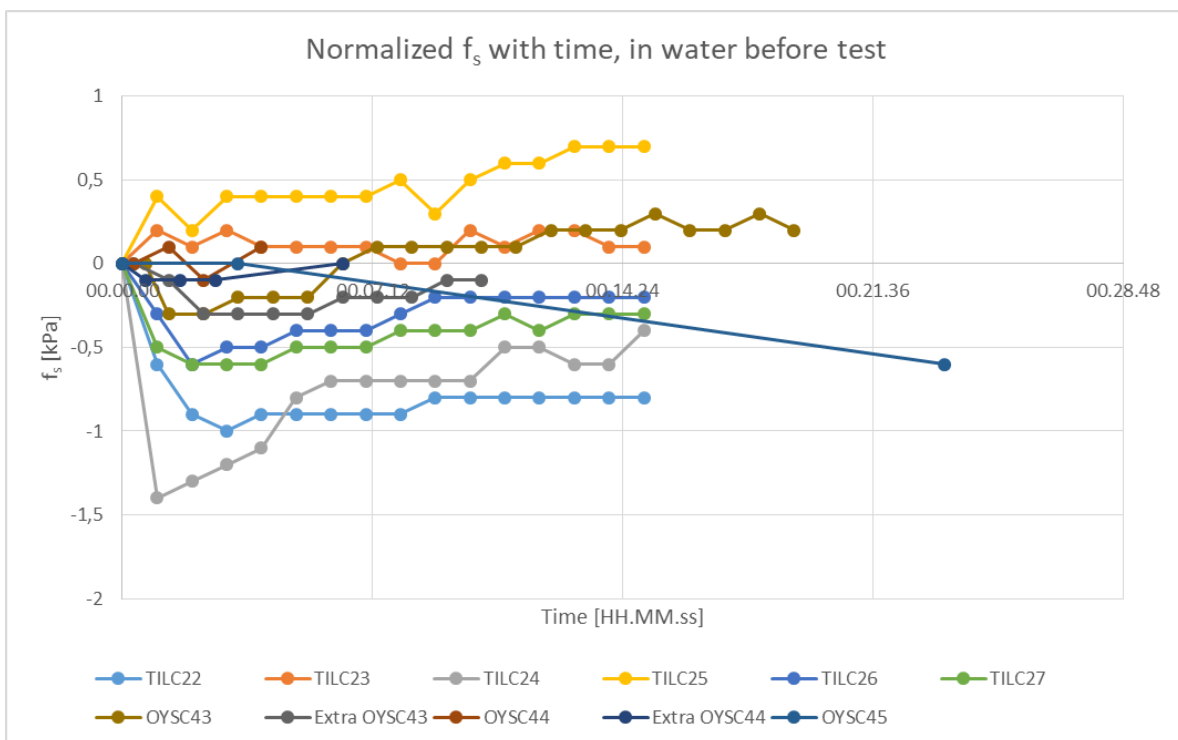


Figure B1.10 Stabilization of f_s with time in water before test. Equal scale for all f_s .

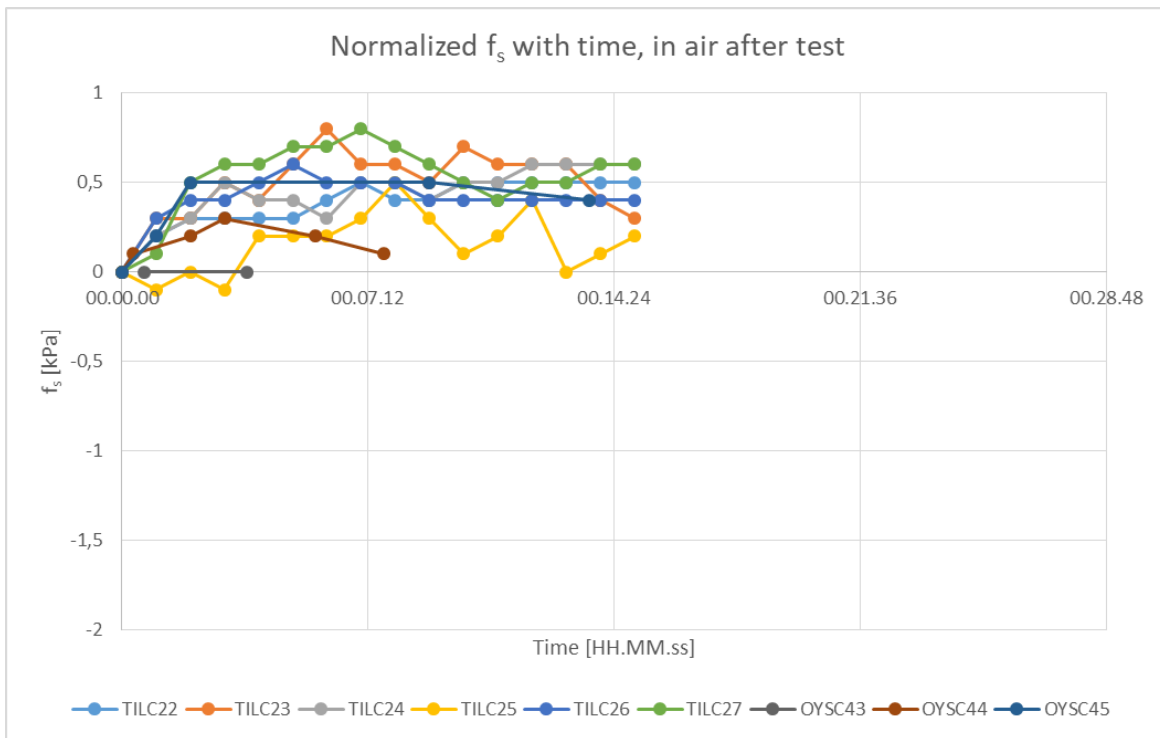


Figure B1.11 Stabilization of f_s with time in air after test. Equal scale for all f_s .

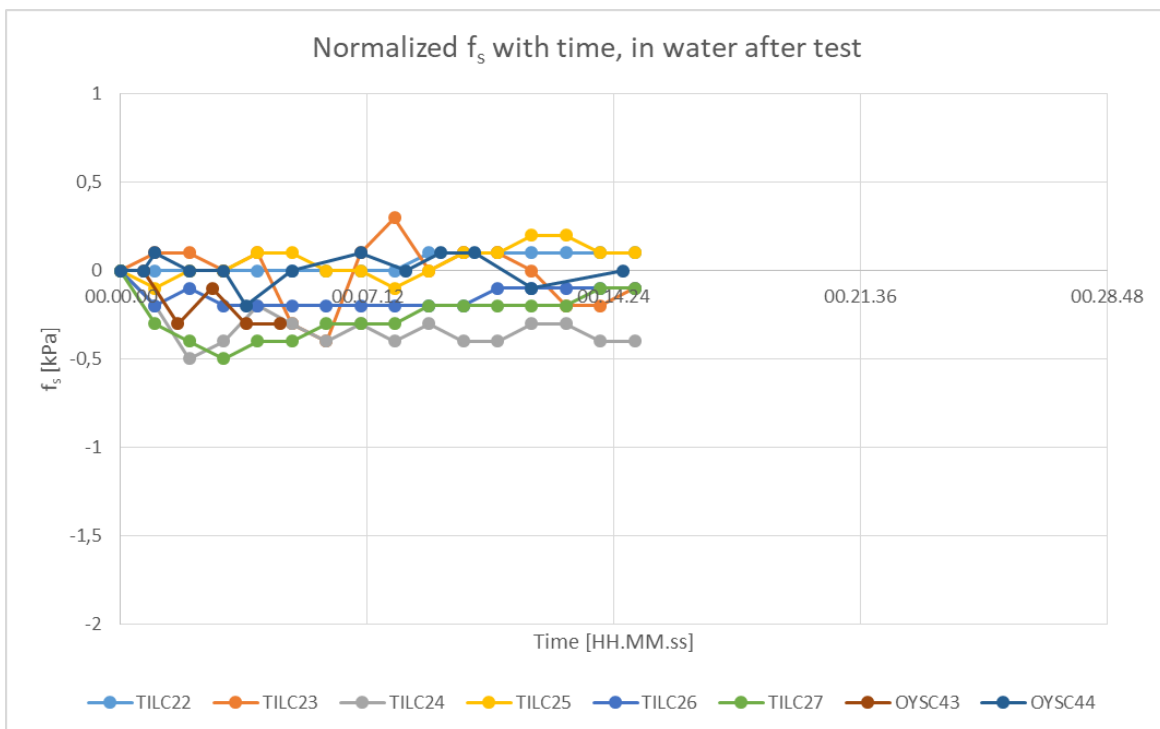


Figure B1.12 Stabilization of f_s with time in water after test. Equal scale for all f_s .

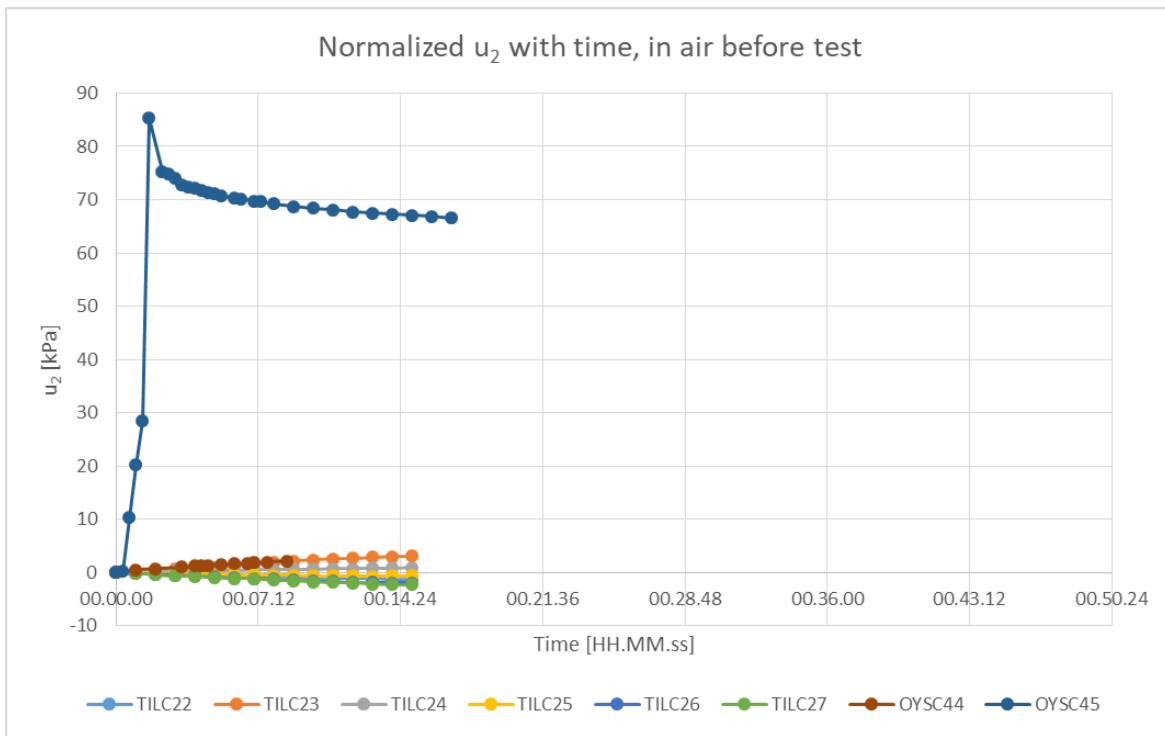


Figure B1.13 Stabilization of u_2 with time in air before test.

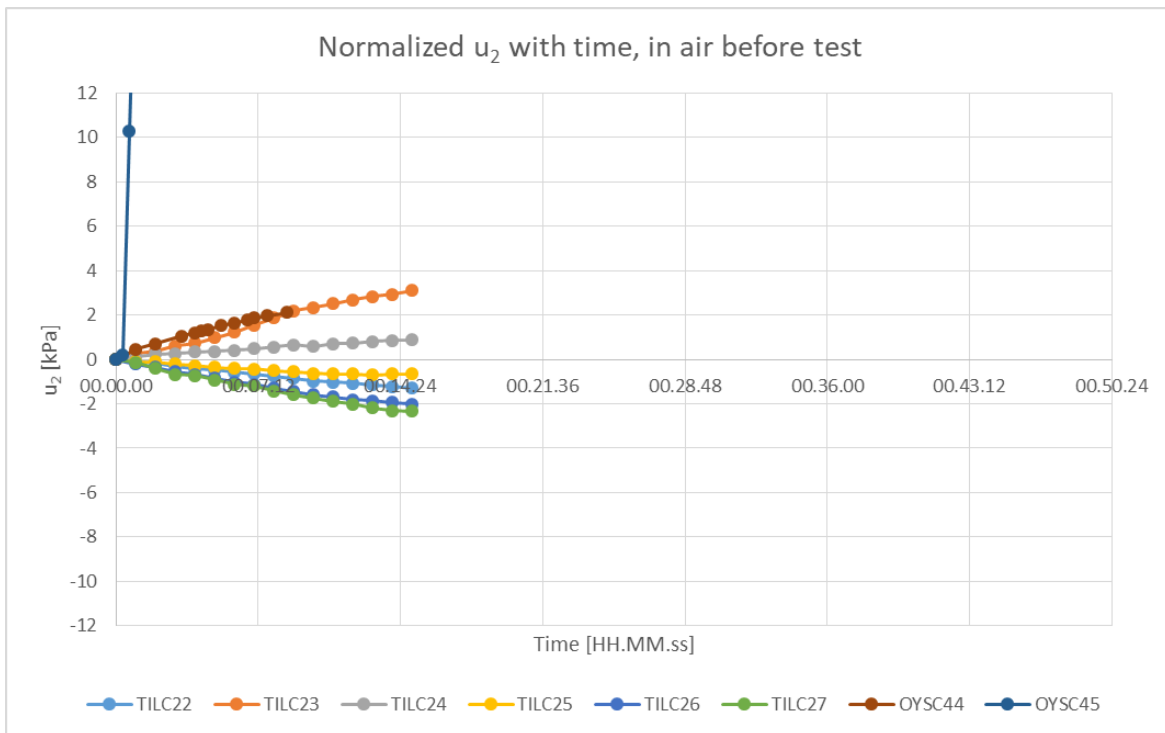


Figure B1.14 Stabilization of u_2 with time in air before test. Equal scale for all u_2 .

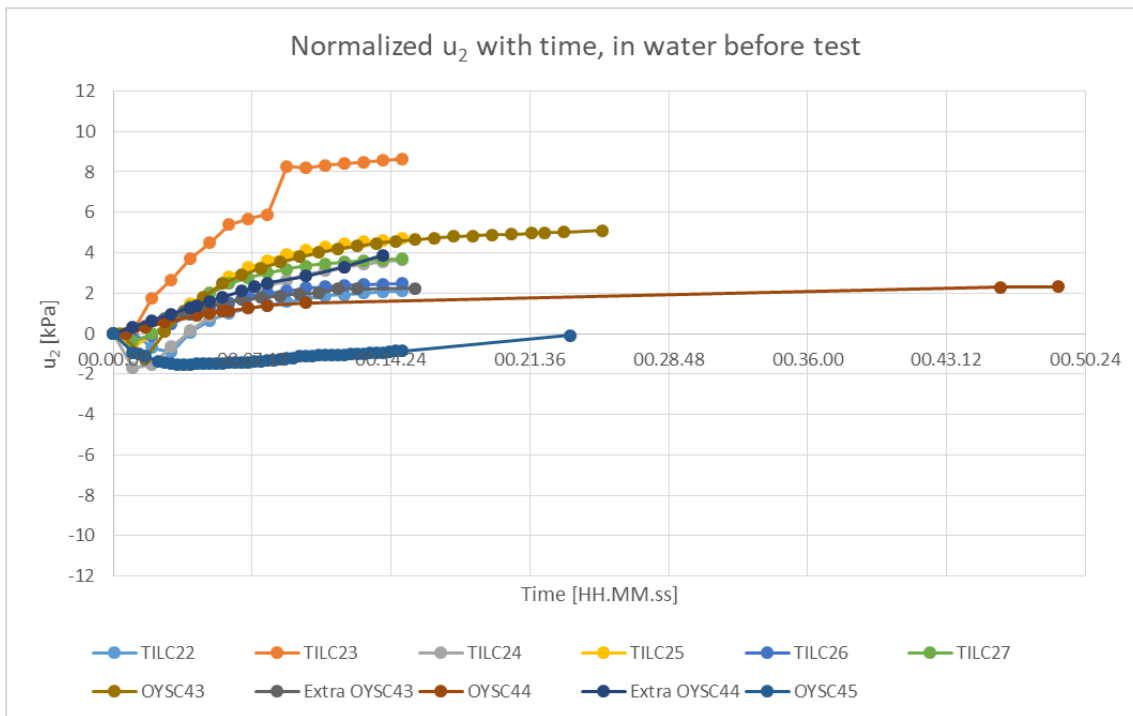


Figure B1.15 Stabilization of u_2 with time in water before test. Equal scale for all u_2 .

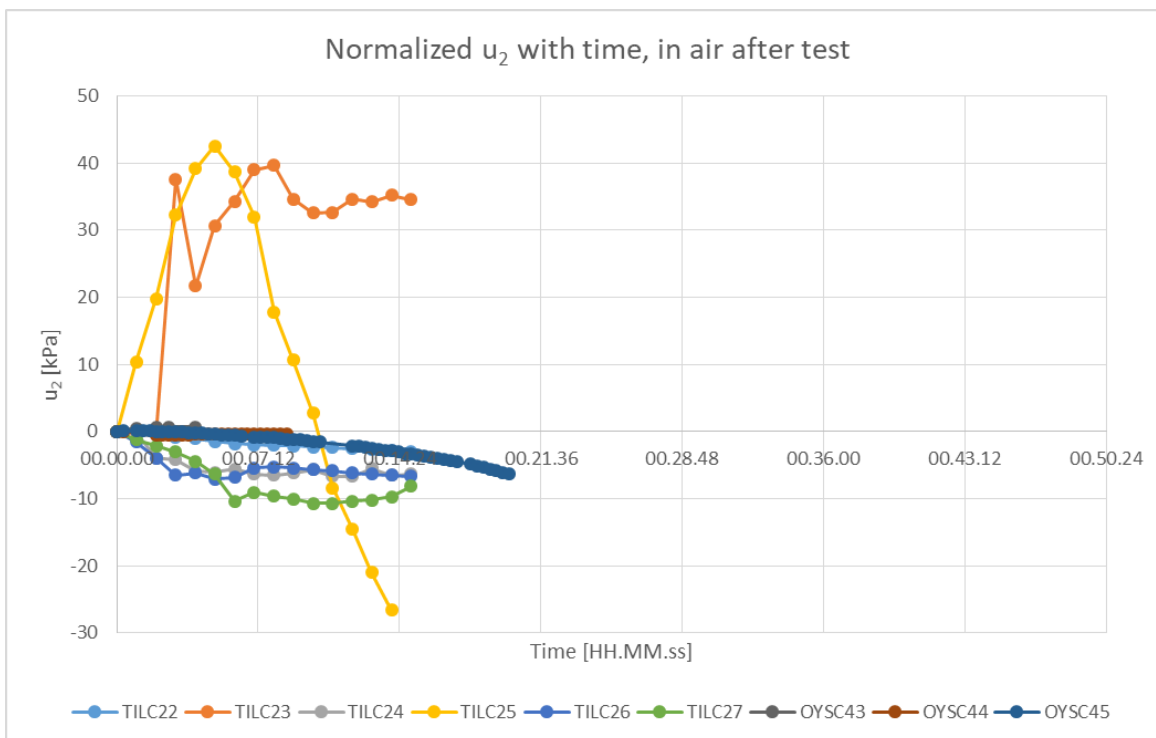


Figure B1.16 Stabilization of u_2 with time in air after test.

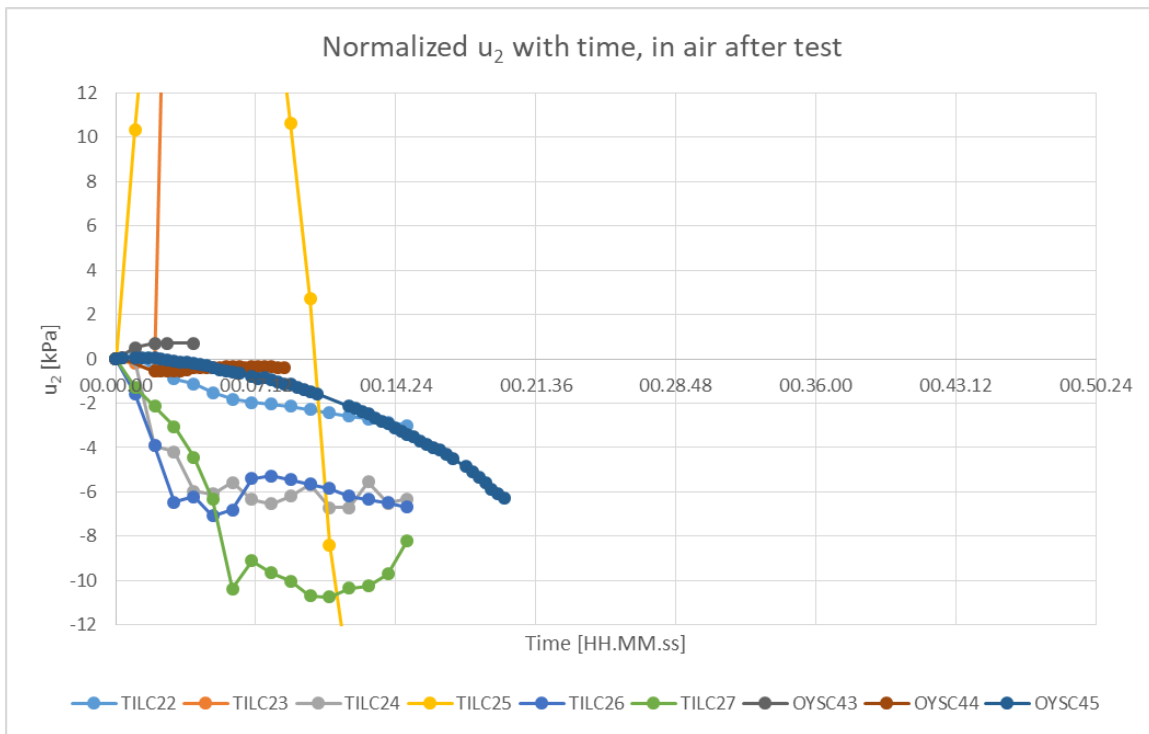


Figure B1.17 Stabilization of u_2 with time in air after test. Equal scale for all u_2 .

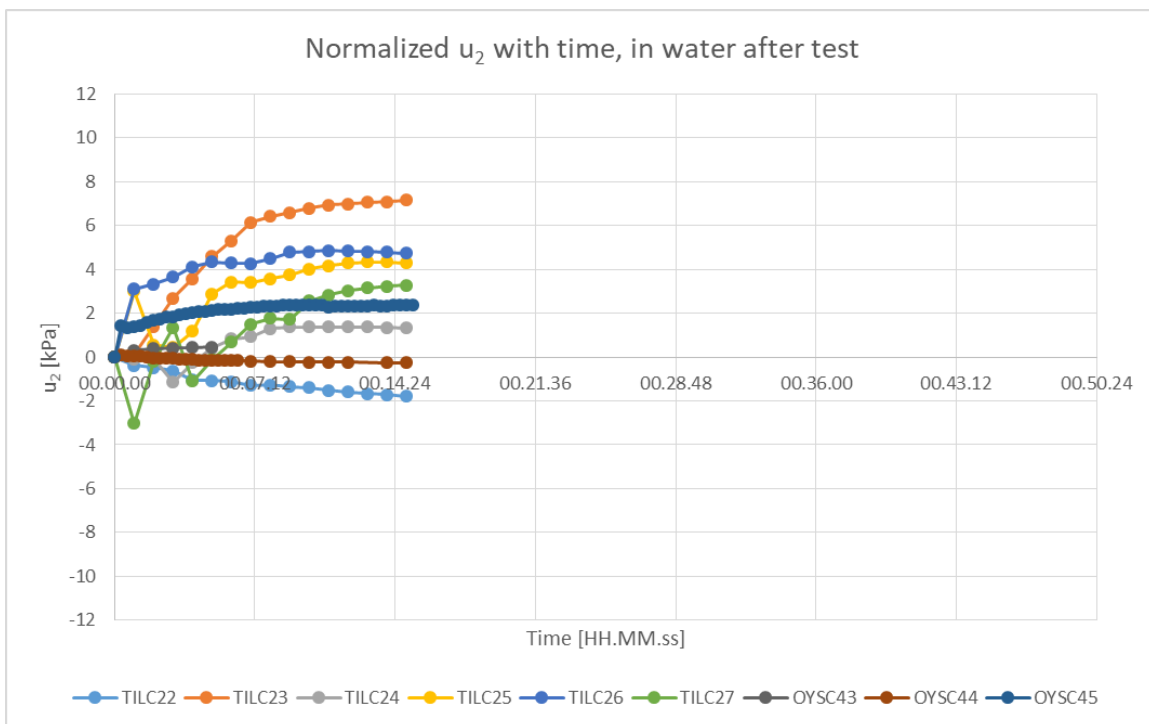


Figure B1.18 Stabilization of u_2 with time in water after test. Equal scale for all u_2 .

Dokumentinformasjon/Document information		
Dokumenttittel/Document title Impact of cone penetrometer type on CPTU results at 4 NGTS sites. Silt, soft clay, sand and quick clay.		Dokumentnr./Document no. 20160154-21-R
Dokumenttype/Type of document Rapport / Report	Oppdragsgiver/Client Research Council of Norway (RCN)	Dato/Date 2020-01-08
Rettigheter til dokumentet iht kontrakt/ Proprietary rights to the document according to contract NGTS		Rev.nr.&dato/Rev.no.&date 0
Distribusjon/Distribution ÅPEN: Skal tilgjengeliggjøres i åpent arkiv (BRAGE) / OPEN: To be published in open archives (BRAGE)		
Emneord/Keywords Norwegian GeoTest Sites, CPTU, cone manufacturers		

Stedfesting/Geographical information	
Land, fylke/Country Norway	Havområde/Offshore area
Kommune/Municipality Fredrikstad	Feltnavn/Field name
Sted/Location Onsøy	Sted/Location
Kartblad/Map	Felt, blokknr./Field, Block No.
UTM-koordinater/UTM-coordinates Sone: Øst: Nord: 32 608 300 6566426	Koordinater/Coordinates Projeksjon, datum: Øst: Nord:

Dokumentkontroll/Document control					
Kvalitetssikring i henhold til/Quality assurance according to NS-EN ISO9001					
Rev/Rev.	Revisjonsgrunnlag/Reason for revision	Egenkontroll av/Self review by:	Sidemannskontroll av/Colleague review by:	Uavhengig kontroll av/Independent review by:	Tverrfaglig kontroll av/Interdisciplinary review by:
Draft	Draft issued for review	2018-11-20 Aleksander Gundersen	2018-11-20 Tom Lunne		
0	Updated with comments	2020-01-07 Aleksander Gundersen	2020-01-07 Tom Lunne		

Dokument godkjent for utsendelse/Document approved for release	Dato/Date 8. januar 2020	Prosjektleder/Project Manager Jean-Sebastien L'Heureux
---	------------------------------------	--